Other SAE books of interest:

Lightweight Electric/Hybrid Vehicle Design
by Ron Hodkinson and John Fenton
(Order No. R-316)

Alternative Fuels Guidebook
by Richard L. Bechtold
(Order No. R-180)

For more information or to order a book, contact SAE Customer Service at
400 Commonwealth Drive, Warrendale, PA 15096-0001;
Web site: http://store.sae.org;
E-mail: CustomerService@sae.org;
Phone: 1-877-606-7323 (USA or Canada) or 724-776-4970
Fax: 724-776-0790

The Winning Solar Car

A Design Guide for Solar Race Car Teams

Douglas R. Carroll

SAE International
Warrendale, Pa.

Library of Congress Cataloging-in-Publication Data

Carroll, Douglas R.
The winning solar car : a design guide for solar race car teams / Douglas R. Carroll.
p. cm.
Includes bibliographical references and index.
ISBN 0-7680-1131-0
1. Solar cars—Design and construction. I. Title.

TL222.C37 2003
629.22'95—dc21 2003052648

SAE International
400 Commonwealth Drive
Warrendale, PA 15096-0001 USA
E-mail: CustomerService@sae.org
Tel: 877-606-7323 (inside USA and Canada)
724-776-4970 (outside USA)
Fax: 724-776-1615

ISBN 0-7680-1131-0

SAE Order No. R-343

Printed in the United States of America.

To my wife Karla,

for putting up with me as I spent an awful lot

of our time learning about solar cars.

Preface

Development of this book began in 1997, after the 1997 Sunrayce event. I had then been involved in designing and building three solar cars that participated in the 1993, 1995, and 1997 Sunrayce events, respectively. As the coach and advisor for a university solar car team, I had the problem of losing some key students with each project. The new students joining the team had the same design misconceptions that the veteran students had when they began and would want to make the same design mistakes that had been made on previous cars. Making the same design mistakes again provides a good educational experience for the students but does not further knowledge of solar car design. To make progress and continually improve our design efforts, I developed a course on solar car design and wrote notes to support the course. The purpose of the course was to get the new students up to speed, and the course focused on what is important in designing a competitive solar car. The notes became a little more formal each time I offered the course, and evolved into this book on solar car design.

The material in this book is based on my experiences designing and building five solar cars over the last twelve years. I have tried to keep the book general and offer design options so that it is not just about how the University of Missouri-Rolla team designs solar cars, but there is a certain amount of bias in our design philosophy. The book was designed to be used in a course that is open to upper-level students majoring in any field of engineering, mathematics, or science. Solar car design is an interdisciplinary topic, and the book was written to be suitable for the junior, senior, and graduate students who would be responsible for designing the car. Students entering the course are assumed to have a fundamental understanding of calculus, differential equations, physics, and chemistry. The book provides an introduction to all aspects of designing, manufacturing, and racing solar cars but does not provide all of the details on any topic. Design groups will have to go deeper than what is provided in this book to design any of the systems on the car. Everyone on the team needs to have a fundamental understanding of what is involved in designing, building, and racing the car. Understanding the "big picture" will help team members make design and manufacturing trade-offs

to stay on schedule and allow time to test and practice racing the car. Testing and practice are an important part of being successful in the competition.

To do well in a solar car race, the team must have a good car, good drivers, good weather information, good strategy, and a well-trained support team. Doing a poor job on any of these elements will hurt the performance of the team in the race. The main focus of this book is on designing the car because that is the most difficult and time-consuming part of the project, but the team needs to recognize that the car is not the whole project. Driver training, accurate weather forecasting, race strategy, and practice in driving the race route make a huge difference in how well the team performs in the competition.

The first two chapters in the book are on energy management, and the information in these chapters is helpful when doing design trade-offs and developing a strategy for racing the car. Chapter 2 includes information on how to drive the car efficiently and is helpful in driver training. Chapter 3 focuses on design methodology and project management and provides an introduction to the general design process. The remaining chapters are about designing the different subsystems of the car. In each chapter, I have referred the reader to books and articles that I have found helpful on designing and building solar cars. The goal of the book is to provide an introduction to all aspects of designing, building, and racing solar cars.

Acknowledgments

When I began working with the solar car team at the University of Missouri-Rolla, I was a new assistant professor and had little understanding of how to design a solar car or how to coach a college car design team. I have received help from many people over the years, and without their help, I could not have been successful. Chancellor John T. Park and Dean O. Robert Mitchell saw value in the project and helped the team get the support, facilities, and funding needed even in the early years when the team was not very successful. The project would have died at an early date without their support and encouragement. Dean Lee W. Saperstein, Dr. D. Ronald Fannin, Dr. E. Keith Stanek, Dr. Ashok Midha, Dr. Henry A. Wiebe, and Dr. David A. Summers provided office space, manufacturing facilities, and technical assistance from their departmental resources in support of the project.

Mr. L. John Tyler spent countless volunteer hours developing an efficient process for manufacturing the body of the car, developing an efficient process for evaluating and testing batteries, and teaching students how to manufacture many of the mechanical components of the car. He has been a key person in developing the practical knowledge required to manufacture a solar car. Dr. C.H. Wu spent many hours explaining to me and the students how solar cells work and how to build a solar array. Dr. K.M. Isaac spent many hours working with me on the aerodynamics of solar cars. Dr. Donald L. Cronin spent many hours teaching me about tire and suspension design. Dr. Paul D. Hirtz was the president and project manager for the team for several years and helped us understand the importance of applying the discipline of project management to the solar car design project.

I owe special thanks to Dr. Patrick J. Starr for talking with me about how he coaches the design teams at the University of Minnesota. He was my mentor in learning how to be an engineering design team coach. Dr. Starr also helped me learn about the technical aspects of designing the chassis and suspension of the solar car. In learning to coach and organize a team, I have also had helpful conversations with my colleagues at other universities: Dr. Michael T. Shelton and Ms. Tina Shelton at California State Polytechnic University-Pomona,

Mr. Art Boyt at Crowder College, Dr. Scott Tolbert at the University of North Dakota, Dr. Joe Ritter and Dr. Steve Shedd at Principia College, Dr. Dennis Waugaman at Texas A&M University, and Mr. Richard T. Whelove at the University of Missouri-Columbia. I also would like to thank Mr. Steve McMullen for his help over the years in developing battery systems.

All solar car teams owe a great deal of thanks to Mr. Dan Eberle, Ms. Kate von Reis, and Ms. Andrea Pagee for staffing the solar car racing headquarters and organizing the races. There would be no solar car races in the United States without their commitment. We also owe many thanks to Mr. Howard Wilson, Mr. Richard King, General Motors Corporation, Electronic Data Systems, and the U.S. Department of Energy for their support of solar car racing.

Table of Contents

Library of Congress Cataloging-in-Publication Data

Carroll, Douglas R.
The winning solar car : a design guide for solar race car teams / Douglas R. Carroll.
p. cm.
Includes bibliographical references and index.
ISBN 0-7680-1131-0
1. Solar cars—Design and construction. I. Title.

TL222.C37 2003
629.22'95—dc21 2003052648

SAE International
400 Commonwealth Drive
Warrendale, PA 15096-0001 USA
E-mail: CustomerService@sae.org
Tel: 877-606-7323 (inside USA and Canada)
724-776-4970 (outside USA)
Fax: 724-776-1615

ISBN 0-7680-1131-0

SAE Order No. R-343

Printed in the United States of America.

To my wife Karla,

for putting up with me as I spent an awful lot

of our time learning about solar cars.

Chapter 1

Introduction

A. Identification of the Problem

The first step in the design process is to define the problem as clearly as possible. There is an iterative process to design, and the design team may not understand the problem well enough at first to give a clear definition. In this case, the problem should be defined as clearly as possible. The definition will be refined as the team works through the design process. Design methodology is discussed in more detail in Chapter 3.

As an example of a race car design problem, circle track racing is more familiar than solar car racing [1-1]. The problem to be solved is to get the car to go around the track as quickly as possible, as illustrated in Fig. 1.1. Speed in the corners is limited primarily by the amount of traction between the tires and the road. Acceleration is limited by the power the engine can provide, the

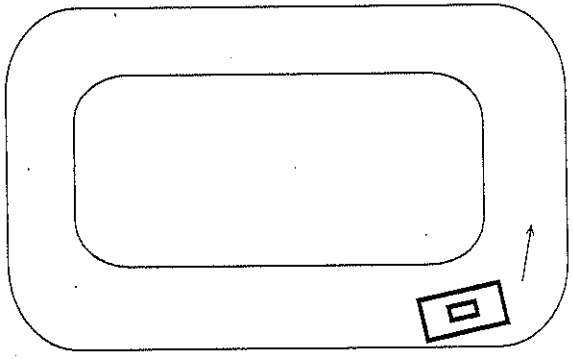

Fig. 1.1 Circle track racing.

efficiency and inertia of the drivetrain, the weight of the car, the aerodynamic drag, and traction between the tires and the road. Braking is limited by the performance of the braking system and traction between the tires and the road. The strategy for circle track racing is as follows:

1. Go around the corner as fast as possible without sliding sideways off the track.

2. Accelerate out of the corner as quickly as possible and continue accelerating down the straightaway.

3. At the last possible minute, hit the brakes to slow down just enough to keep from sliding off the track in the next corner.

From the race strategy, it appears that the most important design aspects for the car are cornering, acceleration, and braking. The next step in problem definition is to determine what aspects of the car contribute most to cornering, acceleration, and braking.

Cornering Performance

1. The tires should be selected so they have a high coefficient of friction between the rubber and the track.

2. A downward aerodynamic force makes a higher normal force on the tires, which makes a higher friction force between the rubber and track. A downward aerodynamic force will improve cornering.

3. The suspension must keep the tires on the road and prevent excessive body roll.

Acceleration Performance

1. Power at the wheels is what provides the acceleration. A high-power engine and good driveline efficiency contribute to getting power to the wheels.

2. Low aerodynamic drag allows the car to accelerate faster and have a higher top speed.

3. The rear tires must have a high coefficient of friction, or they will lose traction and cause the car to spin out of control during acceleration out of the corner.

4. A downward aerodynamic force on the rear tires will help keep rear tires from losing traction. This is why many race cars have a spoiler on the rear.

5. Keeping the car light in weight and minimizing the rotational inertia of the engine and drive system will allow the car to accelerate faster.

Braking Performance

1. The brakes must be capable of slowing the car quickly and smoothly. They must not overheat.

2. The tires must have high coefficient of friction to prevent the car from going out of control when the brakes are applied.

3. Proper suspension and balance are necessary to proportion braking load front and rear, and to prevent nosedive when braking.

Reliability, safety, and ergonomics are also important issues. But from a performance standpoint most of the effort should be spent on tires, aerodynamics, horsepower, brakes, weight reduction, suspension, and handling. Recognizing that there are limited resources, the team must decide how to divide up the resources to build the best overall car.

B. Solar Car Racing

Solar car racing is very different from circle track racing. The reason for starting the chapter with a discussion of circle track racing was to contrast the two problem statements. Performance of the car in cornering, acceleration, and braking is not as important in solar car racing. The primary design

objectives are to make a reliable and energy-efficient car [1-2 to 1-4]. Cornering, acceleration, and braking are secondary issues for solar car design. There are three different types of solar car races, and there are minor variations in the problem statement depending on which type of race the team is preparing for. In any solar car race, a team must design a car that can travel fast and use very little energy. The cars must be large to accommodate the 8 m^2 solar array. A typical car is 1.8 m wide and 5 m long, which is approximately the same footprint as a full-sized automobile. To be competitive the car must be able to travel at 90 km/h (55 mph) using only 1500 W power (2.0 hp). This is a very low power consumption for such a large vehicle, and achieving this level of energy efficiency is the primary design objective.

The World Solar Challenge is a 3000-km cross-country race held in Australia. This was the first large solar car race. It was first held in 1987, and is still regarded as the world championship event. Teams are allowed to drive from 8:00 A.M. to 5:00 P.M. during the day, and there is no maximum speed limit for most of the race. The race is run on the Stewart highway from Darwin to Adelaide. This is an excellent route for solar cars because there is not much traffic. The cars can get up to speed and cruise for hundreds of kilometers without interruption. The World Solar Challenge is an open competition. Teams may use the best technology available for solar cells, batteries, and other systems, regardless of cost. It is very expensive to build a competitive car for this race. The top teams typically travel at an average speed of 90 km/h on the open road. The goal is to drive the 3000 km distance as quickly as possible, and top teams typically travel more than 650 km/day. In the World Solar Challenge teams drive as far as possible during the allotted time each day, and then pull off the road and set up camp for the evening.

The American Solar Challenge is similar to the World Solar Challenge, except that the route, from Chicago to Los Angeles, is longer and more difficult. There is a lot of traffic and many stoplights on this route. It typically takes 2 h to get out of the Chicago area where the race starts. The roads are rough and have lots of potholes, and teams must cross the Rocky Mountains as they go west. The American Solar Challenge is approximately 3700 km (2300 mi) in length. The race is divided into three segments to keep the cars from getting too strung out along the race route. The last leg is very short, so that virtually all of the cars will finish the race within a 2-h period on the last day. This allows for a good publicity opportunity at the finish line. In the World Solar

Challenge there will be several days between the first and last place cars, which makes it more difficult for the press to cover the event. In the American Solar Challenge teams are allowed to drive from 8:00 A.M. to 6:00 P.M. each day. Top teams typically travel at 90 km/h (55 mph) on the open road, but the average speed is lower than in the World Solar Challenge because of the many stops and speed zones on the route. The goal is to get to the end of each segment as quickly as possible and then charge the batteries off the solar array while waiting for the slower teams to arrive. The race is then restarted on the next segment. Top teams will have a full battery pack to start the next segment, while the slower teams will probably have to start with a partial charge in their batteries. The team with the least total time on the three segments is the winner.

Sunrayce was a cross-country race of 1900–2400 km (1200–1500 m) held in the United States. The rules for the race were modeled after the Tour de France bicycle race. Terrestrial-grade solar cells were required and there were limits on the battery technology that teams could use. Limiting the technology that can be used for the solar cells and batteries makes it much less expensive to build a competitive car. Sunrayce was a better engineering competition than the World Solar Challenge or the American Solar Challenge because of the technology limits, but cars that performed well in Sunrayce were not competitive in the world competition, and that hurt the prestige of the event. There were set starting and stopping points for each day of the race, and a typical race day was 250–325 km (150–200 mi). The goal was to drive the distance each day as quickly as possible. Knowing where the teams will start and stop each day makes it much easier to plan the logistics of the race, but it requires more human resources to start and stop the race each day. A Sunrayce-type race is much more expensive to organize than the World Solar Challenge or American Solar Challenge. Sunrayce rules limited the maximum speed to 88 km/h (55 mph), even if the posted speed limit was higher. The top cars had to be energy-efficient enough to travel at 88 km/h or the speed limit under sunny conditions. The last Sunrayce was run in 1999 and it looks like there may not be any more races like this, primarily because of the expense of conducting such an event.

Solar car racing is also conducted on closed tracks. The World Solar Rallye and Dream Cup are probably the best known events. The United States has a race of this type (Formula Sun Grand Prix) which is held in May each year.

In this type of event the cars are allowed to travel as far as possible each day around the track. The allowable driving period is typically from 8:00 A.M. to 5:00 P.M., and the goal is to travel as far as possible during the 3- or 4-day event. The team that travels the farthest is the winner. Conducting the race on a closed track makes it a much safer event, and makes it easier to plan the logistics. Speeds for these races depend on the track. If the track does not have sharp corners, then the cars will get up to speed and cruise at a steady speed all day. Strategy is similar to the road races for solar cars.

The Formula Sun Grand Prix event is held on the Heartland Park track near Topeka, Kansas. The track has very sharp corners. The thin-walled high-efficiency tires that solar cars use are not very durable in hard cornering. Solar cars must slow down to 40 km/h (25 mph) for some of the corners to protect the tires. Even at this rate the tires will last only 3 or 4 h, so pit stops need to be scheduled to change the tires before they blow out. If the car has a flat on the track it will take 30 min for the team to get permission to go out on the track and get it changed. It is difficult to obtain an average speed of 56 km/h (35 mph) on this track. Formula Sun Grand Prix is one of the few solar car events where cornering and handling of the vehicle are important in winning the race. In particular, the tires that are best in the road races may not be best for the Formula Sun event. Giving up some energy efficiency in the tires in exchange for being able to corner faster is an advantage in this race. Maneuverability is important too because there are many vehicles on the track.

In all solar car racing, the cars start the race with a fully charged battery pack. Once the race begins, the batteries can only be charged off the solar array on the car. Charging takes place in the morning before the cars are allowed to begin driving, and in the evening after they are required to stop driving. Teams cannot plug into a generator or power outlet and charge the batteries at night. A good solar race competition should last at least a few days to test the ability of the team and their car in efficiently using solar energy.

Solar cars must run on the very limited amount of energy that the solar array produces. This is what makes solar car racing much different than circle track racing. The design problem for solar car racing is much more focused on energy efficiency goals for the car than performance in acceleration, cornering, and braking. The car must be energy efficient enough to be able to

travel at speeds of 90 km/h (55 mph) on a very limited amount of power. In solar car racing, the following three aspects of the car are focused on:

1. The solar array should gather as much energy as possible. Because the array size is limited to approximately 8 m^2, the array should be as efficient as possible in converting sunlight to electric power. Efficient cells and power point trackers should be used and the array should be wired to get the best overall efficiency from the cells.

2. The car must efficiently use the energy gathered. An energy-efficient car displays the following design features:

   a. The tires must have low rolling resistance.

   b. The vehicle must be lightweight, to reduce rolling resistance.

   c. The car must have low aerodynamic drag.

   d. The motor drive system must be energy efficient.

   e. All of the minor subsystems must consume very little energy. This means using low-resistance wires and connectors and low-power lights and electronics.

3. The car should have energy-efficient batteries. Energy is always flowing into and out of the batteries as the car speeds up and slows down and goes up and down hills. Energy is also stored in the batteries by using the solar array to charge them during the charging periods in the mornings and evenings. Batteries are not 100% efficient. A portion of the energy will be lost as heat every time the battery pack is charged or discharged. Batteries with high efficiency will provide more usable energy to the car because they will generate less heat. As a general rule, if the battery manufacturer suggests a cooling system be used for the batteries, then the batteries are probably not a good choice for solar car racing.

The three performance aspects covered above are most important from the standpoint of the solar car's performance. However, all systems in the car must be well designed and reliable. Reliability is more important than performance.

The team will not win the race if the car breaks down frequently. The philosophy is to first have a well-designed and reliable car, and then to focus on the performance issues.

C. Energy Available and Distances Traveled in Solar Car Racing

The different solar car races we have discussed all allow for approximately 5 kW-h of battery capacity and 8 m^2 of solar array area. It is difficult to measure battery capacity during the scrutineering period before a race, so battery limitations are usually stated in allowable weight, and the allowable weight varies depending on the type of batteries used. Most races now allow for any type of solar cells or batteries to be used in the open class. The competitions usually have a stock class that limits the types of solar cells and batteries that can be used so that a team that cannot afford expensive technology can still be competitive in their class. Stock-class rules usually require that lead-acid batteries and common terrestrial-grade silicon cells be used. A team can spend a great deal of money on two components — solar cells and batteries — and get technology that is considerably better than what is allowed in the stock class. Teams can also spend large amounts of money on expensive composites, titanium chassis and suspension, ultrahigh-efficiency motors, and other components. These items will improve the performance of the car in comparison to more commonly used materials and equipment, but such improvements are small. High-efficiency solar cells and lightweight high-efficiency batteries are the components that make a large difference in the performance of the car.

Whatever the race and class in which the team may be competing, solar cars have a very limited amount of energy to use, and the team must use this energy carefully to get the best performance from their car. The following analysis is an attempt at understanding quantitatively how energy efficient the car must be to be competitive. To achieve this understanding, it is important to consider the energy available and how far the car must travel on that energy.

1. *Batteries*. Battery capacity of 5 kW-h is allowed by the rules. Because the batteries cannot run until they are completely dead without damaging

them, there is about 4.5 kW-h of usable energy in the battery pack. Most races limit the weight of batteries rather than their capacity, because it is easier to weigh the battery than to measure its energy storage capacity. The weight limits are set for the different types of batteries so that the allowable capacity will be approximately 5 kW-h.

2. *Solar Array*. If a stock-class car is being designed, then terrestrial-grade silicon solar cells must be used and the solar array will deliver an average of approximately 800 W on a sunny day while driving. Higher-efficiency (space-grade) cells are available which can deliver 1200–1800 W average power, depending on the efficiency (and usually cost) of the cells. A terrestrial-grade array will deliver 1000 W on the array stand while charging, and a space-grade array will deliver 1.5–2.5 times that much power. These estimates are for a sunny day. The solar array power will be much less on a cloudy day.

3. The cars will have a certain period during the day to drive, usually either 8:00 A.M. to 5:00 P.M. or 8:00 A.M. to 6:00 P.M. The goal is to go as far as possible during the driving time. There will be one or two required media stops during the day, so the allowable driving time is likely to be 8 or 9 h, assuming a stock-class car that begins the day's driving with fully charged batteries. For the purposes of this discussion, it is also assumed that the day is sunny, so that the terrestrial-grade solar array produces 800 W average power, and the race is from 8:00 A.M. to 5:00 P.M. Equation 1.1 shows the energy available for driving during such a day.

$$\begin{array}{c}\text{Energy available} \quad 4.5 \text{ kW-h} + (0.8 \text{ kW})(9 \text{ h}) \\ \text{Battery} + \text{Solar Array} \\ 11.7 \text{ kW-h total energy available for the day}\end{array} \tag{1.1}$$

In an open-class car with a space-grade solar array that produces an average of 1200 W, there will be a total of 15.3 kW-h energy available, 31% more than in a stock-class car. The open-class car will have 31% more power available and, other things equal, will be able to go much faster than the stock-class car.

4. The average power consumption of the car increases as it goes faster. A well-designed stock-class car consumes more power than a well-designed open-class car, primarily because of the weight of the batteries. Stock-class cars require lead-acid batteries, which are much heavier than the high-performance batteries. For the exercises in this chapter, Eqs. 1.2–1.5 will be assumed to be correct. Details of how the equations were developed will be explained in Chapter 2. These equations correspond to well-designed stock and open-class cars. For events outside the United States, speeds are measured in kilometers per hour, and it is convenient to work with a power equation with the speed in kilometers per hour as in Eqs. 1.2 and 1.3.

$$\text{Stock-class power} = [(0.00163)V^3 + (0.0336)V^2 + (5.41)V + 30]\ \text{W} \tag{1.2}$$

$$\text{Open-class power} = [(0.00163)V^3 + (0.0231)V^2 + (3.72)V + 30]\ \text{W} \tag{1.3}$$

where V is the speed in kilometers per hour.

For races in the United States speeds are measured in miles per hour, and it is convenient to work with a power equation with the speed in miles per hour as in Eqs. 1.4 and 1.5. This set of equations represents the same car; the only difference is the change in units.

$$\text{Stock-class power} = [(0.00680)V^3 + (0.0871)V^2 + (8.71)V + 30]\ \text{W} \tag{1.4}$$

$$\text{Open-class power} = [(0.00680)V^3 + (0.0599)V^2 + (5.99)V + 30]\ \text{W} \tag{1.5}$$

where V is the speed in miles per hour.

Throughout this book the equations will be given using metric units, and where it makes sense alternative equations will be given for U.S. common

units, as was the case in the preceding discussion. During a road race, speed limits in the United States are posted in miles per hour. In most of the rest of the world, speed limits are posted in kilometers per hour. Because the driver must respond to the speed limit signs, it makes sense to measure speed in miles per hour for U.S. races, and in kilometers per hour for races held elsewhere in the world.

5. If all the energy in the batteries is used, there may not be enough time to recharge them in the evening and morning. For the exercises in this chapter, it will be assumed that the batteries must be restored to their full charge during the evening and morning charge periods. It will be assumed that there is a total of 4 h of charging time. A terrestrial-grade solar array will produce an average of 1000 W during this period in good sunlight, or a total of 4 kW-h of energy. So a stock-class car can only use 4 kW-h of energy from the batteries and have time to get them fully charged for the next day. A space-grade array will produce quite a bit more power and would be able to use the full amount of energy in the batteries. In cloudy conditions neither array will permit the batteries to be fully charged, so the amount of battery power available decreases during cloudy days.

6. We will now provide an example problem similar to the homework assignment. Assume that a team is driving an open-class car and the array produces 900 W average power while driving and 1100 W while the car is on the array stand. Race time is from 8:00 A.M. to 5:00 P.M. with two required 30-min media stops.

   a. During the 4-h charge period the solar array will be able to put (1100 W)(4 h) energy back into the batteries, so the car can use only 4400 W-h energy from the batteries during the day.

   b. While driving, the solar array will produce an average of 900 W for the 9 h of race time (from 8:00 A.M. to 5:00 P.M.). The total energy available for the car to use is shown in Eq. 1.6.

$$\begin{aligned}\text{Total energy} &= (900\ \text{W})(9\ \text{h}) + 4400\ \text{W-h} \\ &= 12{,}500\ \text{W-h}\end{aligned} \tag{1.6}$$

c. The actual allowable driving time is 8 h because of the two required 30-min media stops. Equation 1.7 must be solved for the speed of the vehicle.

$$12{,}500 \text{ W-h} = [(0.00163)V^3 + (0.0231)V^2 + (3.72)V + 30] \text{ W (8 h)} \quad (1.7)$$

The equation must be solved numerically. The answer is that the car will be able to drive at 86.1 km/h (53.5 mph) during the 8 h it drives, and will be able to travel 689 km (428 m) during the day.

D. Homework Assignment

Find the maximum distance the car can travel for both a stock-class and open-class car. Assume that the car can drive from 8:00 A.M. to 5:00 P.M. and that there will be two required 30-min media stops during the day, so the actual driving time is only 8 h. Assume that there are 4 h of charging time in the evening and morning to get the batteries back up to full charge, and that the batteries must be fully charged after the charging period. There is a maximum of 5 kW-h of available energy in the batteries. Calculate the distance that a stock-class and open-class car can travel for a bright sunny day, a moderately cloudy day, and a very cloudy day with the parameters listed below.

1. *Sunny Day*. The terrestrial-grade array produces 800 W average power while driving and 1000 W on the array stand during the evening and morning charging session. The space-grade array produces 1200 W average power while driving and 1500 W on the array stand during the charging period [618 km (384 m), 758 km (471 m)].

2. *Partly to Mostly Cloudy Day*. The terrestrial-grade array produces 600 W average power while driving and 800 W on the array stand during the evening and morning charging session. The space-grade array produces 900 W average power while driving and 1100 W on the array stand during the charging period [545 km (339 m), 689 km (428 m)].

3. *Very Cloudy Day*. The terrestrial-grade array produces 300 W average power while driving and 300 W on the array stand during the evening and morning charging session. The space-grade array produces 400 W average power while driving and 400 W on the array stand during the charging period [359 km (223 m), 467 km (290 m)].

E. References

1-1. Milliken, W.F., and D.L. Milliken, *Race Car Vehicle Dynamics*, chap. 1, Society of Automotive Engineers, Warrendale, PA, 1995.

1-2. Kyle, C.R., *Racing with the Sun: The 1990 World Solar Challenge*, chap. 3, Society of Automotive Engineers, Warrendale, PA, 1991.

1-3. Storey, J.W.V., A.E.T. Schinckel, and C.R. Kyle, *Solar Racing Cars*, chap. 3, Australian Government Publishing Service, Canberra, Australia, 1994.

1-4. Roche, D.M., A.E.T. Schinckel, J.W.V. Storey, C.P. Humphris, and M.R. Guelden, *Speed of Light: The 1996 World Solar Challenge*, chap. 3, Photovoltaics Special Research Centre, School of Engineering, University of New South Wales, Sydney, Australia, 1997.

Chapter 2

Energy Management Modeling of Solar Car Performance

A. Purpose of Modeling

Modeling allows us to understand quantitatively where the energy is consumed [2-1 to 2-7]. It allows us to focus our effort on the most important aspects when designing the car. After the car is built, modeling allows us to interpret test data and design tests to see which systems are limiting performance of the car. Modeling also allows us to plan race strategy. The goal is to use all the available energy to go as fast as possible, but not run out of energy before getting to the destination. The model developed in this chapter includes Aerodynamics, Rolling Resistance, Solar Array Power, Battery Efficiency, Motor-Drive System Efficiency, Parasitic Losses, Gravitational Energy, and Kinetic Energy.

B. Aerodynamics

Aerodynamic drag accounts for a large portion of the total resistive force when the car is traveling fast. It is less important at slow speeds, but is a significant power loss at any speed above 40 km/h (25 mph). Equation 2.1 is the fundamental equation for aerodynamic drag [2-8].

$$D_A = (0.5)\rho V^2 A C_d \qquad (2.1)$$

where D_A is the aerodynamic drag force, ρ is the density of air, V is the speed of the car, A is a characteristic area for the body of the car (often the projected cross-sectional area when viewed from the front of the car), and C_d is the drag coefficient (a nondimensional quantity related to the shape of the

car body). Typical drag coefficients are $C_d = 2.0$ for a flat plate perpendicular to the airflow, $C_d = 0.05$ for a smooth teardrop shape, and $C_d = 0.1$ for a well-designed solar car, based on frontal area.

Drag area is defined as AC_d. The best solar cars have $AC_d = 0.1–0.15\ m^2$. The drag force is usually measured in newtons, the speed of the car in kilometers per hour, and the frontal area in square meters. Assuming the summertime density of air is $1.17\ kg/m^3$, the drag force equation can be written as shown in Eq. 2.2.

$$D_A = (0.0451)V^2AC_d \tag{2.2}$$

where D_A is the drag force in N, V is the speed of the car in kilometers per hour, and AC_d is the drag area in square meters. The power consumed by aerodynamics (P_A) is the drag force multiplied by the velocity of the car as shown in Eq. 2.3.

$$P_A = (0.5)\rho V^3AC_d \tag{2.3}$$

Most of the modeling in this chapter involves balancing the power used by the car with the power provided to the car, and it is helpful to have power equations using both metric and U.S. customary sets of units as shown in Eqs. 2.4 and 2.5.

$$P_A = (0.0125)V^3AC_d \tag{2.4}$$

where P_A is the aerodynamic power in W, V is the velocity in kilometers per hour, and AC_d is the drag area in square meters.

$$P_A = (0.0523)V^3AC_d \tag{2.5}$$

where P_A is the aerodynamic power in W, V is the velocity in miles per hour, and AC_d is the drag area in square meters.

Another useful term in modeling energy balance is the energy used per kilometer (EPK). The efficiency of the car is commonly measured in watt-hours per kilometer traveled, as shown in Eq. 2.6.

$$EPK_A = (0.0125)V^2AC_d \tag{2.6}$$

The density of air varies with altitude. The above equations for aerodynamic drag were derived assuming a density of $1.17\ kg/m^3$. The actual density of air varies with altitude approximately according to Eq. 2.7 [2-8].

$$\rho = \left(-3.64\times10^{-14}\right)h^3 + \left(3.88\times10^{-9}\right)h^2 - \left(1.18\times10^{-4}\right)h + 1.17 \tag{2.7}$$

where ρ is the density of air in kilograms per cubic meter and h is the height above sea level in meters. The drag force D_A, power P_A, and energy per kilometer EPK_A all vary linearly with the density of air, so corrections can be made for altitude in the above equations by multiplying by the ratio of the actual density to the 1.17 used in deriving the equations, that is, multiplying by $(\rho/1.17)$.

C. Rolling Resistance

Rolling resistance accounts for most of the resistive drag force on the car at low speeds and a significant portion at high speeds. Rolling resistance is directly proportional to the weight of the car, and increases linearly with velocity. The rolling resistance is also dependent on the pavement condition, with rough pavement yielding significantly higher rolling resistance than smooth pavement. Rolling resistance is highly dependent on the tires selected. The energy is dissipated primarily by flexing the sidewalls and treads of the tires as they roll. Thin, high-pressure tires have lower rolling resistance than thick, low-pressure tires. The two companies that have designed tires specifically for solar car racing are Michelin and Bridgestone.

There is no standard test method used by tire manufacturers for measuring rolling resistance, and it is difficult to get information on how the rolling resistance varies with velocity of the car. The following model was based on

empirical tests on passenger tires [2-9]. Equation 2.8 is an empirical approximation of how rolling resistance varies with speed of the vehicle.

$$D_R = C_{rr}\left[1+\frac{V}{161}\right]W \qquad (2.8)$$

where D_R is the drag force in N, C_{rr} is the rolling resistance coefficient, V is the velocity in kilometers per hour, and W is the weight of the car in N. Similar results were obtained by the General Motors (GM) Sunraycer team in testing bicycle tires [2-10].

The speed dependence is largely dependent on the aerodynamics of the wheel and Eq. 2.8 overestimates the drag for aerodynamic wheel designs. Making the wheel more aerodynamic can reduce the rolling resistance significantly at high speeds. Tire pressure is generally 550–850 KPa (80–120 psi). If the Bridgestone or Michelin tires are used, then it is reasonable to assume that the rolling resistance coefficient is approximately 0.005 on smooth roads and 0.006 on rough roads. For road racing, the author's experience is that an average value of $C_{rr} = 0.0055$ has worked well in modeling the performance of the solar cars. Lower values for the rolling resistance coefficients have been reported when testing the tires rolling on smooth steel drums, but those are probably unrealistic for tires rolling on the road. A rough road causes more flexing of the rubber than a smooth road, which increases rolling resistance. On a hot summer day the asphalt can stick to the tires and further increase the rolling resistance. The power consumed by rolling resistance is given by Eq. 2.9.

$$P_R = (0.278)C_{rr}\left[1+\frac{V}{161}\right]WV \qquad (2.9)$$

where P_R is the rolling resistance power in W, W is the weight in newtons, and V is the speed in kilometers per hour. In U.S. customary units, the power equation is given by Eq. 2.10.

$$P_R = (1.99)C_{rr}\left[1+\frac{V}{100}\right]WV \qquad (2.10)$$

where P_R is the rolling resistance power in W, W is the weight in pounds, and V is the speed in miles per hour. The rolling resistance energy used per kilometer traveled is given by Eq. 2.11.

$$EPK_R = C_{rr}\left[1+\frac{V}{161}\right]W \qquad (2.11)$$

where EPK_R is the watt-hours of energy used per kilometer traveled, V is the speed in kilometers per hour, and W is the weight in newtons.

D. Homework Assignment

Assume that the array provides 700 W average power while driving (i.e., do not take into account that the solar energy varies with time of day). There are 4500 W-h of energy available in the battery pack, and no power is lost in the mechanical and electrical systems. Assume that the car weighs 3790 N (850 lb), that the low-speed rolling resistance coefficient of the tires is 0.0055, and that the drag area of the car is 0.2 m^2. These model parameters correspond to an average stock-class car.

1. If the car travels at 90 km/h (55.9 mph), how long will it take before it runs out of energy, and how far will it be able to go at this speed before running out of energy? [2.4 h, 215 km (130 mi)]

2. If the car travels at 70 km/h, how long and how far can it go? [6.38 h, 447 km (264 mi)]

3. If the distance to be traveled for the day is 300 km, what speed should be selected to get there as fast as possible without running out of energy and how long will it take for the car to travel the 300 mi distance? [3.79 h, 79.2 km/h (47.4 mph)]

4. The calculations above were based on an average stock-class car and performance can be improved by getting better solar cells and batteries, or by improving other aspects of the car. Assume that the car is to drive for 8 h/day and the goal is to go as far as possible on the available energy. Change only one parameter at a time in the analysis. (*Explanation:* This

is an important exercise. The goal for most solar car races is to go as far as possible each day. The purpose of this exercise is to begin to understand quantitatively how changing car parameters such as solar array power or aerodynamic drag affects the performance of the car in a race. There are many cases where this type of analysis will be used in evaluating design trade-offs. For example, one body design may produce more solar array power, while a different design has a lower aerodynamic drag. The body design that makes the car perform better, i.e., able to go further in a day, should be selected. There are many other cases where adding weight to the car can improve aerodynamics, increase solar array power, increase battery capacity, or reduce parasitic losses. Cost and manufacturing can also be issues in selecting the design, but in many cases the primary consideration is performance of the car.)

a. Calculate how far the stock-class car above can go in a day. [528 km (328 mi)]

b. Decrease drag area to 0.1 m^2. [624 km (387 mi), Δ = 96 km (59 mi)]

c. Increase array power by 40%. [577 km (358 mi), Δ = 49 km (30 mi)]

d. High-performance batteries increase battery capacity to 5000 W-h and decrease the weight of the vehicle by 1115 N (250 lb). [570 km (354 mi), Δ = 42 km (26 mi)]

e. Decrease weight by 250 N (56 lb). [535 km (333 mi), Δ = 7 km (5 mi)]

f. Decrease rolling resistance coefficient to 0.005. [538 km (334 mi), Δ = 10 km (6 mi)]

5. *Thought Question:* Decreasing aerodynamic drag is labor intensive, but requires very little money. The same is true of reducing the weight of the car by lightening the body, chassis, and other components. Solar cells that are 30% more powerful than the terrestrial-grade cells will cost an extra $30,000, cells that are 50% better than terrestrial-grade will cost an extra $75,000, cells that are 80% better will cost an extra $200,000, and cells that are twice as good will cost an extra $1,000,000. The high-performance batteries will cost about $10,000. Recognizing the resources

and fund-raising ability of the team, where should the effort be focused? What class should the team compete in, stock or open?

E. Solar Array Power

For most races the maximum allowable size for the array is approximately 8 m^2 of solar array area. Terrestrial-grade silicon cells are about 14.5% efficient at converting sunlight to electricity and space-grade cells can be as high as 28% efficient as of the writing of this document. Solar cell efficiency seems to increase every year. At midday in the summer the sunlight intensity is about 1000 W/m^2 at sea level. The maximum solar array power varies from 1160 W for the terrestrial-grade cells to 2240 W for the best space-grade cells. Alpha Centauri, the solar car team from Holland, had a solar array that produced 2200 W peak power in the 2001 World Solar Challenge. Many teams have made terrestrial-grade silicon arrays that produced over 1100 W peak power. As a first approximation, multiplying the 8000 W of power striking the solar array by the efficiency of the solar cells yields a good approximation of the peak power the solar array can produce.

Sunlight intensity increases with altitude. There have been several races across the United States, and all teams noticed a 30% improvement in solar array power (over what the array would produce at sea level) when the car was at an altitude of 1800–2100 m (6000–7000 ft) above sea level. Solar intensity does increase with altitude, but it does not increase by 30%. However, in Sunrayces 1995 and 1997, as teams went across Kansas and the altitude increased from about 300 m on the eastern side to 1200 m on the western side, all teams experienced a marked increase in the power of their solar array. Solar arrays that produced 1000 W in eastern Kansas were producing over 1200 W in western Kansas. This was noticed again in the American Solar Challenge 2001 as teams went across Oklahoma, Texas, New Mexico, and Arizona. The power of the solar array would increase and decrease significantly as the altitude changed.

As a first attempt to explain the increase in solar array power with altitude, a model was developed by assuming that the sunlight intensity varied linearly according to the amount of atmosphere it had to travel through. The solar intensity above the atmosphere and at sea level is known, and it was assumed

that the intensity would vary linearly between these values according to the percentage of atmosphere above the altitude in question. The equation for density of air was integrated to develop an expression for the percentage of the atmosphere above any altitude, and an expression was developed to predict the solar intensity. Unfortunately this model predicts only a few percent increase in solar array power at 2000 m altitude. This approach does not yield a model that accurately predicts what is observed, so the model was discarded. Without more information to make a better model, the best assumption at this point in time is that the array power increases about 5% with every 300 m (1000 ft) increase in altitude. Intensity also varies with clouds and haze.

Solar cell efficiency varies with temperature. It is desirable to keep the cells cool. For silicon cells a rule of thumb is that the power of the array increases 0.5% for every 1°C decrease in temperature. Teams usually spray a distilled water mist on the array to cool the silicon cells. The water slightly attenuates the intensity of the sunlight striking the cells, but the cooling is a larger effect. For silicon cells the water mist will increase the array power by 20% on a hot sunny day. Gallium arsenide (GaAs) cells are not as sensitive to temperature increase, which is one of their advantages. The general consensus is that there is no net benefit to spraying a GaAs array with distilled water, but this has not been thoroughly tested.

The first part of the model development for the solar array is to study how the array power varies with respect to the angle between the array and the sunlight. For angles of misalignment with the sun, the power varies with cos θ of the angle of misalignment, as illustrated in Fig. 2.1. This approximation works well up to angles near 90°, at which point the approximation under predicts array output. For large angles of inclination, the light that is reflected off of surrounding objects becomes significant. For $\theta = 90°$, the array may still gather as much as 10% of its maximum power P_{max}, depending on how reflective the surrounding objects are. For this model, it will be assumed that power varies in accordance with Eq. 2.12 [2-11].

$$P_{Array} = P_{max}\cos(\theta) \qquad (2.12)$$

where P_{Array} is the power produced by the solar array and P_{max} is the power the array produces when aligned with the sun. The power the solar array can

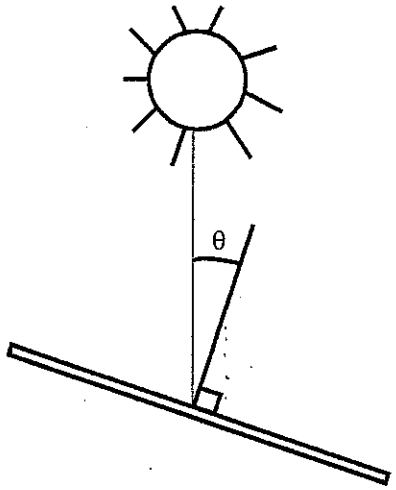

Fig. 2.1 Variation of solar array power with alignment angle.

produce also varies with the time of day. Solar energy is absorbed by the atmosphere, and the further the sunlight must travel through the atmosphere, the more energy is absorbed. Early theories used by solar car teams were that the intensity of the sunlight was proportional to the distance the light traveled through the atmosphere, but testing has shown that this is not a good approximation. When the sun is at an angle of 30° with the horizon, the sunlight must pass through twice as much atmosphere as when it is straight overhead. Testing has shown that the solar array will produce almost as much power with the sun at 30° to the horizon as it does when the sun is straight overhead, provided the array is aligned with the sunlight. Early in the morning, as the sun peeks over the horizon the solar array will not produce nearly as much power as at midday, but the power comes up quickly as the sun rises. An empirical model was developed from testing a nine-cell terrestrial-grade silicon array panel at the University of Missouri-Rolla. This model is probably a good estimate for solar cars with terrestrial-grade silicon arrays. It may be a good estimate for other types of solar arrays, but more testing needs to be done to be sure. If φ is the angle between the sunlight and normal to the ground, as illustrated in Fig. 2.2, then the power that the solar array will produce when aligned with the sun is given approximately by Eq. 2.13.

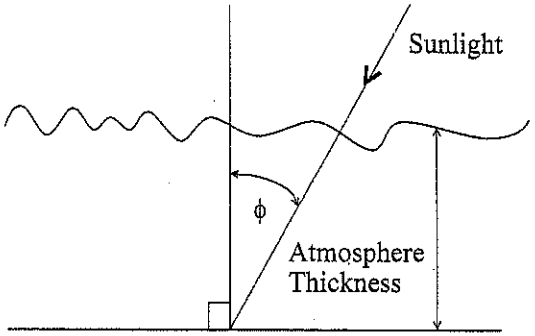

Fig. 2.2 Sunlight latitude angle.

$$\text{Power} = P_{max}\left[\cos(\phi)\right]^{0.3} \tag{2.13}$$

P_{max} is defined as the power the solar array produces at high noon, so an array will have a slightly different P_{max} at different times of the year. The angle ϕ depends on the time of year, time of day, and the latitude of the race. The next step in the modeling effort is to develop an approximate relation for the value of ϕ. The high noon value of ϕ depends only on the time of year and the latitude location of the car. On June 22 the sun is directly over the Tropic of Cancer, 23.5° north, and on December 21 it is directly over the Tropic of Capricorn, 23.5° south. The location of the sun varies approximately according to a sine function between the two tropic lines as shown in Eq. 2.14.

$$\text{Sun latitude location} = 23.5\sin\left(\frac{180(D-82)}{182.5}\right) \tag{2.14}$$

where D is the day of the year. A positive angle means the sun is in the Northern Hemisphere and a negative angle means it is in the Southern Hemisphere. The difference between the latitude location of the car and the location of the sun is the high noon sun angle. As an example suppose that the car is at latitude 37° north. The high noon sun angle on June 22 (day 173) is 13.5°, on May 20 it is 17.2°, and on December 5 it is 59.5°.

Extended after 24 around $\phi_N \approx 22°$ (High noon sun angle)

The angle ϕ varies with the time of day. It is possible to develop a geocentric relationship for ϕ based on the latitude and longitude location, day of the year, and time zone, but this relationship is difficult to work with because sunrise and sunset times vary by about an hour within a time zone. A better approach is to find the high noon sun angle and the sunrise and sunset times for the location of the race. If the race does not start and end in the same place, find the sunrise time for where the race starts and the sunset time for where the race ends and use an average high noon sun angle for the day. The angle ϕ can then be determined from Eq. 2.15.

$$\phi = 90° - (90° - \phi_N)\sin\left(\frac{180(T-SR)}{DL}\right) \tag{2.15}$$

where ϕ_N is the high noon sun angle, T is the time of day in military digital, SR is the sunrise time in military digital, and DL is the day length in military digital time. For computation purposes all of the times in the equations are defined in military digital, so that 1:30 P.M. = 13.5, for example. Combining the ideas of the sun being misaligned with the solar array by an angle θ and the sun being at an angle ϕ with a normal vector to the ground, the power that the solar array will produce is given by Eq. 2.16.

$$P_{Array} = P_{max}\cos(\theta)\left[\cos(\phi)\right]^{0.3} \tag{2.16}$$

When driving it is best to assume that the array is parallel to the ground so that $\theta = \phi$. On the array stand the solar array is aligned with the sun such that $\theta = 0$. The P_{max} term in the equation is the power the solar array would produce at high noon with the array perfectly aligned with the sun.

As an example, assume that the test is performed at a latitude of 36° north in late June so that the sun is near the Tropic of Cancer at 23.5° north. Assume that the solar array would produce 1000 W power when aimed directly at the sun at the high noon sun time. Assume that sunrise is at 5:23 A.M. and sunset is 8:47 P.M. Develop a model for the power the solar array would produce while driving and charging on the array stand.

1. The high noon sun angle is 36° – 23.5° = 12.5°.
2. P_{max} = 1000 W.
3. SR = 5.3833 and DL = 20.7833 – 5.3833 = 15.4 h.

Equation 2.17 shows how the angle between the sun and the ground varies with time of day. Equations 2.18 and 2.19 show how the array power varies with time of day while driving or on the charging stand. The solar array will produce more power on the charging stand because it will be aligned with the sun. The difference is a factor of cos (ϕ). Figure 2.3 shows how the solar array power varies throughout the day for the example above.

$$\phi = 90° - (77.5°)\sin\left(\frac{180(T-5.3833)}{15.4}\right) \qquad (2.17)$$

$$\text{Driving power} = (1000\ \text{W})\left[\cos(\phi)\right]^{1.3} \qquad (2.18)$$

$$\text{Charging power} = (1000\ \text{W})\left[\cos(\phi)\right]^{0.3} \qquad (2.19)$$

Around midday the difference between driving and charging on the array stand is less than 50 W or 5%. At 8:00 A.M. or 6:00 P.M. the difference is approximately 300 W or 30%. Early in the morning and late in the evening the difference is even greater, but the races are usually run between 8:00 A.M. and 6:00 P.M. The example is for a very long day, 15.4 h. There are examples of short days where it may appear to be advantageous to start late and finish early, reducing the driving time over what is allowed. In such cases, the solar array will gather more solar energy, but the car will have to drive faster to cover the same distance, which causes it to use more energy per kilometer (EPK) traveled. In general, it is best to use the full allowable driving time and go slower, but there are exceptions to this rule, especially when the day length is 12 h or less.

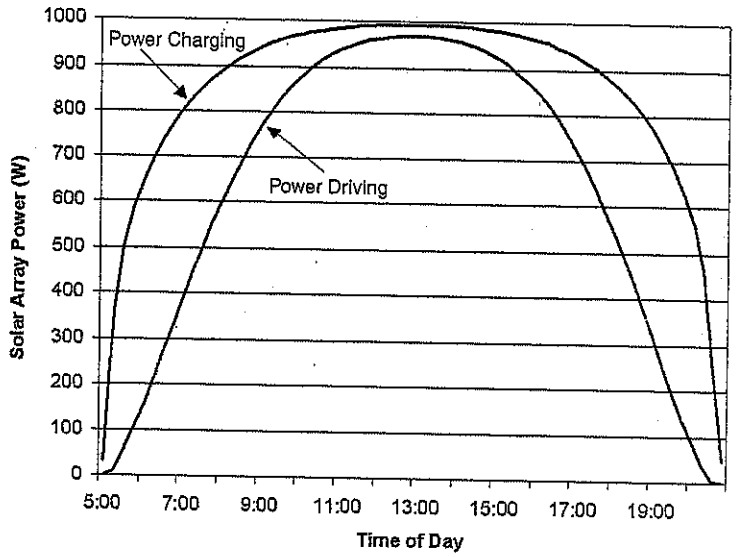

Fig. 2.3 Solar array power and charging on the array stand.

F. Battery Efficiency

In general, batteries are significantly less than 100% efficient in storing energy. Batteries heat up when charging and discharging, converting a significant portion of the energy to heat. As a "rule of thumb," if there is less than 25% difference in array power between putting the array on the charging stand and driving, then it is more energy efficient to be driving. When driving, the power is used directly from the array, avoiding the penalty of storing and retrieving from the batteries.

Most solar cars are equipped with a regenerative braking system that uses the motor to convert the kinetic energy of the car into electric energy, which is then stored in the batteries. Regenerative braking is considerably less than 100% efficient at converting kinetic energy to electrical energy. The energy from regenerative braking is stored in the batteries, which are inefficient. Regenerative braking is usually a power drain on the open road. It is more

energy efficient to coast down the hills and use the gravitational energy directly. Regenerative braking is a benefit in town where the car must stop. At least some of the energy is recovered in the batteries rather than converting it all to heat in the brake disks.

A typical solar car battery pack can deliver 4500 W-h of useful energy at a rate of 1500 W. If the power is drawn out more slowly than this, the batteries can provide more total energy (more than 4500 W-h), and if the power is drawn out faster they provide less total energy (less than 4500 W-h). All battery systems are most efficient when the power is drawn out slowly. Most of the modeling and work has been done on lead-acid batteries and it is not known at this time if the same types of models will work well for the lithium-ion or lithium-polymer batteries that are currently being used on the fastest cars. The Peukert equation, shown in Eq. 2.20, was developed for lead-acid batteries.

$$\text{Energy capacity} = \frac{C}{I^{(n-1)}} \tag{2.20}$$

where C is a constant proportional to the size of the battery, I is the current draw, and n is the Peukert number for the battery. For lead-acid batteries it has been shown that the Peukert number is approximately 1.2 for the most efficient models. The ideal battery would have a Peukert number of 1.0, which would mean that the battery capacity is the same at any current draw. The lithium-ion batteries have a Peukert number between 1.05 and 1.1, which makes them more efficient than the lead-acid batteries. Nickel-metal-hydride batteries are less efficient than lead-acid batteries. Nickel-metal-hydride batteries are lighter in weight, which makes the car use less energy in rolling resistance, but the batteries consume more energy.

In the power management model being developed in this chapter it is more convenient to work with the power being drawn out of the batteries (P) than with the current. System voltage is approximately constant, so the current draw is approximately proportional to the power draw. Equation 2.21 is an approximately equivalent expression of the Peukert equation.

$$\text{Energy capacity} = \frac{C}{P^{(n-1)}} \tag{2.21}$$

where C is a constant proportional to the size of the battery, P is the power draw, and n is the Peukert number for the battery. If the battery capacity is known for two different power draws, then the Peukert model can be fit to the battery system. The Peukert model is best when estimating battery efficiency between the two power draws used in developing the model. It is less accurate when extrapolating outside of the data points, so it is best to use a relatively low and high power draw in developing the model. Data for a set of Delphi lead-acid batteries that many teams have used in the past showed that a typical battery pack has 4500 W-h capacity when providing 1500 W power, and has 3300 W-h capacity when providing 6000 W power. Using these values, the Peukert model for the battery pack is shown in Eq. 2.22.

$$\text{Typical lead-acid capacity} = \frac{23{,}100}{P^{(1.22-1)}} \text{ W-h} \tag{2.22}$$

The Peukert model is a respected way to model battery efficiency, but it is accurate only over a range. The equation greatly overestimates the battery capacity for low power draws. As an example, for a 1-W power draw the equation estimates the battery capacity as 23,100 W-h, which is ridiculous. An estimate will need to be made of the actual low-power battery capacity, which might be 6000 W-h for this example, and place a cap on how high the Peukert equation can estimate battery capacity.

The lithium-ion batteries will have a lower Peukert number. Suppose the battery capacity is 4500 W-h at 1500 W power draw and the Peukert number is 1.08. The model of battery capacity for the lithium-ion batteries is shown in Eq. 2.23.

$$\text{Typical lithium-ion capacity} = \frac{8078}{P^{(1.08-1)}} \text{ W-h} \tag{2.23}$$

The battery capacity equation will be useful when modeling a constant power draw on the battery pack, because it allows for calculation of the total amount of energy available from the pack. The equation will also be used in modeling the car traveling through hilly terrain. For hilly terrain it will be assumed the power draw is constant over a small time period T and the percent decrease

in battery capacity will be calculated for the small time interval. The battery pack starts with 100% capacity, and at 0% capacity the batteries are dead. Figure 2.4 illustrates how battery capacity varies with power draw for the typical lead-acid and lithium-ion battery packs. For both battery systems it was assumed that the maximum capacity for low power usage was 6000 W-h.

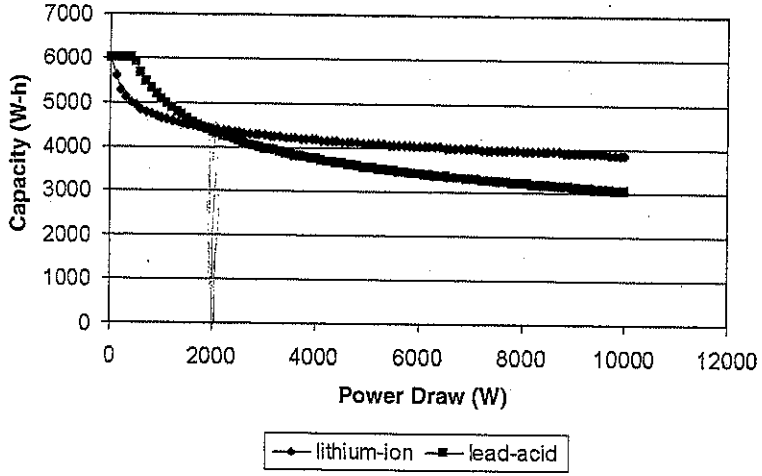

Fig. 2.4 Battery capacity versus power draw.

At high power draws, the lithium-ion batteries will have more usable capacity than the lead-acid batteries. Lithium-ion batteries are also considerably lighter in weight and reduce the rolling resistance of the car, so it is difficult to imagine a situation where the lead-acid batteries are an advantage. The lead-acid batteries do provide more energy than lithium-ion batteries for low current draws that might happen during a cloudy, rainy race, and it is possible that under those conditions there might be an advantage to using the lead-acid batteries.

If a power P is drawn out of the batteries for a time T, then the percentage of the total battery pack that was used up during that period (%C) is given by Eq. 2.24.

$$\%C = \frac{PT}{\left(\frac{C}{P^{(n-1)}}\right)} \times 100\% \qquad (2.24)$$

The denominator in Eq. 2.24 is the total battery capacity at the power draw P and the numerator is the energy used during the time period. This equation is useful when the power draw is not constant, as would be the case for virtually all races. Power is assumed to be constant over a small time period, and the percentage of the battery pack is added up for all the time periods. Once 100% of the battery capacity has been used, the batteries are dead and the car must stop.

G. Motor-Drive System

Solar cars use direct current (dc) brushless electric motors. They are the most efficient motors for the power range required for solar cars. A properly sized motor can be 95% efficient when operating at its maximum revolutions per minute (RPM), and at two-thirds of its rated output. The efficiency decreases at lower revolutions per minute and for very low power outputs. It is very important to match motor output and revolutions per minute to the requirements of the car. An improperly sized motor will be inefficient.

With hills and stops the motor is not always operating at maximum efficiency. The average efficiency of the motor is likely to be in the 90–95% range, depending on how good the motor is and how well it is matched to the power requirements of the car. A single reduction belt or chain drive will take an additional 3–5% of the power, making the motor-drive efficiency in the 85–92% range. For modeling purposes, reasonable assumptions are 94% efficiency for a hub motor and 90% efficiency for a single reduction drive.

H. Parasitic Losses

There are many electrical parasitic losses. The major ones are the battery fan and power converters, which must be on when charging the batteries or driving, that is, all the time. The motor fan must be on when driving, and the turn

signals and brake lights must be used when driving. There are a multitude of connectors, wires, and so forth that all absorb some power.

Mechanical systems absorb power too, even when properly designed. Shock absorbers are an example. Improper design of any system can rob a lot of power from the car in parasitic losses. For modeling purposes, a reasonable assumption for a well-designed car is 10 W of power loss when charging and 30 W when driving.

I. Gravitational Energy

When going uphill, the gravitational resistive force is increased, and when going downhill it is decreased. The gravitational force on the car is given by Eq. 2.25.

$$F_G = W \sin(\theta_G) \tag{2.25}$$

where F_G is the resistive force on the car, W is the weight of the car, and θ_G is the angle of the hill. If the batteries and the regenerative braking systems were 100% efficient, then hills would have only a minor effect on the efficiency of the car. When going uphill, the car draws large currents from the battery, which causes the batteries to operate at a lower efficiency, and reduces the energy efficiency of the car. When going down a steep hill, the car will probably have to use the regenerative braking system to keep the car from exceeding the speed limit. Regenerative braking is better than hitting the brakes, but because the regenerative braking system is inefficient, and the energy generated is stored in the batteries which are inefficient, the car is inefficient when going downhill. Usually the best strategy is to coast downhill as much as possible, but the race rules or speed zones may limit the top speed of the car. The gravitational power is given by Eq. 2.26.

$$P_G = (0.278)WV \sin(\theta_G) \tag{2.26}$$

where P_G is the gravitational power in W, W is the vehicle weight in newtons, V is the speed in kilometers per hour, and θ_G is the angle of the road. In U.S. customary units, the gravitational power is given by Eq. 2.27.

$$P_G = (1.99)WV \sin(\theta_G) \tag{2.27}$$

where P_G is the gravitational power in W, W is the vehicle weight in pounds, V is the speed in miles per hour and θ_G is the angle of the road. The energy used per kilometer (EPK_G) traveled is given by Eq. 2.28.

$$EPK_G = W \sin(\theta_G) \tag{2.28}$$

J. Kinetic Energy

A good strategy for driving in hilly terrain is to allow the car to slow down when going uphill, and speed up when going downhill. Some of the kinetic energy of the car is used to overcome the gravitational energy in climbing the hill, which reduces the power draw from the batteries and allows them to operate at a higher efficiency. Some of the gravitational energy is converted to kinetic energy when going downhill to avoid using the regenerative braking, which is inefficient. Energy can be converted from gravitational to kinetic and back with near 100% efficiency, so this strategy works well in hilly terrain.

Kinetic energy can become very important in track racing too, if there are corners on the track that require the car to slow down. The car might have adequate energy and efficiency to cruise at 40 mph, but there may be corners on the track that are so sharp that the car must slow to 25 mph to avoid going out of control. Track racing with sharp corners is a difficult problem to solve. Slowing for the corners and accelerating out of the corners force the car to operate in an inefficient mode. High-speed cornering increases the rolling resistance of the car, and the thin-walled solar car tires will not stand up to high-speed cornering very well. Track racing is discussed later in the chapter.

K. Modeling: Summary

1. Power/energy to push the car down the road is provided by the solar array and the batteries.

2. Power/energy is consumed by aerodynamic drag, rolling resistance, motor-drive efficiency, and parasitic losses.

3. Gravitational and kinetic power/energy can either provide or consume power, depending on whether the car is traveling uphill or downhill and whether it is speeding up or slowing down.

An energy balance approach is used in developing the model. The power provided by the solar array and batteries must equal the power consumed by aerodynamic drag, rolling resistance, motor-drive system, parasitic losses, gravitational energy, and kinetic energy. The best way to approach this is to first calculate the required power to overcome the aerodynamic drag, rolling resistance, motor-drive efficiency, and parasitic losses. Subtract the power provided by the solar array. Add or subtract the power because of gravitational energy and kinetic energy, depending on whether the car is going uphill or downhill, slowing down or speeding up. The balance of the power must come from the batteries. This is illustrated in the following example.

Example: Assume the car is to run around a flat oval track at 80 km/h and go as far as possible in an 8-h period. Assume that the curves are wide and there is no reason to slow down and that the car never stops. Assume the car travels at 80 km/h until the batteries are dead or until the 8-h period is up. Assume a drag area of 0.12 m^2, a weight of 2700 N, a rolling resistance coefficient of 0.0055, a motor-drive efficiency of 94%, and parasitic losses of 30 W. Assume that the solar array produces a maximum power of 1300 W when directed at the sun and that the batteries used are lithium-ion with a capacity determined by Eq. 2.23. Use the model to calculate how far the car can go in an 8-h period. The power consumed by aerodynamics is given in Eq. 2.29.

$$P_A = (0.0125)(80)^3(0.12) = 768 \text{ W} \tag{2.29}$$

The best cars have a drag area AC_d in the range of 0.10–0.15 m^2, so this would be a typical aerodynamic drag loss for a competitive car. The power consumed by rolling resistance is given by Eq. 2.30.

$$P_R = (0.278)(0.0055)\left[1+\frac{80}{161}\right](2700)(80) = 494 \text{ W} \tag{2.30}$$

The best open-class cars weigh between 2400 and 2900 N, so once again this is a competitive weight for a car. The motor-drive efficiency is assumed to be 94%, which is typical for a hub motor design. Parasitic losses are assumed to be 30 W while driving, which is a typical value for a well-designed car. There is no gravitational power associated with this example because the track is assumed to be flat. There is no kinetic power because the car travels at constant speed.

The power to overcome aerodynamic drag and rolling resistance must go through the motor, so those powers must be divided by the motor-drive efficiency. Parasitic losses do not go through the motor. The total power required to push the car along at 80 km/h is given by Eq. 2.31.

$$P_{Total} = \frac{768+494}{0.94} + 30 = 1373 \text{ W} \tag{2.31}$$

To calculate the power produced by the solar array it is necessary to know the time of day the race starts, the sunrise and sunset times, the high noon sun angle, the maximum power the solar array can produce, the elevation above sea level, and the atmospheric conditions. For this example, assume that the 8 h of driving starts at 9:00 A.M. and stops at 5:00 P.M. Assume a sunny day, and that the track is at sea level. Assume sunrise is at 6:37 A.M. and sunset is at 7:14 P.M., that the high noon sun angle is 22° and the maximum solar array power is 1300 W. A maximum output of 1300 W is typical for a low-cost space-grade solar array with approximately 18% efficient cells. Equations 2.17 and 2.18 can be used to estimate the power produced by the solar array at different times during the day, as shown in Eqs. 2.32 and 2.33.

$$\phi = 90° - (68°)\sin\left(\frac{180(T-6.6167)}{12.6167}\right) \tag{2.32}$$

$$P_{Array} = (1300 \text{ W})\left(\cos(\phi)\right)^{0.3} \tag{2.33}$$

For this example the battery pack is assumed to be lithium-ion, which has a Peukert number of 1.08 and a capacity of 4500 W-h when the power is drawn

out at 1500 W. The constant C in the Peukert equation is 8078, as was illustrated in Eq. 2.23.

The best way to approach this problem is to set up a spreadsheet for the race. At the top of the spreadsheet define the parameters used in the model in such a way that they can be varied. This allows the parameters to be varied in a convenient manner to study the "what if" questions that inevitably come up with a modeling exercise. Table 2.1 shows the left half of the spreadsheet. The spreadsheet is too wide to fit on one page. Explanations for each column in the spreadsheet follow.

Columns 1 and 2. The day is divided into time periods of 30 min in the example. Solar array power varies with time of day, but it does not vary greatly during a 30-min period. The military digital time in the center of the time period is used to calculate the average solar array power for the time period.

Columns 3 and 4. The angle ϕ is calculated using the sunrise and sunset times and the high noon sun angle of 22°. This represents the angle between the sunlight and normal to the ground, and is used to calculate the solar array power. Because the car will be driving around the track, it was assumed that the solar array is parallel to the ground, so the angle of misalignment between the solar array and the sun is ϕ.

Columns 5 and 6. The equations for calculating aerodynamic and rolling resistance are used to fill these columns. Because the values are the same for all times during the day, it is tempting to put these values at the top of the spreadsheet and not make a column for them. In later examples, as the models become more sophisticated, the speed will vary with time of day and the aerodynamic and rolling resistance values will not be constant.

Columns 7 and 8. The total power required to push the car along at 80 km/h is 1372.9 W for this car. Some of the power is provided by the solar array and the rest must be provided by the batteries. The power being drawn out of the batteries gradually runs them down, and when the batteries are dead the car must stop.

TABLE 2.1
EXAMPLE SPREADSHEET

Speed (km/h)	80		Sunrise	6.6167		Peukert No.	1.08
Weight (N)	2700		Day Length	12.6167		Battery C	8078
AC_d (m^2)	0.12		Noon Angle	22			
C_{rr}	0.0055		P_{max}	1300			
Motor Eff.	0.94						
Parasitic Loss	30						
Column 1	Column 2	Column 3	Column 4	Column 5	Column 6	Column 7	Column 8
Time Period	**Military Time**	**Sun Angle ϕ**	**Array Power**	**Aero Power**	**Rolling Power**	**Total Power**	**Battery Power**
9:00–9:30	9.25	48.54	760.6	768.0	494.4	1372.9	612.3
9:30–10:00	9.75	42.17	880.7	768.0	494.4	1372.9	492.2
10:00–10:30	10.25	36.54	978.2	768.0	494.4	1372.9	394.8
10:30–11:00	10.75	31.73	1053.3	768.0	494.4	1372.9	319.7
11:00–11:30	11.25	27.83	1108.0	768.0	494.4	1372.9	264.9
11:30–12:00	11.75	24.89	1145.3	768.0	494.4	1372.9	227.7
12:00–12:30	12.25	22.96	1167.8	768.0	494.4	1372.9	205.2
12:30–1:00	12.75	22.06	1177.6	768.0	494.4	1372.9	195.3
1:00–1:30	13.25	22.22	1175.9	768.0	494.4	1372.9	197.1
1:30–2:00	13.75	23.43	1162.4	768.0	494.4	1372.9	210.5
2:00–2:30	14.25	25.67	1135.8	768.0	494.4	1372.9	237.2
2:30–3:00	14.75	28.90	1093.6	768.0	494.4	1372.9	279.4
3:00–3:30	15.25	33.08	1033.0	768.0	494.4	1372.9	340.0
3:30–4:00	15.75	38.14	951.4	768.0	494.4	1372.9	421.6
4:00–4:30	16.25	44.00	847.1	768.0	494.4	1372.9	525.9
4:30–5:00	16.75	50.58	720.4	768.0	494.4	1372.9	652.6

$P = P_{array}(\cos\phi)^{1.5}$ (Parallel panels close to the ground)

The remainder of the spreadsheet is presented in Table 2.2. The battery power column from Table 2.1 is repeated because the remaining columns track the battery capacity.

TABLE 2.2
REMAINDER OF THE EXAMPLE SPREADSHEET

Column 8	Column 9	Column 10	Column 11	Column 12
Battery Power	Battery Capacity 1	Battery Capacity 2	Battery % Charge	Total % Charge
612.3	4834.4	4834.4	6.33	6.33
492.2	4919.6	4919.6	5.00	11.34
394.8	5007.2	5007.2	3.94	15.28
319.7	5092.4	5092.4	3.14	18.42
264.9	5169.6	5169.6	2.56	20.98
227.7	5232.6	5232.6	2.18	23.15
205.2	5276.3	5276.3	1.94	25.10
195.3	5297.1	5297.1	1.84	26.94
197.1	5293.4	5293.4	1.86	28.80
210.5	5265.5	5265.5	2.00	30.80
237.2	5215.5	5215.5	2.27	33.08
279.4	5147.7	5147.7	2.71	35.79
340.0	5067.5	5067.5	3.35	39.15
421.6	4981.0	4981.0	4.23	43.38
525.9	4893.6	4893.6	5.37	48.75
652.6	4809.9	4809.9	6.78	55.53

Column 9. The second column in Table 2.2 is the ninth column in the spreadsheet table. This column uses the Peukert equation to calculate the battery capacity at the power draw from the battery in column 8.

Column 10. The Peukert equation overestimates the battery capacity at low power draws. This column was made using a logic statement (if-then) to limit the battery capacity to 6000 W-h. In this example the Peukert equation

never estimated battery capacity above 6000 W-h, so the column is identical to column 9. If lead-acid batteries numbers are used with Peukert numbers of 1.22 and 23100, then this column becomes active most of the day.

Columns 11 and 12. In column 11 the power drawn out of the batteries in column 8 is multiplied by the half-hour time period to yield the energy drawn out of the batteries. This energy is divided by the battery capacity at that power draw in column 10 and multiplied by 100% to yield the percentage of the battery pack used during each time period. Column 12 totals the percentage of the battery pack used during the day. In this example 55.53% of the battery pack was used during the day and the car traveled 640 km (8 h at 80 km/h).

Once the spreadsheet is built it is possible to study how changing different things about the car affects the overall results. If this example is a 1-day race, then the team did not use good strategy because they ended up with quite a bit of charge left in the batteries at the end of the day. The speed value in the spreadsheet can be changed until 100% of the battery pack is used by the end of the day. The solution technique is to guess speed values until the desired objective is obtained. For this example 86 km/h uses 100% of the battery capacity by the end of the day. If it is a 1-day race, the best strategy would be to run 86 km/h, which would allow the team to go 688 km during the day and completely use all of the battery capacity.

If this were a multiday race, as most solar car races are, then there are cases when it is a better strategy not to run the batteries all the way down the first day. It is often best to reserve some battery capacity if the evening or next day is going to be cloudy. There will be a time period to charge the batteries with the array on the charging stand after the race period is over, which is 5:00 P.M. for this example. There will be more time to charge the next morning before the race starts at 9:00 A.M. If it is sunny, then the solar array will be able to completely recharge the batteries during the charging periods, and the best strategy is to run the batteries all the way down. If it is to be cloudy, then it may be advantageous to reserve some energy in the battery to have more for the next day. The team must try to use the best strategy for the entire race, not just for 1 day.

The spreadsheet can be used to analyze other issues about the race too. What if the team chooses to use lead-acid batteries that increase the weight by 1100 N and change the battery numbers to 1.22 and 23100? [82.7 km/h, 661.6 km] What if lead-acid batteries and a silicon array of 1000 W maximum power were used? [77.3 km/h, 618.4 km] What if the lithium-ion batteries are used with a 1600-W solar array? [91.1 km/h, 728.8 km] Many other issues can be addressed. The spreadsheet allows the team to study quantitatively how changing performance parameters of the car affects the overall performance. This allows the team to make informed decisions as to where to best focus the resources and human resources available to the team to create the best solar car possible with the resources available.

A problem will develop if too low a speed is chosen in the spreadsheet. In such cases, the solar array will produce more power than is required to push the solar car along, which means it is actually charging the batteries. This causes a negative number to be taken to a fractional power in the Peukert equation, which is not possible mathematically. It is possible to build more logic columns in the spreadsheet to fix this problem. The energy put back into the batteries is the product of power and time, but some of this energy will be converted to heat and lost, so a reasonable assumption must be made as to how much usable energy is put back into the batteries. This problem is amplified when driving in more realistic terrain, which is the topic of the next section. A slight downhill grade will almost always reduce the power consumption to the point that the solar array is charging the batteries, and a steep hill will put the car into regenerative braking mode, which also charges the batteries.

L. Homework Assignment

Develop the spreadsheet in the preceding example.

1. Suppose, using all the same assumptions as in the example that the car starts out going 105 km/h. What time of day and how far will the car go before the batteries are dead? [Batteries are dead a little past 11:30, 270 km (167.8 mi) if linear interpolation is used.]

2. Assume a partly to mostly cloudy day so that the car receives less than 100% of the power from the array that it would receive on a bright sunny day. Add a "cloudiness factor" to the spreadsheet and adjust the solar array power column. What speed should be selected to go as far as possible during the 8-h period for a 70% factor? [78.7 km/h] 50% factor? [73.0 km/h] 30% factor? [66.5 km/h]

3. Suppose there was essentially no energy in the battery pack at the start of the day, and the car had to run on solar power alone. How far could it go in the 8-h period, and what would the speed be in each time increment? [559 km total, speed for first 30-min interval is 60.96 km/h]

M. Hilly, More Realistic Terrain

To study hilly terrain, a data file must be developed that approximates the slope of the road (θ_G) along the race route. A data file was developed for this section of the book, and all of the examples and homework solutions are based on this data file, which can be obtained from the author. The data are modeled on the stretch of Highway 63 south from Rolla, Missouri, to Licking, Missouri, approximately 35 mi of data, and the sample can be repeated to achieve the desired distance of data. This is a relatively clean data set and is useful in illustrating the process of modeling a race along hilly terrain.

For a road race it is necessary to drive the race route and take global positioning system (GPS) readings, feeding them into a computer file. The latitude and longitude readings from the GPS are generally stable enough to be used to track distance along the race route. The altitude readings are generally unstable and must be filtered before they can be used. Just averaging blocks of 10, or even 20 data points is not enough to smooth the altitude data and make them representative of the road. The smoothing program needs to include logic statements that limit the grade of the road to a maximum value reasonable for the road. Interstate highways are usually limited to 4% grade, except in the mountains where the grades may be 6 or 7%. Secondary road grades are usually limited to 6%, with slightly higher grades in mountainous regions. GPS data are often used in developing a strategy model for the car driving along the race route, but the altitude data from GPS have a lot of noise in them. If the grades are not properly smoothed, the model will greatly overestimate the power consumption of the car in the hilly terrain. The procedure for developing this spreadsheet is as follows:

1. Start with the two columns of numbers in the spreadsheet representing the distance along the route and the grade of the road. In the third column put the speed in miles per hour that the car is to be traveling. In developing the spreadsheet and for initial testing it is best to set a constant speed along the route. This is not the most energy-efficient way to drive the route. An algorithm can be developed that allows the car to speed up or slow down an amount each step, depending on the grade of the road, and that limits the top and minimum speeds of the car. Developing this algorithm is a difficult process, and it is best to work with constant speed until the remainder of the spreadsheet is debugged.

2. Calculate the gravitational power in the fourth column using Eq. 2.26. (It will be necessary to convert the grade to an angle.)

3. Calculate the kinetic power in the fifth column. If the speed is assumed to be constant, then the kinetic power is always zero and this column can be ignored. If the velocity changes, then calculate the kinetic power as the change in kinetic energy over the time period. If the velocity is V_i and V_{i-1} at the distances D_i and D_{i-1} along the route, respectively, the kinetic power P_{KE} (in watts) is given by Eq. 2.34.

$$P_{KE} = (5.46\times10^{-7})\,\frac{(V_i^2 - V_{i-1}^2)(V_i + V_{i-1})}{D_i - D_{i-1}}\,W \qquad (2.34)$$

   where W is the weight in newtons, V is the speed in kilometers per hour, and D is distance along the route in kilometers.

4. Calculate the aerodynamic power in the sixth column using Eq. 2.4.

5. Calculate rolling resistance power in the seventh column using Eq. 2.9.

6. Total the fourth, fifth, sixth, and seventh columns in the eighth column to get total power required to push the car down the road. Divide this number by the motor-drive efficiency and add the parasitic losses so column 8 represents the power that must be provided to the motor.

7. Calculate the time period between points (in hours). Divide the distance between points ($D_i - D_{i-1}$) by the average speed between the two points ($V_i + V_{i-1}$)/2 to get the time between points in hours.

8. In column 10, choose a starting time in military digital time, and add column 9 in to get a column that has the time of day in military digital time.

9. Calculate the array power in column 11 using Eqs. 2.15 and 2.16.

10. In column 12, subtract the array power (column 11) from the total required power (column 8) to get the power that must be drawn from the batteries.

11. In column 13, calculate the percent decrease in the battery pack from Eq. 2.24. A problem will emerge. When going down a steep hill the array power will be more than is required to power the car, and there will be a negative power draw from the batteries. This means the motor has kicked into regenerative braking mode and is charging the batteries. But a negative value for P in the battery equation requires that a negative number be raised to a fractional power, a quantity that is not defined. The spreadsheet returns an error everywhere there is regenerative braking. The battery equation is only valid for drawing power out of the batteries. It is not valid for charging the batteries.

The easiest method to resolve the problem is to use a logic statement so that the energy drawn out of the batteries is zero everywhere there is negative power. This is the same as neglecting the energy saved by regenerative braking. Regenerative braking is not a major source of energy, so this is a reasonably good approximation. To include regenerative braking it is necessary to assume an efficiency (50% is a realistic number). The regenerative braking energy should be added to the battery capacity rather than subtracted from it. In practice, it takes several columns to perform the function of keeping track of the energy used from the batteries.

N. Homework Assignment

1. Develop a spreadsheet for modeling a car traveling on hilly terrain, using the hilly terrain data file. Assume the following properties for the car:

a. Drag area = 0.125 m^2
b. Velocity = 90 km/h (constant speed)
c. Rolling resistance coefficient = 0.0055
d. Weight = 2500 N
e. Motor-drive efficiency = 94%
f. Parasitic losses = 30 W
g. Regenerative braking efficiency factor = 0.5
h. Peukert number = 1.08
i. Peukert constant = 8078
j. High noon sun angle = 14°
k. Sunrise = 6:45 A.M.
l. Length of day = 14 h
m. Maximum array power = 1400 W
n. Starting time for race = 8:00 A.M.

2. Do a comparison with the model for traveling on flat terrain by calculating the following:

   a. How far can the car travel in the hilly terrain before running out of energy? [445 km, runs out of power at about 12:57 P.M.]

   b. How far could the car travel on flat terrain? (Set the grade to zero in the model.) [597 km, runs out of power at 2:38 P.M.]

   c. What is the ideal speed to run out of power at 5:00 P.M.? How far will the car go before running out of power? [83.13 km/h, 748 km]

3. The next step is to do a parametric study using the hilly terrain model, and rate the importance of the different parameters in the model, on a realistic range. This is very important for design because we need to know which aspects of the car have the largest impact on overall performance. Use the parameters in question 1 of this homework assignment as the base because they are parameters for a good car. Draw a chart for the variation of each parameter, plotting the distance the car can travel if the race period ends at 5:00 P.M. It is not necessary to use a fine grid of points. Five points per chart is fine. These charts show how varying the parameters over a realistic range affects the overall performance of the car.

a. It is possible to achieve a drag area of 0.30 m^2 without too much effort, assuming a body that encloses the driver and chassis. (An open design would be higher.) The top cars have a drag area in the 0.1–0.15 m^2 range. Plot this chart with a range on drag area from 0.1–0.30 m^2.

b. Claims for rolling resistance coefficients vary a lot because there is no standard method of measuring it. Honda claimed 0.0036 for its Dream III solar car. Passenger car tires typically have a 0.015 rolling resistance coefficient, and that can be reduced to near 0.01 by overinflating the tires. It is unlikely that the car would have a rolling resistance coefficient higher than 0.01, assuming the wheels are properly aligned and the brakes do not drag, so plot this chart for a range of rolling resistance coefficients between 0.0036 and 0.01.

c. Misalignment of the wheels or dragging brakes can significantly increase the rolling resistance, with poorly aligned wheels being the worst offender. Rolling resistance could increase to about 3% of the weight of the car for poorly aligned wheels. Plot a chart allowing rolling resistance to vary from 0.0036 to 0.03, and label the higher rolling resistance as poor wheel alignment, to signify that this can only happen if the team does a poor job in suspension design.

d. Allow the weight of the car to vary between 500 and 1000 lb. The 500-lb value is approximately the lightest-weight solar car ever built. Cars have been built that weigh more than 1000 lb, but at this point any reasonable effort in weight control should keep the weight to less than 1000 lb.

e. An older motor with a single reduction belt or chain drive should be at least 85% efficient, even if the belt or chain is not perfectly aligned, or if a tensioner is used. The best hub motors are 98% efficient. Plot a chart varying motor-drive efficiency from 85 to 98% efficient.

f. Parasitic losses in the electrical system can be very low for a good design to several hundred watts for a poor design. Vary the parasitic losses from zero to 300 W, but label the parasitic losses above 50 W

as poor electrical design to signify that a reasonably good car will not have losses that high.

g. A mediocre array will produce 750 W peak power. High-efficiency cells can be used to make an array that produces 2200 W power. Vary array power from 750 to 2200 W. Please note that this analysis does not account for the fact that a higher powered array will charge the batteries up faster in the evening and morning, which is a significant advantage. Array power is more important than indicated by this graph because the array is used to charge the batteries in the morning and evening.

h. Race rules place limits on the weight of the battery pack to limit the battery capacity to 5 kW-h. Teams can test and screen batteries, and find a set of exceptional batteries of the particular type, and have more than the 5 kW-h of capacity. Adjust the battery capacity formula so that the capacity at a 1500-W power draw varies from 3 to 6 kW-h, using a Peukert number of 1.08. On the same chart draw a line for lead-acid batteries, using a Peukert number of 1.22 and varying the capacity at 1500 W power draw from 3000 to 6000 W-h.

4. From the charts created, write a summary of what aspects of the car have the largest impact on the overall performance. This is one of the most important exercises in the book. To do design trade-offs and build the best car possible with the available resources, it is necessary to understand quantitatively how the different performance parameters of the car affect the overall result.

O. *Extra Credit Homework:* Milford Track (Study of How Hills Affect Solar Car Efficiency)

Qualification for the Sunrayce event was done on GM's Milford track for the 1997 and 1999 Sunrayce events. This track has a very steep hill. The cars start each lap going downhill, and finish by going uphill. Traveling at constant speed around the track is not the most efficient way to drive the course.

The driver must allow the car to speed up going down the hill and slow down when coming back up the hill. The Milford track spreadsheet gives elevation data for the 2.1-mi track. This data file is also available from the author. It is possible to use the model developed in this unit to find the ideal velocity profile of the car going around the track to use the minimum amount of energy per lap, and maintain a given average speed per lap. The driver can study the ideal velocity profile and practice to drive the track in the most energy efficient manner possible. The homework assignment is to use the elevation data for the track and develop the ideal velocity profile for average speeds of 30, 40, and 50 mph. Studying these results will help in understanding the philosophy of driving the car in hilly terrain.

P. *Extra Credit Homework:* Heartland Park Track (Study of How Sharp Corners Affect Solar Car Efficiency)

The Formula Sun event was held on the Heartland Park track, near Topeka, Kansas, in May of 2000, 2001, and 2002. The goal for this event is to have the solar cars travel as many laps as possible in a 3-day period. The Heartland Park track has several sharp corners and a few significant hills. In sunny conditions, the better solar cars have adequate energy to go 50+ mph average speed, but some of the corners are sharp enough that the cars must slow down to below 25 mph. Slowing down for and accelerating out of the corners forces the car to operate in an inefficient manner, and reduces the distance the cars can travel each day. Turn three is a particularly difficult problem because the cars go down a significant grade to the corner, and then must climb a significant grade coming out of the corner.

The Heartland Park spreadsheet, also available from the author, gives elevation and radius of curvature data for the track. The straightaway portions of the track were assigned a radius of curvature of 50,000 ft, since that is essentially straight. The goal is to develop a strategy so that the car consumes as little energy as possible per lap for a given average speed. The strategist will quickly realize that traveling fast in the corners is the most energy-efficient way to drive the track, because it requires less slowing down and accelerating out of the corners.

An additional challenge in this event over the Milford track is that there is a limit to how fast the cars can travel in the corners. The team must decide the g loading the car can withstand in the corners. Solar cars have thin tires, and while the car can withstand a 0.5-g cornering load, the tires may not last very long when cornering this hard. Blowouts will slow the team down a lot more than driving slower and allowing the tires to last longer. Testing must be conducted to find a reliable cornering g load for the car. Once an allowable g loading is established, the strategist can use the model to find the most efficient way to drive the track for a given average speed.

Q. References

2-1. Roche, D.M., A.E.T. Schinckel, J.W.V. Storey, C.P. Humphris, and M.R. Guelden, *Speed of Light: The 1996 World Solar Challenge*, chap. 3, Photovoltaics Special Research Center, University of New South Wales, Sydney, Australia, 1997.

2-2. Tamai, G., *The Leading Edge*, Robert Bentley Publishers, Cambridge, MA, pp. 1–6, 1999.

2-3. Storey, J.W.V., A.E.T. Schinckel, and C.R. Kyle, *Solar Racing Cars*, chap. 3, Australian Government Publishing Service, Canberra, Australia, 1994.

2-4. Kyle, C.R., *Racing with the Sun: The 1990 World Solar Challenge*, chap. 3, Society of Automotive Engineers, Warrendale, PA, 1991.

2-5. McCarthy, L., J. Pieper. A. Rues, and C.H. Wu, "Performance Monitoring in UMR's Solar Car," *IEEE Instrumentation & Measurement Magazine*, pp. 19–23, September 2000.

2-6. Wright, G.S., "Optimal Energy Management for Solar Car Race," *1996 IEEE 39th Midwest Symposium on Circuits & Systems*, pp. 1011–1014.

2-7. Shimizu, Y., Y. Komatsu, M. Totii, and M. Takamuro, "Solar Car Cruising Strategy and Its Supporting System," *JSAE Rev.*, vol. 19, pp. 143–149, 1998.

2-8. Munson, B.R., D.F. Young, and T.H. Okiishi, *Fundamentals of Fluid Mechanics*, John Wiley and Sons, pp. 589, 860–861, New York, 1994.

2-9. Gillespie, T.D., *Fundamentals of Vehicle Dynamics*, Society of Automotive Engineers, Warrendale, PA, p.117, 1992.

2-10. Kyle, C., *GM Sunraycer Case History Lecture 2-3: Sunraycer Wheels, Tires and Brakes*, Society of Automotive Engineers, Warrendale, PA, 1992.

2-11. Goldhammer, L., J. Powe, and G. Ralph, *GM Sunraycer Case History Lecture 3-3: GM Sunraycer Solar Panel*, Society of Automotive Engineers, Warrendale, PA, 1992.

Chapter 3

Design Methodology

A. Introduction

Design methodology is the application of project management principles to an engineering design project. When deadlines are imposed on a large, complex, multidisciplinary project like a solar car, the process must be broken into smaller and more manageable tasks, and the resulting designs must work together as a system. Design methodology, systems engineering, and project management are all closely related topics. A large engineering design project requires that basic project management techniques be employed to ensure that the project is completed on time and on budget, and that it makes the best possible use of the available resources.

There are some generic principles of design methodology that apply to all design projects. The designer must consider the time available to develop the product and the resources available to design, manufacture, and test the product. The designer must consider the history of the product being developed and similar products to gain insight and ideas into how the product should be designed. A process should be put in place to generate ideas for the design and then evaluate and select the best ideas. Some components will be designed and built in-house, while others will be outsourced. Communication between the design groups is required to be sure that the components will work together as a system. It is the performance of the system that must be optimized, not the performance of components or subsystems. Design is an iterative process and the plan should allow for the inevitable testing and redesign.

There are many books available on the subjects of design methodology and systems engineering, and to cover these topics in detail in one chapter is not possible. The goal of this chapter is to cover the most important aspects of design methodology and systems engineering as applied to solar car design.

B. Time and Resources

1. Time

The major solar car races in the world are held every 2 years, so most solar car teams operate on a 2-year schedule. A new car is designed and built every 2 years. There have been cases where a team took 3 or 4 years to design and build a car, but the most common time period is 2 years. The schedule and time allocations for designing, building, testing, redesign, and racing the car must fit into a 2-year period. It must also be recognized that the races are very intense periods that take a lot out of the team members, and there is a recovery time after the race is over where not much is going to get done. If a team participates in more than one race per project, then there is quite a bit of racing and recovery time, which takes away from the design of the next car. Teams typically have about 18 months available to design and build the car and get it ready to race. From a top-down view, the project can be broken into five phases as described below. A schedule should be developed for the project.

a. *Phase 1.* The first phase of the project involves the generation of ideas of how the car will be designed and built. Many ideas will be generated for all aspects of the car. Among the most important are the decisions about what solar cells, batteries, and electric motor and controller the car will use. These are expensive components that have a long lead time. The general shape of the car and driver placement must be decided. The team should also be looking at options of tires and wheels, brakes, steering, suspension components, chassis materials, body materials, power point trackers, rear vision system, turn signals and brake lights, driver controls and interface, and other design options. The culmination of this phase is a decision of how the car will be designed and what materials and components will be used.

b. *Phase 2.* The second phase is the detailed design of the car. The details of how the systems will be designed and built are worked out and materials are ordered. Some of the decisions from the first phase will have to be rehashed. These ideas looked good conceptually, but it was not possible to work out the details to a suitable design. This phase ends when there is a detailed design for all aspects of the car.

c. *Phase 3.* The third phase is manufacturing of the designs. Some designs will have to be modified in order to manufacture them, and some may have to be discarded. Components and subsystems will be bench-tested and modified as necessary to ensure a reliable design. This phase ends when the car is assembled and prepared for testing.

d. *Phase 4.* The fourth phase is testing of the car. Problems that could not be anticipated will surface. These problems will seem obvious and avoidable when they surface, and there will be a temptation to point fingers, but placing blame should be avoided. All cars require some redesign to work out the bugs. This phase ends when the car runs reliably.

e. *Phase 5.* The fifth phase is race preparation. The team should develop race simulations and practice as if running in a race. The drivers will gain experience in driving the car in a race situation and the remainder of the team will gain experience in supporting the car. Specialized tools will be developed to speed up changing tires or performing other routine maintenance or common car problems. This phase ends when the race begins.

Recognizing that the team has approximately 18 months to finish the project, the first phase should be completed in the first 6 months. Some subsystems will be selected much sooner, and once a design concept is selected that particular subsystem can proceed to the detailed design phase. There is overlap in all of these phases. There is no exact time when one phase ends and another begins. Phase three takes about 6 months. If there is only 6 months until the race begins and the team has not started manufacturing the car, then there will be very little testing or race preparation, and the team will almost certainly do poorly in the race. Three months is adequate time to test and redesign and prepare for the race, phases 4 and 5 of the project. This leaves about 3 months for detailed design of the car. Table 3.1 is a GANTT chart showing the recommended time allowances for the five phases of the project.

The project manager must keep the team on schedule, but must also recognize that the schedule is a tool to assist in managing the project. The schedule exists to help the project; the project does not exist to satisfy the schedule. There comes a time when compromises must be made to stay on schedule, and the project manager must be able to convince the designers to make these compromises. It must be a team decision to compromise in the early phases

TABLE 3.1
PROJECT GANTT CHART

Project Phases	Project Month																	
	1	2	3	4	5	6	7	8	9	10	11	12	13	14	15	16	17	18
Phase 1	■	■	■	■	■	■												
Phase 2				■	■	■	■	■	■									
Phase 3									■	■	■	■	■	■	■			
Phase 4																■	■	
Phase 5																	■	■

to allow time for the later phases of the project. The most common mistake in any engineering design project is to spend too much time in phases 1 and 2. Spending more time researching design concepts will result in better concepts. Spending more time detailing the designs will result in better designs. Spending more time on manufacturing, testing, or race preparation will improve the results in those areas. If more time were available, the team could develop a better car. The project manager should be an experienced person with a strong and persuasive personality. It is a good management principle for the project manager *not* to be the principal designer for any subsystem of the car. It is difficult for any person to avoid giving his or her subsystem undue priority and resources.

2. *Resources*

The team will have access to resources to complete the project, and it is important to make the best possible use of the resources available. The most important resource is the time and dedication of the members on the team. The available human resources will be used to raise funds, get material donations and use of facilities, design, build, and test the car, and plan for the publicity events and the race. The more dedicated team members will be willing to use their time to do whatever the team needs most, which is often

fund-raising and keeping the project sponsors informed of team progress. Some team members will only be willing to work on certain aspects of the project, usually their specialty or major interest. The team must find resources for all aspects of the project.

To be successful, all aspects of the project must be done well. A car with great electrical systems and poor mechanical systems will perform poorly in the competition. Great design work with a poor manufacturing effort, or vice versa, does not result in a good car. The team can choose to run in the stock class to reduce the cost of building the car, but there must be enough funds to buy the stock-class components. To be successful the car must be well designed and manufactured and have the right technology in the components, and it must be completed early enough to allow the team to practice and prepare for the competition. The project manager needs to remind the team regularly that all aspects of the project are important, including fund-raising, publicity, logistics planning, and practice runs. These things are just as important as design and manufacturing of the car.

Money is an important resource because some components of the car will have to be purchased. The solar cells are one of the more expensive items. Standard 100-mm^2 single-crystal silicon solar cells cost about $7.00 U.S. each at the time of this printing, and the team will need to buy about 1000 of them to build a solar array and have some spare parts. The cells will have to be strung together and encapsulated. Some teams do this in-house, while others contract it out at a cost of $5,000 to $10,000 U.S. There seems to be no limit as to what can be spent on the high-efficiency space-grade solar cells. Cost goes up exponentially with the efficiency of the cells. The space-grade cells are smaller in size and require a bypass diode for each cell, so the cost of stringing and encapsulating these cells will be much higher than for the silicon cells. Power point trackers will have to be purchased to wire the solar array into the power system, at a cost of a few thousand dollars. It is very difficult to get components for the solar array donated, so the team will need to raise about $20,000 cash for a stock-class solar array. If the team has the funding, getting a more powerful space-grade solar array is one way to significantly improve the performance of the car, and there seems to be no limit as to how much money can be spent in the pursuit of more efficient solar cells.

The other major costs for the project are the motor, batteries, and the logistics costs of participating in the race. A hub motor offers the best overall efficiency. The most economical hub motor system at the time of this printing is the New Generation hub motor and controller, which currently costs about $15,000 U.S. Because of the low production volume, there is a long lead time to get one of these motors. If possible the team should have a spare motor in case of a failure. The spare motor/controller system could be a different, much less expensive system since it will probably not need to be used. A good set of lithium-ion or lithium-polymer batteries will cost from $10,000 to $25,000 U.S. depending on the type and manufacturer. Lead-acid batteries are much less expensive and it may be possible to get them donated. The logistics cost for a U.S. team to participate in the American Solar Challenge is about $15,000 U.S. for food, lodging, and renting the vehicles. It would be about the same cost for an Australian team to participate in the World Solar Challenge. Taking the car overseas greatly increases the logistics cost.

The rest of the car is made from more common and standard materials and components. Included in this category are tires, wheels, brake components, steering components, composites, steel aluminum, wiring, switches, connectors, dc–dc converters, and other electronic components. It would cost approximately $20,000 U.S. to purchase these components, but with some effort, it will be possible to get a substantial amount of them donated. A new team starting with nothing should budget about $75,000 U.S. in cash and donations to build a good stock-class car with a hub motor and to participate in one major event.

Facilities are necessary to build the car and conduct the team business. The team will need office space for planning and management, and shop facilities to manufacture the car. Very few teams will have all of the facilities necessary for manufacturing, so there will be outsourcing for some of the components. No team has ever made their own tires. Even if the team has the facilities, it may be a good decision to contract out certain aspects of the projects. Wheels, brake components, bearings, motor and controller, solar cells and encapsulation, power point trackers, batteries, taillights, horn, and some of the electronics boxes are all examples of components that would be outsourced by most teams. In addition to the facilities the team must have the expertise to manufacture the car.

To practice for and participate in the race, the team will need access to two vans to serve as the lead and chase vehicles, and either a large truck or a truck and trailer to transport the solar car to the event (or to move the car when it breaks down). If the team has a competitive car, the support vehicles need to be fast or they will have difficulty keeping up with the solar car. The support vehicles need to have large fuel tanks, especially for the World Solar Challenge where it is a long way between fuel stations. Many teams have run out of gas trying to keep up with the solar car. A lead and chase van and a truck are the minimum contingent of vehicles for the race. Teams may also have a weather vehicle or scout vehicle which stays 30 km or so ahead of the solar car and radios back detailed information about the road conditions and cloud cover ahead. A separate vehicle may also be used to haul the solar array stand and get things ready for the team when they arrive at the media stops on the race. The array vehicle must be very fast because it will have to pack up the array stand after the solar car leaves the stop, pass the solar car, and arrive at the next media stop at least 15 or 20 min ahead of the solar car to get things ready. There may be other vehicles to haul team gear, pick up supplies, or prepare food for the team. There is a large amount of logistics planning required to run a cross-country race.

C. Study History

Many solar cars have now been built and raced. Some of these have performed very well and others have not. One of the most important parts of design is to study similar products to see what has worked well and what has not worked well in the past. Studying the successful cars will provide some good design alternatives for the system because not all of the good cars are designed the same way. The successful cars do not all have the same body shape. There are several different ways of approaching the body shape that all seem to yield a low aerodynamic drag. There are good design options for almost every system on the car. The important point here is that *most of the good design ideas will come from studying the way the top teams have designed and built their cars.*

It is also important to study the designs that did not work out well, especially if the team is proposing a new and innovative approach to a particular system of the car. It is important to realize that in many cases there was a group of people who believed that they had a great idea, and it was not until they

started testing it that they realized the "fatal flaw." Solar car design is a mature subject, and it is very likely that a new and innovative approach to the design is actually an approach that has been tried in the past and discarded. It is amazing how many poor design ideas continue to be tried, especially by new teams. As an example, teams should have realized after the 1987 World Solar Challenge that an open-wheeled or open-cockpit vehicle has such poor aerodynamics that such a design has no chance of winning the race. No such car has ever won a major race. Yet every event seems to have a few of these designs entered, usually by a new team.

D. Control Innovation

Innovation has advantages and disadvantages. Innovation is necessary for improvement. If the team were to build exactly the same car, project after project, the car would become less and less competitive over time as other teams improve. An innovative design is much more likely to cause problems than a more traditional design. A team that tries a lot of new innovative designs for subsystems on the car is almost certain to have enough problems to keep them from winning the race. Innovation is necessary for improvement, but it needs to be controlled. There needs to be a balance between innovation and the risk of failure.

The riskiest type of innovation occurs when a whole new innovative approach is tried in designing the system. Before accepting such a design approach, the team needs to be sure that the new approach will make the car significantly faster, cheaper, or easier to manufacture than the more traditional approach. If there is not a significant benefit, then taking the risk is poor management of the project. There will be unforeseen problems to be solved when following a traditional approach. Innovative solutions will usually lead to many more unforeseen problems, and there is a chance that they will not work at all. Innovative solutions need to be completed and tested early in the project in case they fail.

The more practical innovations are usually small changes to an existing design, or finding better, faster, or less expensive ways to manufacture the system. Such small changes might be a small reduction in weight through better analysis of the design or a better manufacturing process. Such a change

might be simply finding a lighter-weight component, such as a shock absorber or brake caliper that will work in place of what has been used in the past. The team may find a standard electronics component to replace a component that the team has been designing and building. The standard components tend to be more reliable and less likely to cause problems. Every project seems to bring opportunities to find better batteries and solar cells.

E. Design Process

The process described in this section is a generic six-step method, which is similar to published methods [3-1 to 3-3]. To manage the design of a system, a manager needs a tool that allows projects to be looked at in an objective manner. Design process is a tool that allows the manager to assess how far along the design has progressed and what is likely to be the next step. The manager needs to recognize that this is a tool to assist with the design, and that there are cases where it makes sense to skip steps in the process or to not complete a step before progressing to the next step.

For most design projects, products already exist. The design process begins with some general statements of the needs or desires of what the product should do, and an evaluation of the existing products to see how well they meet the current needs. From these general statements, specifications are developed for the product. The design team will generate ideas and concepts that satisfy the specifications. Many concepts will be generated, and the team will select the concepts that appear to best satisfy the needs and specifications of the product. Detailed designs will be developed for manufacturing the product. The product will then be built and tested. Figure 3.1 is a block diagram of the six-step process.

1. *State Product Needs and Evaluate Existing Solutions.* If there are existing solutions to the problem, the most important part of this step is to evaluate how well those solutions satisfy the needs of the device being designed. The existing solutions may satisfy some needs very well, and there may be a lot of room for improvement with other needs. Some needs may not be addressed at all. It is important to identify the needs and desires that the product is to fulfill. There will probably be some rules or constraints for the product that must be addressed. It is important to

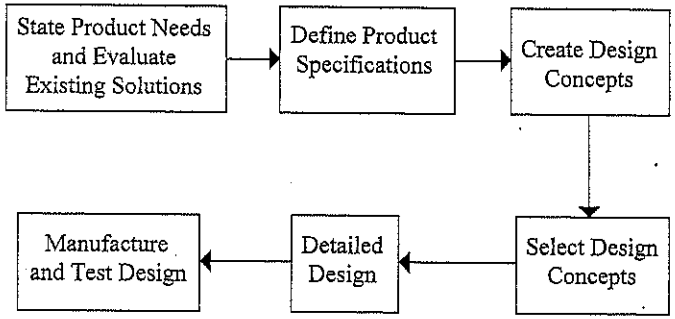

Fig. 3.1 Six-step design process.

carefully study the rules at this point in the design process. The result of this step is a list of statements of what the product should do along with certain rules and constraints. The statements should be nontechnical in nature, and in many ways form a mission statement for the development of the product.

2. *Define Product Specifications.* In this step the goal is to take the nontechnical statements of needs for the product and develop technical design specifications for it. Some of the specifications will be functional requirements, which are functions that the device must perform. In most cases there is a minimum or desirable performance level for device functions that should be part of the specifications. There may be safety or environmental requirements, and specifications need to be developed for those requirements. The primary difference between a statement of need and a specification is that the specification is a quantitative statement.

3. *Create Design Concepts.* The purpose of this step is to create several different design concepts that have the potential of meeting the design specifications. If there are existing products, those products should be included as design concepts. In addition to existing solutions, there may be completely new innovative concepts developed for the product. It is important at this stage to consider a new technology or technologies that has not been used for this product in the past. Useful innovative solutions

usually involve applying new technology to the product. Judgment of whether a design concept is feasible or not should be avoided at this step. The outcome for each design concept is a description of the concept and how it will satisfy the design specifications, usually involving sketches and narrative.

4. *Select Design Concepts.* The goal of this step is to do a fair evaluation of all the design concepts and select the concept that will be used for the product. The selection must be justified on the basis that it is the best solution. As much as possible, quantitative models should be developed to evaluate how well each design concept meets the specifications. One of the most difficult parts of this step in the design process is to not let politics or personalities select the solution. Separate the people from the design concepts. Do not vote on John's design versus Jane's design; vote on design A versus design B. The final solution may include ideas from more than one design, but it is a bad idea to develop a solution that includes something from all the design concepts just to make everyone happy. The goal is to select the best design concept and to be able to justify why it is the best concept.

   People are not machines; they have emotions and feelings. It is important to justify the design decisions made and to convince everyone on the team to support them. There will be problems in detailing and manufacturing the design and getting it to work properly no matter which design concept is selected. Take a little extra time at this step to honestly give fair consideration to all the design concepts, and to evaluate all of them, and to justify the design concept selected based only on the idea that it does the best job in satisfying the specifications. This will help avoid problems later in the design process. Try to get everyone on the team to buy in and support the design selected. When problems arise later, it is not true that the team would not be having those problems if they had selected design A instead of design B. Design A would have a completely different set of problems to overcome.

5. *Detailed Design.* The goal of the detailed design is to work out the details of exactly how the product will be manufactured. There are a lot of decisions to be made about what materials and components will be used in the design, and all of these decisions must be justified to some

extent. A design philosophy must be developed and engineering analysis should be used in sizing and selecting components. Suppliers must be identified for the materials and components and an effort should be made to get the best possible price. The outcome of this phase of the design process is detailed drawings and manufacturing instructions and a list of suppliers and costs for the materials and components for the design.

6. *Manufacture and Test Design.* The final step in the design process is to manufacture a prototype or mock-up of the design and test it to see that it meets the design specifications. There are always some unforeseen problems at this stage that must be overcome. There will probably be some redesign or modifications to the design to make the product work properly. As soon as testing begins, areas of improvement will be identified for the prototype. Some things can be improved with a minor modification, while others require a complete redesign. Decisions will have to be made about whether to address those improvements or to accept the prototype for what it is. The goal should be to make the prototype work as well as possible for the design concept selected.

Once the prototype or mock-up has been tested and modified to make it work as well as possible, the next step in the design process is to evaluate it to see how well it meets the needs that were set in step 1 of the design process. Another way to visualize design is as a circular process, as illustrated in the design spiral in Fig. 3.2. The spiraling outward on the six axes represents improvements in the design as the team gains expertise and understanding of what is involved.

Design methodology is a management tool to help the team progress and improve the design. There are cases where it makes sense to skip a step or to not complete a step before proceeding to the next step, but design progresses in the direction shown. From a management viewpoint it is important to keep the process moving and not get stuck at one point. There is a schedule that must be met in completing the design. One common "sticking point" is creating and selecting design concepts. Teams can spend forever coming up with design concepts and arguing about which is the best solution. A manager may have to step in and force the team to vote and select a concept and move on to detailed design. Detailed design is the other common place where teams get stuck. The design can

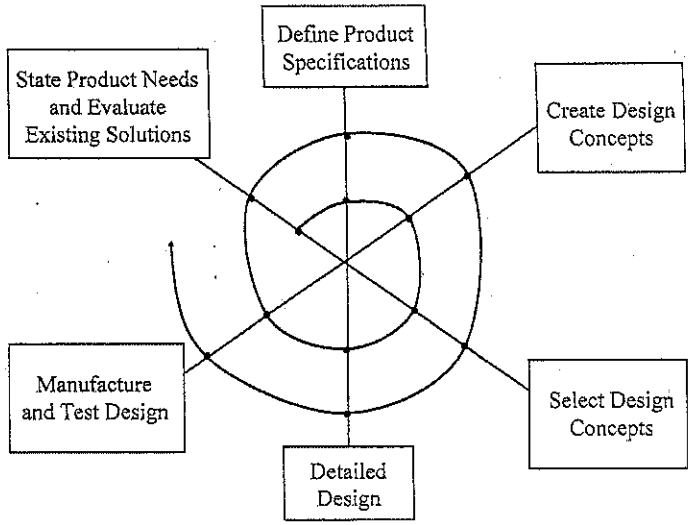

Fig. 3.2 Design spiral.

always be improved by spending more time working on the analysis or looking for better components and suppliers. At some point the team must stop designing and start manufacturing even though the design is not perfect. Design is an iterative process.

F. Solar Car Design Process

The generic design process above applies to solar car design, but some of the details get lost in trying to generalize the process to apply to any design. There are some specific considerations for each step of the design process when it is applied to the design of a solar car, which are detailed below.

1. *State Product Needs and Evaluate Existing Solutions.* There have been many good solar car designs, and the most important part of this step is to study how the best cars have been designed and built. Try to figure out what the top teams are doing to be so successful in the competitions.

The team also needs to study the rules of the competition carefully. Many teams have come to competitions and were disqualified because their car did not meet the race rules. The rules change a little each year, and what was allowed last year may not be allowed this year. The first step in the design process is to come to a good understanding of what has to be accomplished to be competitive.

2. *Define Product Specifications.* The first decision to be made as far as specifications is whether the team will design and build a stock-class or an open-class car. From a design viewpoint the only difference is that the stock-class car uses much heavier batteries and will end up being a much heavier car. The stock-class car is much less expensive to build because it uses less expensive solar cells and batteries. Specifications need to first be developed for the car as a whole, that is, required solar array power, battery capacity and efficiency, motor-drive efficiency, rolling resistance coefficient for the tires, allowable parasitic losses, and weight goals for the body and chassis. Chapter 2 provides a lot of guidance in selecting realistic target values for the open-class and stock-class vehicles.

3. *Create Design Concepts.* The way to approach design concepts differs from system to system on the car. The shape of the body is an important decision that must be made early in the project. There are several good concepts that have worked well for the body shape. Body shape affects the placement of the driver and the balance of the car on the tires. The body must be very aerodynamic for the car to be competitive, so any design concept of body shape must have low aerodynamic drag. There have been many solar cars made that have good aerodynamics, and study of those vehicles is very helpful in developing the body shape. Design concepts for the body shape of the car should include the placement of the driver inside the body of the car. It should be shown that the driver has adequate space to fit in the car, and adequate visibility to drive the car. A center of gravity analysis should also be included to show that the weight of the vehicle can be evenly distributed on the tires.

   For the solar array design, the primary goal is to get the most efficient solar cells that the team can afford. Solar cells are a major cost of the project even for stock-class cars, so it is important to contact all of the manufacturers and get the best price possible on the cells. Money saved

on the cells can be spent on other parts of the car. The team will need to decide whether to develop the expertise and encapsulate the cells in-house or to outsource the encapsulation. Power point trackers will need to be selected that work with the subarray voltage and the battery voltage. There are several companies that make power point trackers and a few teams have designed and built their own trackers. Design concepts for the solar array will center around the solar cells. The team should identify the different possible solar cells for the car as the main part of generating design concepts for the solar array. Design concepts for the solar array should include the efficiency and cost of the solar cells and a basic plan of how the array would be laid out on the car.

There are rules governing the allowable weights for the different types of battery systems. The goal is generally to get as much battery capacity as possible for the allowable weight. There are many battery manufacturers, and the team must contact the manufacturers to see what the options are. Battery technology is changing rapidly, and the best batteries today will probably not be the best batteries 2 years from now. Design concepts for the battery system should include the type and cost of the batteries, the way the batteries would be wired to achieve system voltage, the capacity of the batteries, and an estimate of the efficiency of the batteries.

There are almost an infinite number of choices for the motor-drive system, but most of them are poor choices. If the team has the resources, a high-efficiency brushless dc hub motor should be selected. There are only a few such motors available that are sized properly for solar cars, which limits the design choices. If the team cannot afford or obtain a brushless dc hub motor, then the next best choice is a high-efficiency brushless dc motor with a single reduction chain or belt drive. There are several high-efficiency motors available that are much less expensive than the hub motors. Design concepts for the motor-drive systems should include the cost and estimated efficiency of the system.

The solar array, batteries, and motor-drive systems need to be decided on fairly early in the project because they are expensive items that may have long lead times for delivery. The shape of the body must be decided before the team can get serious about designing the chassis and suspension

systems because body shape determines where the wheels and driver are located. It is important to develop design concepts for these systems early in the project so that the team can select the design concepts to be used and progress with designing and manufacturing the car. There are design options for many of the other systems of the car, but most of those will be explored during the detailed design phase of the project. It is not practical to develop and have the team evaluate design concepts for every aspect of the car. Some of the decisions should be left to the discretion of the person doing the detailed design work for the system.

4. *Select Design Concepts.* One of the earliest steps is to select the design concept for the shape of the car. If the team has several different ideas, then each person or small group should be allowed to develop a presentation of a particular design concept and why it is a good choice and present it to the team. Before any presentations are given to the team, a discussion should be held during which it is decided that everyone will support the decision of the team. The team should then listen to the presentations, discuss the advantages and disadvantages of each, and vote and select the best design. The body shape concept must be selected before design can begin on the body, chassis, or solar array, so this concept must be selected early in the project.

   The team will also need to select the solar cells, batteries, and motor-drive system that will be used on the car. Very few teams will have the funding to get the best of everything, so decisions will need to be made between cost and performance. The power management models in Chapter 2 should be used to help evaluate the amount of performance for the different options. The goal is to make the car as fast as possible using the resources available to the team, and cost has to be a major consideration for these three systems. It may be best for the team to design a stock-class car and greatly reduce costs on the solar cells and batteries. Cost is much less important for other systems. Efficiency and reliability are the main goals in designing most of the mechanical and electrical systems. When making design trade-offs for these systems the goal is to make the car faster and more reliable. Power management models should be developed to help determine which design option will make the car faster.

5. *Detailed Design.* Once the major design concepts have been selected, the team needs to begin developing the details of how the car will be manufactured. Design concepts will be generated and selected as part of the detailed design of the vehicle. There are a lot of options in detailing out the systems. With reference to the design process model, this can be viewed as going through the design process again, skipping the manufacture and test design step, or it can be viewed as a limitation of the model. Design process is a management tool to help lead the team through the design process and keep things moving. Like other management tools it is not an exact science, but it can be very helpful in keeping the process moving and evaluating the progress. Design teams have a tendency to stall out at one step in the process, and this tool can help the project manager know when it is time to step in and force the team to move on to the next step.

   As detailed designs are developed, there will be many times when the team has the choice of designing and manufacturing in-house or outsourcing. Some teams view this as an educational experience and try to do as much in-house as possible. Developing everything in-house can be a good educational experience, but it is poor engineering practice and will probably hurt the performance of the car. All teams outsource the tires, batteries, rod ends, bearings, shocks and springs, resistors, capacitors, and other basic electronic components, and raw materials for manufacturing the body and chassis. The University of New South Wales team is the only one to have manufactured its own solar cells. The team should do what makes sense, and what makes sense depends on the facilities and expertise available to the team. Off-the-shelf electronics components such as power point trackers, dc-dc converters, and battery protection circuitry tend to be much more reliable than systems that are built in-house. There may be cases where it makes sense for the team to design the components in-house and then outsource the manufacturing. The team has a limited amount of calendar time and man-hours for the project. If time can be saved in design and manufacturing, then there will be more time available to test the car and prepare for the race. Testing and preparation make a lot of difference in how well the team performs in the race.

Teams commonly outsource the building of the mold for the body and encapsulation of the solar cells, both of which require long lead times. The body must be designed, the mold built, the body manufactured and painted, and then the solar cells must be put on the body. This takes time and must be done sequentially. The body is usually the critical path in getting the car completed. If the team is going to outsource either the building of the mold or the encapsulation of the solar cells, the designs need to be completed early in the project so that there will be time to write a contract, award it, get it into the company's production schedule, and complete the work on schedule. It is very important to the long-term success of the team to develop a good relationship with the suppliers and companies that the team decides to work with. Most of the same components will be outsourced on subsequent projects, and having a good relationship with companies that can deliver a good product in a timely manner is very helpful.

6. *Manufacture and Test Design.* Manufacturing of a system should begin as soon as the detailed design is done. As was stated above, some systems must be designed earlier in the project than others, and as soon as those designs are complete the manufacturing should begin. Some systems take significantly longer to manufacture than others. The human resources and assets of the team need to be managed to complete everything on time.

Most systems can be bench-tested to be sure that they appear to be working correctly. Bench-testing should be done for all of the electrical systems. Problems will emerge in some of the systems, and redesign or reprogramming can be done to solve those problems. Just because a system works in the lab does not mean that it will work on the car, but it is much easier to solve problems in the lab. Some bench-testing can be done on the mechanical systems to make sure they have clearance to travel through their range of motion, but from a practical standpoint it is not possible to really test the mechanical systems until the car is together and operational.

Once the car is operational, the first step should be to drive the chassis around the parking lot at low speeds. It is best to run the car on battery power only because connecting the solar array into the power system can

sometimes cause unforeseen problems. Problems may emerge during the low-speed testing, and should be corrected until the car runs reliably. Once the car seems to be running reliably, the driver should start pushing harder in the corners to put significant side loads on the suspension and chassis. The car should hit a few potholes or hard bumps. The mechanical systems should be inspected regularly during the tests to be sure they are handling the loads with no unusual deflections or deformations. It is much easier to handle a failure in a parking lot than on the road. Besides testing the car, this process gives the drivers some time learning to drive the car before taking it out on the road.

Once the car seems to be reliable driving around the parking lot, the team should connect the solar array into the power system. Some potential problems are that it produces no power or not as much power as it should, or that it overvoltages the batteries or motor controller. The team may want to put the array in the sun and have it charge a set of inexpensive lead-acid batteries before hooking it into the power system of the car. Once the car seems to work properly with the solar array and body in place, the team needs to start road testing the car and preparing for the race. For road testing, the team should go out with a lead and chase vehicle just as if they were participating in a race. The drivers need a lot of time to learn to drive the car in an efficient manner. A well-trained driver will use 20% less energy than a novice. The strategist for the race needs information on how much power the car will use at different speeds. The team needs to practice changing tires and dealing with other breakdowns. Road races are long multiday events and there will be problems. A well-practiced team will solve those problems faster and help get the car to the finish line sooner. Testing and practicing and getting good data for the energy consumption of the car are very important for success in the race. These factors are much more important than a small improvement in the design of the car.

As the car is being tested, some areas of weakness will be identified. No car is perfect. Design improvements will be proposed and the team will have to decide whether to make the improvements or to live with the existing design. These are not easy decisions. Modifying the car will usually take away test and preparation time, which hurts the car's performance in those areas. The team needs to assess the amount of time

required to make the modification. Design improvements that significantly improve the reliability of the car are generally good candidates. If a system exhibits poor reliability, it is nearly always a good idea to make modifications to improve the reliability. When deciding whether to make performance improvement modifications, the team will have to assess the amount of improvement in performance versus the amount of time that will be taken out of the test schedule.

G. References

3-1. Starr, P.J., and J.V. Carlis, "Introducing the Design Process to Beginners: The Spiral Model," *Proceedings of ASEE Conference,* Paper No. PPR-025, Minneapolis, MN, 2000.

3-2. Ullman, D.G., *The Mechanical Design Process,* McGraw-Hill, New York, 1992.

3-3. Ulrich, K.T., and S.D. Eppinger, *Product Design and Development,* McGraw-Hill, New York, 1995.

Chapter 4

Solar Array Design

Once the race begins, all of the energy the car uses comes from the sun. The power that the solar array produces is one of the most important factors in the performance of the car, and it is important to get as much power as possible. The solar array is also the most expensive component of the car in most designs. There is almost no limit as to how much money can be spent on the solar cells. The least expensive option is polycrystalline silicon cells, which can be 12 or 13% efficient at converting sunlight to electricity. It would cost about $5,000 U.S. at the time of this writing to buy enough cells to cover a solar car. Single-crystal silicon cells are 14.5–15% efficient and cost about $7,000 U.S. The single-crystal silicon cells are the most commonly used solar cells for solar cars. There are also space-grade silicon cells that are above 20% efficiency, and that cost much more than the terrestrial-grade silicon cells. Several companies make gallium arsenide (GaAs) cells that are from 18–28% efficient, and that cost from $25,000 to millions of U.S. dollars depending on the efficiency. There is a limited amount of solar array area allowed by the rules, so higher-efficiency solar cells mean more power, provided the array is designed and built properly. All things equal, 15% efficient cells will produce 25% more power than 12% efficient cells. This chapter covers the fundamentals of how solar cells work, how they are wired into an array panel, how they are integrated with the battery system, and how arrays are diagnosed and repaired.

A. Solar Cell Fundamentals

When a material is placed in the sun, some of the photons from the sun will have more energy associated with them than the energy required to remove an outer valence electron out of its orbit in the material [4-1 to 4-3]. If the photon has adequate energy, it will knock an electron out of orbit creating an

electron-hole pair as illustrated in Fig. 4.1. The hole is an atom that is missing an electron.

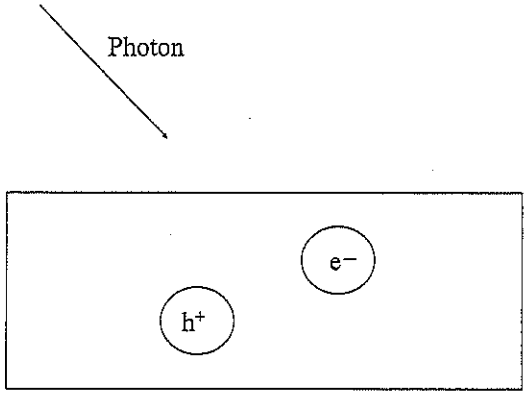

Fig. 4.1 Fundamentals of solar cells.

The free electron will migrate in the material in a random manner. The atom missing an electron may "steal" from one of its neighbors, causing its neighbor to become the hole, and in this manner the hole will migrate in the material. The sunlight will create many electron-hole pairs. When an electron and hole find each other, they recombine (liberating heat) to the equilibrium position. The bombardment of photons striking the material will continue to create electron-hole pairs. As the numbers increase, the probability of an electron recombining with a hole increases. An equilibrium density of free electron-hole pairs will be reached. The density of electron-hole pairs is proportional to the intensity of the sunlight.

Anytime there are free electrons and holes, there is the potential for generating electric power, if it can be organized and controlled. Putting two leads on the material and connecting them to a load as illustrated in Fig. 4.2 will generate a small (insignificant) amount of power.

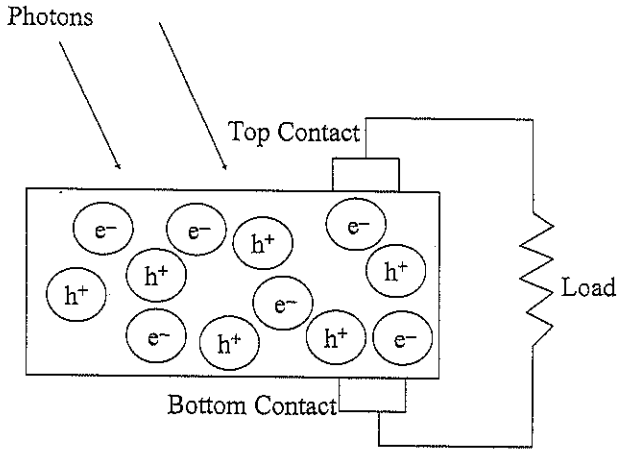

Fig. 4.2 Electron-hole pairs in a material with leads connected.

When a surplus of electrons (e^-) gets near the top contact and a surplus of holes (h^+) gets near the bottom, then some electrons (e^-) will flow into the top lead, generating a current through the load, which is electric power. It is just as likely that a surplus of electrons (e^-) could be near the bottom and a surplus of holes (h^+) near the top, causing current to flow in the opposite direction. The current through the load for this situation is very small and random in direction. This setup would be useless in generating power. The key to generating significant power is to get things organized.

Many materials (most commonly silicon) can be doped with impurities to generate n-type and p-type versions of the material. The n-type material attracts electrons (e^-) and repels holes (h^+), and p-type material attracts holes (h^+) and repels electrons (e^-). There will always be a few holes (h^+) in the n-type and a few electrons (e^-) in the p-type, but the majority of free electrons (e^-) will go to the n-type and the majority of holes (h^+) will go to the p-type. A solar cell is made by putting an n-type layer on top of a p-type layer as illustrated in Fig. 4.3.

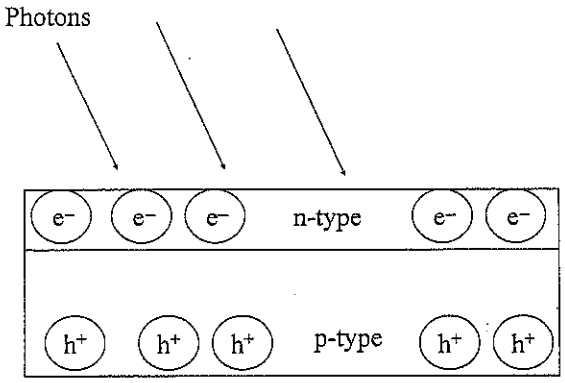

Fig. 4.3 Solar cell schematic.

When a photon liberates an electron (e^-) it will tend to migrate into the top n-type, while the hole (h^+) will tend to migrate into the p-type. The junction forms a barrier, which tends to keep the electrons and holes apart. The electrons (e^-) have like charges and repel each other, and the same is true of the holes (h^+). The solar cell will reach an equilibrium density of free electron-hole pairs, until the driving force to cross the junction and recombine is equal to the driving force of the sun to liberate them. At equilibrium, electron-hole pairs recombine at the same rate they are created.

B. Open-Circuit Voltage

Because there is a surplus of electrons on the top and a surplus of holes on the bottom, there will be a charge difference, which is a voltage between the top and bottom of the cell. Connecting a voltmeter to a lead on the top and on the bottom, as illustrated in Fig. 4.4, allows for the open-circuit voltage of the cell V_{OC} to be measured. V_{OC} depends on the material the cell is made of and the intensity of the sunlight. Higher sunlight intensity generates a higher density of free electron-hole pairs, which increases the open-circuit voltage [4-3 to 4-6].

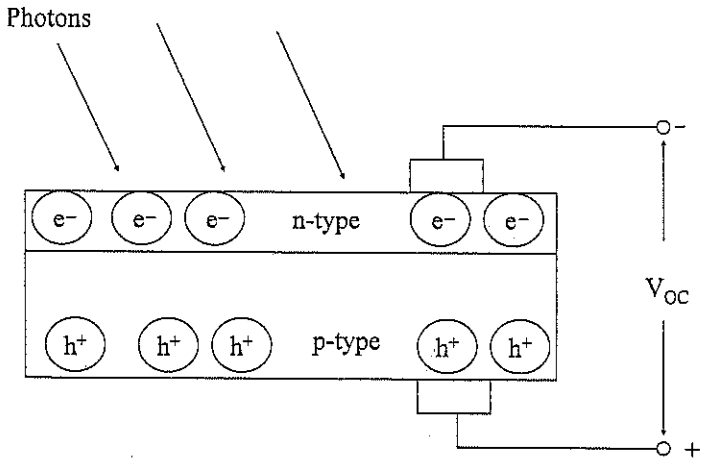

Fig. 4.4 Open-circuit voltage.

C. Short-Circuit Current

If a wire (zero resistance) is connected from the top to the bottom, the electrons will flow into the wire and recombine with the holes on the bottom as illustrated in Fig. 4.5. The voltage across the cell drops to zero and the current flowing through the wire is the short-circuit current. Short-circuit current I_{SC} depends on the material, the intensity of the sunlight, and on how the leads are designed. The electrons and holes must find their way to the leads. The resistance to their mobility in the n-type and p-type materials is the internal resistance R_S of the cell. I_{SC} is almost linearly proportional to the intensity of the sunlight, because the photons must generate electron-hole pairs at the same rate that electrons flow through the wire and recombine with holes on the bottom. I_{SC} is also linearly proportional to the size of the cell [4-3 to 4-6].

Solar cells can be made with either the n-type on top and p-type on bottom or with the p-type on top and n-type on bottom. Either way will work, but most cells are made with the n-type on top. The electrons (e^-) have more "mobility" than the holes (h^+), that is, they move around more freely and easily in the crystal than do the holes. The leads on the top of the solar cell block the

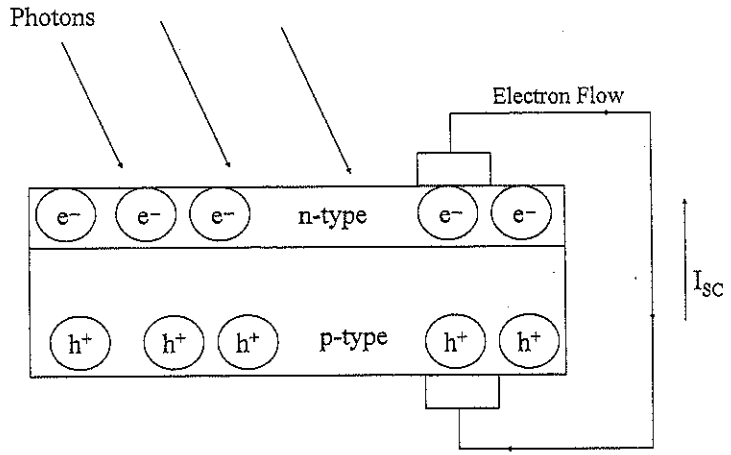

Fig. 4.5 Short-circuit current.

sunlight, so it is desirable to use as small and as few leads as possible on top. The bottom of the cell can be completely coated with silver, making one large lead. If the p-type is placed on the top, the holes h will have to move to the leads on the top, and the solar cell will have more internal resistance than if the n-type is used on top.

D. Solar Cell Efficiency—Solar Spectrum

The sun emits a broad spectrum of light, which means the photons striking the material will have different energies. One of four things can happen when a photon strikes a solar cell.

1. The photon is reflected away and no electric power is generated.

2. The photon does not have enough energy to knock the electron out of orbit. The photon is either reflected out or the energy is converted to heat and no electric power is generated.

3. The photon has exactly the right amount of energy to knock the electron out of orbit. Essentially all of the photon energy is converted to electric power.

4. The photon has more than enough energy to knock the electron out of orbit. The energy required to knock the electron out of orbit will be converted to electric power, and the excess will be converted to heat.

The solar spectrum is illustrated in Fig. 4.6 [4-7]. The AM0 radiation is approximately what is received by satellites above the atmosphere and AM1.5 is approximately what is received at sea level on a clear sunny day. The atmosphere attenuates all wavelengths, and it attenuates some more than others as illustrated in the figure. It is important to understand the AM system when selecting solar cells for the car. Solar cells will produce more power when tested at AM0, but most cells have a higher efficiency rating when tested at AM1.5. When comparing the performance of two different solar cells to decide which ones to buy for the car, it is important that they be compared at the same rating.

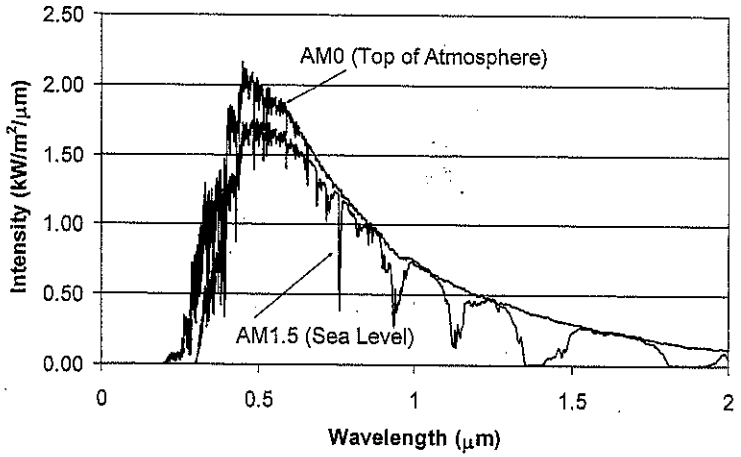

Fig. 4.6 Solar spectrum. (Data for the figure provided by Dr. Judith Lean, U.S. Navy Research Laboratory [4-7].)

If the sun emitted photons that all had the same energy, like a laser, then a material could be chosen for the solar cell that had electron-hole creation energy slightly lower than the photon energy. Nearly all of the energy of the laser light would be converted to electric power for this material. It would have a very high efficiency. This may have applications in space in the distant future. Electricity could be converted to laser light, which could be beamed to a solar collector, which would convert it back to electricity.

However, the sun emits a range of photon energies. For any material chosen, some photons will not have enough energy to liberate an electron and will be wasted. Others will have more than enough energy to liberate an electron, and their excess will be wasted. The material should be selected to match the solar spectrum[4-1]. Silicon is a good choice because it is near the theoretical optimum. A silicon cell can theoretically be 29% efficient in converting sunlight to electricity. Silicon cells have actually been manufactured that are 24% efficient [4-8], but the common grades of single-crystal silicon cells are 12--15% efficient. Amorphous and polycrystalline silicon cells are less efficient.

Gallium arsenide (GaAs) has a higher theoretical efficiency than silicon. The most efficient cells that have been produced were made from GaAs [4-8]. Another advantage of GaAs cells in racing is that their efficiency is not as sensitive to high temperatures, so in the summer the GaAs cells may be significantly more efficient than silicon cells. There are some other exotic materials that have high theoretical efficiency, but have not developed to any extent beyond basic research. Examining the solar spectrum, it can be shown that the ideal material would have a theoretical efficiency of approximately 31%, and GaAs is very near the ideal. The limiting theoretical efficiencies for single-junction cells, and the highest efficiency actually achieved is shown in Fig. 4.7 [4-1, 4-8].

Multijunction cells have been developed to further improve efficiency. The goal is to get high-energy photons to knock high-energy electrons out of orbit, thus converting a higher percentage of their energy to electric power. Low-energy photons would knock low-energy electrons out of orbit and their power would be efficiently converted to electric power. For two band gaps the maximum theoretical efficiency increases to 50%, for three it is 56%, and for 36 it is 72% [4-1]. Multijunction cells were used in a solar car for the first time in a car created by Solar Motions and driven in the 1999 World Solar

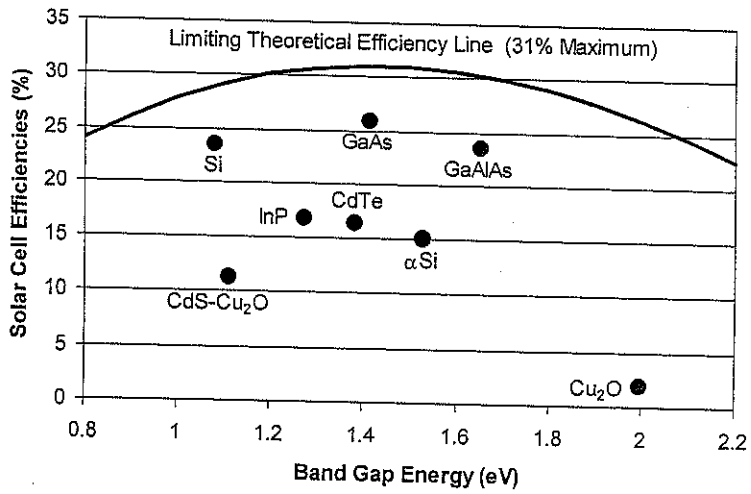

Fig. 4.7 Maximum theoretical efficiency of solar cells. (Theoretical line developed from [4-1], data points from [4-8].)

Challenge. Several teams used multijunction cells in the 2001 American Solar Challenge and World Solar Challenge.

Multijunction cells produce more power in bright sunlight than single-junction cells. The (very limited) race experience up to now shows that the power drops off significantly in cloudy conditions. It may be that the clouds attenuate some wavelengths more than others, causing one junction of the cell to be starved for free electrons. Since the junctions are electrically in series, shutting down one junction would shut down the entire cell. This is just a theory now. There will be a lot of testing in the next 2 years, and a better understanding will be developed of why the multijunction cell output drops so much in cloudy conditions. Multijunction cells are the best solution in bright sunny conditions because they produce the most power. They may or may not be the best solution in cloudy conditions.

E. Solar Cell Model

A solar cell is a p-n junction. It is basically a diode, but it is a special kind of diode. If no sunlight is striking the cell, then it will behave exactly like a diode, allowing current to flow freely in one direction, and preventing flow in the other direction, as illustrated in Fig. 4.8. Notice that the solar cell generates current in the opposite direction so that it will pass current freely as a diode. From a design viewpoint there are two consequences to this.

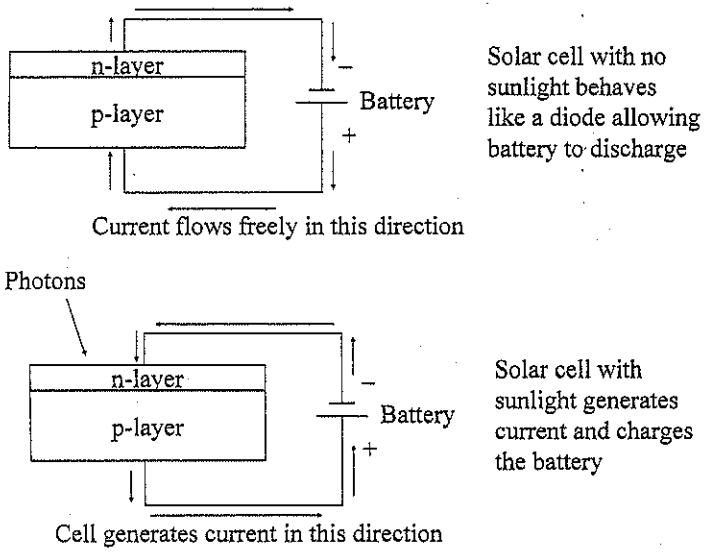

Fig. 4.8 Solar cell–diode model.

1. If a solar array is charging batteries, then a switch or some other means must be included in the circuit. The switch would be used when there is no sunlight on the array, to prevent the batteries from discharging through the array, as illustrated in Fig. 4.9. If the switch is not opened at night, the battery will drive current through the array in the opposite direction and discharge itself.

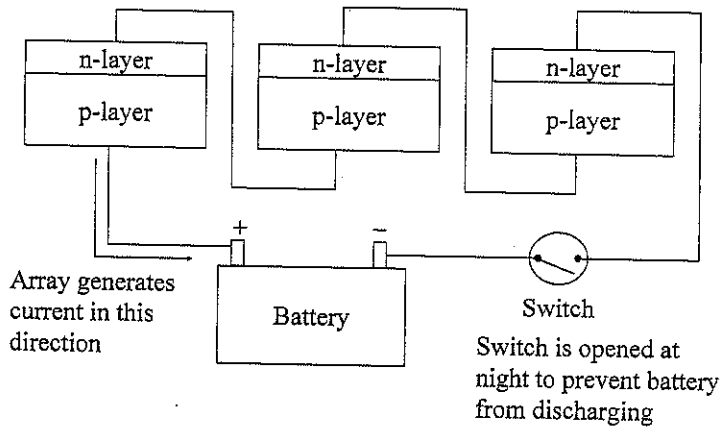

Fig. 4.9 Switch to prevent batteries from discharging.

2. If a single cell in the string is shaded so that it does not receive sunlight, then that cell will not generate any current. The other cells will try to drive current through it, but that is like trying to drive current backward through a diode. One shaded cell will stop current flow from the entire string, even if the other cells are receiving good sunlight. A corollary to this is that the string will produce only as much current as the weakest cell. Careful cell matching is required for a good array design. An electric circuit can be drawn that is analogous to a solar cell, as shown in Fig. 4.10 [4-1].

The analogy of each of the components in Fig. 4.10 and how they are related to the solar cell is explained below:

a. I_L is a current source that is analogous to the potential current the sunlight creates.

b. I_S is the diode saturation current, assuming the cell is completely shaded.

c. R_{SH} is the shunt resistance. Some electron-hole pairs will recombine across the junction. R_{SH} is the resistance to this "current leak." Ideally a

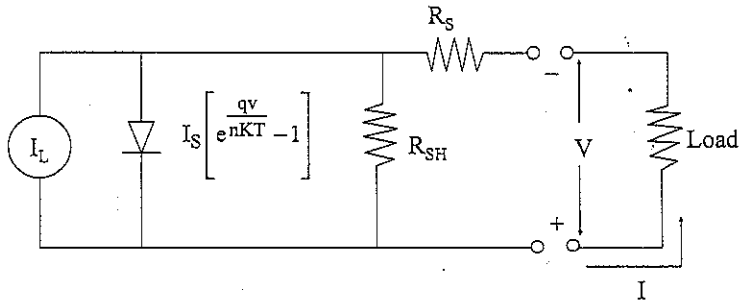

Fig. 4.10 Electrical model of solar cell.

solar cell would have infinite shunt resistance, that is, $R_{SH} = \infty$ ideally, but for real cells that is not possible.

d. R_S is the internal series resistance of the cell. Cells have an internal resistance that absorbs some of the energy they create. Ideally $R_S = 0$, but for real cells that is not possible.

e. I is the output current of the cell.

f. V is the output voltage of the cell.

g. q is the charge of an electron ($1.6021773 \times 10^{-19}$ C), K is Boltzmann's constant (1.380658×10^{-23} J/K), T is absolute temperature, and n is a model parameter that is 1.5 for silicon cells.

It can be shown that the output voltage and current from such a circuit are related by Eq. 4.1.

$$I = I_L - I_S\left[e^{\frac{q}{nKT}(V+IR_S)} - 1\right] - \frac{V+IR_S}{R_{SH}} \qquad (4.1)$$

The above model can be fit to solar cell data using the open-circuit voltage V_{OC} and the short circuit current I_{SC} as illustrated in Eq. 4.2.

$$\begin{aligned} V &= V_{OC} \quad \text{when } I = 0 \\ I &= I_{SC} \quad \text{when } V = 0 \end{aligned} \qquad (4.2)$$

If the series and shunt resistance of the solar cell is known, then a complete model for the cell can be developed, but most solar cell manufacturers do not provide values for these resistances. In such cases, a reasonably accurate model can be developed for the solar cell based on the characteristic resistance R_{CH} of the cell defined in Eq. 4.3 [4-9].

$$R_{CH} = \frac{V_{OC}}{I_{SC}} \qquad (4.3)$$

where V_{OC} is the open-circuit voltage for the cell and I_{SC} is the short-circuit current. The resistances R_S and R_{SH} are related to the characteristic resistance. For a typical silicon solar cell, approximate relations are given in Eq. 4.4 [4-9].

$$\begin{aligned} R_{SH} &= (1000)R_{CH} \\ R_S &= (0.1)R_{CH} \end{aligned} \qquad (4.4)$$

Knowing the open-circuit voltage V_{OC} and short-circuit current I_{SC} an approximate model can be developed for the cell using the above assumptions. The advantage of the approximate model is that only the open-circuit voltage and short-circuit current for the cell need to be known, and it is relatively easy to obtain these values.

Example: Assume $I_{SC} = 3.5$ A and $V_{OC} = 0.62$ V at 300 K. Construct the I-V diagram. For the solution the series and shunt resistances are estimated using Eq. 4.5.

$$R_{CH} = \frac{0.62\ V}{3.5A} = 0.177\ \Omega$$

$$R_S = 0.0177\ \Omega \qquad (4.5)$$

$$R_{SH} = 177\ \Omega$$

Equations 4.6 and 4.7 can be used to solve for I_L and I_S.

$$3.5 = I_L - I_S\left[e^{\left(\frac{1.6021773\times10^{-19}}{(1.5)(1.380658\times10^{-23})(300)}\right)[0+(3.5)(0.0177)]} - 1\right] \qquad (4.6)$$

$$-\frac{0+(3.5)(0.0177)}{177}$$

$$0 = I_L - I_S\left[e^{\left(\frac{1.6021773\times10^{-19}}{(1.5)(1.380658\times10^{-23})(300)}\right)[0.62+(0)(0.0177)]} - 1\right] \qquad (4.7)$$

$$-\frac{0.62+(0)(0.0177)}{177}$$

Solving yields I_L = 3.50035 A and I_S = 3.9813 × 10^{-7} A. Equation 4.8 describes a typical 100 mm × 100 mm silicon terrestrial-grade cell when exposed to bright sunlight:

$$I = 3.50035 - \left(3.9813\times10^{-7}\right)\left[e^{\left(\frac{7736.3}{T}\right)[V+(I)(0.0177)]} - 1\right] \qquad (4.8)$$

$$-\frac{V+(I)(0.0177)}{177}$$

Table 4.1 lists the current versus voltage data for the solar cell. A plot of the I-V curve is shown in Fig. 4.11.

TABLE 4.1
CURRENT VERSUS VOLTAGE DATA

Current	Voltage	Current	Voltage
3.5	0	3.4907	0.32
3.4999	0.02	3.4855	0.34
3.4998	0.04	3.477	0.36
3.4997	0.06	3.463	0.38
3.4995	0.08	3.44	0.4
3.4994	0.1	3.4025	0.42
3.4993	0.12	3.3425	0.44
3.4991	0.14	3.2487	0.46
3.499	0.16	3.1068	0.48
3.4988	0.18	2.9017	0.5
3.4985	0.2	2.62	0.52
3.4982	0.22	2.2539	0.54
3.4977	0.24	1.8025	0.56
3.4969	0.26	1.2707	0.58
3.4957	0.28	0.6666	0.6
3.4938	0.3	0	0.62

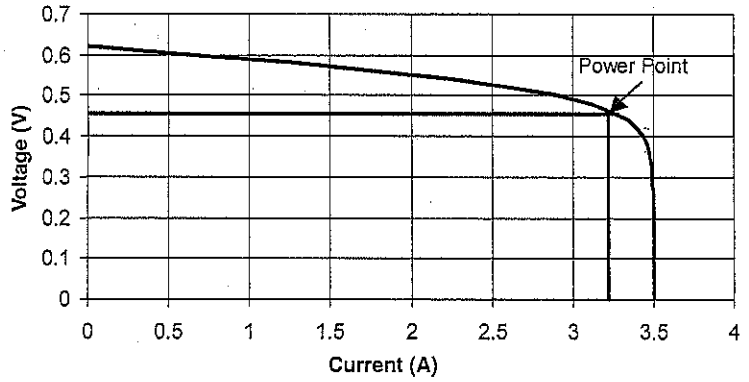

Fig. 4.11 Typical solar cell I-V curve.

The maximum power output for this cell is 1.5 W when I = 3.20 A and V = 0.468 V, as illustrated in Table 4.1. The model can be used to illustrate several things about solar cells and solar arrays.

F. Illumination Level I_L

Open-circuit voltage varies gradually with the illumination level over a broad range of illumination levels. The open-circuit voltage drops off sharply at very low illumination levels. Power point voltage also varies gradually with illumination level. The increase in power from the cell with increased illumination comes primarily from its increased ability to provide current. Short-circuit current and power point current are almost linearly proportional to the illumination level. The power that the cell produces is also almost linearly proportional to illumination level.

The solar cell model can be used to show how voltage, current, and power vary with illumination level. For one-sun illumination (the illumination intensity of the sun on a standard clear day at sea level), I_L was set to 3.5035 and Figs. 4.12 and 4.13 were developed. These illustrate quantitatively how the performance of the cell varies with illumination level.

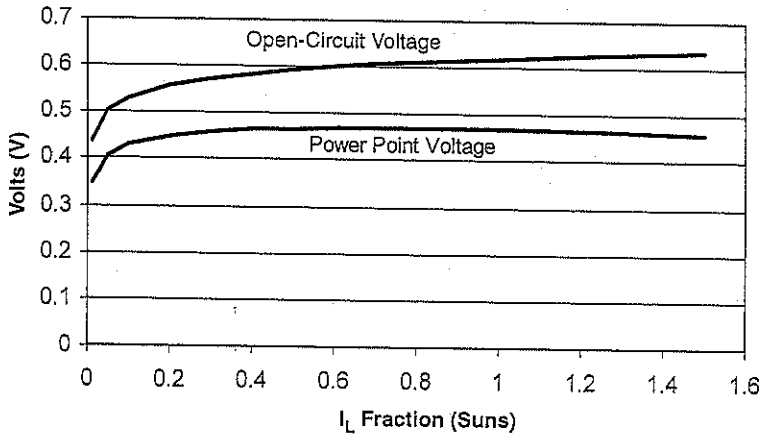

Fig. 4.12 Effect of illumination level on solar cell voltages.

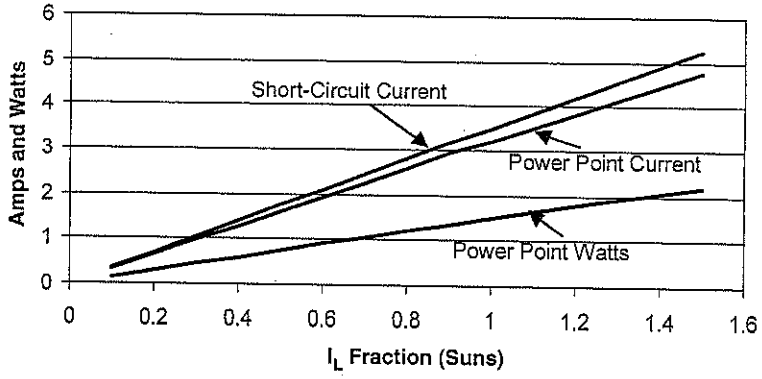

Fig. 4.13 Effect of illumination level on solar cell currents and power.

G. Temperature

The diode saturation current I_S for the solar cell is a function of temperature as illustrated in Eq. 4.9.

$$I_S = I_{S\infty} e^{-\frac{E_g}{nRT}} \tag{4.9}$$

where $I_{S\infty}$ is the saturation current for $T = \infty$ (a fictitious value) and E_g is the band gap energy for the material [4-1]. $E_g = 1.12$ eV for silicon, and for the model cell it was determined that $I_S = 3.9813 \times 10^{-7}$A when T = 300 K. Equation 4.10 shows how the diode saturation current varies with temperature for the model solar cell.

$$I_S = (1.391 \times 10^6)\, e^{-\frac{8664.7}{T}} \tag{4.10}$$

Substituting this for I_S in the model, it is possible to plot how voltage, current, and power vary with temperature. Both open-circuit voltage and power point voltage decrease linearly with temperature as illustrated in Fig. 4.14. The model shows short-circuit current I_{SC} to be constant with temperature as shown in Fig. 4.15. The power point decreases almost linearly with temperature over this range. On the range of 0–100°C (32–212°F) the efficiency of the cell in converting light to electricity decreases the cell output by 0.00617 W for each 1°C rise in temperature, as shown in Fig. 4.16. This leads to a widely accepted "rule of thumb": the array output decreases by 0.5% for every 1°C rise in temperature [4-4 to 4-6].

This rule of thumb is a good estimate for terrestrial-grade silicon cells. The very high-efficiency silicon cells lose about the same (0.617 W/m^2/°C) power, but because they have a higher power density output, this represents only about a 0.3% reduction in power for each 1°C. An advantage of using GaAs cells is that their efficiency does not decrease as rapidly as silicon cells with temperature.

The solar array will heat up considerably in operation because of all the photon energy being converted to heat. Many teams cut holes in the body

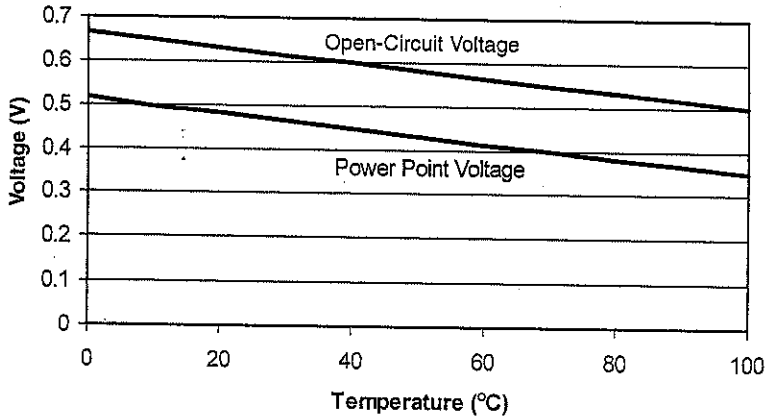

Fig. 4.14 Effect of temperature on solar cell voltages.

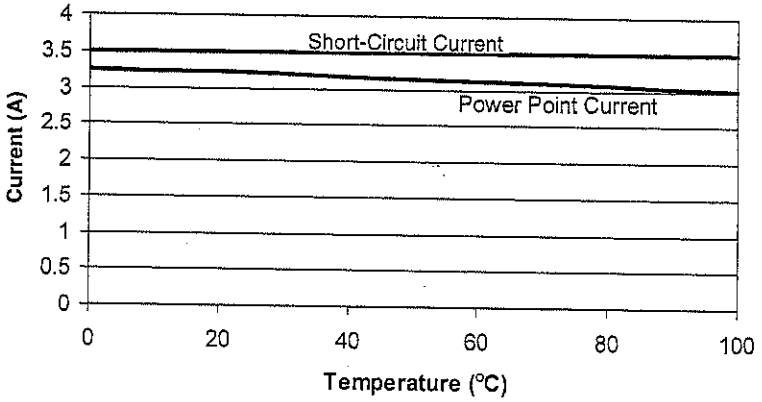

Fig. 4.15 Effect of temperature on solar cell currents.

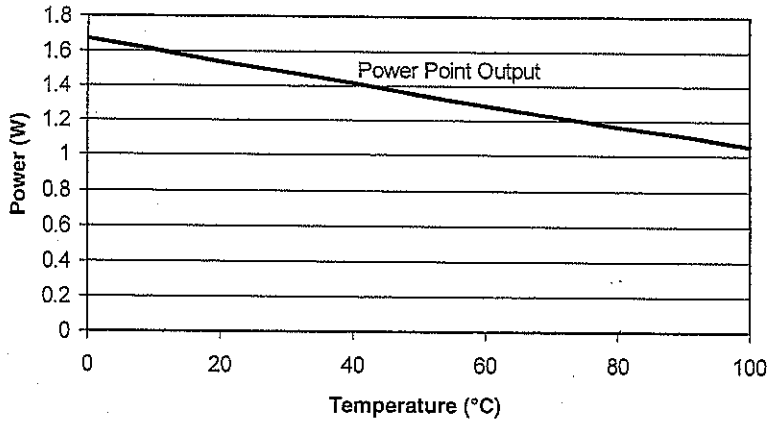

Fig. 4.16 Effect of temperature on solar cell power.

behind the solar cells to keep them cooler while driving. It is common to spray a fine mist of water on the array when it is charging on the array stand to cool the cells. The cells can reach temperatures of 70–80°C when the array is on the charging stand. The evaporative cooling of water droplets can reduce the temperature to 30°C and thus provide a 15–20% increase in array power on a bright, hot sunny day. Distilled water should be used to avoid leaving mineral deposits on the array. It is the evaporative cooling that cools the cells, so a fine mist is better than flooding the cells with water.

Cooling the silicon cells increases power output by increasing the voltage output of the solar array; cooling does not increase the current output significantly. This can be verified experimentally by connecting a multimeter to measure open-circuit voltage of a silicon cell, and then placing the cell in the sun. As the cell heats up the open-circuit voltage will decrease significantly. The experiment can be repeated by hooking the multimeter to measure short circuit current, and it will be observed that the current does not change significantly as the cell heats up. The same effect happens with GaAs cells, but the decrease in voltage is less significant.

Most teams feel that spraying the GaAs cells with distilled water will not significantly increase the power they produce. Cooling the cells will increase the voltage they produce, but the water droplets will block some of the sunlight and decrease the current the cells produce. No careful study has been done to determine if spraying the GaAs cells has a net increase or decrease on their power output, so the answer is not known at this time. Spraying the silicon cells with water will significantly increase the power they produce.

Some teams have tried to develop cooling systems that operate while the car is driving, but such systems add weight and use power. So far no team has developed a system that produces a net gain in energy efficiency. Water spray systems require that the water weight be carried when the car is driving, and forced air cooling systems absorb a lot of electric power.

H. Coatings

The solar array must be coated to keep it from shorting out when it gets wet. A major disadvantage of a coating is that it insulates the cells and makes them hotter and less efficient. However, to be able to spray water on the array and cool it or drive in the rain, the array must have a waterproof coating. There have been very few solar car races during whch it did not rain at least 1 day.

Stationary arrays such as those used on the roofs of buildings commonly use a glass coating because the glass is more scratch resistant than polymer coatings. However, glass is too heavy for solar cars. Polymer coatings are always used on solar cars, and it is important to be careful when cleaning the car so that the coating is not scratched. Tedlar, Tefzel, Lexan, and Epoxy have all been used successfully. The primary goal is to provide a thin coating that allows the light through and protects the cells from water. In recent years two minor improvements have been tried.

1. *Antireflection Coatings.* Bare solar cells reflect a significant portion of the light that hits them, especially light coming from oblique angles. Typically the array coatings have an index of refraction of 1.0–1.5, which will bend the light rays and direct them more toward the solar cells [4-4 to 4-6, 4-10]. Antireflection coatings will direct a higher

percentage of the light into the cells than using no coating at all. Ideally the coating would have an index of refraction of 1.0, so finding suitable polymers with an index of refraction between 1.0 and 1.5 will slightly increase array power as compared to bare cells. Approximately 4% increase in array power is the maximum possible benefit of using an antireflection coating instead of bare cells.

2. *Texturing.* Texturing the surface of the coating will have very little effect on normal incident light rays, but will assist in absorbing the oblique angle rays, as illustrated in Fig. 4.17 [4-4]. The disadvantage of texturing is that it makes it difficult to clean the solar array. Dust particles get down into the valleys of the texture and are difficult to remove. A coating that is easy to scratch and difficult to clean is undesirable, so most solar car arrays do not use a textured coating.

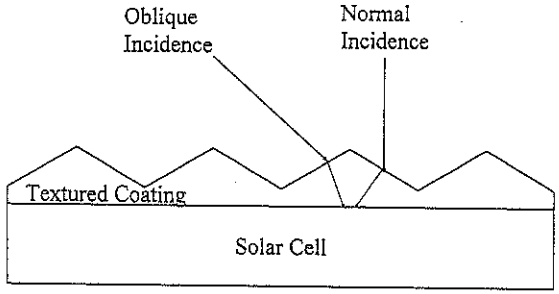

Fig. 4.17 Textured coating for solar arrays.

I. Wiring the Solar Array

There are some important considerations in wiring the cells into an array. The array voltage must be matched with the battery system voltage and the power point trackers [4-4 to 4-6, 4-11]. Ideally the array voltage should be slightly higher than the battery system voltage. This allows for the use of a step-down transformer, which is more efficient than a step-up transformer. To achieve a typical battery system voltage of 100 V, many cells must be wired in series as illustrated in Fig. 4.18.

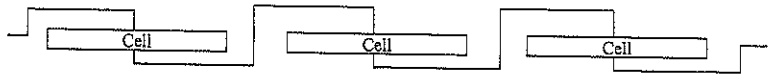

Fig. 4.18 Series wiring of solar cells.

In a series wiring circuit, the same current passes through all the solar cells. It is important that all cells in the string have approximately the same power point current. As an example, consider two cells in series that have different power point currents. Cell no. 1 has a power point of 1.497 W at 0.468 V and 3.199 A, and cell no. 2 has a power point of 1.0546 W at 0.470 V and 2.244 A.

If both cells could operate at their power point, the two cells could generate $1.497 + 1.0546 = 2.5516$ W between them. But if these two cells are wired in series, they must both carry the same current, and so they cannot both operate at their power points. If the current carried by the two cells is I and the voltages provided are V_1 and V_2, then the wiring schematic is as shown in Fig. 4.19.

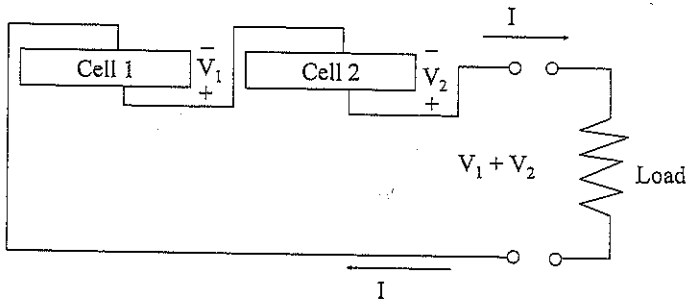

Power Output = $I(V_1 + V_2)$

Fig. 4.19 Wiring schematic of mismatched solar cells.

Fig. 4.20 shows I-V curves for cell no. 1 and cell no. 2 using the model developed in the previous section.

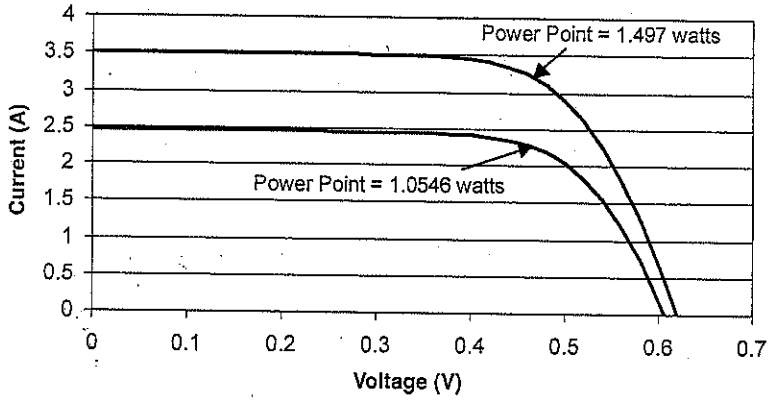

Fig. 4.20 I-V curves for mismatched cells.

To maximize the power, it is necessary to maximize the quantity $I(V_1 + V_2)$. The power point current for the two cells in series will be near the power point current for the weaker cell (cell no. 2). Table 4.2 shows the current, voltage, and power of each cell, and the total power of the two cells in series. This table was used to find the power point of the two cells if wired in series.

The true maximum output is 2.292 W when I = 2.34 A, V_2 = 0.4436 V, and V_1 = 0.5357 V. The weakest cell has a power point current of 2.244 A, and at that current the two cells would produce 2.2675 W. The true power point for the two cells in series is only slightly greater than what would be calculated by assuming that the power point current for the two cells is the same as the power point current of the weakest cell. Two bounds can be set for the power point current for a string of cells. The power point current will be greater than the lowest power point current of any cell in the string, and the power point current will be less than the short-circuit current for any cell in the string. *The true power point current for a string of cells will be between the power point current and short-circuit current of the weakest cell in the string.*

TABLE 4.2
DATA FOR MISMATCHED CELLS WIRED IN SERIES

Series Current	Cell No. 2 Voltage	Cell No. 1 Voltage	Cell No. 2 Power	Cell No.1 Power	Total Power
2.21	0.4766	0.5421	1.053286	1.198041	2.251327
2.22	0.4747	0.5416	1.053834	1.202352	2.256186
2.23	0.4728	0.5412	1.054344	1.206876	2.261220
2.24	0.4708	0.5407	1.054592	1.211168	2.265760
2.25	0.4687	0.5402	1.054575	1.215450	2.270025
2.26	0.4665	0.5397	1.054290	1.219722	2.274012
2.27	0.4642	0.5392	1.053734	1.223984	2.277718
2.28	0.4618	0.5387	1.052904	1.228236	2.281140
2.29	0.4592	0.5382	1.051568	1.232478	2.284046
2.30	0.4565	0.5377	1.049950	1.236710	2.286660
2.31	0.4536	0.5372	1.047816	1.240932	2.288748
2.32	0.4505	0.5367	1.045160	1.245144	2.290304
2.33	0.4470	0.5362	1.041510	1.249346	2.290856
2.34	0.4436	0.5357	1.038024	1.253538	2.291562
2.35	0.4396	0.5352	1.033060	1.257720	2.290780
2.36	0.4352	0.5347	1.027072	1.261892	2.288964
2.37	0.4304	0.5341	1.020048	1.265817	2.285865
2.38	0.4248	0.5337	1.011024	1.270206	2.281230
2.39	0.4185	0.5331	1.000215	1.274109	2.274324
2.40	0.4110	0.5326	0.986400	1.278240	2.264640

It is tedious generating the numbers for the spreadsheet when there are several cells in a string. I_P for the string will be between I_P and I_{SC} of the weakest cell ($I_{Pweakest} < I_{Pstring} < I_{SCweakest}$). In most cases there is not a large difference between I_P and I_{SC} of the weakest cell. A good first approximation is to assume that the power point current for the string is halfway between the power point and short-circuit currents for the weakest cell, as illustrated in Eq. 4.11.

$$I_{P\,string} \approx \left[\frac{I_P + I_{SC}}{2}\right]_{\text{for weakest cell}} \tag{4.11}$$

Example. Assume there are ten cells in a string. Nine are good like cell no. 1 and one is weak like cell no. 2. What is the estimated power of the string? Equation 4.12 shows the calculations involved in estimating the power output of the string.

Assume

$$I_P = \frac{2.244 + 2.45}{2} = 2.347 \text{ A}$$

$$V_{1-9} = 0.5354 \text{ volts}$$

$$V_{10} = 0.4408 \text{ volts} \tag{4.12}$$

$$\text{Power} = 9(2.347)(0.5354) + (2.347)(0.4408) = 12.344 \text{ W}$$

An important thing to notice is that if the one weak cell were removed, then each of the nine good cells would produce 3.199 A at 0.468 V for a total of 13.474 W, which is more than the ten cells produce. *So the tenth cell is actually reducing the power of the string.* It would be better to wire around the weak cell and cut it out of the string. This example helps to explain why it is so important to match cells in a string so they all have approximately the same power point current. Sometimes the cells are cut into smaller pieces, so that the array or portions of the array are made up of small cells. The power point current is linearly proportional to the size of the cell, so it would never be proper to put cells of different sizes in the same string.

J. Shading of the Array

If one cell in a string is shaded, then its illumination level current (I_L) will be drastically reduced. The one shaded cell will have a greatly reduced short-circuit and power point current, and will limit the current in other cells in the string. If the cell is completely shaded and receives no solar energy, then the cell will act as a diode blocking the current and the string of cells will pass essentially zero current. The power output of the entire string will be zero. Bypass diodes are incorporated into the array wiring to bypass weak or damaged strings, but it does not take much shading to dramatically lower the power output of the array, even with the bypass diodes.

K. Cell Matching

Solar cells should be matched so that all the cells in a string have the same power point current. There will be minor variations from cell to cell even when they are of the same type and out of the same lot. One approach to matching is to measure the I-V curve for every cell and group them so that they are as perfectly matched as possible. This is a lot of effort for a small gain in power if the cells are first quality terrestrial-grade, because there is very little difference from cell to cell. First-quality terrestrial-grade silicon cells are not usually matched because it is not worth the time and cost. Matching is very helpful if the team receives a donation of space-grade "rejects," and wishes to pick out the best cells and match them as best as possible. Matching is very important for space-grade cells because the power point varies a lot from cell to cell, even for first-quality space-grade cells.

L. Angling of Cells in a String

The body of the car will be curved to optimize aerodynamics, and the cells will be placed on a curved surface as illustrated in Fig. 4-21. This causes different cells in the string to have different angles with respect to the sun. In turn, this gives them different I_L currents, which makes their power point currents different, which makes them poorly matched.

The I_L current varies approximately with the cosine of the angle θ between the sun and the cell as was shown in Chapter 2. If the angle between two

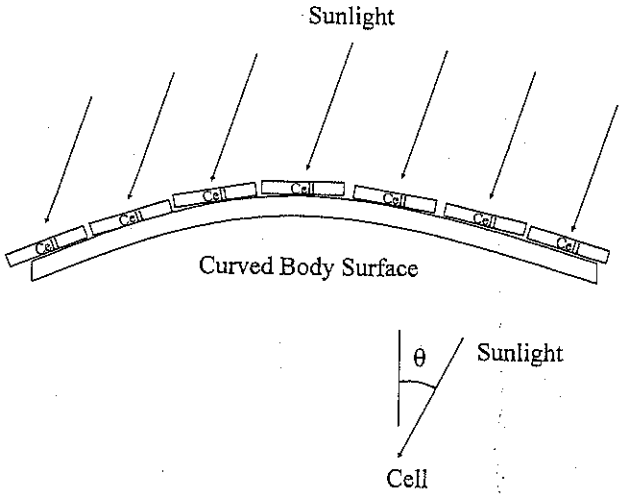

Fig. 4.21 Solar cells on a curved body surface.

perfectly matched cells is $\theta_2 - \theta_1$, then the mismatch of power introduced can be approximated as shown in Eq. 4.13. Table 4.3 shows approximate power losses for different sun angles and mismatch angles.

$$\text{Mismatch power} = \left[\cos(\theta_1) - \cos(\theta_2)\right] \times 100\% \qquad (4.13)$$

The mismatch power is an estimate of what percentage of power output will be lost because the cells in an array have different angles to the sun. On the charging stand the solar array will be directed at the sun so that presumably some of the solar cells in the array would have a zero sun angle. In this case even a 10° misalignment in the array would cause only 1.52% reduction in power. Misalignment of cells in the solar array is less critical when the array is pointed at the sun, as it would be on the charging stand. When driving the car, the solar array will not be aligned with the sun, and misalignment of the cells in the subarrays becomes more critical. Early morning and late evening sun angles can be 50° or higher and the reduction in power due to misalignment of cells in the subarrays becomes very significant.

TABLE 4.3
ESTIMATED POWER LOSS DUE TO MISALIGNMENT OF SOLAR CELLS

θ_1	θ_2	Mismatch	θ_1	θ_2	Mismatch
0	2°	0.06%	10°	12°	0.67%
0	4°	0.24%	10°	14°	1.45%
0	6°	0.55%	10°	16°	2.35%
0	8°	0.97%	10°	18°	3.38%
0	10°	1.52%	10°	20°	4.51%
30°	32°	1.80%	50°	52°	2.71%
30°	34°	3.70%	50°	54°	5.50%
30°	36°	5.70%	50°	56°	8.36%
30°	38°	7.80%	50°	58°	11.29%
30°	40°	10.00%	50°	60°	14.28%

Ideally all cells in the subarray should be parallel, or as parallel as possible. The subarrays should be laid out on the body to keep the cells as parallel as possible. As an example, if the body is a simple curve as shown in Fig 4.22, and there are three arrays on the body, there is a good way and bad way to place the arrays on the body. The good placement keeps the cells in the individual subarrays as parallel as possible. The bad placement causes the cells on the opposite sides of the body to be very unparallel. The good placement will produce considerably more power than the bad placement while driving, especially during early morning and late evening driving. The difference when charging on the array stand will not be as great.

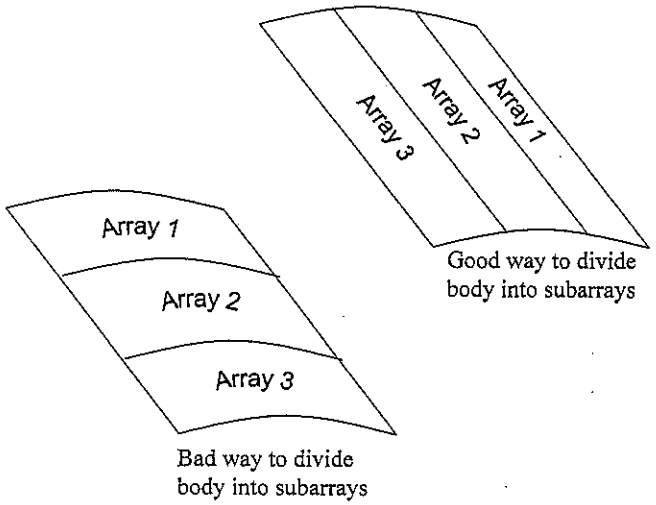

Fig. 4.22 Arranging subarrays on a curved body.

M. Shingling of Cells

The cells come with very thin silver strips to collect the electrons. These strips are connected to wider buses as shown in Fig. 4.23. These collectors are necessary for the cell to produce electricity, but block the sunlight from the cell, reducing the illumination level. Making these collectors too small increases the series resistance of the cell R_S. Getting maximum power from the cell involves a compromise between blocking some of the sunlight and reducing the series resistance of the cell.

Shingling of cells involves cutting the cells into smaller pieces and overlapping to cover the wide buses. The cells must be cut to the shape shown in Fig. 4.24.

After being cut, the pieces must be matched so that all of the cells in any string have very close to the same power point current I_P. Cells are then overlapped as shown in Fig. 4.25 so that the wide buses are no longer blocking the sunlight.

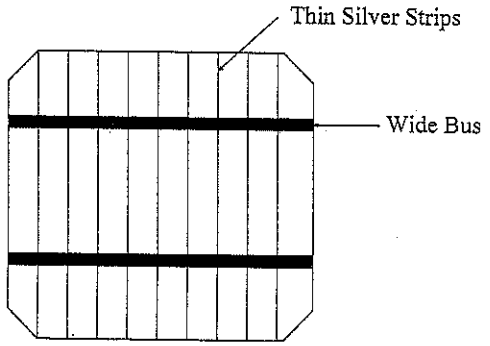

Fig. 4.23 Solar cell thin silver strips and wide bus.

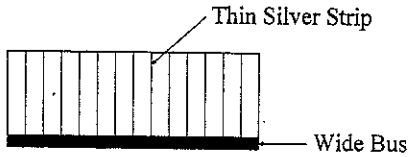

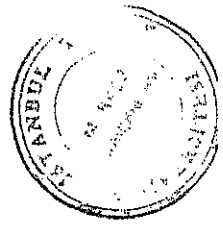

Fig. 4.24 Cut cell prepared for shingling.

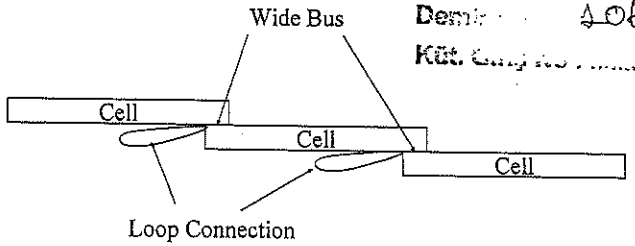

Fig. 4.25 Shingled cells.

A loop-type connection is generally made between the bottom of one cell to the wide bus on the cell below. Direct solder connections are not used because thermal expansion of the array will inevitably break the connection. Shingling covers the wide bus bars, and thus increases the percent coverage (and array power) by a few percent. It is a lot of work for a small benefit, but shingling will increase array power by a few percent.

N. Series-Paralleling of Cells

This is an advanced topic that requires considerable effort in matching short strings of cells [4-12]. Series-paralleling is an important topic if the team is using GaAs solar cells, or is shingling small silicon cells. When small cells are used, it may be impractical to have a single string of cells for each subarray because it would create too many subarrays. As an example, consider double-junction GaAs solar cells with a power point voltage of 2.0 V. The nominal battery voltage is 100 V, and the array voltage might be set at 150 V so that step-down power trackers can be used. It would be necessary to wire 75 solar cells in series to achieve the desired array voltage. It takes approximately 3000 of these solar cells to make the 8-m^2 array allowed by the race rules, so there would be 40 subarrays if they were wired in single strings. The team would need to buy 40 power trackers and find a place for them on the car. All of the subarrays would need to be debugged and monitored, and this is impractical. If the team is going to use space-grade cells, then some series-paralleling will be necessary.

Within each short string (3–10 cells) the cells are matched in series as closely as possible by power point current. The short strings are matched in parallel by power point voltage as illustrated in Fig. 4.26. Two strings that have the same power point voltage can be put in parallel.

The power output for this case is $(I_{P1} + I_{P2})\, V_P$, and because both strings have the same V_P this is equal to the maximum total power the two strings can produce. This series-parallel module is connected to another as shown in Fig. 4.27.

To maximize the power output of the solar array, the short strings must be matched so that the currents match as shown in Eq. 4.14.

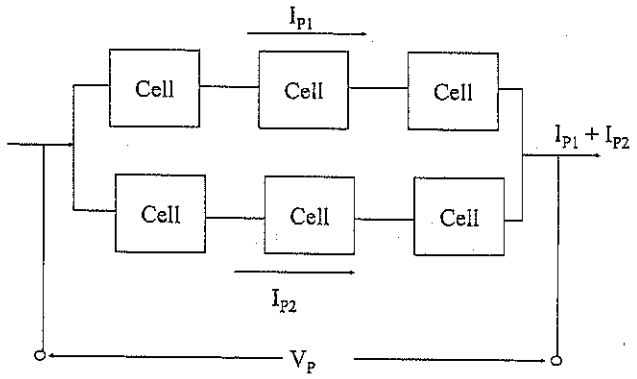

Fig. 4.26 Series-paralleling of solar cells.

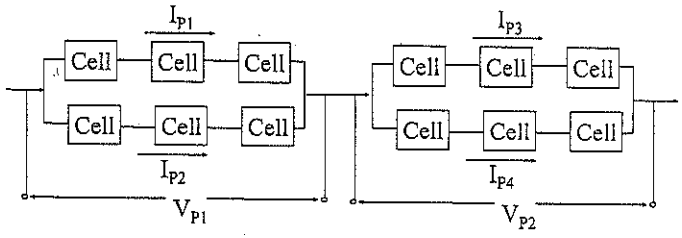

Fig. 4.27 Connecting series-parallel modules.

$$I_{P1} + I_{P2} = I_{P3} + I_{P4} \tag{4.14}$$

The advantages to series-paralleling are that it is possible to better match the solar cells and it is possible to wire more solar cells into the same power tracker and have fewer subarrays to debug and monitor. Three to ten subarrays is an acceptable number; the ideal number is five or six. Individual cells are made into short strings with all cells in the individual strings having the same I_P. The short strings are matched by V_P of the string. Then there is more flexibility in matching total current for two strings.

Example: $I_{P1} = 3.0$ A, $V_{P1} = 1.4$ V

$I_{P2} = 3.25$ A, $V_{P1} = 1.4$ V

$I_{P3} = 3.1$ A, $V_{P1} = 1.35$ V

$I_{P4} = 3.15$ A, $V_{P1} = 1.35$ V

By putting the cells together in the series-parallel arrangement in Fig. 4.27, each short string can operate at its power point, and the total power is the sum of the power points for the four short strings. On the other hand, if any two of the strings were placed in series, then they would be mismatched to some extent.

Series-paralleling was first proposed as a way to better match terrestrial-grade silicon cells. It offers the possibility of better overall matching, but it is a *lot* of work for a small gain and is probably not worth the effort. When small solar cells are used, it is necessary to use series-paralleling to reduce the number of subarrays to a reasonable number. This is the practical application of series-paralleling the solar cells.

O. Bypass Diodes

Diodes are usually wired around short strings to prevent one cell from completely blocking the current. The diodes are not active unless a reverse voltage develops across them. In Fig. 4.28, assume that each of the good cells produce 0.5 V at the power point, and that the bypass diode is wired around four cells as shown.

In Fig. 4.28(a) all cells are good and no current flows through the bypass diode. The voltage gain across the six cells will be 3.0 V, and if the cells are producing 3 A, these six cells produce 9 W power. In Fig. 4.28(b) there is a "bad cell" indicated. The other cells are trying to drive current through it, reversing the voltage across it. Without a diode, the bad cell would not allow any current to pass, and the power output would be zero. The bypass diode allows current to flow around the four cells in the middle, essentially cutting them out of the circuit. Two volts are lost due to bypassing the four cells. It

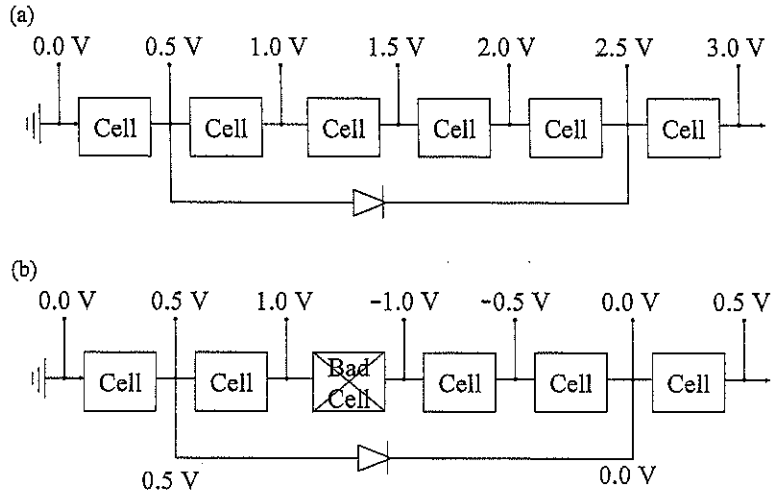

Fig. 4.28 Bypass diodes. (a) No current passes through diode. (b) Current passes through diode; 0.5 lost to forward-bias diode.

will require approximately an additional 0.5 V to forward-bias the diode and allow it to conduct current, so a total of 2.5 V are lost to bypass the bad cell. The case shown in Fig. 4.28(b) will produce only 1.5 W power, so the one bad cell causes a 7.5 W power loss for the string. The current will flow freely through the diode, and allow the rest of the string to continue to produce power. The purpose of bypass diodes is to allow the array to continue to produce power when a small fraction of cells are damaged or shaded.

A common approach is to use bypass diodes around every 5--7 cells for silicon arrays. Many GaAs cells require a diode for every cell because reversing voltage across the cell will cause permanent damage to the cell. Space applications also use diodes around every cell, but the diodes add weight and complexity and some top teams have chosen not to use them at all on silicon arrays. The cells are very reliable unless mechanically damaged. Under low-light conditions, the diodes can bypass portions of the array that are undamaged, effectively shutting down the array. This is not a great loss since the array would not produce much power under low-light conditions anyway.

Bypass diodes and no-bypass diodes for the silicon arrays have both been used successfully.

P. Array Diagnosis and Repair

It is difficult to diagnose and determine what is wrong with an array. The best strategy is to carefully match the cells and to be careful with the array so that nothing goes wrong. The team should carefully consider any repair, because the repair procedure often causes more damage. It is very difficult to remove cells from the array without damaging adjacent cells. Repairing the array during the race may require that the repairer stand in front of the array blocking sunlight from hitting the array, which greatly reduces the power the array generates while being repaired. The "hurry up" attitude that inevitably occurs makes it likely that the array will be further damaged. It may be better to simply let the bypass diode do its job and accept a slightly lower array output during the race.

If the output of the array seems to be reduced, the first step is a visual inspection to identify cells that are cracked or damaged. A single crack across a cell often does not reduce its power output, so just because a cell is cracked does not mean it is bad. Cracks are the most common form of damage, but other types of damage do occur. The main bus leads can delaminate from the cell. Water and condensation can cause corrosion of the leads or cells and damage the array. The polymer coating can degrade and reduce the power output from the array. If the array appears to be producing less power than it should, a good visual inspection will often identify the likely problems.

The array should be checked with a voltmeter to identify "bad" cells. The array must be placed in the sun and loaded by charging the batteries. The person measuring the voltages must be careful not to shade the subarray because a partially shaded cell will appear to be "bad" even though it is in good condition. If possible, check voltages from behind the array. It is best to start by checking for voltage across the bypass diodes. The schematic shown in Fig. 4.29 is a 6 × 5 panel with bypass diodes around every six cells. The "good" strings will show a voltage of approximately 3 V, while the string with the "bad" cell will show a voltage of approximately –0.5 V, that is, the voltage required to forward-bias the diode as illustrated in the figure. A string with a "weak" cell may have part of the current going through the diode and

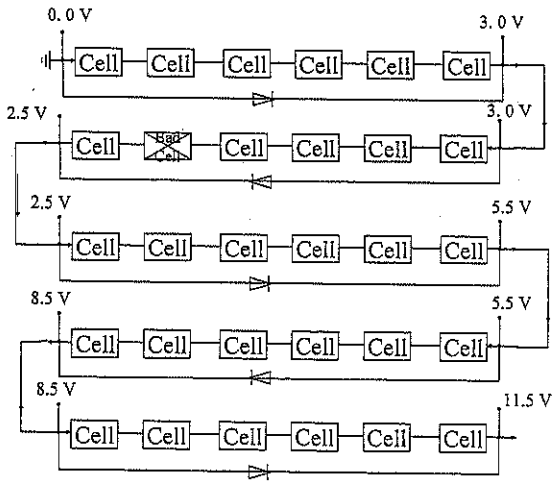

Fig. 4.29 Diagnosing solar array damage.

part of it going through the string, but this is rare. The strings usually test either "good" or "bad" unless the array is wet and shorting out in places. If the array is wet and shorting out the readings will be difficult to interpret. It is necessary to dry the array first and then try to diagnose it.

The second string in Fig. 4.29 has the "bad" cell and the voltage across this string will be approximately 0.5 V. The other strings will have a voltage of 3.0 V. Once the string with the "bad" cell is identified, the voltmeter can be used to check for which cell is bad. It may be necessary to put needles on the voltmeter leads to push through the coating. The "good" cells in the string will be producing their open-circuit voltage, which is approximately 0.5 V. The "bad" cell will have a voltage drop such that the voltage for the string drops approximately 0.5 V, which in this case would be –3.0 V, as illustrated in Fig. 4.30.

Once the "bad" cell has been identified, the best approach for repairing it needs to be determined. For this case the "bad" cell causes a voltage loss of approximately 3.5 V, and if the string carries 3 A the power loss is 10.5 W.

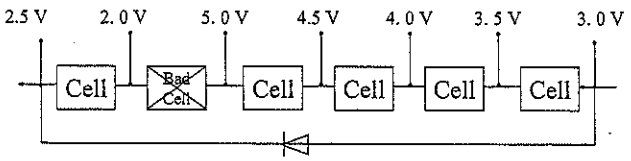

Fig. 4.30 Identifying a bad solar cell electrically.

There are circumstances where it is best to live with a 10.5-W power loss and do nothing. During the race, doing nothing is often the best thing to do.

If a repair is to be attempted, the least intrusive approach is to wire around the "bad" cell. This is sometimes referred to as "shorting out the bad cell" since the wiring connects the top of the bad cell to the bottom, shorting it out. But shorting out the cell is not the goal. The goal is to provide a path for the current to flow through without having to go through the "bad" cell. Fig. 4.31 illustrates the wiring that must be done.

The coating must be removed from the top of the two cells on the main bus leads. A short piece of wire is laid on top and soldered to the top of the two cells as illustrated in Fig. 4.31. Care should be taken when removing the coating and doing the soldering. It is easy to crack the adjacent "good" cell that defeats the whole repair procedure. A common mistake is to connect the "bad" cell to the wrong adjacent "good" cell. *Be careful to jumper to the correct cell!*

This repair allows the current to flow from the "good" cell on the left, around the "bad" cell and to the top of the next "good" cell. This string of six cells would produce approximately 2.5 V and 3 A, or 7.5 W. If the repair is not done, the current must flow through the bypass diode, and 0.5 V will be lost in the string of six cells, causing it to produce –1.5 W. The repair will increase the power from the array by approximately 9 W over using the bypass diode. With this repair the only loss of power is the one "bad" cell, approximately 1.5 W. (All of the numerical values in this analysis are for 100 mm × 100 mm terrestrial-grade silicon cells. The principles are the same for other cells, but the numeric values will be different.)

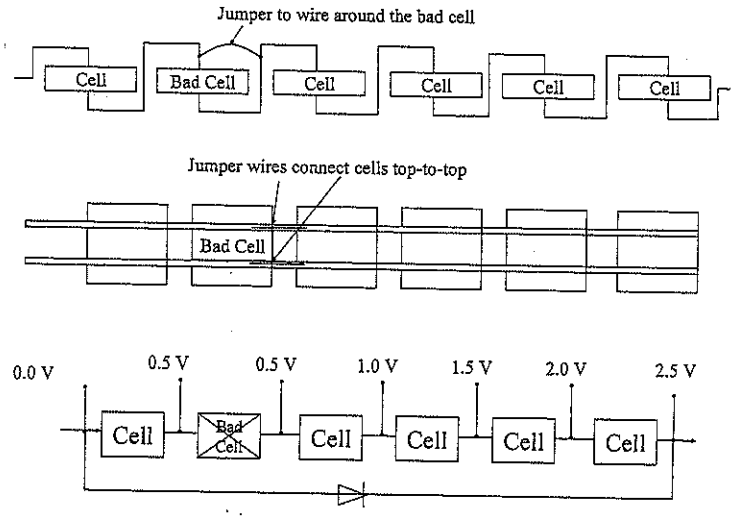

Fig. 4.31 Wiring around a bad solar cell.

If only one cell is bad, the repair procedure above is probably the best solution. Losing one cell is not a significant loss of array power. In some cases several cells may be damaged, and it may be possible to replace a string of cells or a panel of cells. Replacing a string or panel is much more difficult and time-consuming than wiring around a cell. There is a much greater likelihood of further damaging the array when removing and installing the new string or panel. The advantage of replacing a string or panel is that it restores the array to its full maximum power.

Q. Matching Array Voltage with Battery Voltage

The array voltage must be matched with the battery voltage and the power point trackers. Most arrays use step-down transformers in the power point trackers, so the array voltage must be higher than the battery voltage, or the step-down transformers will not work. It was previously shown that V_{OC} and V_P decrease as the illumination level decreases and when temperature

increases. When the voltage produced by the array is less than the battery voltage, then the power point trackers will think the batteries are charged and shut down. If the car uses eight 12-V lead-acid batteries in series, then at full charge each battery will produce about 14 V. That is, it will take 14 V to drive any current into them as they approach full charge. So the array must produce a minimum of 112 V. In designing the array, it must be decided where the low-light cutoff should be. This will determine the number of cells required for each subarray. The following issues should be considered in deciding the number of cells in a subarray.

1. To generate power at 0.01 suns, then the V_P is 0.347 V, and 323 cells wired in series are required to generate the required 112 V. If the array is designed to shut down at 0.05 suns, then each cell produces $V_P = 0.406$ V and 276 cells in series are required. For 0.10 suns V_P is 0.429 V and 261 cells are required.

2. The power point tracker will operate most efficiently when the array voltage is only slightly higher than the battery voltage. There will be a maximum array voltage the tracker can handle too.

3. The array may get damaged during the race, and damage will reduce the array voltage. If the bad cells drop the voltage too much, then the array produces no power.

4. The cells on the car must be divided evenly into subarrays, and there are only so many cells that will fit into an 8-m^2 array. Cells can be cut to make half-cell subarrays if necessary. Subarray size must be selected so that the voltage will fall into the operating range of the power point trackers. Selecting a high voltage allows the array to produce power at low light levels, and when it is partially shaded or damaged. A higher voltage is desirable from a reliability standpoint, but the array will operate more efficiently if the voltage is matched with the battery voltage.

R. Power Point Trackers

The simplest way to use a solar array is to connect it directly to the battery pack as illustrated in Fig. 4.32. If there are enough cells in series to make the array voltage higher than the battery voltage, the array will produce power

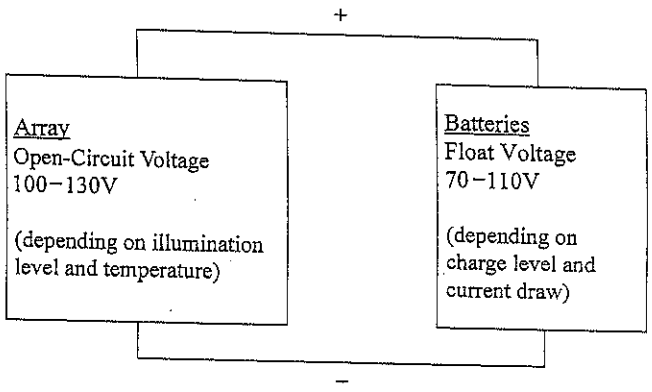

Fig. 4.32 Direct wiring of solar array to battery pack.

and charge the batteries. This method of wiring the array to the batteries is simple, inexpensive, and reliable.

If the array is matched with the battery pack as illustrated in Fig. 4.32, then under most conditions the array will produce power and charge the batteries. Overall, this design would be about 75% efficient in using the amount of energy the array can produce. Because of its low cost and simplicity, this is the way many terrestrial solar arrays are designed and wired.

1. When the battery voltage equals the power point voltage of the array, the system is nearly 100% efficient.

2. When the battery voltage is below the power point voltage, the efficiency is approximately the ratio of the voltages.

3. When the battery voltage is above the array power point voltage, the efficiency drops off sharply.

4. When the battery voltage is above the array open-circuit voltage, no power is produced.

The primary consideration in this simple design is to keep the power point voltage greater than the battery voltage for nearly all conditions. Making the solar array voltage very high ensures that the array always produces some power, but the power produced will be low. There is an optimum "match" between array power point voltage and battery float voltage, where the system will be about 75% efficient.

After understanding the simple wiring system above, it is easy to explain why solar cars use power point trackers. Ideally the array should operate at its power point voltage producing as much power as possible all the time. Then a very high-efficiency dc–dc converter would convert the power that the solar array produces to the correct battery voltage. This is the role of the power point trackers, and using them increases the amount of power from the array by 20–25% over the simple wiring configuration. Power point trackers are typically 97–98% efficient in using the power potential of the solar array.

Step-Down Converters. The most popular trackers are the step-down trackers, so named because the array power point voltage is designed to always be higher than the battery voltage. The fundamentals of how this type of power point tracker works is illustrated in Fig. 4.33.

1. When the switch S is closed, the full array voltage is applied, pushing current through the inductor L and into the batteries. The voltage across the batteries increases.

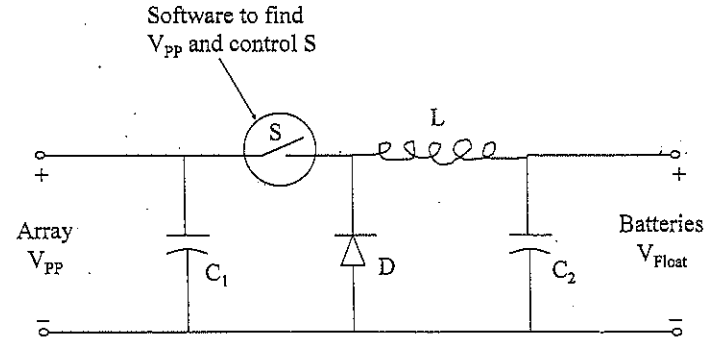

Fig. 4.33 Step-down power point tracker.

2. When the battery voltage is getting too high, the switch S opens, disconnecting the array from the batteries. Current will continue to flow up through the diode D as the inductor L and capacitor C_2 both push current into the battery. Capacitor C_1 is charged up during this part of the cycle.

3. As the voltage to the battery goes down near the float voltage, the switch S is closed again, and the array and capacitor C_1 push current through the inductor and into the batteries. Current through the diode D ceases and capacitor C_2 is charged up during this part of the cycle.

The cycle described above repeats. The software takes readings from sensors measuring the array voltage and current. The opening and closing of switch S [metal oxide semiconductor field-effect transitor (MOSFET) switch] causes a "ripple" in the array voltage and current. This "ripple" allows the software to hunt around and determine the power point voltage V_{PP}. By controlling the frequency with which the switch opens and closes, and the percentage of time it is open (or closed), the power point trackers can keep the array operating very near its power point voltage and keep the output at the battery voltage. The primary power loss mechanisms in the power point trackers are resistive losses primarily in the inductor, switching losses in the MOSFET switch S (a MOSFET is a very energy-efficient switch), capacitive losses as the capacitors are charged and discharged, and the energy to forward-bias the diode. The diode is the largest energy loss, but all of these are significant.

All of the power flowing through the power point tracker must flow through the inductor. To minimize power losses, an inductor with a resistance as low as possible should be selected. The switching, capacitive, and diode losses occur each time the switch is opened and closed, so operating at a slower frequency is desirable. The switching frequency goes up as the power point voltage of the solar array becomes larger than the battery voltage. That is, if the power point voltage of the array is slightly higher than the battery voltage, then the switching frequency is low. If the power point voltage of the array is much higher than battery voltage, the switching frequency must be higher. So even when using trackers, the system is most efficient when the array voltage is matched with the battery voltage.

Step-Up Converters. For step-up converters to work properly, the power point voltage of the solar array must be lower than the battery voltage. The advantage of this type of converter is that the array can be broken into smaller subarrays, allowing better cell matching, less sensitivity to shadows, and less power loss because of broken cells. This is only an advantage for the large silicon cells. Step-up converters are generally not a good idea if small solar cells are being used. The disadvantages of using step-up converters are that the current flowing into the trackers is higher than for step-down converters, so i^2R losses are increased, and if the tracker fails it is more difficult to develop a work-around procedure to directly connect the array to the batteries. A diagram of a step-up power point tracker is shown in Fig. 4.34.

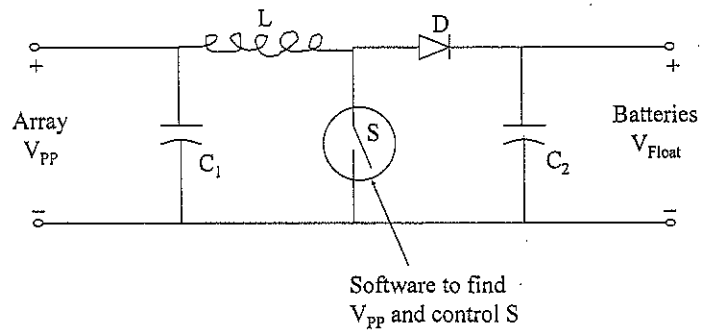

Fig. 4.34 Step-up power point tracker.

Step-up converters are inherently about 1% less efficient than step-down converters because of the additional i^2R loss, but from a system viewpoint, they can probably extract as much or more total power from the large silicon cells because of better cell matching and less sensitivity to shadows. The step-up converter operates most efficiently when the power point voltage of the solar array is only slightly less than the battery voltage.

Up/Down Converters. By inverting the output voltage and using two MOSFET switches, it is possible to make a converter that can step up or down. The diode is replaced with a second MOSFET switch, and the software

to control the two switches is much more complex, but this is the most efficient design. Up/down converters are still in the development stage. They are not well tested at this point, and so their reliability is questionable. But it will not be too many years before this type of converter is used in solar car racing. An up/down power point tracker is illustrated in Fig. 4.35.

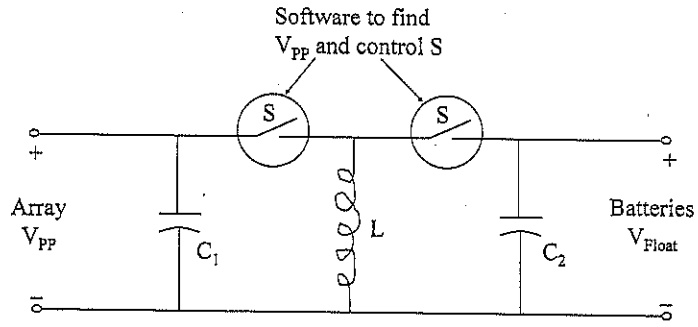

Fig. 4.35 Up/down power point tracker.

The up/down converter operates most efficiently when the power point voltage of the solar array is equal to the battery voltage, so the subarray size should be such that this is approximately correct most of the time.

S. Extreme Low-Light/No-Light OFF Switch

In a no-light condition, the solar cells will act like diodes, allowing current to flow backward through them. The batteries could potentially drain themselves by pumping current backward through the cells. All power point trackers prevent this from happening, so this is a moot point if power point trackers are being used. The switch also prevents the solar array from producing power and provides a level of safety when working on the electrical systems. A switch should be installed to disconnect the array from the batteries at night as illustrated in Fig. 4.36. If the cells are wired directly to the batteries, a diode may be used in addition to the switch, but the diode will drop the array voltage approximately 0.5 V and should not be used unless absolutely

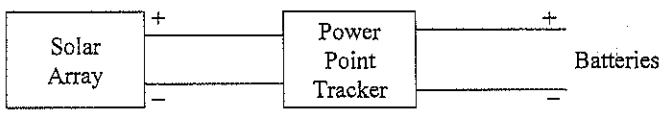

Wiring with Power Point Trackers

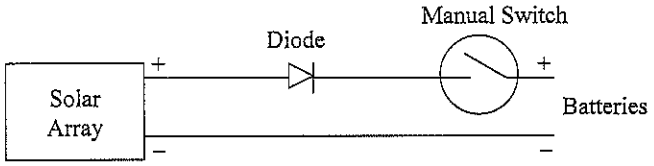

Direct Wiring with a Diode

Fig. 4.36 Main power switch wiring.

necessary. In addition to the main power switch for the solar array, the team may want to consider wiring in a switch for each subarray so that individual subarrays can be turned on and off. Being able to turn individual subarrays on and off is often helpful in diagnosing array problems.

T. Homework

1. Construct I-V diagrams for solar cells A and B below. Please construct one graph with both I-V curves on it.

   Cell A: Open-circuit voltage = 0.63 V
   Short-circuit current = 3.6 A

   Cell B: Open-circuit voltage = 0.60 V
   Short-circuit current = 2.67 A

   [Assume $R_{CH} = V_{OC}/I_{SC}$, $R_S = (0.1)R_{CH}$, and $R_{SH} = (1000)R_{CH}$, Temperature = 300 K, n = 1.5]

2. Find the power point for cells A and B above, and locate the power point on the I-V diagrams of problem 1 above. [A = 1.569 W at V = 0.477 V and I = 3.290 A, B = 1.098 W at V = 0.452 V and I = 2.428 W] Find the power point for cells A and B wired in series. [2.4467 W at I = 2.54 A] Comparing the individual power points to the series power point, what percentage of power is lost by wiring these two cells in series? [8.3% loss in power]

3. Consider a series string of ten cells that are all exactly like cell A above.

   a. What is the ideal power point for the string? [15.69 W]

   b. Suppose one cell is slightly shaded, so that the illumination level (I_L) is reduced to 75% of its original value. What is the power point of the string? [13.8 W at 2.67 A]

   c. *Bonus Question:* Suppose the string is placed on a surface curved into the shape of a circular arc as shown in Fig. 4.37, with the sun shining in the direction shown. What is the power point of the string? (I_L varies with cos θ alignment with the sun.)[15.069 W at 3.13 A; 18° arc is a 4% reduction in power compared to a flat array]

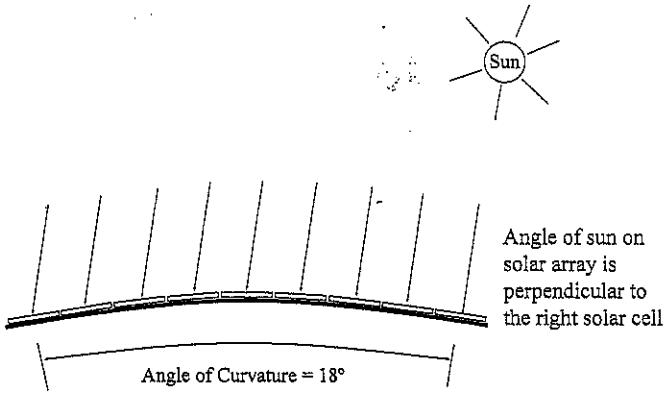

Fig. 4.37 Solar cells on a curved body.

U. References

4-1. Sze, S.M., *Physics of Semiconductor Devices*, chap. 14, John Wiley and Sons, New York, 1981.

4-2. Komp, R.J., *Practical Voltaics: Electricity from Solar Cells*, Aatec Publications, Ann Arbor, MI, 1995.

4-3. Goldhammer, L., J. Powe, and G. Ralph, *GM Sunraycer Case History Lecture 3-3: GM Sunraycer Solar Panel*, Society of Automotive Engineers, Warrendale, PA, 1992.

4-4. Roche, D.M., A.E.T. Schinckel, J.W.V. Storey, C.P. Humphris, and M.R. Guelden, *Speed of Light: The 1996 World Solar Challenge*, chap. 6, Photovoltaics Special Research Center, University of New South Wales, Sydney, Australia, 1997.

4-5. Storey, J.W.V., A.E.T. Schinckel, and C.R. Kyle, *Solar Racing Cars*, chap. 6, Australian Government Publishing Service, Canberra, Australia, 1994.

4-6. Kyle, C.R., *Racing with The Sun: The 1990 World Solar Challenge*, chap. 4, Society of Automotive Engineers, Warrendale, PA, 1991.

4-7. Lean, J., "The Sun's Radiation and Its Relevance for Earth," *Annu. Rev. Astron. Astrophys.*, vol. 35, pp. 33–67, 1997.

4-8. Green, M.A., K. Emery, K. Bucher, D.L. King, and S. Igari, "Solar Cell Efficiency Tables (Version 9)," *Prog. Photovoltaics: Res. Applic.*, vol. 5, issue 1, pp. 51–54, 1997.

4-9. Wu, C.H., personal conversation, 1997.

4-10. Zhao, J., A. Wang, P. Altermatt, and M.A. Green, "Twenty-four Percent Efficient Silicon Solar Cells with Double Layer Antireflection Coatings and Reduced Resistance Loss," *Appl. Phys. Lett.* vol. 66, issue 26, pp. 3636–3638, 1999.

4-11. Cocconi, A., and W. Rippel, *GM Sunraycer Case History Lecture 3-1: The Sunraycer Power System*, Society of Automotive Engineers, Warrendale, PA, 1992.

4-12. Roche, D., H. Outhred, and R.J. Kaye, "Analysis and Control of Mismatch Power Loss in Photovoltaic Arrays," *Prog. Photovoltaics: Res. Applic.*, vol. 3, pp. 115–127, 1995.

Chapter 5

Aerodynamics of Solar Cars

A. Fundamentals

To be competitive, a solar car must travel at sustained speeds of 90 km/h, and at those speeds aerodynamic drag is the single largest power drain. It is important to understand what can be done to minimize the aerodynamic drag on the car, and what drag reduction is necessary to have a competitive car. The aerodynamic drag for the car can come from five sources [5-1 to 5-5].

1. *Flow Separation.* For relatively unaerodynamically shaped bluff bodies like automobiles, the flow will separate from the body near the sharp corners in the body shape and create spinning vortices of turbulence. Flow separation causes a high drag force on the body, and is to be avoided. Streamlined bodies like solar cars have very little flow separation.

2. *Skin Friction.* As the air flows over a streamlined body, there is friction between the air and the body, which causes a drag force on the body. Skin friction is the dominant drag force for streamlined bodies like solar cars. Skin friction drag will be proportional to the total surface area of the car, so reducing surface area will tend to reduce the skin friction drag.

3. *Boundary Layer Pressure Loss.* As the air flows over the body, a boundary layer develops. The boundary layer is a layer of air flowing over the body, between the body and the free-stream flow. Air outside the boundary layer is flowing undisturbed, that is, flowing at the free-stream velocity. The boundary layer gets thicker as it progresses from the front of the car to the rear. The thick boundary layer at the rear of the car makes the rear stagnation pressure less than the front stagnation pressure, so there is an effective pressure drop along the length of the body, which causes a

drag force on the body. (The pressure on the front of the car is higher than on the rear.) Thicker bodies have a larger pressure drop, so making the body thin reduces the drag because of boundary layer pressure loss. For a streamlined body this term is less significant than skin friction drag, but is not insignificant.

4. *Induced Drag.* All streamlined bodies are capable of generating lift if they are given an angle of attack relative to the airstream. The drag on the body increases as the lift (up or down) increases. Minimum drag occurs when the body has zero lift, and so the angle of attack of the car should be adjusted to zero lift.

5. *Interference Drag.* This is drag because of imperfections in the body such as joints or seams, and drag because of the mating of the canopy or fairings to the body.

Equation 5.1 is the fundamental equation for aerodynamic drag force on a car [5-4].

$$\text{Drag force} = \frac{1}{2}\rho V^2 A C_d \qquad (5.1)$$

where ρ is the density of air ($\approx$1.17 kg/m^3 for summer conditions at sea level), V is the car velocity, A is the characteristic area, and C_d is the drag coefficient.

The power required to overcome aerodynamic drag is the product of the drag force and the velocity of the car, and is given in general by Eq. 5.2 [5-4].

$$\text{Power} = \frac{1}{2}\rho V^3 A C_d \qquad (5.2)$$

The density of air varies with temperature and altitude. Assuming a reasonable summertime value for air density at sea level of 1.17 kg/m^3, the power formula becomes Eq. 5.3.

$$\text{Power} = (0.01256) V^3 A C_d \qquad (5.3)$$

where V is the car velocity in kilometers per hour, AC_d is the drag area in square meters, and Power is the power requirement for aerodynamic drag in watts.

If the race occurs at an altitude above sea level, the density of air can be estimated from Eq. 5.4 [5-4].

$$\rho = (-3.64\times10^{-14})h^3 + (3.89\times10^{-9})h^2 + (-1.18\times10^{-4})h + 1.17 \qquad (5.4)$$

where ρ is the density of air in kilograms per cubic meter, and h is the height above sea level in meters.

If the temperature is exceptionally cold or hot, the universal gas law [$\rho_1 T_1 = \rho_2 T_2$] can be used to correct the density for temperature. The temperature for a density of 1.17 kg/m^3 is 305 K (32°C) and 1 atm of pressure.

The drag coefficient is measured based on the characteristic area. The drag coefficient C_d makes no sense unless the characteristic area on which it is based is defined. Automotive engineers have used the "frontal area," which is the projected area of the car when viewed from the front, as the characteristic area. Aerospace engineers have used the "planform area," the projected area when viewed from the top, or the "wetted area," which is the total surface area of the vehicle.

The characteristic area that should be used in the drag equations depends on the shape of the object. Bluff-shaped bodies, like typical automobiles, have a lot of flow separation as the air flows over the body. Flow separation causes turbulence in the flow, which causes a lot of pressure drag on the body. When pressure drag dominates, it is best to use frontal area as the characteristic area, because drag is approximately proportional to frontal area.

When the body has a good aerodynamic shape so that the flow stays attached to the body and there is little turbulence, either planform or wetted area may be the best choice for the characteristic area. Drag for this type of flow is dominated by skin friction drag, which is caused by the friction between the air and the body, and is approximately proportional to the amount of surface area exposed to the flow.

B. Car Body Shape

The minimum drag shape for a three-dimensional (3-D) body is the teardrop or torpedo shape as illustrated in Fig. 5.1(a) [5-4, 5-5]. Solar cars need to modify that shape to accommodate the solar array. Race rules require that the entire solar array must fit in a rectangular box, and for most races the area of the solar array is limited to approximately 8 m^2. The body shape that will have minimal drag and accommodate a square array on the top surface can be achieved by widening and flattening the basic teardrop shape as illustrated in Fig. 5.1(b). The current international rules for a one-person car limit the car dimensions to 5 m long and 1.8 m wide so there is the potential of having 9 m^2 of solar array area. But some of the potential array area is lost because of rounding of the nose of the car, and some is lost because of the canopy, so in practice the car will have approximately 8 m^2 of solar array area. International rules allow a two-person car to be 6 m long and 2 m wide. A two-person car can realistically have about 11 m^2 of solar array area.

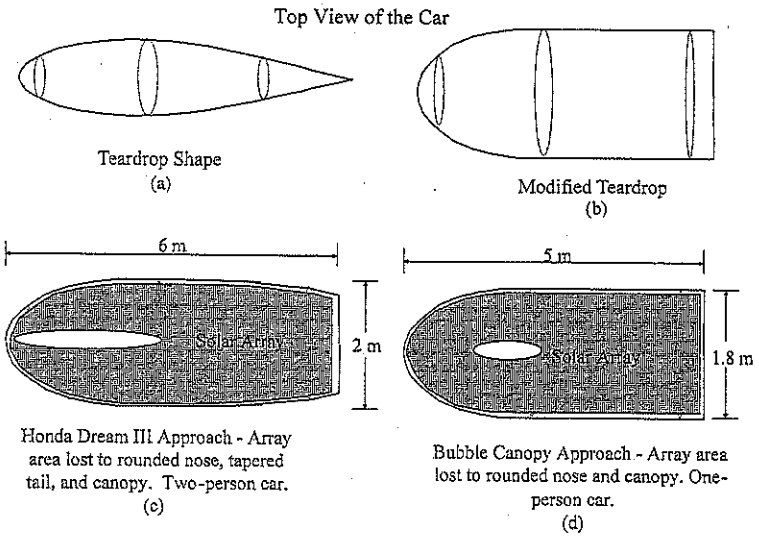

Fig. 5.1 Aerodynamic body shape development.

Most teams give up some array area to minimize the aerodynamic drag on the car. Reducing the array area reduces the power the array will produce, so the reduction in aerodynamic drag must be more significant than the reduction in array power. In making Honda Dream III, winner of the 1996 World Solar Challenge, the design team chose to move the array forward on the rounded nose portion of the car, taper the tail of the car, and put a canopy on the top [5-6, 5-7]. The makers of the car gave up a significant amount of solar array area to minimize the drag on the car, as illustrated in Fig. 5.1(c). Honda is one of the few teams that tapers the tail to reduce aerodynamic drag. They also had a very large canopy that was blended into the body to minimize canopy drag, which significantly reduced the size of the solar array. The most common solar car design is a one-person car with a bubble canopy as illustrated in Fig. 5.1(d) [5-7 to 5-9]. For most teams it is much easier to manufacture the body if it is of constant width along most of the length as is illustrated in Fig. 5.1(d), and this approach will yield a larger solar array than Fig. 5.1(c).

C. Camber

The teardrop shape yields the lowest drag when the body is traveling in free-stream air. That is, if the body were high above the ground and traveling through still air, the teardrop shape would yield the lowest drag, and the modified teardrop shapes above would be the best choice for a solar car body. But for cars traveling near the ground, there is a "ground effect" that increases the drag on the teardrop shape as it is brought close to the ground. This effect was first studied by Klemperer in the early 1900s [5-10], and more precisely by Morelli [5-1, 5-10]. It was discovered that cambering the teardrop shape, as illustrated in Fig. 5.2, would reduce the drag when the body was traveling near the ground [5-1, 5-10, 5-11]. As the body moves closer to the ground, more camber is required to minimize the drag. For solar cars, cambering the body will reduce the body drag 5–10% compared with using a symmetric shape.

In Fig. 5.2, the symmetric and cambered shapes have the same thickness and length. The symmetric shape will have lower drag in free-stream flow, and the cambered shape will have lower drag near the ground. The side view of the solar car body should have a cambered shape to take advantage of the 5–10% reduction in drag on the body.

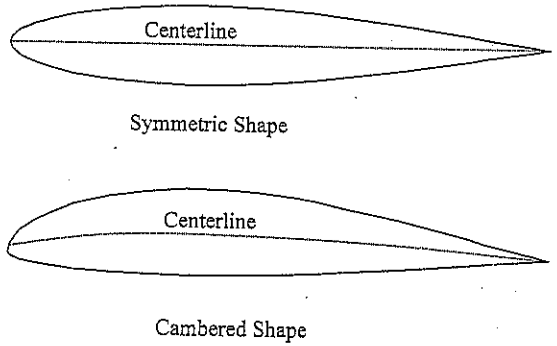

Fig. 5.2 Cambering the airfoil. Side view of the car.

The National Advisory Committee for Aeronautics (NACA) 66 series airfoils were developed to promote laminar flow over as much of the length as possible, and are among the shapes with the lowest drag. They have poor lift-to-drag characteristics, and are not used much for aircraft wing design, but are a good shape for the solar car body. Because the goal is to minimize the drag, the NACA 66 series is probably a good place to start in developing a body design. Table 5.1 lists the points for the basic NACA 66 symmetric shape with a maximum thickness of 10% of the chord length [5-12].

Using the data in the table, it is possible to construct a cambered shape for the body that will minimize the drag. The designer will need to decide how to place the driver inside the car, as this is what will probably determine the minimum thickness of the car. The designer will also need to decide how to place the array on the top of the car. The first exercise will be to learn how to construct a body shape for a car that is to be 5 m long and 49 cm thick at the thickest point.

Example. For the first exercise the car will be assumed to be 5 m long and 49 cm thick. The thickness is 9.8% of the chord length, and the standard shape given is 10%, so we first have to adjust the thickness of the 10% shape. This is accomplished by multiplying all of the Y values in the 10% column of Table 5.1 by 0.98 to generate the desired shape. All of the values in the X and

TABLE 5.1
NACA 66 SERIES

X % Chord	Y 10%
0	0
0.5	0.759
0.75	0.913
1.25	1.141
2.5	1.516
5.0	2.087
7.5	2.536
10	2.917
15	3.530
20	4.001
25	4.363
30	4.636
35	4.832
40	4.953
45	5.000
50	4.971
55	4.865
60	4.665
65	4.302
70	3.787
75	3.176
80	2.494
85	1.773
90	1.054
95	0.408
100	0

Y columns are then multiplied by the chord length of 5 m to generate the full-scale shape of the car. The shape generated is shown in Fig. 5.3.

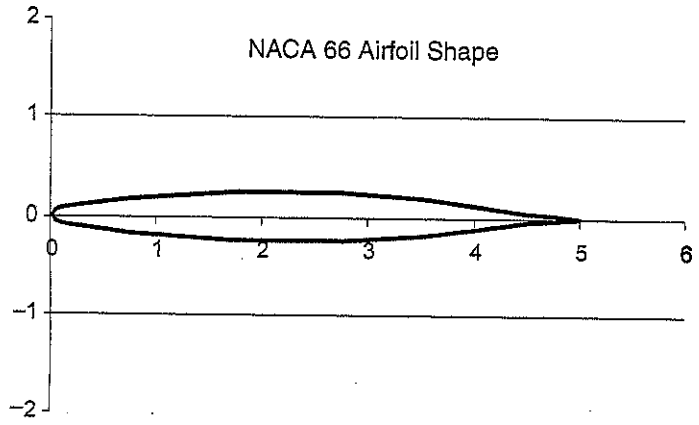

Fig. 5.3 Scaled body shape.

The next step is to camber the shape to design for the ground effect. For cars traveling approximately 10 in. off the ground, the shape should be cambered 2–5% of the chord length to minimize the drag. Getting the camber to exactly the minimum drag shape is not necessary. The drag does not vary much between 2 and 5% camber. It is easier to manufacture the chassis and make the interface between the bottom of the chassis and wheel fairings if the bottom of the car is flat, so the camber that yields an approximately flat bottom should be chosen.

To camber the airfoil, first select the point where the thickness is a maximum (X_{max}, Y_{max}), which would be the point (2.25, 0.245) for the shape above. The length L for this shape is 5 m, and the percent camber is C%. The Y values will all be shifted up by the Y_{adj} factor defined in Eq. 5.5.

$$Y_{adj} = \frac{C\%L(LX - X^2)}{100X_{max}(L - X_{max})} = \frac{(2.7)(5)(5X - X^2)}{100(2.25)(5 - 2.25)} \text{ for this example} \quad (5.5)$$

The shape in Fig. 5.3 was cambered by 2.7% to achieve the approximately flat bottom shown in Fig. 5.4.

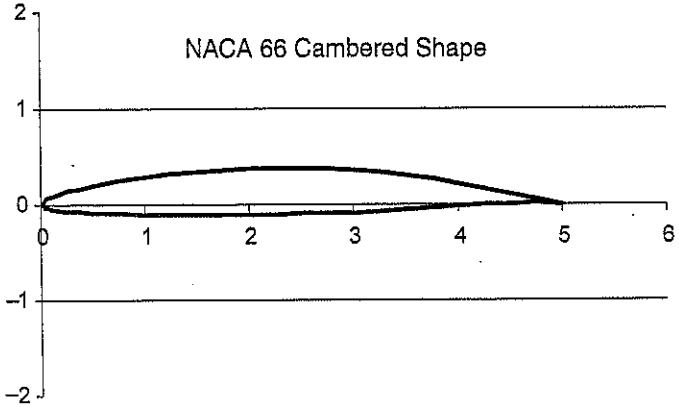

Fig. 5.4 Cambered body shape.

The bottom of the car should be flat along the portion where the front wheels will interface with the chassis. On the actual car body shape, the flat portion on the bottom might be extended back to about 3.5 m from the nose to make it easier to manufacture the interface between the body and chassis. Curvature on the nose in front of the wheels is desirable because gradual curvature will promote laminar flow on the belly of the car and reduce the drag. The rear should come to a "knife edge" to allow the air flowing under the car to smoothly rejoin the air flowing over the top. Table 5.2 contains the data for the basic airfoil shape, the symmetric airfoil scaled to 5 m length and 49 cm thickness, and the cambered airfoil. The first half of the table from 0 to 100% is the top of the car body and the second half from 100 to 0% is the bottom of the car body.

TABLE 5.2
CAMBERED AIRFOIL DEVELOPMENT

Basic Shape		Symmetric Airfoil		2.7% Cambered Airfoil	
X % Chord	Y 10%	X	Y	X	Y
0	0	0	0	0	0
0.5	0.759	0.025	0.037191	0.025	0.039905
0.75	0.913	0.0375	0.044737	0.0375	0.048797
1.25	1.141	0.0625	0.055909	0.0625	0.062642
2.5	1.516	0.125	0.074284	0.125	0.087579
5.0	2.087	0.25	0.102263	0.25	0.128172
7.5	2.536	0.375	0.124264	0.375	0.162105
10	2.917	0.5	0.142933	0.5	0.192024
15	3.530	0.75	0.17297	0.75	0.242515
20	4.001	1	0.196049	1	0.283322
25	4.363	1.25	0.213787	1.25	0.31606
30	4.636	1.5	0.227164	1.5	0.341709
35	4.832	1.75	0.236768	1.75	0.360859
40	4.953	2	0.242697	2	0.373606
45	5.000	2.25	0.245	2.25	0.38
50	4.971	2.5	0.243579	2.5	0.379943
55	4.865	2.75	0.238385	2.75	0.373385
60	4.665	3	0.228585	3	0.359494
65	4.302	3.25	0.210798	3.25	0.334889
70	3.787	3.5	0.185563	3.5	0.300108
75	3.176	3.75	0.155624	3.75	0.257897
80	2.494	4	0.122206	4	0.209479
85	1.773	4.25	0.086877	4.25	0.156422
90	1.054	4.5	0.051646	4.5	0.100737
95	0.408	4.75	0.019992	4.75	0.045901
100	0	5	0	5	0
95	−0.408	4.75	−0.01999	4.75	−0.005917
90	−1.054	4.5	−0.05165	4.5	−0.00256
85	−1.773	4.25	−0.08688	4.25	−0.01733
80	−2.494	4	−0.12221	4	−0.03493
75	−3.176	3.75	−0.15562	3.75	−0.05335
70	−3.787	3.5	−0.18556	3.5	−0.07102
65	−4.302	3.25	−0.2108	3.25	−0.08671
60	−4.665	3	−0.22859	3	−0.09768
55	−4.865	2.75	−0.23839	2.75	−0.10339
50	−4.971	2.5	−0.24358	2.5	−0.10722
45	−5	2.25	−0.245	2.25	−0.11
40	−4.953	2	−0.2427	2	−0.11179
35	−4.832	1.75	−0.23677	1.75	−0.11268
30	−4.636	1.5	−0.22716	1.5	−0.11262
25	−4.363	1.25	−0.21379	1.25	−0.11151
20	−4.001	1	−0.19605	1	−0.10878
15	−3.53	0.75	−0.17297	0.75	−0.10342
10	−2.917	0.5	−0.14293	0.5	−0.09384
7.5	−2.536	0.375	−0.12426	0.375	−0.08642
5	−2.087	0.25	−0.10226	0.25	−0.07635
2.5	−1.516	0.125	−0.07428	0.125	−0.06099
1.25	−1.141	0.0625	−0.05591	0.0625	−0.04918
0.75	−0.913	0.0375	−0.04474	0.0375	−0.04068
0.5	−0.759	0.025	−0.03719	0.025	−0.03448
0	0	0	0	0	0

The cambered shape will have a very low aerodynamic drag. It will be very close to the lowest drag possible for a body that is 5 m long and 49 cm thick. The NACA 66 series airfoils have their maximum thickness at 45% along the length, and are well suited for cars that have the driver in the middle. If the driver is to be near the front, a standard airfoil with the maximum thickness at 30% along the length will work out better. Grid points for a standard airfoil shape are given in Table 5.3.

TABLE 5.3
STANDARD AIRFOIL

X	Y
0	0
0.5	2.000
1.25	3.788
2.5	5.229
5	7.109
7.5	8.400
10	9.365
15	10.691
20	11.475
25	11.883
30	12.004
40	11.607
50	10.588
60	9.127
70	7.328
80	5.247
90	2.896
95	1.613
100	0

The cambered shape is the side view of the car. The next step is to get the top view. The method that yields the lowest drag is to use a truncated airfoil shape, but a lot of array area is lost when using this shape. Most teams do not use the truncated airfoil shape, but the method is provided here because it is the shape with the lowest drag. A standard airfoil shape is chosen such that the maximum thickness is close to the nose, so that the car body will achieve its maximum thickness as far forward as possible. The standard airfoil in Table 5.3 works well for the truncated airfoil design [5-12].

The maximum width of the airfoil can be adjusted to the maximum width of the car, and the length should be adjusted so that the end of the car occurs at approximately 60% chord length. For a car that is 5 m long and 2 m wide, the top view for a low-drag shape would look like Fig. 5.5. This is very similar to the top view of the Honda Dream III car [5-6, 5-7]. The problem with this shape is that it is difficult to fit a rectangular array on it without losing a lot of solar array area, but this is close to the minimum-drag shape for the top view of a solar car with a reasonable-sized solar array.

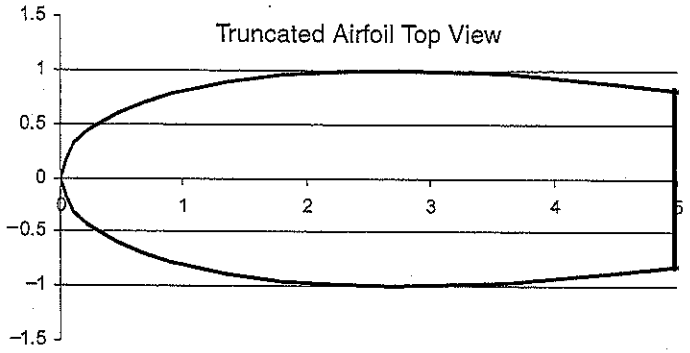

Fig. 5.5 Top view of car with truncated airfoil shape.

Most teams choose to round the nose as illustrated in Fig. 5.6 [5-7 to 5-9, 5-13]. Rounding the nose in this way makes the solar array larger. The shape of the nose is very important in minimizing the aerodynamic drag, and shaping the nose is an area where computational fluid mechanic analysis is helpful. The body is usually of constant width to the end of the tail, with no

taper on the tail. Making the body of constant width makes it much easier to fit a rectangular array on top, and this type of body is much easier to manufacture. Tapering the tail, as shown in Fig. 5.5, will make it more difficult to manufacture the body, but will reduce the drag.

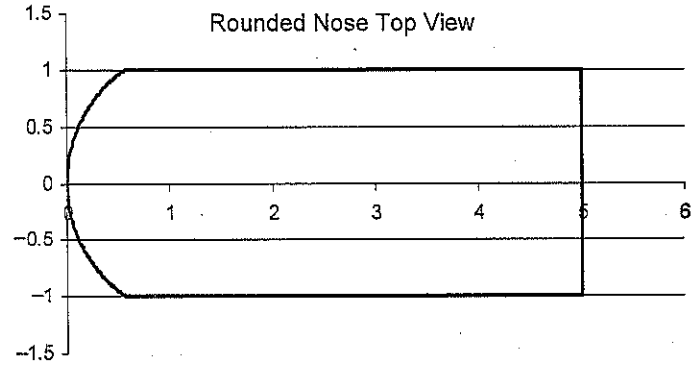

Fig. 5.6 Top view of car with rounded nose.

In constructing the front view of the body, the lowest-drag shape would be to use an ellipse with the proper width and height for each section along the length of the body. But to get a good interface between the front fairings and the chassis, it is desirable to make the chassis flat in regions near the front wheels. The front fairings must turn when the front wheels turn, and it is difficult to make a good interface on a curved surface. The rear wheels do not turn and the fairing can be mounted rigidly to the body, so it is possible to mount the rear fairing(s) on a curved surface.

Homework Assignment. Choose a body length and thickness and go through the exercise of adjusting the thickness, adjusting for camber, developing a top view, and a 3-D sketch of the car body. Do not try to optimize the shape of the body at this point. Select a reasonable length and thickness for the car, select the shape that has approximately the right thickness-to-length ratio, adjust the thickness, incorporate camber to make the bottom approximately flat, design a top view, and draw the figures. Please turn in a side view, top view, and 3-D sketch along with the detailed calculations.

D. Reynolds Number

The Reynolds number (Re) is a dimensionless quantity that is used to characterize the flow as either laminar, transitional, or turbulent according to the definition in Eq. 5.6 [5-1, 5-4].

$$\begin{array}{ll} 100 < Re < 3\times10^5 & \text{Laminar} \\ 3\times10^5 < Re < 5\times10^5 & \text{Transitional} \\ Re > 5\times10^5 & \text{Turbulent} \end{array} \qquad (5.6)$$

The Reynolds number is defined in Eq. 5.7.

$$Re = \frac{\rho V D}{\mu} = \frac{V D}{\nu} \qquad (5.7)$$

where ρ is the density of the fluid, V is the flow velocity (car velocity), D is a characteristic length (car length), μ is the fluid viscosity, and ν is the fluid kinematic viscosity ($1.46 \times 5\ 10^{-4}$ m^2/s or $1.57 \times 10^{3-4}$ ft^2/s for air). Assuming that the car is 5 m long and traveling at 90 km/h (25 m/s) the Reynolds number is 8,400,000, which is in the turbulent flow region. The boundary layer flow for the car will be predominantly turbulent boundary layer, even for relatively low velocities of the car, that is, $Re > 5 \times 10^5$ for any car and velocity of interest. There will be a region of laminar flow over the nose of the body which can be estimated by modeling it as flow over a flat plate as shown in Eq. 5.8.

$$5\times10^5 = \frac{(25)(D)}{1.46\times10^{-5}} \Rightarrow D = 29.2 \text{ cm} \qquad (5.8)$$

If the body were flat and parallel to the flow, it would be reasonable to expect laminar flow to exist over the first 29.2 cm of the nose of the car at 90 km/h. If the nose is curved so that the body gradually gets thicker from the nose backward, it is possible to extend the laminar flow well beyond 29.2 cm. The 1987 GM Sunraycer was designed so it had laminar flow over the front 2 m of the car, but at a lower speed than 90 km/h. Laminar flow is desirable

Collected sun changes with θ and ϕ; integrate θ values over the surface to obtain albeted sun?

because it reduces the drag on the body, but achieving 2 m of laminar flow requires very careful design of the nose of the car. For most teams, achieving 0.5–1.0 m of laminar flow is more realistic, and even that much will require careful attention to details. Any small bump or irregularity will trip the flow and cause it to transition to turbulent boundary flow. On the top surface it is usually either the seam for the canopy or the edge of the array that causes flow transition. On the bottom surface it is usually either the seam between the body and belly pan or the front fairings.

E. Body Drag Area Calculations

In the early days of solar car racing, teams were using different definitions for the characteristic area of the car. There was a lot of variation in the reported drag coefficients, and it was difficult to interpret the results and compare designs. Some teams reported drag coefficients less than 0.01 based on total wetted area of the car, while others reported drag coefficients larger than 0.1 based on the frontal area. The drag area AC_d is a consistent way to compare two designs, and is commonly measured in square meters.

In this section a method is developed to estimate the drag area of a solar car. The drag is broken down into components of the car (body, canopy, fairings, etc.), and the drag areas of the components are added to yield the total drag area. Each component will have its own characteristic area and drag coefficient. The best solar cars in the world have drag areas of 0.1–0.15 m^2 at 90 km/h. To be competitive the car must achieve a total drag area in this range.

The information in this section has been developed over a period of about 5 years, in a rather ad hoc manner at the University of Missouri-Rolla. Many of the formulas used come from the books by Tamai [5-1] and Munson, Young, and Okiishi [5-4]. The goal has been to develop a systematic method of estimating the drag area of a solar car design, but there was not enough information available in these and other references to develop a purely scientific approach. There is a wealth of data on the drag area of well-designed solar cars [5-7 to 5-9]. The basis for the formulas used in this section are scientific, but some of the formulas were "adjusted" using "engineering judgment" until the procedure yielded accurate estimates for the solar cars for which data were available. The procedure is not perfect, but it is straightforward and seems to consistently yield an answer that is within 10% of the

published values for aerodynamically shaped solar cars. The information in this section is helpful in designing and optimizing the aerodynamics of a solar car and in comparing the aerodynamic drag of different solar car designs. It is a helpful design tool, but some parts are not scientifically rigorous.

F. Body Drag Introduction

The nose of the car body should be rounded like an airfoil nose. It should also be smooth with no seams to "trip the boundary layer," as discussed above. It is not difficult to obtain laminar flow over the first 30 cm of the length of the car. If the nose is rounded like an airfoil, it is possible to extend laminar flow beyond 30 cm to the first seam in the body. The designer should be realistic in deciding where the flow will transition from laminar to turbulent boundary layer. It is very difficult to achieve more than 1 m of laminar flow under any circumstances. Designers have attempted the "seamless joint" between body panels, but are seldom successful. Any small bump or irregularity in the surface finish will cause the flow to transition.

Figure 5.7 shows how the skin friction drag varies along the length of the car for laminar flow and for turbulent boundary layer flow [5-1, 5-4]. The figure

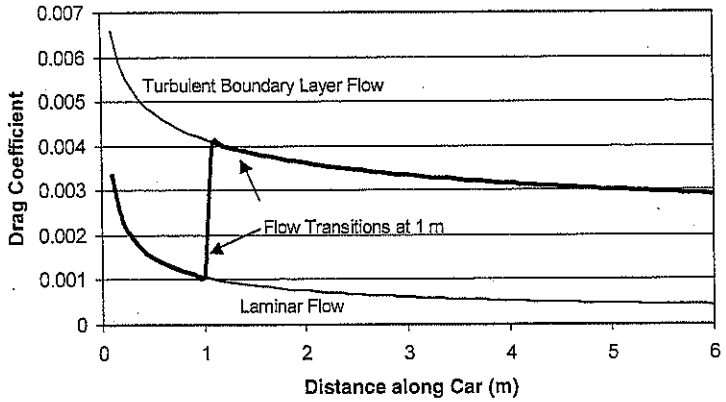

Fig. 5.7 Drag coefficient as the flow transitions from laminar to turbulent boundary layer.

shows an abrupt change from laminar flow to turbulent boundary layer, which is a simplification. In reality there will be a region of transition, but this approximation works well for estimating drag on the body. Laminar flow drag is always less, so it is advantageous to have as much laminar flow as possible. In both cases the drag is highest at the nose of the car, and decreases toward the rear of the car. The total area under the curve(s) represents the total drag on the car. Delaying the transition from laminar to turbulent boundary layer flow reduces the area under the curve, and thus reduces total drag on the car. A shorter car will have less drag than a longer car if they both have the same amount of laminar flow. The reduction in drag achieved by shortening the car comes from removing some of the lower drag region at the rear of the car. A longer car can have less total drag than a shorter car if the longer car has more laminar flow on the nose. Analysis shows that lengthening the car by lengthening the nose and adding more laminar flow length will almost always reduce the total drag on the car. The designer must be realistic about the laminar flow that can be achieved when designing the car, but should achieve as much as possible.

If the nose is designed to gradually widen, as illustrated in Fig. 5.8, it is possible to maintain laminar flow for a significant distance. The widening of the nose gives a pressure gradient on the surface that is conducive to laminar

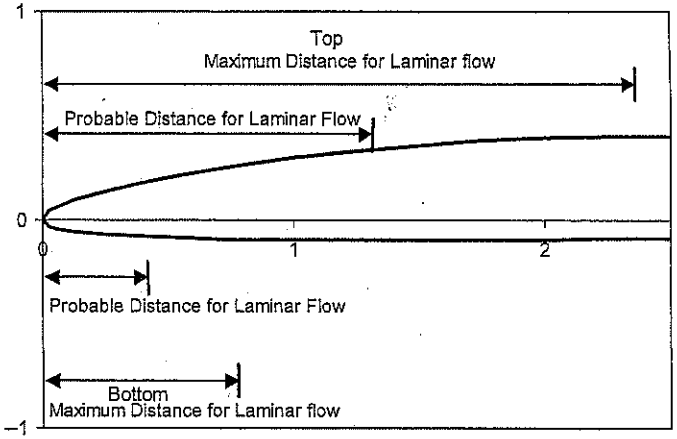

Fig. 5.8 Laminar flow distance on the nose.

flow. It is not possible to have laminar flow beyond where the body reaches maximum thickness, as illustrated in Fig. 5.8. A more probable transition point is located between one-half and two-thirds of the measurement at which the body reaches maximum thickness, as illustrated in Fig. 5.8, and this assumes that there are no seams or bumps on the nose. It is very unlikely that laminar flow will carry beyond a seam or bump on the surface.

Body Drag Coefficients. The drag coefficients vary along the length of the car because the local Reynolds number (Rex) varies along the length. The local Reynolds number is defined in Eq. 5.9 [5-4].

$$Rex = \frac{Vx}{\nu} \tag{5.9}$$

where x is the distance from the nose of the car, V is the car velocity, and ν is the kinematic viscosity of air. The local drag coefficient for laminar flow is given by Eq. 5.10 [5-4].

$$C_{d\ laminar} = \frac{0.664}{\sqrt{Rex}} \tag{5.10}$$

The local drag coefficient for turbulent flow is highly dependent on the surface roughness. If the surface is infinitely smooth, the local drag coefficient is given by Eq. 5.11 [5-4].

$$C_{d\ turbulent} = \frac{0.0576}{(Rex)^{0.2}} \tag{5.11}$$

If the surface is not smooth, it is customary to characterize the surface roughness as a characteristic surface "bump height" divided by the length of the car (ε/L). For this case the average drag coefficient can be estimated by Eq. 5.12 [5-4].

$$C_{d\ turbulent\ rough} = \left[1.89 - 1.62\ \log_{10}\left(\frac{\varepsilon}{L}\right)\right]^{-2.5} \tag{5.12}$$

The average drag coefficient for the surface is obtained by integrating the drag coefficients along the length of the car. The equation for the drag coefficient for a rough surface is an estimate, and the designer should be careful when using it. Two calculations should be made, one assuming an infinitely smooth surface and one with the rough surface. There are cases where the equations will yield a lower drag coefficient for a rough surface, but in reality the rough surface will never have a lower drag than a smooth surface. The designer should calculate for the smooth and rough surface and choose the larger drag coefficient as the best estimate.

If the total length of the body is L and the boundary layer transitions at L_T on top and L_B on the bottom, the average drag coefficients for the top and bottom are calculated by integrating the local drag coefficients along the length of the car. Average drag coefficients for the perfectly smooth surface are obtained from Eqs. 5.13 and 5.14.

$$C_{dTop} = \frac{1.328}{\sqrt{Re}}\sqrt{\frac{L_T}{L}} + \frac{0.072}{(Re)^{0.2}}\left[1 - \left(\frac{L_T}{L}\right)^{0.8}\right] \tag{5.13}$$

$$C_{dBottom} = \frac{1.328}{\sqrt{Re}}\sqrt{\frac{L_B}{L}} + \frac{0.072}{(Re)^{0.2}}\left[1 - \left(\frac{L_B}{L}\right)^{0.8}\right] \tag{5.14}$$

The Reynolds number in these formulas is the global Reynolds number (Re), based on the length of the car, not the local Reynolds number (Rex). The average drag coefficient for the rough surface can be obtained from Eqs. 5.15 and 5.16.

$$C_{dTop} = \frac{1.328}{\sqrt{Re}}\sqrt{\frac{L_T}{L}} + \frac{L - L_T}{L}\left[1.89 - 1.62\ \log_{10}\left(\frac{\varepsilon}{L}\right)^{-2.5}\right] \tag{5.15}$$

$$C_{dBottom} = \frac{1.328}{\sqrt{Re}}\sqrt{\frac{L_B}{L}} + \frac{L - L_B}{L}\left[1.89 - 1.62\ \log_{10}\left(\frac{\varepsilon}{L}\right)^{-2.5}\right] \tag{5.16}$$

Example. Assume that the car is 5.5 m long, and that the flow transitions at 0.9 m on the top and at 0.5 m on the bottom. Assume that the car is traveling at 72.4 km/h (45 mph), and that the "bump height" is 0.5 mm. Calculate the drag coefficients for the top and bottom of the car.

Solution. The calculation for the Reynolds number where 72.4 km/h = 20.13 m/s is shown in Eq. 5.17.

$$\mathrm{Re} = \frac{(20.13)(5.5)}{1.46\times10^{-5}} = 7.584\times10^{6} \tag{5.17}$$

Calculations of the drag coefficients for the perfectly smooth surface are shown in Eqs. 5.18 and 5.19.

$$C_{dTop} = \frac{1.328}{\sqrt{\mathrm{Re}}}\sqrt{\frac{0.9}{5.5}} + \frac{0.072}{(\mathrm{Re})^{0.2}}\left[1-\left(\frac{0.9}{5.5}\right)^{0.8}\right] = 0.00251 \tag{5.18}$$

$$C_{dBottom} = \frac{1.328}{\sqrt{\mathrm{Re}}}\sqrt{\frac{0.5}{5.5}} + \frac{0.072}{(\mathrm{Re})^{0.2}}\left[1-\left(\frac{0.5}{5.5}\right)^{0.8}\right] = 0.00273 \tag{5.19}$$

Calculations for the rough surface are shown in Eqs. 5.20 and 5.21.

$$C_{dTop} = \frac{1.328}{\sqrt{\mathrm{Re}}}\sqrt{\frac{0.9}{5.5}} + \frac{5.5-0.9}{5.5}\left[1.89-162\log_{10}\left(\frac{0.0005}{5.5}\right)\right]^{-2.5} = 0.00424 \tag{5.20}$$

$$C_{dBottom} = \frac{1.328}{\sqrt{\mathrm{Re}}}\sqrt{\frac{0.5}{5.5}} + \frac{5.5-0.5}{5.5}\left[1.89-162\log_{10}\left(\frac{0.0005}{5.5}\right)\right]^{-2.5} = 0.00454 \tag{5.21}$$

So for this case the drag coefficient for the top would be 0.00424, and for the bottom it would be 0.00454. For a perfectly smooth surface the drag coefficient is a function of the velocity of the car, because the Reynolds number is

a function of velocity. For the rough surface equation there is a small dependence on velocity, but the drag coefficient is almost constant.

Figure 5.9 shows how the drag coefficients of the top of the car in the example above vary with velocity in the range of 55–105 km/h. The assumption in the original power management model was that the drag coefficient was constant for any speed. This chart shows that for a perfectly smooth surface the drag area is not constant, but decreases with speed because the Reynolds number increases with speed.

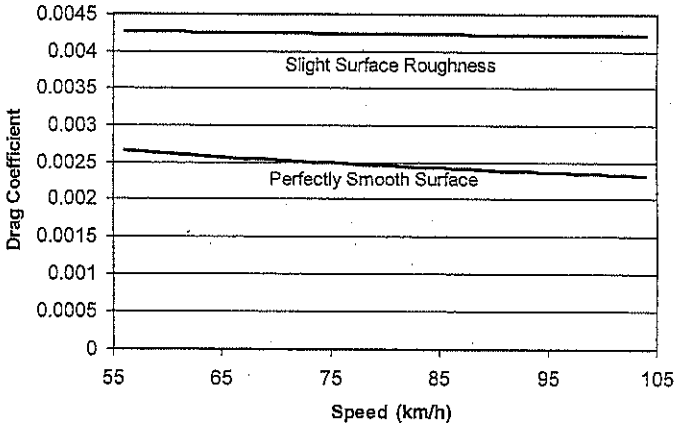

Fig. 5.9 Variation of drag coefficient with car speed.

Body Surface Area. The drag areas for the top and bottom of the car would be the drag coefficients multiplied by the surface areas. Because it is difficult to calculate the surface area of a curved body like this, it will be estimated from the planview area. The planview area of the car is estimated by looking at the top view of the car and estimating the total area in square meters. The designer may need to draw the top view carefully and to scale on a grid and count the squares to make an accurate estimate of the planview area PA.

The skin friction drag on the body is proportional to the surface area, and surface area increases with the thickness of the body. If t is the maximum

thickness of the body of length L, the total surface area A is given approximately by Eq. 5.22 [5-1].

$$A = 2PA\left[1+2\left(\frac{t}{L}\right)+60\left(\frac{t}{L}\right)^4\right] \qquad (5.22)$$

This formula assumes that a smooth, well-rounded body shape was used. Cross sections of the body, when viewed from the front, should be elliptical. This can be a problem for thicker bodies because the top of the car near the sides becomes very rounded, and it is difficult to place the solar array on it. Some teams choose to make the cross sections of the body more rectangular with rounded corners, rather than elliptical. This increases the surface area, and hence the drag of the body. Figure 5.10 illustrates how to estimate the surface area of the body for different cross-sectional shapes.

If cross sections are elliptical, use the surface area calculated by Eq. 5.22.

If cross sections are rectangular with rounded corners, multiply the surface area calculated by Eq. 5.22 by a factor that depends on the radii of the corners.

r = 3 in., Factor = 1.1
r = 2 in., Factor = 1.15
r = 1 in., Factor = 1.2

Fig. 5.10 Correction factor for bodies with nonelliptical cross sections.

The designer must use good judgment in determining the surface area of the body. There may be cases where the body is drawn in a computer-assisted design (CAD) package, and the software may be used to calculate the surface area. The goal is to get a realistic estimate of the surface area of the body,

and the CAD package will probably be more accurate than the previous analysis. The above analysis is most useful for preliminary design analysis, to compare different designs and to help in selecting a design concept.

Boundary Layer Pressure Loss. A thicker body will have a higher boundary layer pressure loss. As the air flows around the body, the boundary layer thickness increases, and the rear stagnation pressure is always less than the front stagnation pressure. This pressure drop causes drag on the body, and thicker bodies tend to have more boundary layer pressure loss than thin bodies. This pressure loss can be alleviated to some extent by tapering the tail. If the maximum width of the car is W and the tail is gradually tapered so that the width of the tail at the back of the car is WT, the correction for boundary layer pressure loss BLPL is given by Eq. 5.23 [5-1].

$$BLPL = \left[1+1.5\left(\frac{WT}{W}\right)\left(\frac{t}{L}\right)^{1.5}+19\left(\frac{WT}{W}\right)\left(\frac{t}{L}\right)^6\right] \qquad (5.23)$$

This formula is valid only for small amounts of taper where $0.75\,W < WT < W$. The drag area for the body of the car can be estimated from Eq. 5.24.

$$AC_{dBody} = A\left(\frac{C_{d\ Top}+C_{d\ Bottom}}{2}\right)BLPL \qquad (5.24)$$

Example. Consider the top view of the body with the rounded nose shown in Fig. 5.11. The spreadsheet plot is adjusted to make a reasonably fine grid to calculate the planview area PA. Each square represents 0.25 m^2 of planview area. There are 34 whole squares and 6 partial squares for this shape. The total area is estimated as

$$PA = (0.25)[34+2(0.99)+2(0.4)+2(0.9)] = 9.645\ m^2 \qquad (5.25)$$

The length of the body is 5 m and the thickness was assumed to be 49 cm. Plugging into Eq. 5.22, the total surface area of the car is 23.18 m^2 as shown in Eq. 5.26.

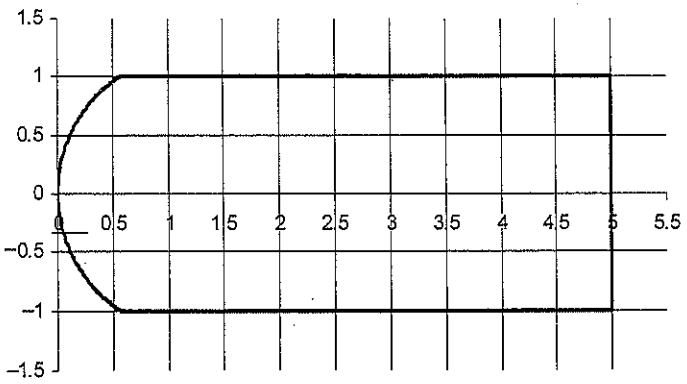

Fig. 5.11 Example of planview area calculation.

$$A = 2(9.645)\left[1+2\left(\frac{0.49}{5}\right)+60\left(\frac{0.49}{5}\right)^4\right] = 23.18\ \text{m}^2 \qquad (5.26)$$

There is no taper on the tail, so WT/W is unity. The BLPL factor is 1.046 as shown in Eq. 5.27.

$$BLPL = \left[1+1.5\left(\frac{2}{2}\right)\left(\frac{0.49}{5}\right)^{1.5}+19\left(\frac{2}{2}\right)\left(\frac{0.49}{5}\right)^6\right] = 1.046 \qquad (5.27)$$

The drag coefficients for the top and bottom depend on where the flow transitions from laminar to turbulent boundary layer, and on the surface roughness. Assume that the array starts 1 m back from the nose and is the full width of the car. On the bottom assume that the front-wheel fairing extends to within 0.75 m of the nose of the car. The flow transitions at 1.0 m on the top and at 0.75 m on the bottom. Assume that the surface roughness "bump height" is 0.1 mm. To calculate the Reynolds number assume that the car is traveling at 88.5 km/h (55 mph). The Reynolds number is calculated in Eq. 5.28.

$$Re = \frac{(24.6)(5)}{1.46\times10^{-5}} = 8.432\times10^6 \qquad (5.28)$$

Calculations for the drag coefficients for the perfectly smooth surface are shown in Eqs. 5.29 and 5.30.

$$C_{dTop} = \frac{1.328}{\sqrt{Re}}\sqrt{\frac{1.0}{5.0}}+\frac{0.072}{(Re)^{0.2}}\left[1-\left(\frac{1.0}{5.0}\right)^{0.8}\right] = 0.00235 \qquad (5.29)$$

$$C_{dBottom} = \frac{1.328}{\sqrt{Re}}\sqrt{\frac{0.75}{5.0}}+\frac{0.072}{(Re)^{0.2}}\left[1-\left(\frac{0.75}{5.0}\right)^{0.8}\right] = 0.00249 \qquad (5.30)$$

Calculations for the rough surface drag coefficients are shown in Eqs. 5.31 and 5.32.

$$C_{dTop} = \frac{1.328}{\sqrt{Re}}\sqrt{\frac{1.0}{5.0}}+\frac{5.0-1.0}{5.0}\left[1.89-1.62\log_{10}\left(\frac{0.0001}{5.0}\right)\right]^{-2.5} = 0.00308 \qquad (5.31)$$

$$C_{dTop} = \frac{1.328}{\sqrt{Re}}\sqrt{\frac{0.75}{5.0}}+\frac{5.0-0.75}{5.0}\left[1.89-1.62\log_{10}\left(\frac{0.0001}{5.0}\right)\right]^{-2.5} = 0.00323 \qquad (5.32)$$

There is a little more laminar flow on the top, so the drag coefficient for the top is a little less than for the bottom. The drag area for the body of the car is then estimated from Eq. 5.33.

$$AC_{dBody} = (23.18)\left(\frac{0.00308+0.00323}{2}\right)1.046 = 0.0765\ \text{m}^2 \qquad (5.33)$$

This is a typical value for a well-streamlined solar car body. The drag area of the body will represent two-thirds to three-fourths the total drag area of a

well-designed car. The rest of the drag area comes primarily from flow around the wheels and fairings and to a lesser extent flow around the canopy.

Short Wide Car Versus Long Slender Car. The designer may ask, "For a given planview area and thickness, will a short wide car or a long slender car have less drag area?" The longer car will have a higher Reynolds number, and the Reynolds number is in the denominator when calculating the drag coefficients. Therefore, a long slender car will usually have a lower drag coefficient and drag area. Exceptions to this rule may occur if the short wide car can have more laminar flow, but in general the long slender car will have lower drag.

Homework. Calculate the drag area for the body described as follows: body length is 5 m, body width is 1.8 m, planview area is 8.75 m^2, thickness is 0.45 m, laminar flow is 0.5 m on the top of the car and 0.3 m on the bottom of the car, surface roughness is 0.2 mm on the top and 0.1 mm on the bottom, and all cross sections are elliptical. Assume that the tail of the car is not tapered. (1) Calculate drag area for 64.4 km/h (40 mph). [0.07649 m^2] (2) Assume that the laminar flow can be increased to 1.0 m on top and 0.6 m on the bottom and recalculate the drag area. What is the percentage reduction in drag area? [0.06988 m^2, 8.64%]

Angular Change in the Surface of the Body. An angular change in the body is undesirable from an aerodynamic aspect, but may be beneficial to another aspect of the car. Accordingly, there may be an abrupt change in the body angle because of design trade-offs. The increase in drag area because of an abrupt change can be estimated from the angle and distance over which the angular change occurs, as illustrated in Fig. 5.12.

If the angular change is less than 5° there is essentially no change in aerodynamic drag in the region. For larger angles the increase in drag area can be estimated from Table 5.4. If this change in angle occurs over some width b of the car, the increase in drag area is shown in Eq. 5.34.

$$ACd = (0.3\ m)\ \sin(\theta) b(\Delta C_D) \qquad (5.34)$$

If the distance is less than 30 cm, use the actual distance rather than 30 cm. This term is added to the turbulent boundary flow term for this area. That is,

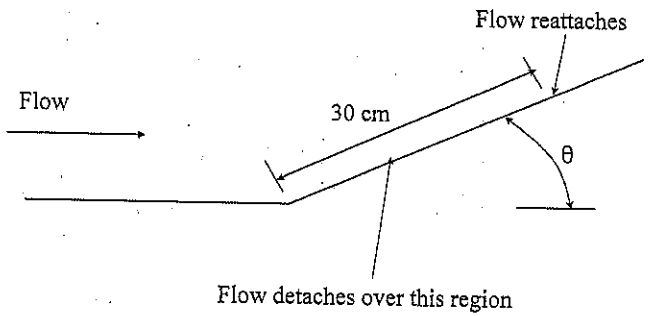

Fig. 5.12 Abrupt change in body angle.

TABLE 5.4
ABRUPT ANGULAR CHANGE

$\theta < 5°$	$\Delta C_D = 0.00$
$\theta = 10°$	$\Delta C_D = 0.10$
$\theta = 15°$	$\Delta C_D = 0.20$
$\theta = 20°$	$\Delta C_D = 0.25$
$\theta = 30°$	$\Delta C_D = 0.35$
$\theta = 45°$	$\Delta C_D = 0.50$
$\theta \geq 60°$	$\Delta C_D = 0.75$

this estimate accounts for the increase in drag because of the change in angle on the surface.

Example. To shorten the total length of the car, the tail is tapered as shown in Fig. 5.13. If the tail is 1.8 m wide, find the increase in drag area.

The 18° angles are measured for lines parallel to the top and bottom surfaces. Interpolating, $C_d = 0.23$ and the distance is less than 30 cm, so 25 cm = 0.25 m

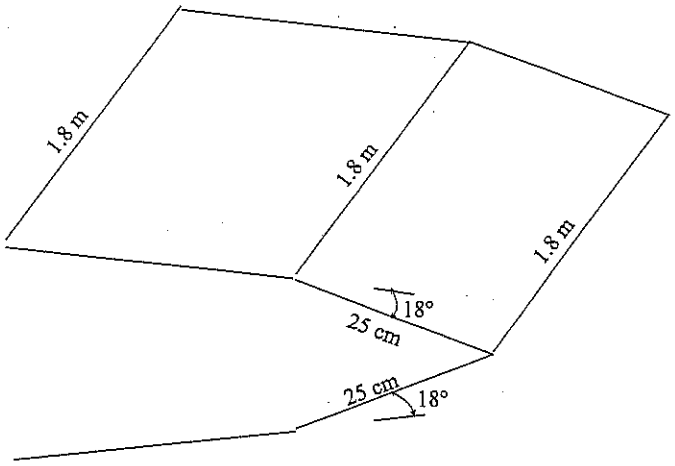

Fig. 5.13 Change in body angle to taper the tail.

will be used as the distance. The increase in drag area for the tapered tail is shown in Eq. 5.35.

$$AC_d = [0.25 \sin (18)](1.8)(0.23) \times 2 = 0.064 \text{ m}^2 \qquad (5.35)$$

This is a large drag penalty. The drag that comes from tapering the tail in this way is almost as much as the total drag on an aerodynamically shaped body. Body designs that lead to flow separation are very undesirable.

G. Canopy Drag

To estimate drag on the canopy, it is necessary to consider the shape of the canopies that are used, and also the information available for similar shapes. Many bubble canopies are ellipsoidal and so the best approximation in most cases is to use the drag on a half-ellipsoid solid. In the following analysis, it is assumed that the canopy width is approximately equal to the canopy height. The analysis is reasonable provided that the width is at least half the height,

and no more than twice the height. Most bubble canopies will fall in this range. The drag area for an ellipsoidal-shaped canopy can be estimated using Fig. 5.14 and Table 5.5 [5-4].

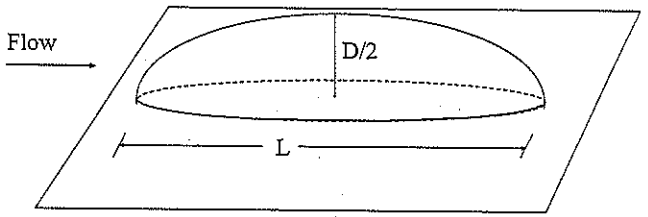

D = twice the canopy height, which would be the diameter of the ellipsoid solid
L = canopy length

Fig. 5.14 Flow over the canopy.

TABLE 5.5
ELLIPSOIDAL BUBBLE CANOPIES

L/D	AC_D
1.0	(7.85×10^{-2}) LD
2.0	(2.36×10^{-2}) LD
3.0	(1.02×10^{-2}) LD
4.0	(5.89×10^{-2}) LD
5.0	(3.93×10^{-2}) LD
7.0 (or more)	$(0.0157)D^2$

In addition to the drag on the canopy, there will be an interference drag caused by flow around the canopy interfering with flow on the body. To account for this, the turbulent boundary flow under the canopy will be included in the

total drag of the car. Even though the body area under the canopy is not exposed to the airflow and has no real aerodynamic drag, it should be included in the AC_D calculation for turbulent boundary layer flow on the body, to account for the interference drag around the canopy. Interference drag is proportional to the size of the canopy, so this is a reasonable approach.

In doing the CAD drawings for the body, the body will be drawn first and then components like the canopy will be added. It will be convenient to calculate the total drag on the body shape, and then add the drag of the components as they are added on. The approach illustrated here is to consistently add the drag on the body under the component added to account for the interference drag. This has the further "stability" advantage that adding things to the body will always increase the drag, which must be true.

Example. Consider a canopy that is 1.3 m long and 45 cm tall. The L/D ratio is calculated in Eq. 5.36.

$$\frac{L}{D}=\frac{1.3}{0.9}=1.444 \tag{5.36}$$

Use linear interpolation to obtain Eq. 5.37 and calculate the increase in drag area because of the canopy.

$$AC_d=(5.41\times10^{-2})(1.3)(0.9)=0.063\ m^2 \tag{5.37}$$

This is a large drag area because the canopy is large. Suppose the length of the canopy is increased to 2 m to reduce the drag. The drag area for this case is calculated in Eq. 5.38.

$$\frac{L}{D}=\frac{2.0}{0.9}=2.222 \Rightarrow AC_d=(2.06\times10^{-2})(2.0)(0.9)=0.037\ m^2 \tag{5.38}$$

Making the canopy long and slender helps reduce drag area. Suppose the length is increased to 3.6 m, making for a ridiculously long canopy. The drag area for this case is calculated in Eq. 5.39.

$$\frac{L}{D}=4.0,\ AC_d=(5.89\times10^{-3})(3.6)(0.9)=0.019\ m^2 \tag{5.39}$$

Clearly, a canopy 3.6 m long is impractical. Even a canopy 2 m long is questionable. Suppose the height of the original canopy is reduced to 30 cm. Equation 5.40 shows the drag area for this shorter canopy design.

$$\frac{L}{D}=2.17,\ AC_d=(2.14\times10^{-2})(1.3)(0.6)=0.017\ m^2 \tag{5.40}$$

These examples illustrate that it is more important to make the canopy shorter (reducing D) than to increase its length to give it a larger L/D ratio. Of course, the canopy must be able to accommodate the driver's head, but it should be as small as possible. These drag area calculations assume that the canopy is smooth. If it is not smooth because of a joint in the canopy, turbulence will be generated and the drag area will be higher.

Idealized Canopy Shape. A great deal of research has been done to determine the ideal shape for a canopy of a given size [5-1]. When viewed from the front, the canopy should be blended into the body with a small radius to minimize the frontal area. When viewed from the side, the canopy should be blended in with a large radius so that the side view of the canopy is "bell-shaped" [5-1]. Figure 5.15 illustrates the ideal canopy shape as viewed from the front and sides.

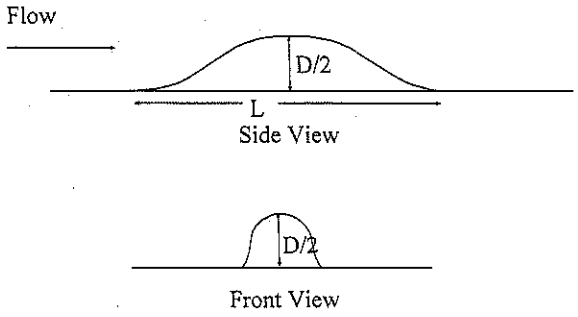

Fig. 5.15 Ideal canopy shape.

If this ideal canopy shape is used, then the canopy drag is reduced considerably, as compared with the ellipsoid design. However, this shape takes up a lot of space on the top of the car, and may reduce the size of the solar array. Teams may choose to "blunt" the front and/or rear of the canopy making it look more like the ellipsoidal canopy illustrated in Fig. 5.14. Table 5.6 lists correction factors for using the ideal shape. The drag area calculated using the ellipsoid formulas should be multiplied by the appropriate correction factor to estimate drag because of the canopy.

TABLE 5.6
CORRECTION FACTORS FOR "IDEALIZED" CANOPY

Blunted Front—Blunted Rear	1.0
Ideal Front—Blunted Rear	0.667
Blunted Front—Ideal Rear	0.357
Ideal Front—Ideal Rear	0.256

The designer may need to use judgment in deciding if the canopy is of ideal shape, or somewhere between ideal and blunted. Another correction factor can be added to account for the width of the canopy. If the width is w and the height is D/2, then the drag area can be adjusted by the canopy width correction factor in Eq. 5.41.

$$\text{Canopy width correction factor} = \sqrt{\frac{w}{D}} \tag{5.41}$$

Example. Assume that the canopy is 30 cm tall, 40 cm wide, and 150 cm long. It is blunted on the front, and ideal-shaped in the rear. Calculation of the drag area is shown in Eq. 5.42.

$$\frac{L}{D} = \frac{150}{60} = 2.5 \Rightarrow AC_d = (1.69\times10^{-2})(1.5)(0.6)(0.357)\sqrt{\frac{40}{60}} = 0.00443\ m^2 \tag{5.42}$$

Homework. Assume that the minimum-sized canopy required is 30 cm tall and 30 cm wide. An ellipsoidal-shaped canopy is 60 cm long. A canopy with idealized front or rear is 90 cm long, and a canopy with both the front and rear of idealized shape is 120 cm long. Assume that there is a rectangular cutout in the array for the canopy and that the solar cells produce 150 W/m^2. If the car is traveling 64.4 km/h (40 mph), what is the best shape for the canopy? [Ellipsoid canopy consumes 94.6 W and displaces 27 W of array area, idealized front consumes 61.5 W and displaces 40.5 W array power, idealized rear consumes 32.9 W and displaces 40.5 W array power, idealized front and rear consumes 14.6 W and displaces 54 W array power. Idealized front and rear is best, but idealized rear is almost as good.]

H. Other Shapes Protruding into the Airstream

Other items protruding into the airstream are typically rods, mirrors, and fins. Exposed items are generally undesirable. There are cases when exposed mirrors might allow the designer to reduce the size of the canopy, and the decrease in drag from reducing the size of the canopy may offset the drag caused by the exposed mirrors. For the World Solar Challenge the cars are required to be 1 m tall, and teams have placed a small aerodynamic fin on top of their canopy to meet this rule. This is another case where an item protruding into the airstream may reduce the overall drag of the car. Fins have also been used to stabilize airflow over the surface of cars, especially in crosswind conditions. Such fins increase the drag of the car, and should only be used if necessary. Exposed suspension components cause high drag forces, and are always undesirable. Figures 5.16 and 5.17 may be helpful in estimating drag on exposed components [5-4].

Example. Suppose that 50-mm-diameter flat mirrors are mounted on 6-mm-diameter rods 20 cm above the body as illustrated in Fig. 5.18. Estimate the drag area for two mirrors.

To reduce drag on the mirrors, assume a hemispheric leading edge was used on the mirrors and that an airfoil-shaped rod (aero rod) was used in place of the round rods. The drag area for the mirrors is estimated using Eq. 5.43.

$$AC_d = 2[(0.42)\pi(0.025)^2] + 2[(0.006)(0.2)(0.2)] = 0.0021\ m^2 \tag{5.43}$$

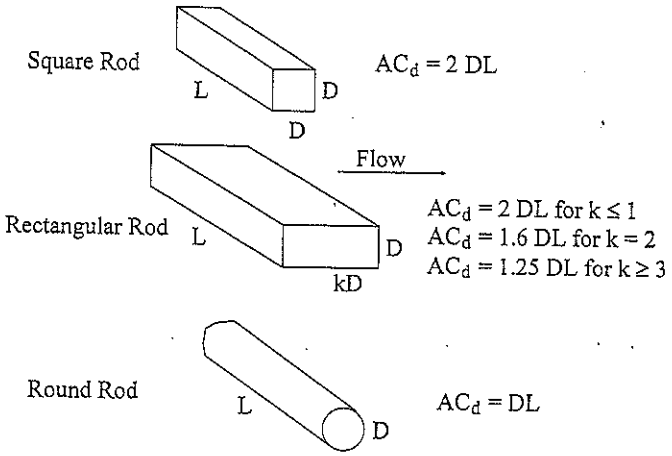

Fig. 5.16 Drag areas of common shapes I.

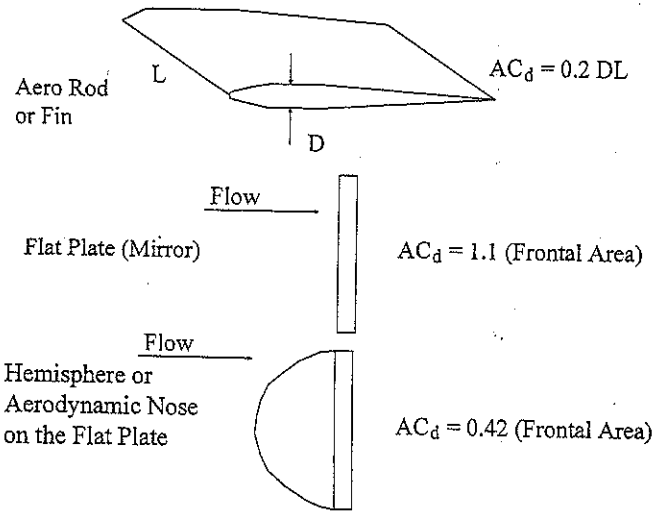

Fig. 5.17 Drag areas of common shapes II.

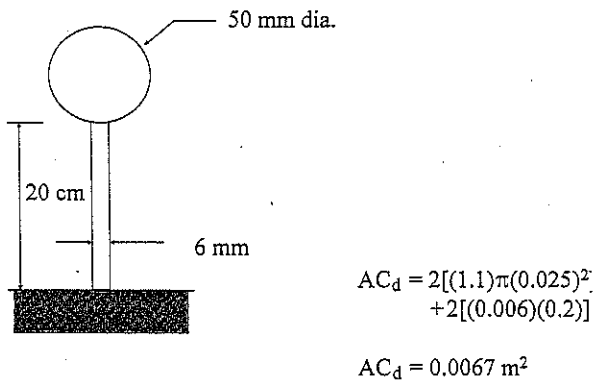

Fig. 5.18 Drag area of a mirror.

Putting the mirrors inside the canopy requires a larger, higher drag area canopy, but eliminates the external mirror drag. A drag area of $0.0021 m^2$ is not that high, when the target drag area for the whole car is 0.1–0.15 m^2. The designer could probably make the mirrors and rods smaller, and reduce the mirror drag to something insignificant.

I. Drag Caused by the Wheels

The flow around the wheels and fairings will contribute at least 20% of the drag of the vehicle, even if these areas are well designed. Poor design around the wheels can easily make this the most significant drag on the car, even larger than the drag on the body. It is very important to do a good job in interfacing the wheels with the body. Many teams have focused all their effort on the body and canopy and neglected the wheels. There is only one canopy, but there are three or four wheels, so this is poor judgment.

In general, the wheels should fit up inside the body as much as possible, making the fairings short. This reduces drag on the fairings. About 10 cm of wheel should be exposed below the fairings. The belly of the car body should be at least 25 cm off the ground to minimize the ground effects drag, so the ideal fairing would be about 15 cm tall if the bottom of the car is flat and 25 cm

off the ground around the wheels. Most teams set the belly further off the ground and round the bottom of the car so that typical fairings are 25–30 cm tall. The fairings should have an aerodynamic shape with as small of a frontal area as possible. The ideal shape for the fairings when viewed from the side is the same as the ideal shape for the canopy when viewed from the side. A large radius should be used to interface the fairings to the body, if possible. Because the fairings must turn with the wheels, a compromise is almost always made between aerodynamics and mechanical complexity. Keeping the wheels up inside the body makes the fairings shorter and helps make them easier to design, but necessitates a thick body design.

The fairings should fit tightly around the tires, and should be sealed to prevent air from flowing up into the car. Ventilation drag, because of air flowing up into the car through the wheel wells, can be a major source of drag. Tight-fitting fairings and sealed wheel wells are the best way to minimize ventilation drag. The following sections illustrate how to estimate drag around the wheels.

Exposed Wheels. Flow separation exists around all exposed portions of the wheels. Making the exposed portion of the tire–wheel combination a smooth shape helps, but it is not possible to keep the flow attached to the exposed wheels. The best chance for achieving attached flow is on the fairing, but it is not desirable to have the fairing go all the way down to the ground. Besides the obvious ground clearance requirement, making the fairings too long will increase the aerodynamic drag on the car.

The portion of the tire in contact with the road has a zero velocity as illustrated in Fig. 5.19. The drag coefficient of the exposed tire and wheel is higher than the fairing, but the tire and wheel have a much lower velocity. The fairing travels at the same speed as the car, but the portion of the tire near the road has a very low velocity. Aerodynamic drag is proportional to the square of the velocity, so there is an optimal amount of the wheel to leave exposed to minimize the total drag. The more tire exposed, the higher the average velocity of the exposed tire and wheel. The top of the tire is traveling at twice the speed of the car, so it is very undesirable to have the top portions of the wheels exposed.

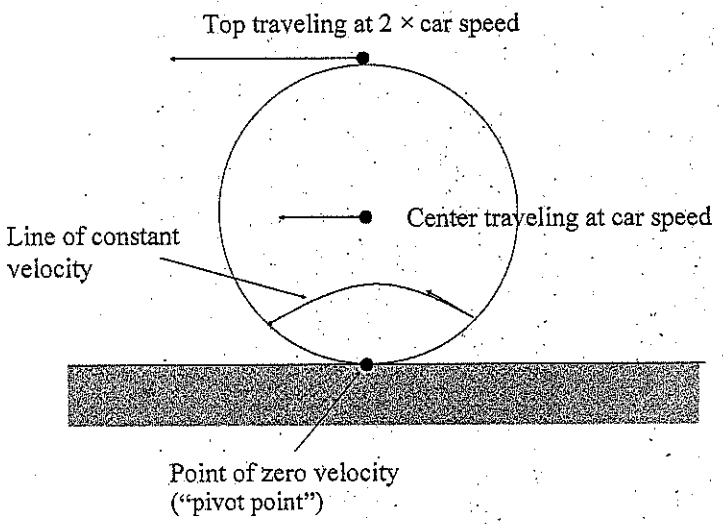

Fig. 5.19 Drag of exposed wheels.

The exposed portion of the wheel will behave like a bluff body, having a drag coefficient of approximately 2 based on the frontal area, but the average velocity will be less than that of the car. If the tire has a radius R and the car is traveling at velocity V_{car}, the average velocity of the tire (V_{tire})at some point h above the ground is shown in Eq. 5.44.

$$V_{tire} = V_{car}\left(\frac{h}{2R}\right) \tag{5.44}$$

Figure 5.20 illustrates an exposed wheel height of h below the fairing. If the tire has a width of b, then the frontal area is hb and the drag area based on the average velocity of the tire is $AC_d = 2hb$. The drag force, based on the velocity of the car, is then estimated using Eq. 5.45.

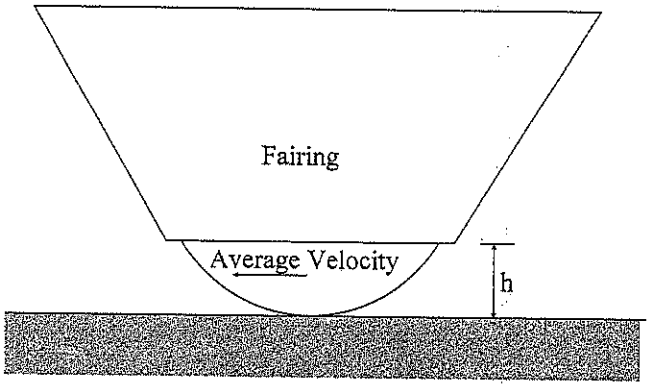

Fig. 5.20 Wheel velocity.

$$\text{Drag force} = \frac{1}{2}\rho V_{car}^2\left(\frac{h^2}{4R^2}\right)(2hb) = \frac{1}{2}\rho V_{car}^2\left(\frac{h^3 b}{2R^2}\right) \qquad (5.45)$$

Making the exposed frontal area hb smaller decreases the drag area directly. Making the tire radius R larger decreases the drag area by lowering the average velocity of the exposed portion of the tire. The drag area for the exposed portion of the wheel can be calculated using Eq. 5.46.

$$AC_d = \left(\frac{h^3 b}{2R^2}\right) \qquad (5.46)$$

Wheel Fairings. To estimate the drag on the fairings, an approach similar to the canopy will be used, except that fairings are more like an elliptic prism than an ellipsoid. For an elliptic prism of length L, width D, and height h, the drag area can be estimated using Fig. 5.21 and Table 5.7 [5-4].

An ellipse is not the most aerodynamic shape for the fairings. It is best to use an airfoil shape, though it is sometimes more difficult to interface the airfoil

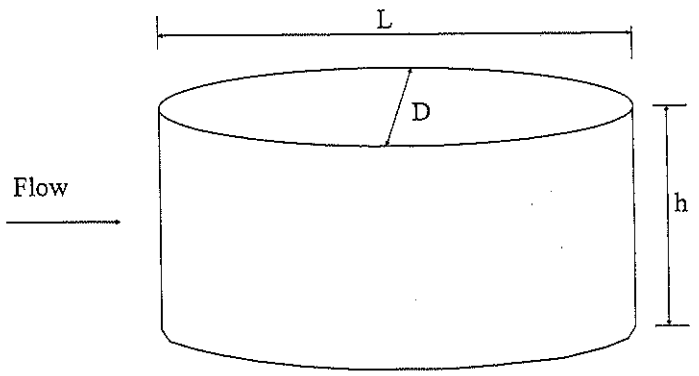

Fig. 5.21 Flow around an elliptic prism.

TABLE 5.7
ELLIPTIC WHEEL FAIRINGS

L/D	AC_d
1.0	0.5 hL
2.0	0.15 hL
3.0	0.067 hL
4.0	0.040 hL
5.0	0.025 hL
7.0 or more	0.1 hD

with the body and chassis. Because the fairing is attached to the body, the drag for the airfoil will not be as low as it would be if the airfoil were in free-stream flow. For an airfoil-shaped fairing, Table 5.8 should be used to estimate the drag area.

TABLE 5.8
AIRFOIL WHEEL FAIRINGS

L/D	AC_d
2.0	0.04 hL
3.0	0.025 hL
4.0 or more	0.1 hD

Example. Estimate the drag area for the wheel and fairing shown in Fig. 5.22. The tire is 5 cm wide and has a diameter of 48 cm. The fairing has an elliptic cross section with D = 15 cm and L = 50 cm at the bottom, and D = 30 cm and L = 1.1 m at the top, as shown in Fig. 5.22.

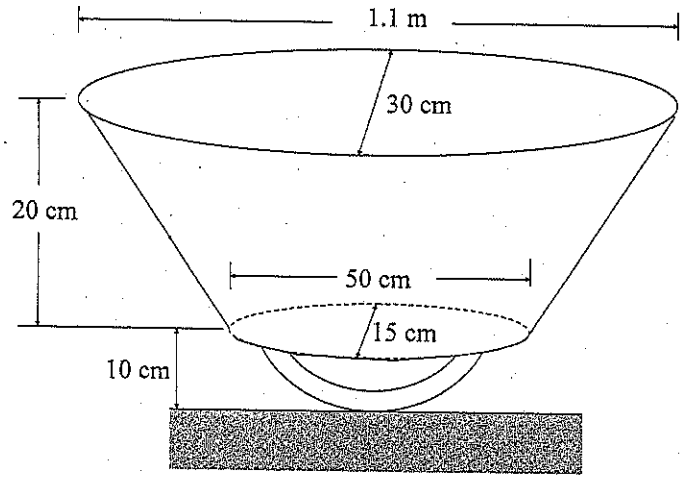

Fig. 5.22 Wheel fairing drag example.

Equation 5.47 estimates drag area for the exposed wheel.

$$AC_d = \frac{h^3 b}{2R^2} = \frac{(0.1)^3(0.05)}{2(0.24)^2} = 0.00043 \text{ m}^2 \qquad (5.47)$$

The average length of the fairing is (1.1 + 0.5)/2 = 0.8 m, and the average width is (0.3 + 0.15)/2 = 0.225 m. Equations 5.48–5.50 show calculations for the drag of the wheel fairing.

$$\frac{L}{D} = \frac{0.8}{0.225} = 3.56 \qquad (5.48)$$

Interpolating,

$$AC_d = 0.052 \text{ hL} = 0.052(0.2)(0.8) = 0.00832 \text{ m}^2 \qquad (5.49)$$

$$\text{Total } AC_d = 0.00832 + 0.00043 = 0.00875 \text{ m}^2 \qquad (5.50)$$

If the clearance is increased to 15 cm, shortening the fairing to 15 cm and increasing the exposed wheel to 15 cm, the calculations can be redone to yield a drag area of 0.00146 m^2 for the exposed wheels and 0.00624 m^2 for the fairing, a total of 0.00770 m^2. This shows that increasing the ground clearance under the fairing can reduce the drag on the car for a wide fairing like the one in the example. The fairing should be small and narrow to give maximum benefit, and the fairing in the example is a poor design. It would be better to use no fairings and leave half the wheels exposed than to use a large wide fairing like this one. If the average thickness is reduced to 10 cm and the average length is reduced to 70 cm, then L/D = 7. The drag area for this narrow-fairing design is shown in Eq. 5.51.

$$\text{Total } AC_d = (0.1)(0.2)(0.1) + 0.00043 = 0.00243 \text{ m}^2 \qquad (5.51)$$

Increasing the ground clearance to 15 cm for this narrow fairing makes the drag area 0.00296 m^2, which is an increase. Further improvements in reducing drag on the fairings can be achieved by using an airfoil shape.

Homework. Assume that the bottom of the car is to travel 30 cm above the ground, and the goal is to design a fairing to minimize the drag on the vehicle. The average fairing width is 15 cm, and the average fairing length is 75 cm to fit it around the wheel. The tire is 5 cm wide and 48 cm in diameter. Find the ground clearance that minimizes the drag on the wheel and fairing assembly for an elliptic-shaped fairing and an airfoil-shaped fairing. [12 cm for the elliptic shape and 10.7 cm for the airfoil shape]

Leading and Trailing Fairings (Taco Fairings). Teams have employed leading and trailing fairings on the wheels to reduce drag, as illustrated in Fig. 5.23. These are sometimes called taco fairings because they look a little like taco shells in front of and behind the wheel. The advantage of taco fairings over the full fairings is that they do not have to turn with the wheels. They can be mounted to the belly pan of the car, which is much simpler mechanically than mounting them on the kingpin. The disadvantage of these fairings is that they have higher drag than the full fairings. There may be cases where the reduction in mechanical complexity is more important than the reduction in aerodynamic drag.

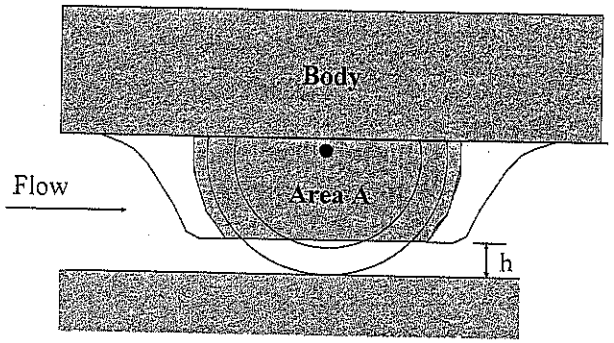

Fig. 5.23 Taco fairings.

To analyze the drag area for this design, include the frontal area of the taco fairings multiplied by a drag coefficient of 0.1, include the turbulent flow over the surfaces of the wheel as twice the exposed area (front and back) multiplied by a drag coefficient of 0.015, and include the term for the exposed portion of the wheel, as illustrated in Eq. 5.52. The leading and trailing fairings should be the same width as the tire.

$$\text{Total drag area} = (\text{fairing frontal area})(0.1) + 2A(0.015) + \frac{h^3 b}{2D^2} \qquad (5.52)$$

Example. Assume that the belly of the car is 30 cm above the ground and that the ground clearance h to the fairings is 10 cm. The fairings are 5 cm wide and the area A is estimated to be 960 cm^2. Find the drag area for the taco fairing arrangement. Assume that the tire is 5 cm wide and 48 cm in diameter. Equation 5.53 shows the example drag area calculation.

$$AC_d = (0.2)(0.05)(0.1) + 2(0.096)(0.015) + \frac{(0.1)^3(0.05)}{2(0.24)^2} = 0.00431\ m^2 \qquad (5.53)$$

If the wheels were not faired at all, that is, they are exposed, the drag area would be 0.0117 m^2 as shown in Eq. 5.54.

$$AC_d = \frac{(0.3)^3(0.05)}{2(0.24)^2} = 0.0117\ m^2 \qquad (5.54)$$

The conclusion to be drawn is that leading and trailing fairings are significantly better than no fairings. They are simple and unlikely to interfere with the wheel as it bumps up and down and turns. The leading and trailing fairings will probably have fewer reliability problems than full fairings. However, the minimum drag area comes from a small, thin, aerodynamic fairing wrapped around the tire. In summary, the drag area for a well-designed full fairing was 0.00243 m^2, for the taco fairings it was 0.00431 m^2, and for the fully exposed wheels it was 0.01170 m^2. In the absence of other analysis, these numbers can be used to estimate the value of designing fairings. At 88.5 km/h (55 mph), the power lost because of four fairings (or exposed

wheels) would be 85, 150, and 407 W, respectively, for the full, taco, and exposed wheel designs. Flow around the wheels also contributes to ventilation drag, as illustrated in the following section.

J. Ventilation

The driver, batteries, motor, and some electronics equipment require ventilation to keep from overheating. Ventilation always increases the drag of the car, and is thus undesirable. Uncontrolled ventilation can add a significant drag to the car. It is important to seal the body and provide only the ventilation needed.

Most of the air that flows into the car comes in through the wheel fairings as illustrated in Fig. 5.24. There is also usually a small vent to provide fresh air for the driver. Any air that is taken into the car will be accelerated from zero speed to the speed of the car. The kinetic energy of the mass of air is increased, and this energy must be provided by the power system of the car.

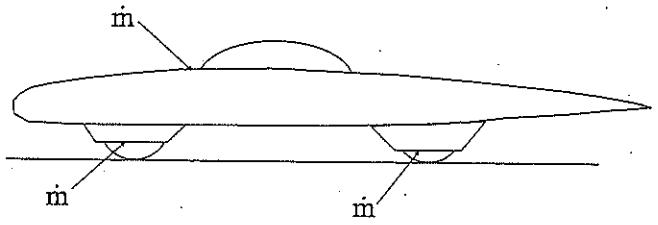

Fig. 5.24 Ventilation drag.

For a mass flow rate into the car of m, the power required is shown in Eq. 5.55.

$$\text{Power} = \frac{1}{2}\dot{m}V^2 \qquad (5.55)$$

If the car is traveling at 90 km/h (25 m/s), it does not take a large hole to allow 1 m^3 of air per second into the car. Because 1 m^3 of air has more than

1 kg of mass, the mass flow rate into a poorly sealed car could easily be 1 kg/s. A ventilation rate of 1 kg/s would absorb 300 W of power, which is more than the drag on all the fairings combined. It is very important to control the ventilation rate allowing air to enter the car.

The most obvious way to control ventilation is to seal the holes and prevent air from flowing into the car. Body seams should be tight to prevent air from entering through the seams. There should be one small vent directing air at the driver's neck and face. The driver should open this vent only if he or she is hot. The battery box must be vented into a wheel well. All air that is forced out of the battery box will be replaced by air from within the car, which must be drawn in through the cracks and seams. So all the air exiting the battery box will be replaced with air from outside the car, which adds to the ventilation drag. In general, the goal is to provide only necessary ventilation. By following this philosophy, the drag that arises because adequate ventilation is provided to the driver, batteries, electronics, and motor will be small compared to that arising from other sources.

The most significant ventilation drag comes from the flow into the wheel wells. Large holes must be provided for the wheels and tires, and it is inevitable that a significant amount of air will flow up into the wheel wells. This ventilation causes significant drag for the car, and the goal should be to minimize flow up into the wheel wells. There are two ways to minimize the ventilation drag around the wheels.

1. *Minimize the wheel hole opening.* The front wheels should fit through an hourglass-shaped opening in the belly pan. The hole should be large enough to allow the wheel to turn and bump up and down, but should be as small as possible. If fairings are used, they should fit as tightly as is practical around the tires and wheels to minimize the area available for air to flow up into the wheel wells. The fairings should be tapered about 10° as shown in Fig. 5.25, to help reduce the amount of air that is scooped up by the rear-wheel fairings.

2. *Seal the wheel wells.* The wheel wells should be sealed so that any air entering the wheel hole opening must also exit the wheel hole opening. Sealing the wheel wells will create a "back pressure" that will help keep the air from entering through the wheel hole openings. If the wheel wells

Cut an hourglass hole in the belly pan for the front wheels to minimize the size of the hole.

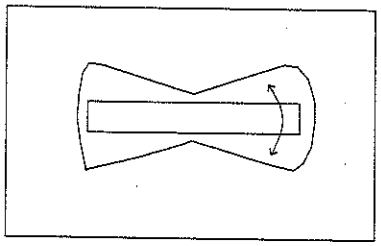

Taper the rear of the fairing approximately 10° to reduce the amount of air scooped up by the rear of the fairing.

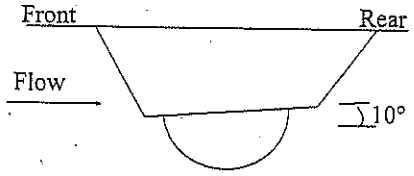

Fig. 5.25 Minimize wheel hole openings.

are open so that air can flow into the car, significantly more air will flow up into the wheel wells. The wheel wells should be as small as possible. A wheel well that fits tightly around the tire and wheel will seal better than one that is large and spacious.

The amount of drag caused by a ventilation hole depends on the orientation of the hole with respect to the flow, and on how well the volume behind the hole is sealed. It is possible to estimate the drag area for holes that are parallel and perpendicular to the airflow. The designer should recognize that these are estimates, and that volumes are usually not sealed or unsealed, but somewhere in between. Table 5.9 can be used to estimate the drag area for ventilation holes.

Example. Two vents, each 3 cm wide and 10 cm tall, are cut into the canopy to provide ventilation to the driver's face. The increase in drag area is calculated in Eq. 5.56.

$$AC_d = 2(0.03)(0.1)(0.52) = 0.0031\ m^2 \quad \text{[unsealed area]} \qquad (5.56)$$

TABLE 5.9
VENTILATION SUMMARY

Hole perpendicular to the flow	AC_d = (0.52)A (Unsealed area) AC_d = (0.26)A (Sealed area)
Hole parallel to the flow	AC_d = (0.13)A (Unsealed area) AC_d = (0.065)A (Sealed area)

The opening in the bottom of a wheel fairing is approximately 0.025 m^2. The drag area for a sealed and unsealed wheel well is calculated in Eq. 5.57, assuming this hole size.

$$AC_d \text{ (sealed)} = (0.065)(0.025) = 0.001625\ m^2$$

$$AC_d \text{ (unsealed)} = (0.13)(0.025) = 0.00325\ m^2 \qquad (5.57)$$

K. Wingtip Drag

Corners on the body generate vortices that increase the drag on the car. Such vortices occur at the wingtips on airplanes, hence the name wingtip drag. To minimize wingtip drag, the car body should be positioned so that it generates zero lift. This position yields the smallest drag for the car. Suspension adjustments should be made to achieve zero angle of attack. Zero lift is the single most important factor in reducing wingtip drag. If the body generates lift, up or down, there will be an *induced* drag, proportional to the lift generated. Induced drag acts on the car in addition to wingtip drag, and offsets any advantage gained by generating lift on the car. The car should be positioned for zero lift, and such positioning will require some trial and error and experimentation to find the zero lift point.

Round Corners. Use as large a radius of curvature as is prudent in the corners. The wingtip drag can be estimated for a car with a maximum cross-sectional profile as shown in Fig. 5.26.

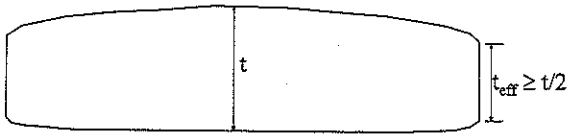

Fig. 5.26 Round corners prevent wingtip drag.

For the purposes of analysis, assume the car is of length L and has a maximum thickness of t. If the corners are rounded, then use t_{eff} as the distance between the inner parts of the curved radius as shown. *But*, as a minimum $t_{eff} = t/2$. That is, no matter how rounded the corners are, use t_{eff} as at least half the maximum thickness of the car. Equation 5.58 shows how to calculate the increase in drag area for wingtip drag [5-4].

$$AC_d = \left(\frac{\pi}{4} t_{eff} L\right)(0.15)\left(\frac{t_{eff}}{L}\right)^2 \text{ for each side} \qquad (5.58)$$

Example. Assume that a car's length is 5.5 m, that its maximum thickness is 40 cm, and that its corners have a radius of curvature of 2.5 cm. Equation 5.59 shows how to estimate wingtip drag area for two sides of the car.

$$AC_d = \left(\frac{\pi}{4}(0.35)(5.5)\right)(0.15)\left(\frac{0.35}{5.5}\right)^2 \times 2 = 0.00184 \text{ m}^2 \qquad (5.59)$$

L. Induced Drag

When a body is positioned with an angle of attack, it generates either upward or downward lift, and there is an increase in the drag called induced drag. Race cars running on circular tracks are designed aerodynamically so that downward lift will push the car downward on the track to improve traction. This allows the car to perform better in cornering and acceleration. Traction is not an issue in solar car design. The designer's goal is to minimize the drag. The angle of attack of the body should be adjusted to generate zero lift,

and thus zero induced drag [5-14]. After the car is built and is being tested, yarn strips can be taped near the rear of the car to help determine if the car is generating lift as it is being driven down the road. The rear swing arm should be adjusted to raise or lower the rear and zero the lift as best as possible. Power consumption data can also help determine when the lowest drag coefficient is achieved. It is better to generate a little upward lift than a little downward lift. Some teams have deliberately tilted the body of the car to generate a small amount of upward lift because this allowed the flow to stay laminar longer on the bottom of the car [5-1]. Accepting a small amount of induced drag in exchange for more laminar flow on the nose may be a good trade-off.

M. Summary

The following list is a summary of how the drag area would be divided up for an excellent car.

1.	Body drag area	= 0.0765 m^2
2.	No angular changes in body	= 0.0 m^2
3.	Canopy 30 cm tall × 1.5 m long	= 0.0063 m^2
4.	No rods or mirrors	= 0.0 m^2
5.	Well-designed wheel fairings for four wheels (0.00243 m^2/wheel)	= 0.00972 m^2
6.	Ventilation (four sealed wheels plus the driver)	= 0.0096 m^2
7.	Wingtip drag	= 0.00184 m^2
	Total	**0.104 m^2**

The main drag area sources are the body, canopy, exposed wheels and fairings, and ventilation system. Accordingly, certain goals must be set when designing the car.

- The body should have a smooth aerodynamic shape everywhere to keep the flow attached and to eliminate pressure drag. This is of paramount importance; there can be no compromise.

- Fairings should be developed that fit tightly around the tires and leave approximately 10 cm of exposed wheel area.

- The wheel wells must be sealed to control the ventilation. The openings around the tires should be small and sealed.

- The canopy should be small. It is especially important to make the canopy as short in height as possible. But the canopy must be large enough to hold the rearview mirror or external mirrors will be needed.

- The car should be designed to minimize the total surface area of the body, while incorporating 8 m^2 of solar array area on top.

N. Side Winds

Finally we will study the aerodynamic effect of side winds on the car. Solar car bodies are much more aerodynamic than passenger car bodies, and the side winds have a different effect. For side winds on the car, there is a side flow combined with a front flow, and the result is that the flow passes over the body at some angle θ as shown in Fig. 5.27. If the design is for a side wind of velocity V_S with the car traveling at velocity V, then flow is at some angle θ relative to the body.

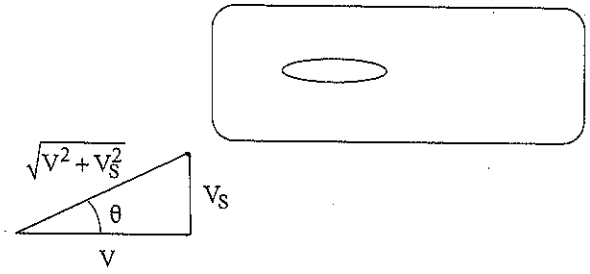

Fig. 5.27 Angled flow over the body.

The velocity of the air flowing over the car increases because of the side wind, and because drag is proportional to the square of velocity, it would appear that the drag would increase. If the flow stays attached to the body, then (for small angles θ) the drag force will increase due primarily to the increase in velocity over the car. The drag force has a lateral component that increases rolling resistance, and a direct component, drag on the car. The drag area will increase by the factor in Eq. 5.60, assuming a rolling resistance coefficient of C_{rr}.

$$\text{Factor} = \left(\frac{\sqrt{V^2+V_S^2}}{V}\right)\left(\cos\theta + (C_{rr})\sin\theta\right) \qquad (5.60)$$

This equation shows that the drag is almost constant for a side flow, which is approximately correct as long as the flow stays attached to the body. At some angle, the flow will begin to separate around the canopy and fairings, and there will be a sharp increase in drag. Equation 5.60 is not valid once an angle is reached where the flow begins to separate. It is difficult to quantify when the flow will detach, but the goal should be to design the body, canopy, and fairings so that the flow will stay attached for flow angles up to perhaps 30°. This will minimize the drag on the car when there is a side wind.

Sailing. If the flow stays attached to the body in a side wind, there will be a "sailing" effect which may reduce the drag of the car. The car body will behave like an airfoil with a slight angle of attack. With an angle of attack, an aerodynamically shaped body generates a lift force perpendicular to the flow and an induced drag force parallel to the flow. If the flow stays attached to the body, the lift force will be much higher than the induced drag, so that the combined lift and drag generate a thrust on the car in the direction the car is traveling and a side load that increases rolling resistance. Most of the combined force is to the side, but the wheels on the car prevent it from going sideways, just as the keel on a sailboat prevents the boat from going sideways. The side load does increase rolling resistance, so it is not quite as simple as is illustrated in Fig. 5.28.

If the flow stays attached, the lift and induced drag will generate a net thrust on the car, pushing it forward. There is still the drag term from the drag area

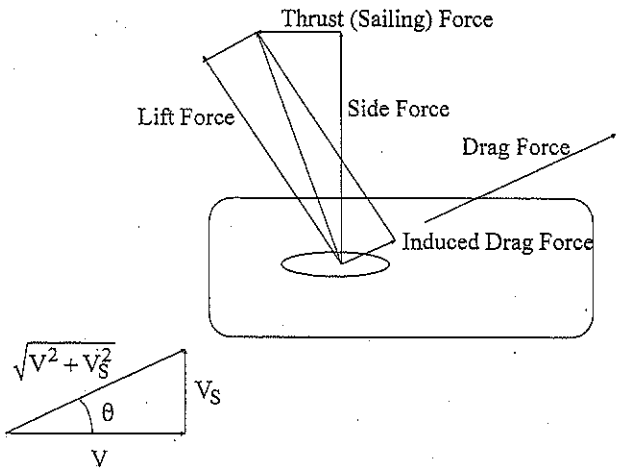

Fig. 5.28 Vector schematic for sailing.

that was previously calculated, and the thrust will not overcome this drag, but it is possible for the aerodynamic drag to be reduced by a side wind. For a body like a solar car, it would be reasonable for the induced drag to increase with the angle of attack θ for small angles of attack. The lift also increases with the angle of attack until the flow starts to separate, at which point the lift drops off dramatically and the drag increases dramatically.

Flow separation on the body is analogous to stalling of the airfoil. The lift is reduced and the drag increased. At some angle of attack the flow will begin to separate around the canopy and fairings, and the drag will increase sharply. The Biel solar car, which ran in the 1993 and 1996 World Solar Challenge, had a minimum drag for an angle of attack of about 20° because of the sailing effect [5-7].

If the car body is modeled as an ellipsoid-type airfoil, and typical lift-to-drag ratios are used for the angles of attack, Fig. 5.29 can be generated showing how the apparent drag area varies with a side wind. In the analysis the side wind was increased to generate an angle of attack. The net velocity increased

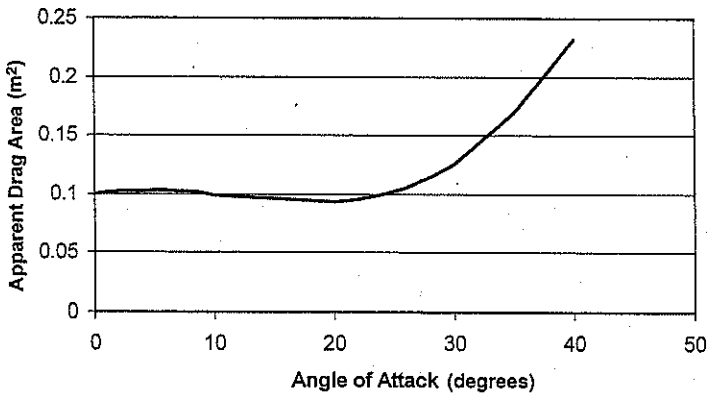

Fig. 5.29 Effect of sailing on drag.

with the angle of attack, as illustrated in Fig. 5.28. Parameters were adjusted so that the minimum drag would occur at 20° to correspond with data from the Biel car [5-7].

Homework. The best homework for this unit is to locate an existing solar car and measure it and calculate the drag area. Results from this analysis can be compared to the results obtained from the power consumption data for the car. If it is a well-designed solar car the drag area should be between 0.1 and 0.15 m^2. If a solar car is not available, photographs of solar cars can be used to get approximate dimensions and to go through the analysis. A lot of understanding may be gained by analyzing one or two existing designs.

O. Computational Fluid Mechanics (CFM)

The method of analysis outlined in this chapter can be used to develop a solar car body with a good aerodynamic design. If the side view of the body is that of a cambered airfoil, and if the body is smooth and rounded as suggested in this chapter, a low body drag will be achieved. If the top view is that of an airfoil like the Honda Dream III, it is unlikely that the computational fluid mechanics (CFM) analysis will yield any drag reduction in the body shape.

Airfoils are well understood and are the lowest drag shapes. If the CFM analysis yielded a different answer, the designer should be suspicious that something in the CFM model is wrong.

Nose Design. Most teams do not design the top view of the car to be an airfoil shape like the Honda Dream III because that shape greatly reduces the size of the solar array and because it is difficult to manufacture a body of that shape. The nose should be rounded to an extent, but the ideal shape of the rounded nose is not well understood now. CFM analysis can be helpful in refining the shape of the nose of the car. The streamlines going around the nose should be smooth and there should be a gradually increasing pressure gradient.

Canopy and Fairing Interfaces. The information in this chapter should provide a good basis for designing the interface between the canopy and body and the fairings and body. Some refinement may be possible using CFM analysis. The streamlines should flow around the canopy and fairings and rejoin behind them. The pressure will increase as the flow approaches the canopy and fairings, and will drop significantly as the flow goes around them. A large pressure drop indicates flow separation, so the design can be modified to control the pressure drop.

Side Winds. CFM codes excel in modeling an angled flow over the car body. Many different angles can be studied and the pressure plots are helpful in determining when flow separation will occur. Refinement of the sides of the body and the interfaces between the canopy and fairings and the body can improve the aerodynamics of the car in a side wind.

In summary, CFM codes can be helpful in refining the shape of the body. The codes are not capable of predicting an accurate value for the drag area of the vehicle, but they are capable of comparing two designs.

P. Wind Tunnel Testing

Wind tunnel testing of the car or of models can be helpful in refining the shape. If models are used, they must be accurate for the tests to be meaningful. Getting good information from a wind tunnel test requires expertise. Before attempting wind tunnel testing the team should consult with an expert

to help plan the tests to be conducted and to help interpret the results. Building a rough model of the car and having a novice test it in the wind tunnel may be fun and interesting, but it will not help design the car.

Q. References

5-1. Tamai, G., *The Leading Edge*, Robert Bentley Publishers, Cambridge, MA, 1999.

5-2. Gillespie, T.D., *Fundamentals of Vehicle Dynamics*, chap. 4, Society of Automotive Engineers, Warrendale, PA, 1992.

5-3. Milliken, W.F., and D.L. Milliken, *Race Car Vehicle Dynamics*, chap. 3, Society of Automotive Engineers, Warrendale, PA, 1995.

5-4. Munson, B.R., D.F. Young, and T.H. Okiishi, *Fundamentals of Fluid Mechanics*, John Wiley and Sons, New York, 1994.

5-5. Katz, J., *Race Car Vehicle Aerodynamics*, Robert Bentley Publishers, Cambridge, MA, 1995.

5-6. Ozawa, H., S. Nishikawa, and Higashida, D. "Development of Aerodynamics for a Solar Race Car," *JSAE Rev.*, vol. 19, pp. 343–349, 1998.

5-7. Roche, D.M., A.E.T. Schinckel, J.W.V. Storey, C.P. Humphris, and M.R. Guelden, *Speed of Light: The 1996 World Solar Challenge*, chap. 5, Photovoltaics Special Research Center, University of New South Wales, Sydney, Australia, 1997.

5-8. Storey, J.W.V., A.E.T. Schinckel, and C.R. Kyle, *Solar Racing Cars*, chap. 4, Australian Government Publishing Service, Canberra, Australia, 1994.

5-9. Kyle, C.R., *Racing with the Sun: The 1990 World Solar Challenge*, chap. 5, Society of Automotive Engineers, Warrendale, PA, 1991.

5-10. Hucho, W.H., *Aerodynamics of Road Vehicles*, Society of Automotive Engineers, Warrendale, PA, 1998.

5-11. Lissaman, P., *GM Sunraycer Case History Lecture 2-1: Concepts in the Aerodynamic Drag of Road Vehicles*, Society of Automotive Engineers, Warrendale, PA, 1992.

5-12. Abbot, I.H., *Theory of Winged Sections*, Dover Publications, New York, 1959.

5-13. Hibbs, B., *GM Sunraycer Case History Lecture 2-2: Sunraycer Aerodynamic Development*, Society of Automotive Engineers, Warrendale, PA, 1992.

5-14. Fukuda, H., K. Yanagimoto, H. China, and K. Nakagawa, "Improvement of Vehicle by Wake Control," *JSAE Rev.*, vol. 16, pp. 151–155, 1995.

Chapter 6

Composite Materials

A. Body Structure

The body structure of solar cars is made from foam or honeycomb core composite materials, sometimes called sandwich composites. These materials are very lightweight and have high stiffness [6-1 to 6-3]. The structure of these materials is illustrated in Fig. 6.1.

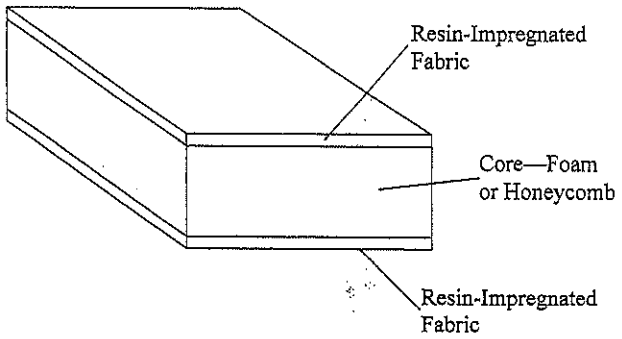

Fig. 6.1 Sandwich composite construction.

The core has a resin-impregnated fabric bonded to each side, which is why it is often called a sandwich composite. The materials required to make the composite are as follows:

1. *Fabric.* The fabric is made from either glass, graphite, or Kevlar fibers woven into a fabric similar to the cloth from which men's dress shirts are

made. Use of these high-strength structural fibers comes from their historical development for the aerospace industry. Tests have shown that nylon, polyester, or cotton fibers would have the required strength for many applications and be much less expensive. Strength of the fabric is seldom what limits the strength of the composite. The problem in using common fabric is that it was not designed to work with the resin. Department store fabrics may absorb too much resin, making a heavy composite, or may not bond well with the core, making a weak composite.

2. *Core.* Honeycomb core has been made from aluminum, paper, and phenolic polymer or blends. It provides the highest strength-to-weight ratio of the core materials, but it is more difficult to get a good bond between the core and fabric with honeycomb core than with foam core. Vacuum bagging is required to get a good bond, and this complicates the manufacturing process. Styrofoam and other polymer foams have also been used for the core. The trend has been to use styrofoam core, primarily because it is lightweight, inexpensive, easy to work with, and gives a good bond with the fabric. Foam core makes the manufacturing much easier because a good bond between the fabric and core can be obtained without vacuum bagging. It does make a significantly weaker composite than can be achieved with honeycomb core, so the honeycomb is the best choice for components that require high strength.

3. *Resin.* Epoxy is used almost exclusively for the resin, but there are many types of epoxy. Polyester resin is inferior to epoxy. For solar cars the most important component in the composite is the resin. If the team is on a limited budget, it is best to skimp on the foam and fabric and buy good resin. The resin is also the toxic portion of the lay-up. It is important for the safety of the team members to get a low-toxicity epoxy resin.

B. Body Strength Requirement

Solar car bodies are a unique and interesting topic in designing with composites. The loads on the body are small, and almost any composite will be strong enough if a box beam type of construction is used. The main goal is to find lightweight fabric and core to design as lightweight a body as possible. The entire body, including the canopy, solar cells, encapsulate, and electronics

will probably weigh less than 535 N (120 lb), which is very lightweight for a car body that is 5 m long, 1.8 m wide, and 0.4 m thick. About half of this weight comes from the solar cells, encapsulate, and electronics. Most of the loads on the body are proportional to its weight, so keeping the body light in weight helps reduce the loads the body must carry.

The most significant load case for the body is the load applied by the team members as they remove and replace the body or carry it around. The body must be strong enough so it will not be damaged by the point loads applied by hands lifting and carrying it. This strength comes primarily from the placement of internal body ribs supporting the body surface. Team members will not be able to see the internal rib structure of the body once it is built, so it is good design strategy to have enough internal ribs to carry a load of 225 N (50 lb) spread over the area of a person's hand anywhere on the bottom or side of the body. The ribs should go through to the top of the car too to ensure that the stiffness is adequate to prevent flexing and vibration of the solar array. The body must also be able to carry the weight of the solar array and aerodynamic loading, but these loads are spread over large areas and are much less likely to damage the body than the loads required to pick the body up and carry it around. Most of the remainder of the significant body loads come from the connections between the body and chassis or body and array stand, and are discussed in the next section.

C. Attachment Points

The loads can become large at the attachment points, where the body is attached to the chassis or array stand. There are several instances of specific loads that must be considered when designing attachment points. If the body is hinged on the chassis to facilitate driver egress, the egress loads will be approximately equal to the weight of the car body. The body will have to be tilted upward by either the driver or a spring actuator. This load(s), and the loads on the hinges, will be on the order of the weight of the body. The body may have to be reinforced in these areas to carry the loads.

The car will hit bumps when driving that will transmit dynamic loads to the body equal to two or three times the weight of the body. These loads must be carried by the attachment mechanisms between the body and chassis. For a

conservative design, each of the attachment points should be able to carry a load equal to three times the weight of the body without causing damage to the body. The bump loads will actually be divided among the connection points and most of them will not see a load equal to three times the weight of the body, but the bump loads happen continuously while driving the car. The connections must be overdesigned to prevent fatigue failure in this area.

The body will be placed on an array stand for morning and evening charging of the batteries. Loads on the array stand will be less than the bump loads. If the body is attached to the array stand in the same manner that it is attached to the chassis, satisfying the bump load requirements for the chassis will make the attachment points adequate for the array stand. If a different attachment system is used, the attachment points must be able to carry the weight of the body and the wind loading that inevitably happens when the body is tilted toward the sun in the early morning and late evening. The attachment points should be able to carry two times the weight of the body for a conservative design.

If careful attention is paid to the aerodynamic design, the aerodynamic loads will be less than 120 N (25 lb) when the car is being driven in still air. Side winds and passing trucks may increase the aerodynamic loads to 450 N (100 lb) in normal driving conditions, and the load could be in any direction. (A poor aerodynamic design could result in much higher loads.) Designing for bump loading is generally adequate for aerodynamic loading. The most important difference is that the connections must be able to carry the loads in all directions, not just up and down.

The connections must also carry cornering and braking loads, and there may be other loads for equipment attached to the body. In most cases designing the body-to-chassis connections to carry three times the weight of the body, and designing the array stand connections to carry two times the weight of the body will be adequate for all load cases.

D. Body Support Plates or Angles

For most designs, the interface between the chassis and body has the body resting on plates or angles as illustrated in Fig. 6.2. For a steel or aluminum

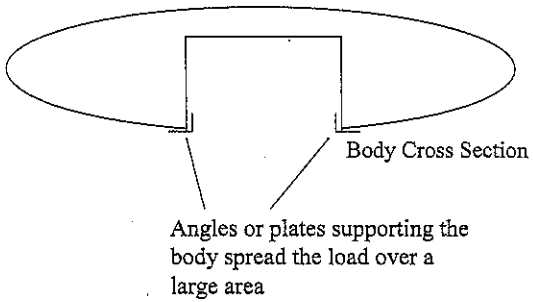

Fig. 6.2 Angles or plates supporting the body.

chassis design the supports are usually angles. For a composite chassis design they are usually composite plates. The body must be lifted off the chassis as it is put on the array stand, so for most designs it makes sense to have overlapping plates supporting the body. The plates also help provide a seal between the body and chassis to reduce ventilation drag. The plates or angles that the body rests on when it is placed on the chassis should be large to spread the load and reduce the stress on the body near the attachment points. Most of the time the load is downward (gravity), so spreading out the load reduces stress on the body and chassis for the prevailing gravitational loading.

Besides the supporting angles or plates, there must be connections that firmly hold the body down on the chassis, preventing it from bouncing up and down or sliding fore or aft. The connectors may require a more substantial core than foam or honeycomb. Wood or aluminum may be used for the core locally to increase the strength as illustrated in Fig. 6.3.

It may be prudent to add a couple of layers of fabric to further reinforce areas near connections. The connection should be capable of holding at least three times the weight of the body, nominally 1600 N (360 lb), to be sure that it will be reliable. There is a temptation to skimp on materials in the connector areas to reduce weight, which can make the connectors unreliable.

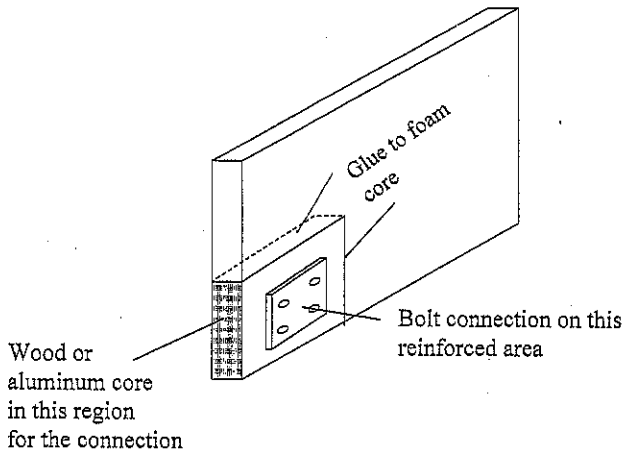

Fig. 6.3 Reinforcing areas near connections.

E. Quality of Lay-Up

Quality of the lay-up is of paramount importance, and this means (primarily) putting the epoxy where it is needed, and not putting it where it is not needed. Cleanliness is very important too.

1. The core must have a clean surface so it will be possible to get a good bond with the fabric. The best choice for a clean, smooth surface is the blue styrofoam commonly used as insulation for homes in construction. This foam is inexpensive, and comes with a plastic sheeting on both sides. Remove the sheeting just prior to lay-up, as illustrated in Fig. 6.4, to ensure a clean, smooth surface for bonding.

   If honeycomb core is chosen, or a foam core that has been hot-wired or sanded to shape, the surface will be porous. It is very difficult to get this surface clean once it is dirty, so be sure to keep it clean or preferably in its wrapper until time to use it. It is almost impossible to keep resin from flowing into the pores or honeycomb cells during lay-up, and so a porous or honeycomb core tends to absorb more resin than an extruded foam

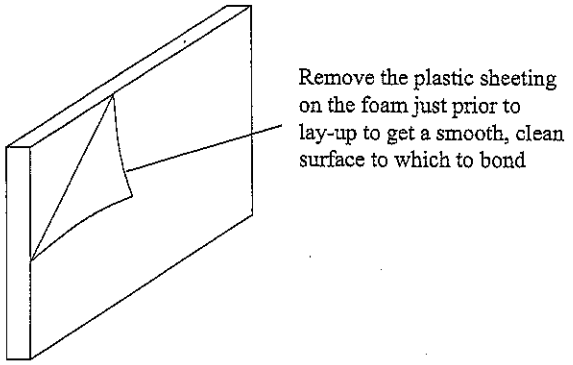

Fig. 6.4 Removing plastic sheeting from foam core.

core with a smooth surface. Honeycomb may have a lower density than the extruded foam core, and theoretically makes a lighter composite, but some allowance must be made for the extra resin that will be absorbed by the honeycomb core.

2. The resin must be worked into the fabric to fully wet the fabric, and to bond it to the foam. There should be no air bubbles or dry areas under the foam, because this reduces the bonding between the core and the fabric.

3. Excess resin should be removed from the surface with a squeegee to keep it smooth and to keep the car light in weight. Care must be taken because a little extra resin everywhere adds a lot of weight to the car. Small blobs on the car's surface increase the surface roughness and aerodynamic drag.

4. The fabric will be put on in pieces, and the edges of the pieces must be blended in with the squeegee to keep the surface smooth. The main quality goals are:

   a. Bonding should be complete at the interfaces and joints with no air pockets or dry areas. This makes the structure strong.

b. No excess resin should flow down into the honeycomb or foam pores, and there should be no excess resin blobs on the surface of the body. This keeps the structure lightweight.

c. The surface should be kept smooth to reduce aerodynamic drag on the car.

5. There is always some body work to be done after laying up the body. Being careful throughout the process to keep the body smooth reduces the amount of body work, which saves work and reduces the weight of the body.

F. Box Beam Construction

A box beam construction technique integrates the top and bottom of the car into one unit, similar to a box. Internal ribs are used to stiffen the top and bottom panels and to reduce the vibration or flexing of the panels. A box beam construction technique makes a lightweight rigid body structure. The body will need to have a cutout to allow it to fit down on the chassis, so it is not a complete box, but many teams have used this box beam approach to make a rigid lightweight body structure.

The other approach is to have only the top of the car body removed when placing the solar array on the charging stand, and many teams have used this approach. For this approach, honeycomb core composites are required to provide the required strength and stiffness to the top of the car, and there will probably need to be some stiffening ribs on the back of the top to further stiffen it. This makes the top of the car heavier than it would be with a box beam construction, but it may be a good design trade-off for certain chassis designs.

The body is really a nonstructural component of the car because the loads are so small. From a structural viewpoint, the main efforts in designing the body are in finding lightweight composite materials because with a box beam construction almost any composite is strong enough for the body. Loads on the chassis are much higher, and the chassis is a safety-critical structural item. The challenges in designing a composite chassis are as follows:

1. The biggest challenge is to determine the precise strength of the composite material used. A test procedure is required to determine the strength and stiffness of the composite material. The strength is highly dependent on the manufacturing process, and a high-quality and reliable manufacturing process must be developed in conjunction with the strength and stiffness testing. It must be possible to tailor the strength of the composite to the strength required in various areas on the body and chassis.

2. Analysis techniques, including finite element codes, must be available that can deal with the unique material properties of core-type composites. These techniques must be able to analytically determine the lay-up process to be used in various areas on the chassis.

Many teams use composites for the chassis of the car. Premade honeycomb composite panels are available and are a good choice for the chassis. The panels can be cut just like plywood and glued together to make a box-type chassis. This process requires significantly fewer man-hours to manufacture than a welded metal tube-frame chassis. The strength and stiffness of the composites are not as well understood as the metals, and because of this a composite chassis is usually a little heavier than a properly designed welded metal tube-frame chassis.

G. Mold and Body Construction

Once the body is designed and the materials are selected, it must be manufactured. A mold is required to hold the composites to the required shape during manufacturing. Most teams use a three-dimensional mold to make the body. Building the mold requires a lot of work and time, so some teams have adopted the rib mold approach described below.

1. Make a wooden rib structure that approximates the shape of the top of the car. Ideally the body shape should be drawn as a solid model or a surface model in a CAD package. The computer model can then be "sliced" every 20 or 30 cm along the length to get shape profiles for the top of the body. A numerically controlled cutter can be used to cut the ribs out using the drawing files, or if that is not available a large plotter can be used to print out the rib shapes full scale. The plots can be glued

or taped to wooden sheets, and the shapes can be cut out with a band saw. The wooden ribs should be cut with respect to reference planes as illustrated in Fig. 6.5, so that it will be easier to align the ribs in the mold.

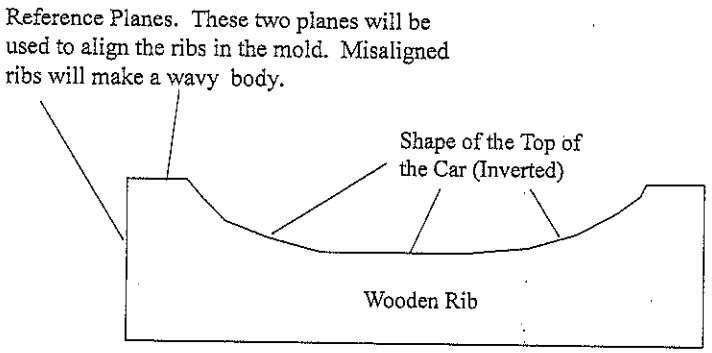

Fig. 6.5 Wooden ribs for the mold.

2. Once the wooden ribs are cut out, they are placed into a wooden mold and aligned so that the mold forms the inverted shape of the top of the car as illustrated in Fig. 6.6. Care should be taken to get the ribs properly aligned in the mold and firmly anchored in place. The accuracy of the body shape depends on getting the ribs aligned.

3. Sheets of foam are glued together to make a single piece large enough to make the top of the car. For complex curves on the body, it will be necessary to cut out a sliver of the foam to make it fit in the mold as illustrated in Fig. 6.7. To do this, cut the foam, and allow it to overlap and push it down into place. Mark the overlap sliver and cut it out.

   The plastic sheeting should not be removed from the foam as it is fit to the mold. This will help ensure a clean surface for bonding. After the foam is fit to the mold, it should be glued in place on the bottom side to the ribs. Use epoxy to glue it to the mold so it will stay firmly attached. The plastic sheeting is what is actually glued to the ribs, not the foam.

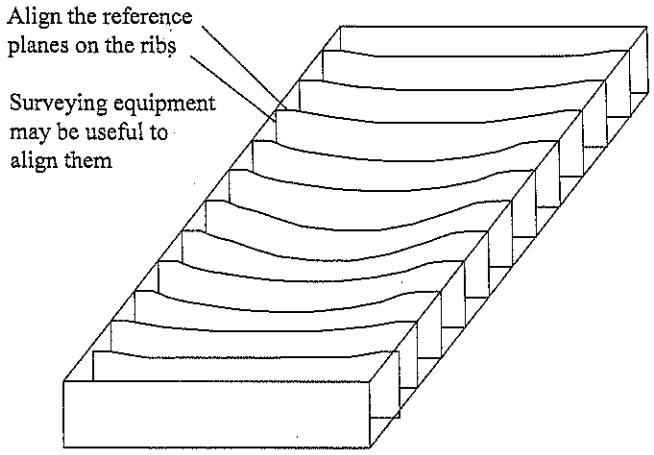

Fig. 6.6 Rib mold.

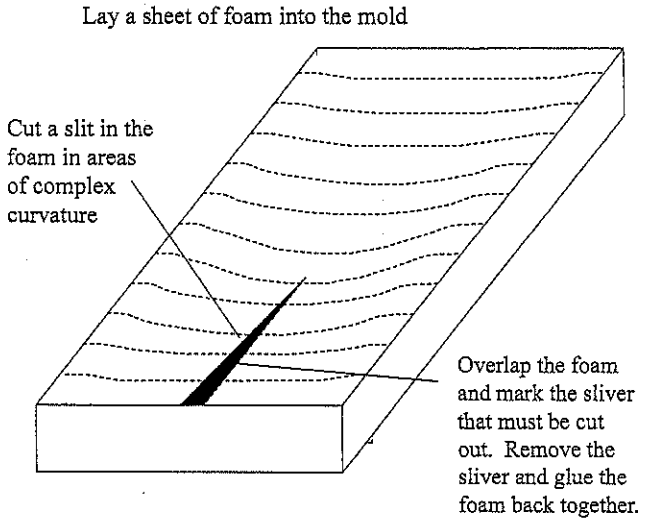

Fig. 6.7 Laying the first sheet in the mold.

4. Once the foam is securely glued to the ribs, clean the top of the foam and remove the plastic sheeting on that side. Cover the foam with a layer of fabric and resin and let it cure. Peel ply should be placed on the areas where ribs are to be attached so it will be easier to make a good bond between the fabric and the foam ribs that will be placed inside the body. Peel ply is designed to not bond well with the epoxy so it can be peeled off later. The peel ply will leave a clean, slightly rough surface that is ready for bonding with the ribs.

5. Make the foam ribs that will be used as interior ribs for the car body. Be sure that the interior ribs will not line up exactly with the wooden ribs in the mold, or they will be difficult to hold in place while the resin cures. The internal ribs typically have a very low stress. Foam ribs are adequate for the internal ribs. No composite fabric need be applied to them. The top and bottom panels need a composite fabric on both sides, and regions near where the body is connected to the chassis may need multiple layers of fabric to reinforce the connections.

6. Glue the interior ribs in place on the top. If possible, hold or tape the rib in place until the epoxy cures. Weights can also be balanced on top of the ribs to hold them in place. If necessary use Sheetrock screws to hold the ribs in place while the epoxy cures. Sheetrock screws hold the pieces tightly together and create a good bond, but they leave holes in the top surface and create body work later, which increases the weight of the body. Figure 6.8 illustrates the process of using Sheetrock screws. The screws should be removed after the epoxy cures to reduce weight.

7. Tape joints should be made on the ribs to be sure they are well bonded to the top. The tape joints are made from resin-impregnated fabric. There is no benefit in overlapping the joints more than 25 mm (1 in.).

8. The bottom of the car should be fabricated over the ribs that are attached to the top of the car. The bottom is glued to the ribs and held in place with weights or Sheetrock screws. If fabric is to be used on both sides of the bottom, it must be placed on the inside before the bottom panel is attached over the ribs.

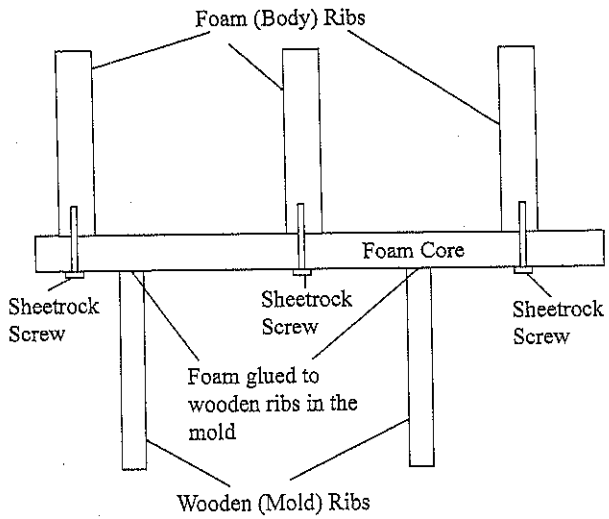

Fig. 6.8 Placing body ribs.

9. If possible, tape joints should be applied to the bottom and ribs. It will be difficult to reach some of these, and access holes may need to be cut for the tape joints, or it may not be practical to use tape joints everywhere on the bottom.

10. As much as possible, the foam core should be bent into the shape of the car body. This yields the best and lightest-weight laminate. However, there will be areas on the nose, tail, and edges that have too much curvature, and it will not be possible to bend foam sheets into shape. There are several options for finishing the edges.

    a. Foam blocks can be sanded into shape and glued onto the body in its current state. (At this point the outside part of the body has not been covered with fabric.) This is usually the simplest approach, and it has the advantage of being the most durable. The disadvantage is that it is the heaviest approach.

b. Foam ribs can be made that approximate the desired shape; and then these regions can be covered with Mylar sheeting. This is very lightweight, but degrades the aerodynamics slightly, and the Mylar is easily torn. Mylar requires considerable maintenance. It will need to be replaced many times during the life of the car.

c. Foam blocks can be sanded into shape as in option (a) and covered with fabric, which is allowed to cure. Paint thinner can be used to dissolve the foam away leaving a fabric shell of the correct shape. The shell may require ribs to hold its shape, or it may be stiff enough without the ribs. The shell is then attached to the body using tape joints. This is lighter in weight than the solid foam and more durable than Mylar, but it is also very time-consuming and easily damaged.

11. After the body shape is complete, the entire exposed surface should be covered with fabric, being sure to make the surface as smooth as possible. If the foam is not smooth, then the fabric over it will not be smooth either. It is best to perform the body work before covering the surface with fabric. The fabric creates rough areas where pieces are overlapped. When practical, make the overlaps on the top (under the solar cells) or in other places that will not be exposed to airflow when driving. This process will yield a very lightweight and aerodynamic body.

H. Strength and Stiffness of Honeycomb and Foam Core Composites

Most solar car teams (including corporate teams) do not have the expertise and quality control to optimize the design of the composite body. Composites offer the flexibility of altering the core material and/or thickness, the number of layers of fabric, fabric type and weight, and the resin used. Minimizing the weight is desirable, but it is not an easy task. The strength of these materials is highly dependent on the manufacturing process used. Testing should be done to measure the strength of the material, and the results can be used to do stress analysis on the body and optimize the design.

Before the team starts on a testing and analysis program, an estimate should be made of the possible benefits, that is, the weight that might be saved. Are

lighter materials available? If the lightest-weight core and fabric available were used, it does not help to do an analysis and find that a lighter-weight fabric or core would be adequate. A foam core body like the one described above will weigh less than 350 N (80 lb). The solar array and miscellaneous electronic components will add about 175 N (40 lb), bringing the total weight of the body to less than 535 N (120 lb). With careful attention to detail, bodies of this type have been produced that weigh 450 N (100 lb). The solar array weight can be reduced by using thinner cells and coatings, but the thinner cells may not be as efficient, and thinner coatings may produce a rougher surface or not protect the cells. The maximum possible weight savings for the body is 350 N (80 lb) (making its weight zero), and a more realistic weight savings is 50 N (11 lb). It may not be worth the extra testing and design efforts to optimize the body design. The team may be better off spending that time and effort on other aspects of the car.

1. *Tensile Strength.* Tensile strength is governed by the strength of the fabric. Fabric strength is governed by the strength of the fibers used. Fabric strength is generally measured in newtons per meter width, indicating the amount of force [in newtons (N)] required to break a strip of fabric 1 m wide. A test that can be performed to measure tensile strength is the tension test. A piece of composite is cut into a tensile specimen as illustrated in Fig. 6.9 and then tested. It will probably be necessary to replace the core material with wood on the ends that fit into the machine grips to prevent crushing of the composite.

   If P_{max} is the breaking load of the fabric and w is the width of the specimen, the strength of the fabric is given by Eq. 6.1.

$$\text{Fabric strength} = \frac{P_{max}}{2w} \tag{6.1}$$

   Structural fabrics such as glass, graphite, or Kevlar usually have a rated strength from the manufacturer. Composite strength is highly dependent on the manufacturing process, so testing should be done to measure the strength. The composite may not achieve the full manufacturers' rating.

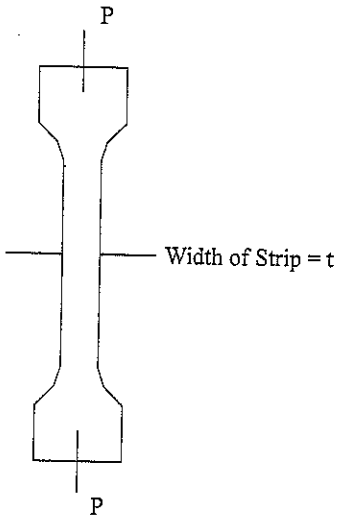

Fig. 6.9 Tensile specimen.

The stiffness of the composite fabric in tension can also be measured if a gauge is used to measure the strain e. The force per inch width can be plotted against strain, and the slope of the linear region is the stiffness (E/w) in newtons per meter. Typical results of a tension test are illustrated in Fig. 6.10.

Example. A tensile specimen was tested and the load-deflection data shown in Fig. 6.11 were taken. The foam core has a thickness of 1 cm. Find the strength and stiffness of the composite fabric.

Calculations for fabric strength and stiffness are shown in Eqs. 6.2 and 6.3.

$$\text{Fabric strength} = \frac{1100\ \text{N}}{2(0.019\ \text{m})} = 28{,}900\ \text{N/m width} \qquad (6.2)$$

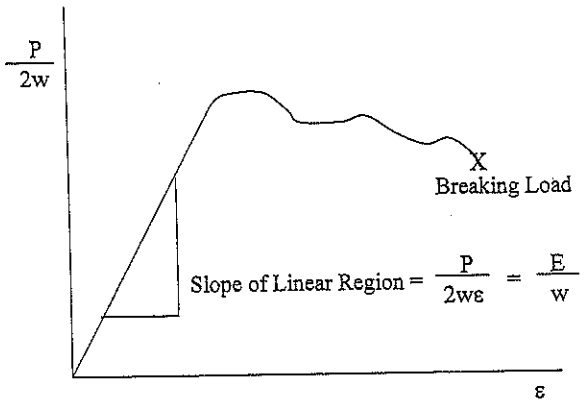

Fig. 6.10 Tensile test results.

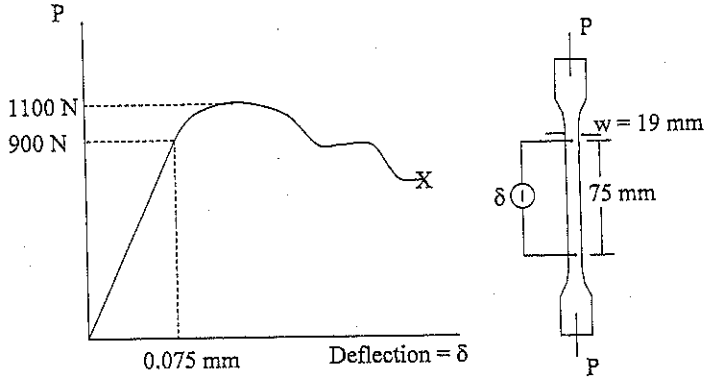

Fig. 6.11 Tensile test example.

$$\text{Fabric stiffness} = \frac{900\text{ N}}{2(0.019\text{ m})\left(\frac{0.075\text{ mm}}{75\text{ mm}}\right)} = 23{,}700{,}000\text{ N/m width} \qquad (6.3)$$

Assuming fabric on both sides, a 1-cm-wide strip could support 2(0.01)(28,900) = 578 N tensile force.

Example. Suppose the fabric above is placed on both sides of a foam core 2 cm thick. What would the strength of the composite be? [28,900 N/m. The tensile strength does not depend on the core used because the core does not contribute significantly to tensile strength of the composite.]

2. *Compression Strength.* A compression test is similar to a tensile test except that the specimen is much shorter in length and is loaded in compression instead of tension. Rectangular blocks of the material are crushed between two steel load platens as illustrated in Fig. 6.12. The block is loaded in compression as shown, and the failure load P_{max} is measured.

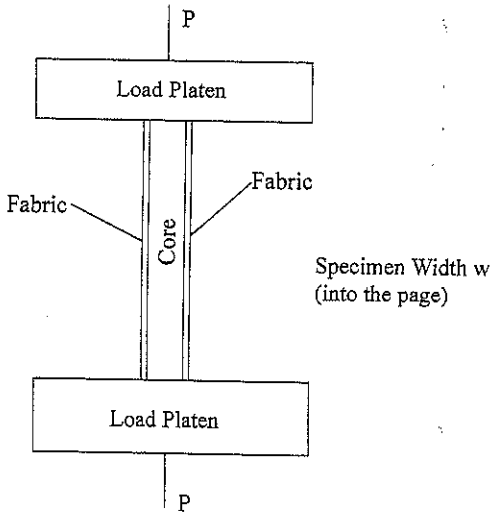

Fig. 6.12 Compression test.

The strength of the fabric in compression is then calculated using Eq. 6.4.

$$\text{Fabric strength} = \frac{P_{max}}{2w} \qquad (6.4)$$

where w is the width of the specimen.

To obtain accurate results, the length L of the specimen should be short enough to get local buckling of the fabric, and not global buckling of the sample as illustrated in Fig. 6.13.

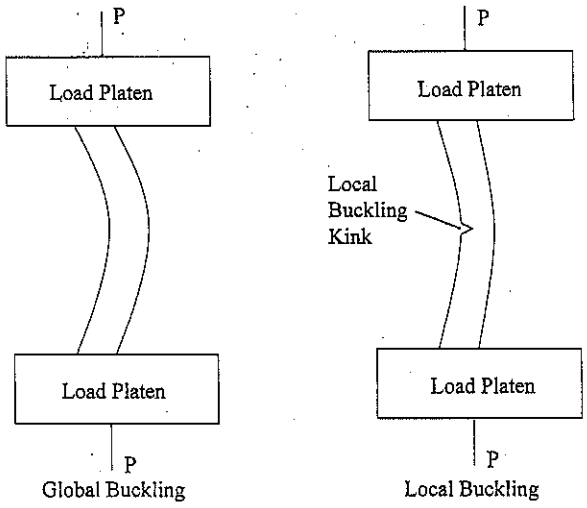

Fig. 6.13 Buckling of the composite specimen.

The specimen should not bow out significantly before it kinks. Ideally a kink would form on both sides, but that does not usually happen. This test yields a good estimate of the compression strength of the composite. The compression strength depends on the fabric, the quality of the bonding, and the "through-the-thickness" stiffness of the core material. A foam core has much lower stiffness than a honeycomb core. The local buckling kink forms by the fabric buckling into the core, and so a

high-stiffness core like honeycomb will help prevent the buckling kinks and increase the compression strength of the composite compared to the softer foam core material. Poor bonding yields a low-strength composite regardless of the core of fabric materials used. Large-celled honeycomb often has poor compression and flexure strength because of kinks forming over the large cells. A thicker fabric will have higher compression strength, but this comes at the expense of a large increase in weight.

Example. Suppose a foam core composite is tested as illustrated in Fig. 6.14. Find the strength and stiffness of the fabric. The failure mode is local buckling, that is, kinking of the fabric.

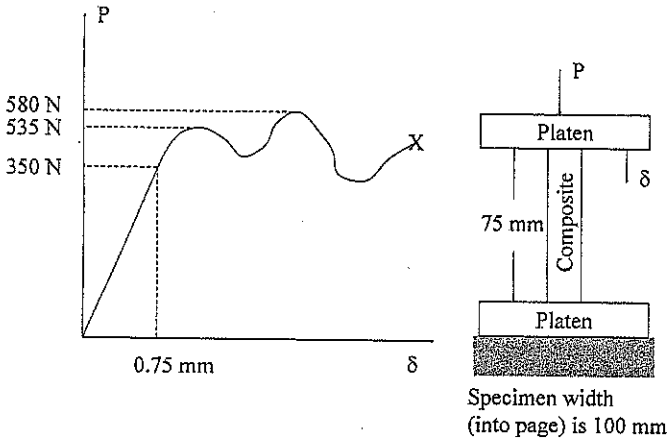

Fig. 6.14 Example of a compression test.

The strength and stiffness of the composite in compression are calculated in Eqs. 6.5 and 6.6.

$$\text{Fabric strength} = \frac{535\ \text{N}}{2(0.1\ \text{m})} = 2675\ \text{N/m} \qquad (6.5)$$

$$\text{Fabric stiffness} = \frac{350\ \text{N}}{2(0.1\ \text{m})\left(\frac{0.75\ \text{mm}}{75\ \text{mm}}\right)} = 175{,}000\ \text{N/m} \qquad (6.6)$$

A 1-cm-wide strip of the composite with fabric on both sides would have a compression strength of 53.5 N. The strength value in compression is much lower than the tensile strength values, which is typical for foam core composites.

Example. Suppose a thicker foam core were used. Would the compression strength be different? [If the foam is of the same type, the compression strength would be approximately the same, 2675 N/m, though the thicker foam would increase the strength to some degree. If a different type of foam were used the compression strength would change. A stiffer foam would yield a higher strength and a softer foam a lower strength. A honeycomb core would yield a higher compression strength.]

3. *Flexure Strength.* Flexure tests are a combined tension and compression test, and are a good test method for foam or honeycomb core materials. When a panel is bent, one side is in tension and the other is in compression. The shear and bending moment diagrams for the test are illustrated in Fig. 6.15.

   For this simple loading case, the fabric on top is in compression and the bottom is in tension. Assuming good bonding between the fabric and core, there are three possible failure modes, as illustrated in Fig. 6.16.

   a. *Tensile Failure.* The fabric tears or breaks on the bottom side. Tensile failure is rare for foam core or honeycomb core composites. Compression failure or delamination failure are the usual modes.

   b. *Compression Failure.* The fabric on the top surface buckles down into the core, yielding a crease in the panel. Honeycomb core has a much higher resistance to this type of failure than foam core, which is why the honeycomb core generally yields a higher compression and flexure strength. Low-density foam core yields a low buckling strength, but the strength is dependent on the fabric and resin used, not just the core.

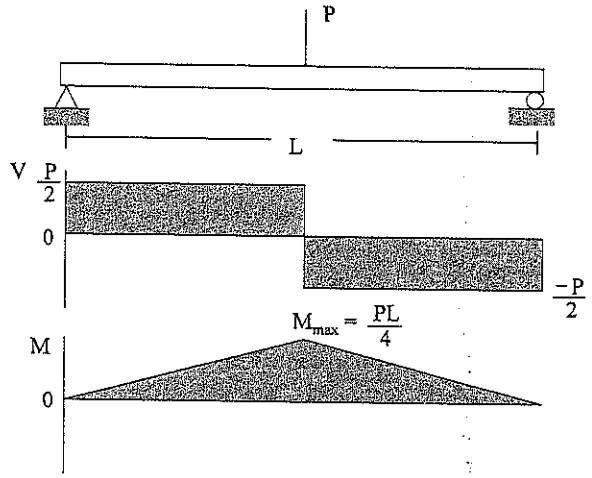

Fig. 6.15 Shear and bending moment diagrams for a flexure test.

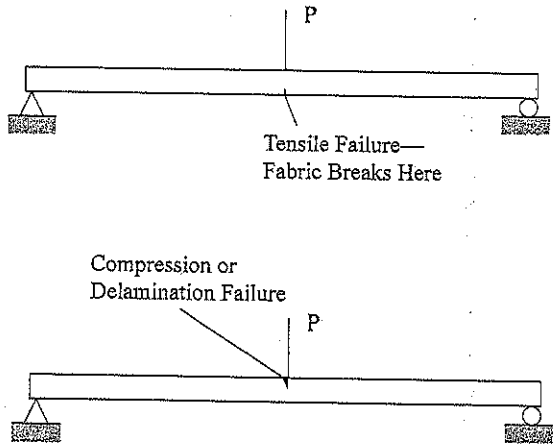

Fig. 6.16 Flexure test.

c. *Delamination Failure.* The fabric on the top of the specimen delaminates from the core and buckles outward away from the core. This is more common for honeycomb composites than for foam core composites. Large cell honeycomb composites often exhibit this failure mode.

The failure mode determines whether the tensile, compression, or delamination strength of the composite is calculated. In the test, a maximum bending moment M_{max} will be reached and the strength of the composite is given by Eq. 6.7.

$$\text{Composite strength} = \frac{M_{max}}{t} \tag{6.7}$$

where t is the thickness of the composite. The force per unit width is obtained by dividing by the width w of the specimen. If the specimen is supported on a span L and loaded in the center with P_{max}, the strength of the composite is given by Eq. 6.8.

$$\text{Composite strength} = \frac{M_{max}}{wt} = \frac{P_{max}L}{4wt} \tag{6.8}$$

Example. A Kevlar/foam composite is tested on a 30-cm span. The specimens are 10 cm wide and 15 mm thick, and fail on the compression side by buckling into the foam (compression failure) when a load of 70 N is applied. Find the compression strength of the fabric.

Solution. The strength is calculated in Eq. 6.9.

$$\text{Composite strength} = \frac{(70\text{ N})(0.3\text{ m})}{4(0.1\text{ m})(0.015\text{ m})} = 3500\text{ N/m} \tag{6.9}$$

Example. Suppose a cantilever beam is to carry the 90-N load illustrated in Fig. 6.17. If the beam is 60 cm wide, what is the required foam thickness? Use a safety factor of 3, limiting the compression load in the fabric to (3500/3) N/m.

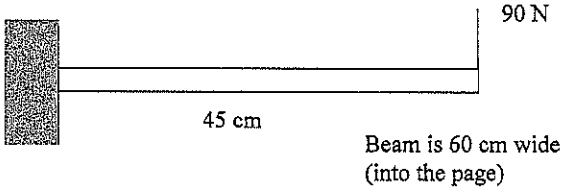

Fig. 6.17 Example of flexure strength.

The solution is given in Eqs. 6.10–6.12.

$$M_{max} = (90\ N)(0.45\ m) = 40.5\ N/m \tag{6.10}$$

$$\frac{3500\ N/m}{3} = \frac{40.5\ N/m}{(0.6\ m)(t)} \tag{6.11}$$

$$t = 58\ mm \tag{6.12}$$

The foam core should be 58 mm thick to carry the load. This illustrates how the experimental data can be used to design composite panels to carry a bending load.

The flexure test can also be used to estimate the stiffness of the composite. Stiffness is important to reduce vibration of the body panels, and to prevent cracking of the cells. However, it is difficult to say what stiffness is required, so the usefulness of this information is questionable. Stiffness data are necessary to do finite element modeling of the composite structure. The flexure test will yield a load-deflection curve similar to the one shown in Fig. 6.18.

The flexure stiffness of the composite beam is characterized by the term EI, and for this load case EI is given by Eq. 6.13.

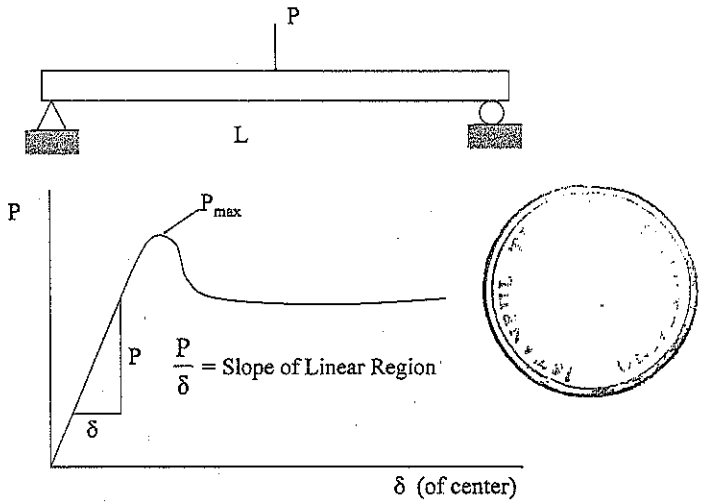

Fig. 6.18 Example of flexure stiffness.

$$EI = \left(\frac{P}{\delta}\right)\frac{L^3}{48} \tag{6.13}$$

where P/δ is the slope of the load-deflection curve. The useful number for design is the stiffness per unit width, as shown in Eq. 6.14.

$$\left(\frac{EI}{w}\right)_C = \left(\frac{P}{\delta}\right)\frac{L^3}{48w} \tag{6.14}$$

Knowing the stiffness per unit width of the composite, it is possible to estimate the stiffness per unit width of the fabric. This is useful in extrapolating the stiffness data to other core thicknesses. The stiffness of the fabric depends on the type of core material used, so it is not correct to extrapolate to other types of core material. The cross section of the composite is illustrated in Fig. 6.19.

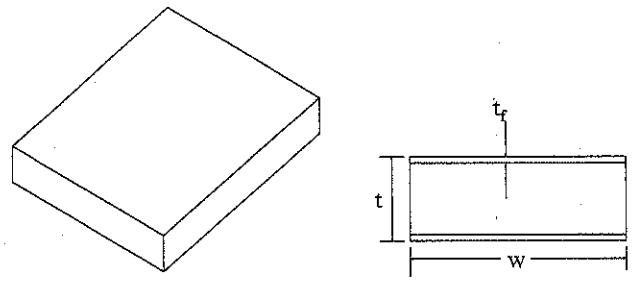

Fig. 6.19 Example of composite cross section.

Assuming that the core contributes very little to the overall stiffness, the moment of inertia I of the specimen is given by Eq. 6.15.

$$I \approx \left[\frac{wt_f^3}{12} + wt_f\left(\frac{t}{2}\right)^2\right](2) \tag{6.15}$$

where t_f is the thickness of the fabric, t is the thickness of the specimen, and w is the width of the specimen. Since $t_f << t$, the first term is small compared to the second and the moment of inertia can be approximated by Eq. 6.16.

$$I \approx \frac{wt_f t^2}{2} \tag{6.16}$$

With these approximations, the modulus of elasticity (E) for the fabric is then given by Eq. 6.17.

$$E = \frac{\left(\frac{EI}{w}\right)_C}{\frac{t_f t^2}{2}} \tag{6.17}$$

For composite fabric, the modulus comes primarily from the fibers, so it is customary to multiply E by the fabric thickness t_f to get the stiffness per unit width $(E/w)_{fabric}$ as shown in Eq. 6.18.

$$\left(\frac{E}{w}\right)_{fabric} = \frac{\left(\frac{EI}{w}\right)_C}{\frac{t^2}{2}} \tag{6.18}$$

The fabric stiffness can be used to estimate the beam stiffness when the same fabric is used on a core of different thickness. As stated, fabric stiffness depends on the core material used, so the fabric stiffness measured in this type of test cannot be used for different types of core materials, only different thicknesses of the same core material.

Example. A beam that is 10 cm wide and 19 mm thick is tested on a 30-cm span and the results are shown graphically in Fig. 6.20. Find the stiffness of the fabric.

Solution. Calculations of the stiffness of the fabric are illustrated in Eqs. 6.19 and 6.20.

$$\left(\frac{EI}{w}\right)_C = \left(\frac{P}{\delta}\right)\frac{L^3}{48w} = (3300)\frac{(0.3)^3}{48(0.1)} = 18.56 \text{ N/m} \tag{6.19}$$

$$\left(\frac{E}{w}\right)_{fabric} = \frac{\left(\frac{EI}{w}\right)_C}{\frac{t^2}{2}} = \frac{18.56}{\frac{(0.019)^2}{2}} = 103{,}000 \text{ N/m} \tag{6.20}$$

Example. Find the stiffness of the composite if a piece of foam 25 mm thick (the same type of foam) is used for the core. The stiffness is estimated in Eq. 6.21.

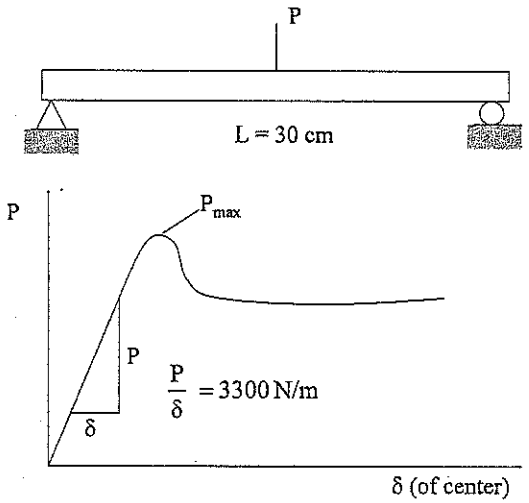

Fig. 6.20 Flexure test results.

$$\left(\frac{EI}{w}\right)_C = \left(\frac{E}{w}\right)_{fabric}\left(\frac{t^2}{2}\right) = (103{,}000)\left(\frac{0.025^2}{2}\right) = 64.4\ \text{N/m} \qquad (6.21)$$

which is a significantly higher stiffness than for the 19-mm core.

I. Composites Assignment

1. An Excel data file is available from the author that contains data for three compression specimens and three flexure specimens. Plot load versus deflection for each of the specimens tested. (Plot load as the y-axis and deflection as the x-axis.) The first part of the file for each test is header information that can be ignored, although it does give the maximum load for the test that is helpful in calculating the strengths. There are three columns of numbers below the header. The first column is a counter, giving the number of data points. The second column gives

the displacement of the crosshead of the machine (and therefore of the specimen) in inches. The third column displays the load on the specimen.

2. For the flexure specimens calculate the compressive strength of the fabric when loaded in flexure. Also calculate the composite stiffness and the fabric stiffness in compression.

   Compressive strength of the fabric = $(P_{max})(L)/[4(w)(t)]$

   P_{max} = maximum load on the composite
   L = span of the fixture = 21 cm
   w = specimen width = 2.25 in.
   t = specimen thickness = 0.625 in.

   Composite stiffness = $(P/d)L^3/[48(t)]$
   (P/δ) = slope of the linear portion of the load-deflection curve
   L = span of the fixtures = 21 cm
   t = specimen thickness = 0.625 in.

   Fabric stiffness in compression = composite stiffness/$[t^2/2]$

3. Calculate the compressive strength and compressive stiffness of the fabric for the compression test on foam core composites.

   Compression strength = P_{max} /[2(w)]
   P_{max} = maximum load on the specimen
   w = specimen width = 3.0 in.
   (There is a factor of 2 because there is fabric on both sides.)

   Fabric compressive stiffness = $(P/\delta)h/[2(w)]$
   (P/δ) = slope of the linear region of the load-deflection curve
   w = specimen width = 3.0 in.
   h = specimen height = 3.0 in.

J. References

6-1. Morgan, R., and M. Cowley, *GM Sunraycer Case History Lecture 5-2: Structure (Composite Shell)*, Society of Automotive Engineers, Warrendale, PA, 1992.

6-2. Roche, D. M., A.E.T. Schinckel, J.W.V. Storey, C.P. Humphris, and M.R. Guelden, *Speed of Light: The 1996 World Solar Challenge*, chap. 4, Photovoltaics Special Research Center, University of New South Wales, Sydney, Australia, 1997.

6-3. Storey, J.W.V., A.E.T. Schinckel, and C.R. Kyle, *Solar Racing Cars*, chap. 5, Australian Government Publishing Service, Canberra, Australia, 1994.

Chapter 7

Car Balance and Spring Rates

A. Car Balance and Moment of Inertia

The suspension isolates the car and driver from the harshness of the road surface. Probably the biggest benefit of a suspension in solar car racing is that it keeps the body of the car from bouncing around too much when the car hits bumps, which reduces the aerodynamic drag on the car [7-1]. The suspension helps keep the tires on the road when the car hits bumps, which provides better handling and control of the vehicle. Keeping the tires on the road also eliminates some of the skidding that occurs when a tire leaves the road and then comes back down and makes contact, which reduces the rolling resistance and tire wear on the vehicle [7-1 to 7-4]. The first step in designing the suspension is to balance the car and select the spring and damper rates for the front and rear. These rates will be used to calculate spring constants for the individual wheels once the geometry is developed. To calculate spring rates the wheelbase, weight of the car, and moment of inertia of the car must be known. The center of gravity (CG) will be located between the front and rear axles as illustrated in Fig. 7.1.

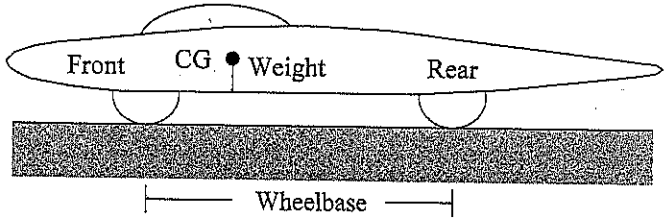

Fig. 7.1 Center of gravity (CG) and wheelbase.

The weight of the car is typically about 2700 N (600 lb) for an open-class car and 3700 N (850 lb) for a stock-class car. The wheelbase is typically 2.0–2.5 m (80–100 in.). Selecting the design weight and wheelbase of the car are conceptual decisions. There is no analysis to help determine an exact estimate for weight or wheelbase. It must be based on what has been accomplished with cars of similar design. The battery technology to be used is the main impact on the weight estimate of the car. A well-designed solar car with lead-acid batteries will weigh approximately 3700 N (850 lb), while a similar car with lithium-polymer batteries will weigh 2700 N (600 lb).

Most solar cars are three-wheeled vehicles with two wheels in front and a single rear wheel. For stability, a three-wheeled vehicle should be balanced so that there is an approximately equal weight on all of the tires [7-5]. The CG for most cars should be closer to the front axle than to the rear as illustrated in Fig. 7.1. Another issue is that solar cars usually have active brakes only on the front wheels, with regenerative braking on the rear wheel. It is difficult to design a brake system for the drive wheel, especially for a hub motor drive, so even the four-wheeled cars usually have active brakes only on the front. To ensure proper braking performance, the weight must be balanced so that 60–70% of the weight is on the front wheels, even for four-wheeled cars. This will ensure that the car will be able to stop in a reasonable distance. U.S. races have a braking test requirement that the car be able to stop with approximately a 0.5 g deceleration, including the reaction time of the driver, and it will be difficult to pass the braking test if less than 60% of the weight is on the front wheels.

Center of gravity and polar moment of inertia are elementary topics, but the general process needs to be tailored to solar cars. Several assumptions must be made to get started, and the best way to illustrate the process is with an example. For the example, assume a 2.5-m (98-in.) wheelbase and a total weight of 3700 N (830 lb) for the car (a stock-class vehicle). The main weights for the car are 785 N (176 lb) for the driver, 1500 N (336 lb) for the batteries, and 535 N (120 lb) for the body and solar array. To bring the total to 3700 N, assume that "everything else" weighs 880 N (197 lb), and that the weight is evenly distributed over the chassis so that the CG of the "everything else" weight is centered between the two axles. The CG for the 535-N body load is assumed to be at the center of the car body. The battery and

driver weights can be moved to achieve the required 60–70% of the weight on the front wheels. Figure 7.2 illustrates the example.

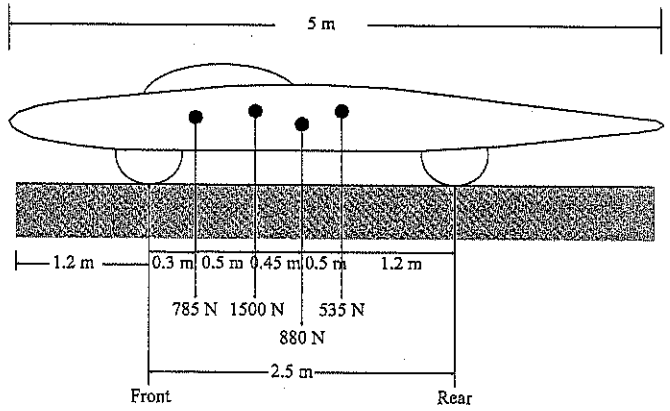

Fig. 7.2 Center of gravity (CG) example.

The calculation method for determining the CG is shown in Eq. 7.1. The CG of the car is located 87.3 cm behind the front wheel axle. The weight distribution is calculated in Eqs. 7.2 and 7.3.

$$CG = \frac{(785)(0.3)+(1500)(0.8)+(880)(1.25)+(535)(1.3)}{3700} = 0.873 \text{ m} \quad (7.1)$$

$$\text{Front} = \frac{2.5-0.873}{2.5} \times 100\% = 65.1\% \quad (7.2)$$

$$\text{Rear} = \frac{0.873}{2.5} \times 100\% = 34.9\% \quad (7.3)$$

In the design example shown in Fig. 7.2, 65.1% of the weight is on the front wheel axle, which would work out well for the car. If the CG was too far

back or forward, then the various weights in the car or the wheels would need to be moved to achieve a balance of weight. This can usually be accomplished by moving the driver and/or batteries, but in some cases it is necessary to move the front and rear wheels forward or backward with respect to the chassis to achieve the proper weight balance. The designer must be realistic about where to place the driver and batteries. There must be adequate space in front of the driver for his or her legs, and the driver and batteries cannot occupy the same space. Once a proper CG is achieved, the polar moment of inertia can be calculated.

The polar moment of inertia for the car can be estimated by treating the driver and battery masses as point masses. The body of the car is treated as if the mass is distributed evenly over the length of the car and the "everything else" is treated as if the mass is distributed evenly over the wheelbase. The polar moment of inertia for an object with its mass distributed over a length L is $mL^2/12$. For point masses the polar moment is the mass multiplied by the distance to the CG squared (md^2). The calculation for the polar moment of inertia J for this example is shown in Eq. 7.4.

$$\begin{aligned} J = &\left(\frac{785}{9.81}\right)(0.873-0.3)^2 + \left(\frac{1500}{9.81}\right)(0.873-0.8)^2 + \\ &\left(\frac{880}{9.81}\right)(1.25-0.873)^2 + \left(\frac{880}{9.81}\right)\frac{2.5^2}{12} + \\ &\left(\frac{535}{9.81}\right)(1.3-0.873)^2 + \left(\frac{535}{9.81}\right)\frac{(5)^2}{12} \\ &= 210 \text{ kg m}^2 \end{aligned} \tag{7.4}$$

The design example shown in Fig. 7.2 puts the batteries, the heaviest weight in the vehicle, near the CG, which reduces the polar moment of inertia. Lowering the polar moment of inertia improves the handling performance of the car and is desirable, but handling is not critical in solar car racing. Still, it is a good idea to keep the driver and batteries near the CG and to keep the body centered over the wheels. It will make the car handle a little better.

Once estimates have been made for the mass, mass moment, CG, and wheelbase, it is possible to calculate the spring rates for the front and rear. Spring rates are selected to provide an energy-efficient suspension, and to provide a reasonably soft ride for the driver (along with the batteries and other components).

B. Selecting Spring Rates

If possible, we would choose to have no suspension. It absorbs energy in the shock absorbers and it greatly increases the mechanical complexity. A suspension complicates the steering and wheel alignment of the car. However, without a suspension the wheels will transmit extremely high loads to the chassis and body and driver when the car hits a bump. The tires would bounce off the ground when the car hit a bump and would skid to some extent when they came back down on the ground, causing tire wear and increasing rolling resistance. The chassis and body would have to be much stronger and heavier if there were no suspension, and the constant jolting around would be hard on the driver and many other components. The suspension also helps keep the body from jolting around when the car hits a bump, which helps reduce the aerodynamic drag on the car. In considering the total picture of designing a solar car, the suspension reduces the overall weight of the car, makes it much more comfortable to drive, and improves the overall energy efficiency of the car.

In general, a softer suspension is more comfortable. However, as the suspension is designed to be softer, the designer quickly discovers that more travel is required in the suspension for the increase in softness. A soft suspension deflects more than a firm suspension for the same bump, so more travel must be designed into the suspension to prevent it from bottoming out.

The characteristic number that describes the softness or firmness of a suspension is the frequency of vibration. A suspension with a lower frequency of vibration will be softer, and one with a higher frequency of vibration will be firmer. Many years of experience have lead to an empirical upper limit of 2.5 Hz for the ride frequency. Race cars and high-performance sports cars will have suspensions that are tuned to near a 2.5 Hz ride frequency [7-1 to 7-3]. Luxury cars are tuned to a ride frequency nearer to 1 Hz [7-2].

The first step in designing the suspension is to choose the spring rates for the front and rear wheels. The solar car designer will choose to tune to a ride frequency of near 2.5 Hz, because that yields a better efficiency in the suspension, that is, it will absorb less energy than a soft suspension. A simple spring-mass model can be used to make a first estimate of the spring rates, and then the spring rates can be refined using a more complex model.

1. *Simple Model.* The front and rear of the car are treated as if they were independent of each other, and modeled as a mass on a spring as illustrated in Fig. 7.3. The governing differential equation is shown in Eq. 7.5.

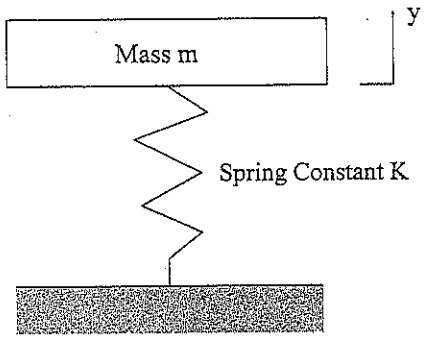

Fig. 7.3 Simple spring rate model.

$$m\frac{d^2y}{dt^2} = -ky \tag{7.5}$$

where m is the mass and k is the spring constant. The natural frequency ω is as shown in Eq. 7.6.

$$\omega = \sqrt{\frac{k}{m}} \tag{7.6}$$

To use the simple model, only the weight W on the particular tire needs to be measured. Assuming that the weight on the wheel is given in newtons, the spring rate in N/m is given in Eq. 7.7.

$$k = \frac{W[(2.5)(2\pi)]^2}{(9.81)} = 25.2\ W\ (N/m) \tag{7.7}$$

In U.S. common units, the weight on the wheel will be measured in pounds and the spring constants will be given in pounds per inch. Equation 7.8 can be used to estimate the spring rates in U.S. common units.

$$k = \frac{W[(2.5)(2\pi)]^2}{(12)(32.2)} = 0.639\ W\ (lb/in.) \tag{7.8}$$

This calculation can be used to estimate the spring rates for each wheel. The model neglects the pitching of the car, and the coupling of the front and rear suspensions, and is not the most accurate method to achieve the 2.5 Hz ride frequency, but it is a simple model to use. Multiply the weight on the wheel by the constant factor, and the result is approximately equal to the desired spring rate. The main reason to use this model is to generate some approximate values for the spring rates to compare to the more complex solution below. The simple model should generate spring rate values that are within 25% of the optimal value.

2. *Complex Model.* The complex model includes the pitching of the car and coupling of the front and rear suspensions. It neglects the stiffness of the tires and road and the damping of the shock absorbers. There have been extremely complex models developed that include these effects [7-2 to 7-4], but experience in using the models have led to the simplifications presented here. Stiffness of the road surface, the tires, the chassis, and the shock absorbers all contribute to the spring rate of the car. It is impossible to get accurate values for these terms, and this makes it impossible to analytically calculate the required spring constants for the suspension. Some experimentation will be required after the car is built to ensure that the springs are acceptable. The solutions that come out of

the complex model have been used in designing solar car suspensions and will yield spring rates that are close to correct.

The model illustrated in Fig. 7.4 assumes that the car has a mass of m, a polar mass moment of inertia of J around the center of mass, a spring rate of k_1 in the front and k_2 in the rear, and that the center of mass is L_1 from the front and L_2 from the rear as shown in Fig. 7.4. Balancing forces in the y direction and moments around the center of mass yields the governing differential equations found in Eqs. 7.9 and 7.10.

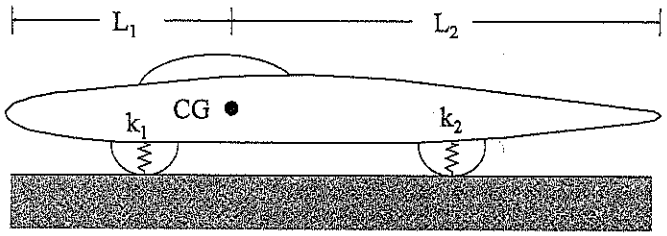

k_1 and k_2 are the spring rates for the front and rear suspensions, respectively. They are not the spring constants for the front and rear springs. The spring constants depend on the geometry of the suspensions.

Fig. 7.4 Front and rear spring rates' model.

$$m\frac{d^2y_c}{dt^2} = -k_1y_1 - k_2y_2 \tag{7.9}$$

$$J\frac{d^2\theta}{dt^2} = k_1y_1L_1 - k_2y_2L_2 \tag{7.10}$$

where y_1, y_2, and y_c are the vertical displacements of the front, rear, and center of mass, respectively, and θ is the pitch angle of the car. The kinematic relations are shown in Eqs. 7.11 and 7.12.

$$\frac{y_2 - y_c}{L_2} = \theta \tag{7.11}$$

$$\frac{y_c - y_1}{L_1} = \theta \tag{7.12}$$

Equations 7.9–7.12 can be combined to yield Eqs. 7.13 and 7.14 for the bounce of the center of mass, y_c, and the pitch angle θ of the car [7-2].

$$mJ\frac{d^4y_c}{dt^4} = \left[m\left(k_2L_2^2 + k_1L_1^2\right) + \left(k_1 + k_2\right)J\right]\frac{d^2y_c}{dt^2} + \left[\left(k_1 + k_2\right)\left(k_1L_1^2 + k_2L_2^2\right) - \left(k_1L_1 + k_2L_2\right)^2\right]y_c \tag{7.13}$$

$$mJ\frac{d^4\theta}{dt^4} = \left[m\left(k_2L_2^2 + k_1L_1^2\right) + \left(k_1 + k_2\right)J\right]\frac{d^2\theta}{dt^2} + \left[\left(k_1 + k_2\right)\left(k_1L_1^2 + k_2L_2^2\right) - \left(k_1L_1 + k_2L_2\right)^2\right]\theta \tag{7.14}$$

The general solution to these equations is quite complex. For design of the spring rates, only the two natural frequencies need to be known, which are the bounce and pitch frequencies of vibration. New terms, α_1 and α_2, are defined in Eqs. 7.15 and 7.16 [7-2].

$$\alpha_1 = \frac{k_1 + k_2}{m} \tag{7.15}$$

$$\alpha_2 = \frac{k_1 L_1^2 + k_2 L_2^2}{J} \qquad (7.16)$$

If the car is envisioned as having a bouncing, straight up and down motion, and the spring constants are k_1 and k_2, and the total mass of the car is m, then from the equation for α_1 it might be reasonable to assume that α_1 is the square of the bounce frequency for the car. Here, α_1 will be approximately equal to the square of the bounce frequency, but not exactly equal because of coupling between bouncing and pitching.

If the motion of the car is envisioned as making the car pitch back and forth front and rear, and the spring constants are k_1 and k_2, and the total mass moment of inertia for this pitching motion of the car is J, extrapolating from some basic dynamics of motion for pitching, it might be reasonable to assume that α_2 is the square of the pitch frequency. Here, α_2 will be approximately equal to the square of the pitching frequency, but not exactly equal because of coupling between bouncing and pitching.

If the front and rear of the car tend to bounce up and down with the same natural frequency, as calculated by the simple model, then there is no coupling between bouncing and pitching, and α_1 and α_2 will be the squares of bounce and pitch frequencies, respectively. If α_1 and α_2 have different natural frequencies, then there is a coupling factor β given in Eq. 7.17 [7-2].

$$\beta^2 = \frac{(k_1 L_1 - k_2 L_2)^2}{mJ} \qquad (7.17)$$

If the front and rear of the car bounce with the same natural frequency, then $k_1 L_1 = k_2 L_2$ and β^2 is zero. These three terms (α_1, α_2, β) are like the components of the second-order tensor of vibration of the vehicle, because they behave like a second-order tensor in calculating the natural frequencies of vibration of the car. The bounce and pitch frequencies of the car are the principal frequencies given by Eq. 7.18 [7-2].

$$\omega^2 = \frac{\alpha_1 + \alpha_2}{2} \pm \sqrt{\left(\frac{\alpha_1 - \alpha_2}{2}\right)^2 + \beta^2} \qquad (7.18)$$

There are four roots to the equation above, two positive and two negative. The positive ones are the natural frequencies of vibration. Note that if β is zero, ($k_1 L_1 = k_2 L_2$), the natural frequencies of vibration are the square roots of α_1 and α_2. This is an interesting special case, but is not desirable in a suspension design. Some coupling of bounce and pitch results in a smoother ride than when the frequencies are uncoupled.

The goal is to design an energy-efficient suspension, and it can be shown that limiting the travel limits the amount of energy the suspension absorbs when it hits a bump. This consideration must be balanced against avoiding frequencies that would give the driver motion sickness or dizziness. The goal is to select spring rates for the front and rear of the car (k_1 and k_2) that satisfy the conditions of low energy absorption and reasonable driver comfort. From the standpoint of energy efficiency, the higher the frequency the better, but drivers start running into problems when the frequencies are above 2.5 Hz. The compromise for solar car racing (and for other race cars) is to set the spring rates so that both the bounce and pitch frequencies are near but below 2.5 Hz.

Maurice Olley developed some "rules of thumb" in the 1930s that are still used today in selecting spring rates for cars [7-2]. These are rules that do not have to be satisfied exactly, but they are good guidelines in selecting the spring rates for the car. The goal should be to keep the bounce and pitch frequencies below 2.5 Hz.

1. The front suspension should have a spring rate about 30% lower than the rear, for a weight distribution of 50-50 front and rear. If the weight distribution is unequal, then k_1/W_1 should be about 30% less than k_2/W_2.

2. The bounce and pitch frequencies should be close together, and the bounce frequency should not be more than 1.2 times the pitch frequency. A higher ratio results in interference kicks that degrade the performance of the suspension.

3. For passenger cars, the bounce and pitch frequencies should be about 1.3 Hz or less to give a nice smooth ride. Solar cars can sacrifice a smooth ride for energy efficiency, as long as it does not get into the range of causing the driver motion sickness or dizziness.

4. The roll frequency should be approximately equal to the bounce and pitch frequencies. Roll frequency has not been discussed. Sway bars are added to passenger cars to stiffen the response when cornering and they increase the roll frequency. Sway bars add weight and complexity, and they are not used in solar cars. Cornering performance is not a priority, and the cornering performance of solar cars is generally not very good. Sway bars increase the spring rate relative to roll without increasing it relative to bounce and pitch, and are quite useful in balancing all the frequencies for the car. As solar cars continue to get faster, sway bars may be used in the track races.

C. Homework

The purpose of this assignment is to estimate spring rates for the front and rear of the car shown in Fig. 7.5. It was decided to divide the car into four main weights: the batteries, driver, body, and chassis/miscellaneous components. Total weight for the car and driver was estimated to be 3790 N (850 lb), and so the weights were proportioned to add up to 3790 N. The center of gravity (CG) for the body was estimated to be at the centroid along its length at x = 250 cm (98 in.). The chassis extends approximately from the front of the car to the rear axle, so its CG was estimated to be halfway along this span at x = 158 cm (62 in.). The driver and battery CGs were placed where the items were to be located on the chassis as illustrated in Fig. 7.5.

1. Calculate the x-component of the CG for the car and estimate the weight on the front and rear. [CG at x = 158.2 cm (62.36 in.), front weight = 2573 N (575.8 lb), rear weight = 1217 N (274.2 lb)]

2. Use the simple method to make a first estimate of the required spring rates for the front and rear of the car. [Front = 64,850 N·m (368 lb/in.), rear = 30,658 N·m (175 lb/in.) These are total spring rates for the front and rear, respectively. If there are two front wheels, each front wheel

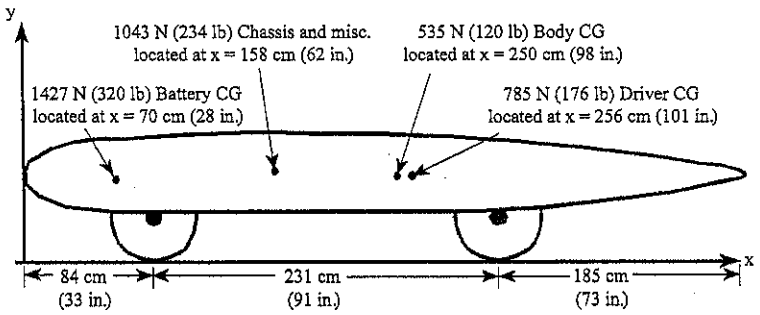

Fig. 7.5 Homework problem for calculating spring rates.

will have a spring rate of half the front value calculated. For a single rear wheel, the spring rate is the full value calculated.]

3. In preparation for the more complex analysis method, estimate the polar mass moment of the car. [Treat the body and chassis as slender members so that their contributions are $J = mL^2/12 + m(x - x_c)^2$. Treat the batteries and driver as point masses so that their contributions are $J = m(x - x_c)^2$. Body = 159.6 kg m^2 (116.6 slug-ft^2), chassis = 47.3 kg m^2 (34.8 slug-ft^2), batteries = 113.0 kg m^2 (81.5 slug-ft^2), driver = 76.6 kg m^2 (56.7 slug-ft^2), total = 396.6 kg m^2 (289.6 slug-ft^2)]

4. Use the spring rates from the simple model above and calculate values for α_1, α_2, β^2, and the pitch and bounce natural frequencies. [α_1 = 247 rad^2/s^2, α_2 = 280 rad^2/s^2, $\beta^2 = 0$ (β^2 will always be zero when values from the simple model are used), ω_1 = 2.74 Hz, ω_2 = 2.42 Hz. So the spring rates should be decreased from the simple estimate to ride rates below 2.5 Hz. This design might cause motion sickness for the driver.]

5. *(Extra Credit)* Adjust the spring rates and incorporate some coupling (β^2) to help dampen out the bumps. Develop a more "ideal" ride rate design. [k_1 = 56,000 N·m (320 lb/in.), k_2 = 25,000 N·m (140 lb/in.) yields ride frequencies that are just below the allowable 2.5 Hz. This is just one solution; there are many acceptable solutions.]

D. References

7-1. Drees, H., *GM Sunraycer Case History Lecture 5-3: Sunraycer Suspension System*, Society of Automotive Engineers, Warrendale, PA, 1992.

7-2. Gillespie, T.D., *Fundamentals of Vehicle Dynamics*, chap. 5, Society of Automotive Engineers, Warrendale, PA, 1992.

7-3. Milliken, W.F., and D.L. Milliken, *Race Car Vehicle Dynamics*, chap. 6, Society of Automotive Engineers, Warrendale, PA, 1995.

7-4. Bastow, D., and G. Howard, *Car Suspension and Handling*, chap. 3, Society of Automotive Engineers, Warrendale, PA, 1993.

7-5. Starr, P., "Designing Stable Three Wheeled Vehicles, with Application to Solar Powered Racing Cars," unpublished work, May 1996.

Chapter 8

Tires and Rolling Resistance

A. Tire Selection

In a well-designed solar car, approximately 35% of all the energy used at 90 km/h (56 mph) will go toward overcoming rolling resistance. The percentage is even higher for slower speeds. On a cloudy day, if the car is traveling at 45 km/h (28 mph), the rolling resistance may consume 70% of all the energy used.

The tires are the primary factor in rolling resistance, and it is very important to select tires that have a low rolling resistance coefficient [8-1 to 8-3]. Currently the best choices are the tires manufactured by Michelin and Bridgestone specifically for solar car racing. These were not available for the early cars, such as the GM Sunraycer. The Sunraycer team did a lot of research in selecting the best bicycle tires for their car. Equation 8.1 was developed based on theory and experiment, and is helpful in understanding the rolling resistance of tires [8-1].

$$C_{rr} = K\left(\frac{W_0}{W}\right)\left(\frac{P}{P_0}\right)^{0.3072}\left[D_w - \sqrt{D_w^2 - \frac{\left(\frac{4W}{\pi}\right)\left(2.456 + (0.251)D_w\right)}{19.58 + 5975P}}\right] \quad (8.1)$$

where D_w is the tire diameter, P is the pressure in the tire, and W is the weight on the tire. The term K in Eq. 8.1 is an experimental quantity that must be determined from a rolling resistance test conducted with a weight W_0 on the tire and a tire pressure of P_0. Because of the empirical nature of Eq. 8.1,

units for D_w must be inches, W and W_0 must be in pounds, and P and P_0 must be in pounds per square inch. In a rolling resistance test, the force required to make the tire roll along is measured, as illustrated in Fig. 8.1.

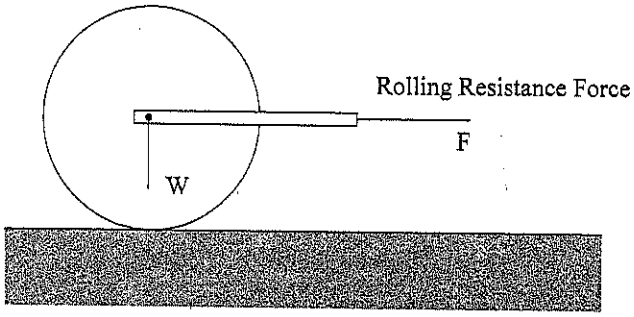

The rolling resistance force turns out to be proportional to the weight on the tire, so it is convenient to define a rolling resistance coefficient C_{rr}.

Fig. 8.1 Rolling resistance test.

In the test, the rolling resistance coefficient is defined as shown in Eq. 8.2.

$$C_{rr} = \frac{F}{W} \tag{8.2}$$

The experimental constant K must be determined from a test where the weight on the tire is W_0, the diameter of the tires is D_w, and the pressure is P_0. The coefficient of rolling resistance C_{rr} is measured from the test, and the value for K is selected to fit the formula. If a tire of diameter D_w is tested at a pressure P_0, with a weight W_0 applied to the wheel, and the rolling resistance force is F, then K is found from Eq. 8.3.

$$K = \frac{\frac{F}{W_0}}{\left(\frac{W_0}{W_0}\right)\left(\frac{P_0}{P_0}\right)^{0.3072}\left[D_w - \sqrt{D_w^2 - \frac{\left(\frac{4W_0}{\pi}\right)\left(2.456 + (0.251)D_w\right)}{19.58 + 5975P_0}}\right]} \tag{8.3}$$

Once K is known, the formula can be used to study how changing the pressure, diameter, and weight on the wheel affects the rolling resistance coefficient of the tire. In developing the following charts, it was assumed that F = 1.25 lb was measured for a weight W_0 = 250 lb at a pressure P_0 = 80 psi and the tire diameter is D_w = 19 in. The rolling resistance coefficient was 1.25/250 = 0.005 for the test, a value typical for solar car tires.

Increasing the diameter of the tire will reduce rolling resistance. However, large tires are difficult to incorporate into the body design. A large tire will increase height of the car because the top of the car must be above the tire. Tall wheel fairings will have to be used, which increases the aerodynamic drag on the vehicle. Large tires are also heavier and absorb more rotational kinetic energy when driving. So a compromise must be reached when selecting tire diameter. Bridgestone tires have a diameter of about 19.5 in., and the Michelin tires have a diameter of about 22 in. Figure 8.2 illustrates how tire diameter affects the rolling resistance coefficient. Assuming similar tire designs, that is, everything is the same except the diameter, the rolling resistance coefficient would vary as illustrated in Fig. 8.2.

The rolling resistance coefficient is almost constant with the weight on the tire, as illustrated in Fig. 8.3. A slight increase is observed with increased weight, but it is very slight. Rolling resistance force is the product of the weight on the tire and C_{rr}, so the rolling resistance force increases with weight on the tire, but the rolling resistance coefficient is almost constant with weight. All tires have weight limits, and exceeding the weight limit on the tire will cause a disproportionate increase in rolling resistance. But assuming that the tire is being used in the weight range it was designed for, the rolling resistance coefficient is essentially constant.

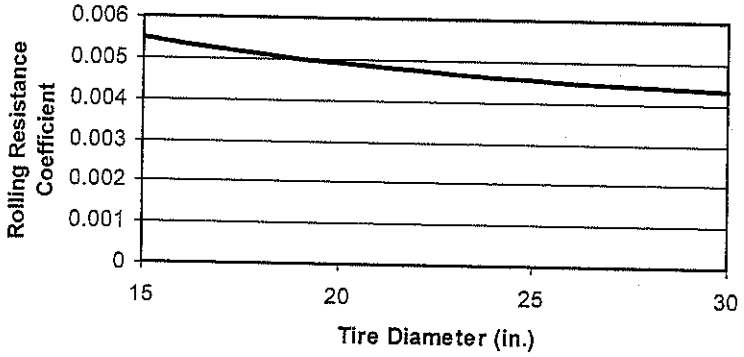

Fig. 8.2 Effect of tire diameter on rolling resistance.

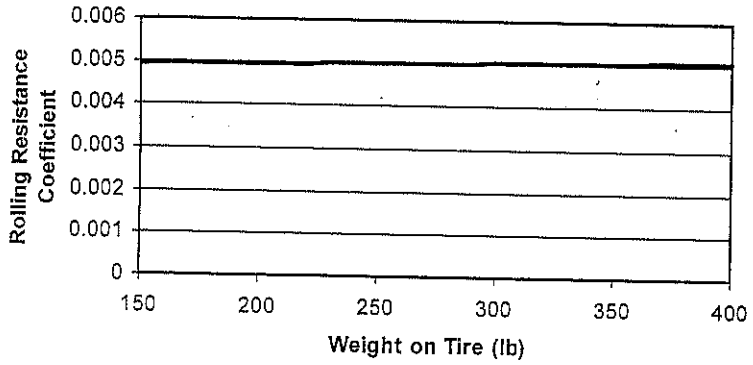

Fig. 8.3 Effect of weight on rolling resistance.

Rolling resistance decreases as the pressure in the tire is increased. High-pressure tires are desirable, but there is a limit to what the tires can withstand. Raising the pressure makes the tires more likely to be damaged by road hazards, and you do not win races sitting on the side of the road changing tires. General Motors tested bicycle tires for the GM Sunraycer, and the resulting data showed that rolling resistance decreased even when the tires were pressurized well beyond the manufacturer's rated pressure. So

for rolling resistance, the best approach is to start with the highest-rated manufacturer's recommendation for the tires, and test the durability by driving the car. Increasing tire pressure will decrease rolling resistance and increase the probability of a flat tire or blowout. Choose the highest pressure the team is comfortable with. Figure 8.4 shows how the rolling resistance coefficient varies with tire pressure.

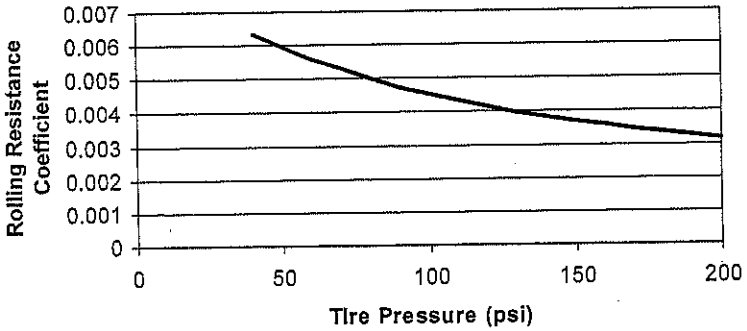

Fig. 8.4 Effect of tire pressure on rolling resistance.

Example. Assume that the car weighs 800 lb and is traveling at 55 mph. What is the reduction in power required to overcome rolling resistance if the pressure in the tires is increased from 80 psi ($C_{rr} = 0.005$) to 120 psi ($C_{rr} = 0.00415$)?

The power to overcome rolling resistance is calculated in Eqs. 8.4 and 8.5.

$$\text{Power} = (1.99)(800)(0.005)\left[1+\frac{55}{100}\right]55 = 679 \text{ W} \qquad (8.4)$$

$$\text{Power} = (1.99)(800)(0.00415)\left[1+\frac{55}{100}\right]55 = 563 \text{ W} \qquad (8.5)$$

Changing the inflation pressure from 80 to 120 psi will reduce the power consumption of the car by 116 W at 55 mph. If the car uses 2000 W available to go 55 mph, a typical value for an 800-lb car, the savings of 116 W is a power savings of about 6%. This is significant, but not tremendously significant. It is worth some effort to determine the highest pressure that can safely be used in the tires. On cloudy days, the energy savings is more significant, and it may be worth more risk to inflate the tires to a higher pressure.

The data also show that rolling resistance decreases with tire diameter. If the team decides to change from a 19-in.-diameter tire (C_{rr} = 0.005) to a 26-in.-diameter tire (C_{rr} = 0.0045) there will be a power savings of 67.9 W, or about 3% of the total power used. This would be significant too, and should be considered. However, using 26-in.-diameter tires will require taller fairings and increase the aerodynamic resistance, so large-diameter tires may not mean a net benefit for the car.

B. Rolling Resistance Phenomenon

Where does the rolling resistance come from? This question always comes up when discussing rolling resistance. The answer is that the energy is primarily absorbed by the rubber in the tires [8-1, 8-4 to 8-6]. If a piece of rubber is flexed back and forth it heats up as it absorbs the mechanical energy required to perform the flexing action. The portion of the tire in contact with the road has been deformed a little because of the weight on the tire. The deformation is a flexing of the rubber in the area of the tire near the ground—the tread and sidewalls of the tire are flexed slightly. As the tire rolls, the rubber is constantly being flexed back and forth as different parts of the tire come in contact with the ground. The rubber absorbs energy and the tire heats up. This is the primary source of rolling resistance for pneumatic tires rolling on concrete or asphalt pavement. The heat generated can cause tire failure, especially if the tires are underinflated so that the magnitude of the flexing is large.

To minimize rolling resistance it is necessary to minimize the energy absorbed by the flexing of the tires. There are several ways to reduce rolling resistance.

1. The amount of deformation (flexing) at the road surface is proportional to the weight on the tire. Reducing the weight on the tire reduces the amount of energy the tire absorbs while rolling. Lighter-weight cars have lower rolling resistance.

2. Increasing the pressure in the tire reduces how much it deforms under load. Therefore, increasing the pressure reduces the flexing of the rubber, which reduces the energy absorbed by the tire, which in turn reduces the rolling resistance.

3. Flexing a thin sheet of rubber takes less energy than flexing a thick sheet, so thin-walled tires have lower rolling resistance. Several experiments have shown that worn tires have a lower rolling resistance than new tires of the same type. Thin tires have low puncture resistance too, so lower rolling resistance must be balanced with safety and reliability.

4. Large-diameter tires have a different-shaped "contact patch" than small-diameter tires. Large-diameter tires have less curvature (larger radius of curvature) and tend to make a longer and narrower contact patch. This reduces flexing, especially in the sidewalls of the tires. Figure 8.5 illustrates contact patch shapes for tires [8-1].

Static equilibrium requires that the contact patch area multiplied by the average pressure on the contact patch equal the weight on the tire. If two tires have the same pressure, the contact patch area will be approximately the same for both tires. This is especially true for the thin-walled tires used on solar cars. Large-diameter tires have a narrower contact patch, which means that the sidewalls flex out less under load. Less flexing means less energy absorbed, and therefore larger tires have lower rolling resistance.

As the tire pressure increases, the contact patch area decreases. The pressure between the tire tread and road surface increases, and so the tire is more susceptible to road damage. The type of tire tread is important too. A tire with a smooth tread (termed *slicks*) is more energy efficient than a treaded tire. Tire treads deform under load, bending together or apart, and this action absorbs energy in addition to the flexing of the body of the tire.

The driving surface also impacts the rolling resistance of the tires. A smooth driving surface has a lower rolling resistance than a rough surface, because it causes fewer deformations in the rubber. Surface roughness on the road

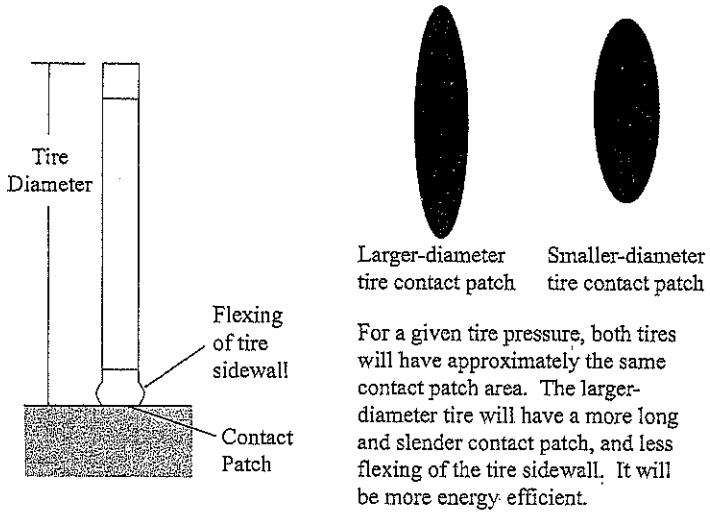

Fig. 8.5 Tire contact patch shape.

causes the tire to deflect in the shape of the roughness as it rolls over it, which causes the rubber to absorb more energy than for a smooth surface.

Road Surface Deformation. The other component of rolling resistance is deformation of the road surface [8-4]. Pneumatic tires in contact with a concrete or asphalt surface absorb much more energy than the road surface, and so energy lost to road surface deformations is insignificant. At the other extreme is driving in sand, where deformation of the road surface (sand) is the dominant factor in rolling resistance. Road surface deformation is insignificant for solar car racing, unless one is dealing with a race down the beach.

The issue of road surface deformation is discussed here primarily because the novice will suggest using a rigid tire, or a tire made of a very hard material that will not deform under load. If the tire is rigid, the energy absorbed by the tire will be zero, which might seem to be a more energy-efficient situation. For example, steel wheels running on steel rails (as in a railroad)

are more efficient than pneumatic tires running on a road surface. But steel wheels running on an asphalt or concrete surface expend a large amount of energy crushing the small rocks on the road surface. Therefore, pneumatic tires are the best solution for driving on pavement.

Homework. Assume that a rolling resistance test was performed on a tire under the following conditions: the tire was pressurized to 80 psi, the weight on the tire was 250 lb, and the outer diameter of the tire was 19 in. Under these conditions the rolling resistance coefficient was measured to be 0.005.

1. Plot how the rolling resistance coefficient would vary as a function of the diameter of the tire, for similar tires under the same 250-lb load and 80 psi pressure. Vary the tire diameter from 15 to 30 in.

2. Plot how the rolling resistance coefficient would vary as a function of the weight on the tire, assuming that the diameter is 19 in. and the tire is pressurized to 80 psi. Allow the weight to vary from 150 to 400 lb.

3. Plot how the rolling resistance coefficient would vary with the pressure in the tire, assuming the tire diameter is 19 in. and the weight on the tire is 250 lb. Vary the pressure from 40 to 200 psi.

C. Energy Loss Model for Tire Misalignment

Tires absorb energy through rolling resistance when they are aligned with the direction of travel. They absorb more energy when they are not properly aligned. The misalignment can be caused by poor stiffness in the suspension or chassis structure, loose-fitting connections in the suspension, bumpy or non-Ackerman steering, or simply not adjusting the toe-in of the wheels so they are aligned properly. Suspension geometry design is covered in Chapter 9. The purpose of this model is to understand and quantify the energy losses caused by wheel misalignment. Figure 8.6 illustrates a misaligned tire.

As the tire rolls, the leading edge would like to travel along a straight line distance b relative to the trailing edge. However, when the leading edge makes contact with the pavement, it would need to slide laterally a distance ($b \sin\theta$) relative to the pavement to travel along a straight line to the trailing

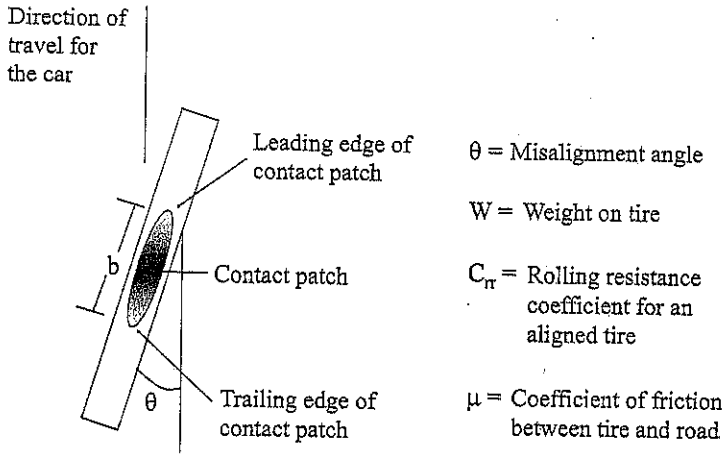

Fig. 8.6 Energy loss model for tire misalignment.

edge. If the tire were very rigid, the tread would have to slide relative to the pavement, but tires are not rigid. The sidewalls of the tire allow the tread to flex sideways to some extent, allowing the tread to "roll" around the side of the rim to some degree. The difference between a rigid tire and a flexible tire is illustrated in Fig. 8.7.

The misalignment angle θ is often called the slip angle [8-4 to 8-6], although for small misalignments the tires do not actually slide relative to the pavement. For small misalignments the tires deform and accommodate the misalignment. For large misalignments there will be significant sliding between the tires and the road. Tires are flexible to a large extent, so this behavior is much more like that of the "flexible" tire in Fig. 8.7 above than the behavior of the "rigid" tire, but there is always some sliding on the trailing edge of the contact patch, even for very flexible tires. The high-pressure tires used for solar car racing are much more rigid than tires used in passenger cars, so alignment for solar car tires is more critical than for passenger car tires.

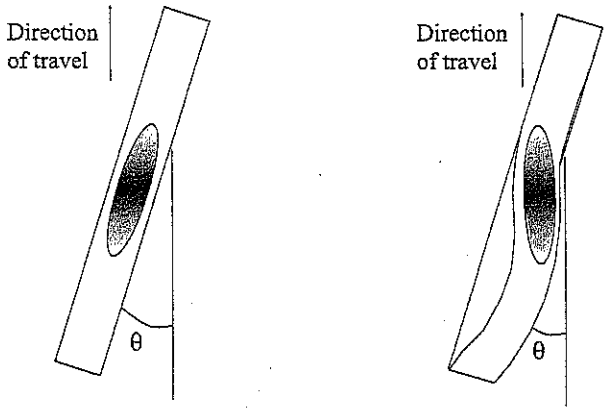

"Rigid" tire. The contact patch must slide laterally (to the left) as the tire rolls.

"Flexible" tire. The tread flexes allowing the contact patch to be aligned with the direction of travel.

Fig. 8.7 Rigid and flexible tires.

1. *Rigid Tire Model.* The simplest model assumes that the tire is rigid and that the tread slides sideways against the pavement. This yields a high estimate for the rolling resistance, but is a place to start in understanding quantitatively how misalignment increases rolling resistance. The rigid tire model is illustrated in Fig. 8.8.

   The energy absorbed in rolling the tire a distance equal to the contact patch length b is the rolling resistance force multiplied by the rolling distance plus the friction force multiplied by the sliding distance, as illustrated in Eq. 8.6.

$$\text{Energy absorbed} = WC_{rr}b\cos(\theta) + \mu Wb\sin(\theta) \qquad (8.6)$$

   where W is the weight on the tire and μ is the coefficient of friction between the tire and the road. Dividing the energy absorbed by the

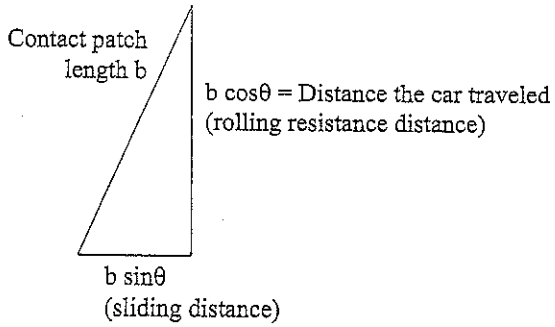

Fig. 8.8 Rigid tire model parameters.

distance traveled, the force required to overcome the total rolling resistance of the tires is obtained in Eq. 8.7.

$$\text{Force} = WC_{rr} + \mu W \tan\theta \tag{8.7}$$

The effective rolling resistance coefficient C'_{rr} is the force divided by the weight on the wheel. For a rigid tire, the effective rolling resistance coefficient for a misalignment angle of θ is given by Eq. 8.8.

$$C'_{rr} = C_{rr} + \mu \tan\theta \tag{8.8}$$

For a solar car, the typical rolling resistance for the tire is $C_{rr} = 0.005$, and the coefficient of friction between the tire and road is approximately $\mu = 0.8$. Figure 8.9 shows how the effective rolling resistance coefficient C'_{rr} varies with angle of misalignment, for misalignments up to 3° for the simple (rigid tire) model.

The chart in Fig. 8.9 shows that the rolling resistance would increase by almost a factor of ten for a misalignment angle of 3°, and that the increase in rolling resistance is very significant even for small angles of misalignment.

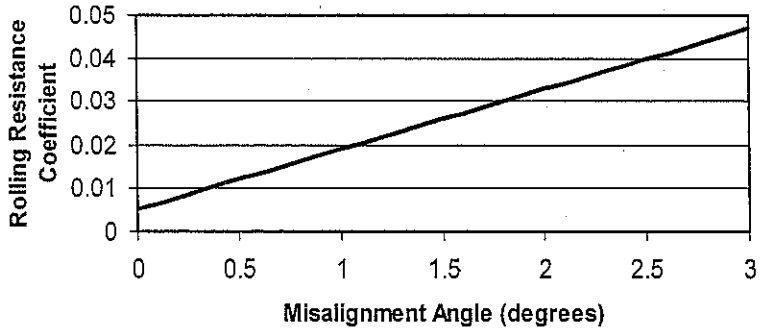

Fig. 8.9 Effect of tire misalignment on rolling resistance—rigid tire model.

Example. Assume that the car weighs 3567 N (800 lb) and that there is 2230 N (500 lb) total on the two front wheels of the car. The toe adjustment is set wrong so that each of the front tires is out of alignment by 1° and the coefficient of friction between the tire and road is 0.8. (This corresponds to 2° of toe misalignment.) Find the increase in energy consumption caused by the front tires of the car being misaligned, compared to tires that are properly aligned. Equation 8.9 calculates the power consumed by the misalignment if the car is traveling at 64 km/h (40 mph).

$$\text{Power} = (0.278)(64)(2230)\left(1+\frac{64}{161}\right)(0.005+(0.8)\sin(1^\circ)) = 1051\text{ W} \tag{8.9}$$

If the wheels were aligned, the rolling resistance power would be 277 W, so the 1° misalignment almost quadruples the rolling resistance of the front tires on the car. Alignment is quite important, but this simple model overestimates the drag penalty caused by wheel misalignment. The flexible tire model gives a more realistic estimate of the drag penalty caused by wheel misalignment, but it is also more complex.

2. *Flexible Tire Model.* The tire has some lateral flexibility, and will flex sideways for some distance rather than sliding sideways. Some or all of

the distance (b sinθ) will be taken up by flexing of the tire. As a first approximation, assume that the tire tread flexes laterally some distance δ for a given lateral load F, so that F = kδ as illustrated in Fig. 8.10. The tire will flex laterally until the lateral load exceeds the friction force between the tire and the road, at which point the tire will slide laterally. Figure 8.10 illustrates the assumptions of this model.

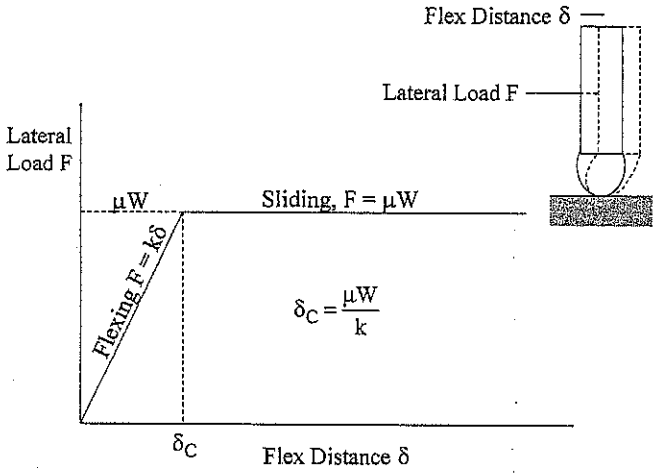

Fig. 8.10 Flexible tire model.

For the misalignment to be fully taken up by flexing the tire, the lateral movement of the tread (b sinθ) must be less than or equal to δ_C. If (b sinθ) is greater than δ_C some of the lateral movement will be taken up by flexing, and the rest by sliding. Rolling resistance comes from flexing of the tire, so the additional flexing because of the lateral load will increase the rolling resistance, but not as much as the sliding of the tire. A weight W on the tire causes a rolling resistance force of WC_{rr}, and the force comes primarily from flexing rubber in the tire. As a first approximation, it could be assumed that a lateral load F on the tire would cause the same amount of rolling resistance, so that the rolling resistance force for a weight and lateral load on the car is given by Eq. 8.10.

$$\text{Rolling resistance force} = WC_{rr} + FC_{rr} \tag{8.10}$$

The fundamental idea behind this assumption is that a lateral force causes approximately the same amount of flexing of the tire as a weight force of the same value. This is just an assumption, and an argument could be made that lateral loads cause more deflection or less deflection than vertical loads. This is the first of several approximations that must be made to get results out of the flexible tire model. Two cases must be considered when considering this model.

Case 1. All of the lateral motion is taken up by the flexing of the tire. If b sinθ < δ_C, all of the tire's lateral motion can be attributed to flexing and there will be no slipping between the tire and the road. The lateral load on the tire is expressed as kb sinθ, and the effective rolling resistance coefficient C'_{rr} is given by Eq. 8.11.

$$C'_{rr} = \left(1 + \frac{kb\sin\theta}{W}\right) C_{rr} \tag{8.11}$$

Case 2. Some of the tire's lateral motion is attributed to flexing and some to sliding. The tire can accommodate a maximum lateral motion of δ_C without slipping. If b sinθ > δ_C, an amount δ_C is taken up by flexing of the tire and the rest of the lateral motion is taken up by sliding the tire on the pavement. It can be shown that the effective rolling resistance coefficient C'_{rr} for this case is given by Eq. 8.12.

$$C'_{rr} = C_{rr} + \mu C_{rr} + \left(\frac{b\sin\theta - \frac{\mu W}{k}}{b\cos\theta}\right)\mu \tag{8.12}$$

To use this model, it is necessary to measure a lateral stiffness value for the tires (k) and a contact patch length (b). These quantities are not always known, and vary from tire to tire, along with the pressure in the tire and with the weight on the tire. The method discussed below allows these quantities to be estimated so that results can be obtained from the model, but a better approach

involves developing experiments and measuring these quantities for the tires being used.

Assuming an oval shape, the contact patch is related to the pressure P in the tires approximately as shown in Eq. 8.13.

$$P = \frac{W}{\frac{\pi}{4}ab} \tag{8.13}$$

where W is the weight on the tire, a is the minor axis of the ellipse, and b is the major axis (and contact patch length). If the contact patch has an aspect ratio (r_p = b/a), the contact patch length (b) is given by Eq. 8.14.

$$b = \sqrt{\frac{4(r_p)W}{\pi P}} \tag{8.14}$$

For solar car tires and most bicycle tires, $r_p = 3$ (approximately). The aspect ratio is less for passenger car tires. The contact patch length can then be approximated from the weight on the tires and the pressure in the tires. For example, if the weight on the tire is 1338 N (300 lb), and the tire is pressurized to 793 kPa (115 psi), the contact patch length would be 8.03 cm (3.16 in.), and the width would be 2.67 cm (1.05 in.). This figure is approximately correct for Bridgestone solar car tires.

The stiffness of the tire (k) increases with increasing pressure. A test was performed at the University of Missouri-Rolla on Bridgestone tires and it was found that a reasonable estimate for k for the tires when pressurized to 689 kPa (100 psi) is 700 kN/m (4000 lb/in.). That is, it would take approximately 446 N (100 lb) lateral load to deflect the tire laterally 0.635 mm (0.025 in.). Increasing the pressure in the tires would increase the k value, but it is not known if this increase is linearly proportional to the pressure or not.

In the formula, a higher k value will increase the rolling resistance, so it might seem that reducing the pressure in the tires to reduce the k value would lower the rolling resistance. However, C_{rr} and the contact patch length b

both decrease with increasing pressure. The tires will never be perfectly aligned, and there will be an optimum pressure for a given misalignment that will minimize rolling resistance. This "optimum" pressure may be greater than the pressure that is safe for the tires, and safety and reliability are more important than lowering rolling resistance. If the pressure is high enough to cause sliding of the tires, there is a very marginal reduction in C_{rr} for increasing pressure. Common sense is required in selecting the best tire pressure.

Example. Assume that there is a weight W = 250 lb on the tire, and the tire is out of alignment. Plot how the rolling resistance coefficient varies with misalignment for P = 80, 110, and 140 psi. Assuming an aspect ratio of three, the contact patch length can be estimated from Eq. 8.15.

$$b = \sqrt{\frac{(12)(250)}{P}} \tag{8.15}$$

The lateral stiffness of the tire is probably not exactly linear with respect to the pressure in the tire, but it would certainly increase with the pressure in the tire. For the purposes of this model it was assumed that k varied linearly with pressure in the tire according to Eq. 8.16.

$$k = (40)P \tag{8.16}$$

The coefficient of friction between the tires and the road was assumed to be $\mu = 0.8$. It was also assumed that the rolling resistance coefficient for the tires was 0.005 when the weight on the tire was 250 lb and the pressure in the tire was 100 psi. The diameter of the tires was assumed to be 19 in. Using the tire model in Eq. 8.1, Eq. 8.17 shows how the rolling resistance coefficient C_{rr} varies with tire pressure.

$$C_{rr} = 49.367\left(\frac{P}{100}\right)^{0.3072}\left[19 - \sqrt{19^2 - \frac{2299.7}{19.58 + (5975)(P)}}\right] \tag{8.17}$$

Figure 8.11 shows how the effective rolling resistance of the tire varies with the pressure to which the tire is inflated and the angle of misalignment.

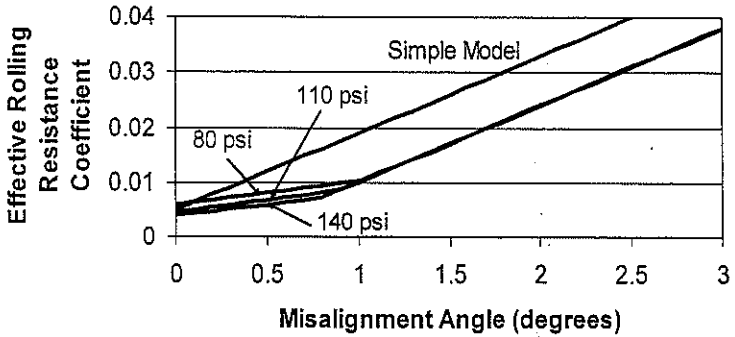

Fig. 8.11 Effects of tire pressure and misalignment angle on rolling resistance—flexible tire model.

If the tires are reasonably well aligned, a higher tire pressure yields a significantly lower rolling resistance. If the tires are misaligned 1°, there is very little difference in rolling resistance for tires inflated to 80, 110, and 140 psi pressure. Careful examination of the data shows that the high-pressure tire actually has slightly higher rolling resistance than the low-pressure tire for misalignment angles of 1° or more. If there is a large angle of misalignment, a lower-pressure tire will be able to accommodate the misalignment better, and will have a (very slightly) lower rolling resistance. Another benefit is that the lower-pressure tire is less likely to be damaged in use, that is, it is less likely to blow out.

The flexible tire model yields a low estimate of the rolling resistance because it assumes no slipping for small tire misalignments. In reality there is always some slipping near the rear of the contact patch. Actual rolling resistance for a given tire misalignment lies somewhere between the simple and complex models. These models illustrate that it is most important to keep the tires aligned. Small misalignments cause significant increases in the rolling resistance.

D. References

8-1. Kyle, C., *GM Sunraycer Case History Lecture 2-3: Sunraycer Wheels, Tires and Brakes*, Society of Automotive Engineers, Warrendale, PA, 1992.

8-2. Roche, D.M., A.E.T. Schinckel, J.W.V. Storey, C.P. Humphris, and M.R. Guelden, *Speed of Light: The 1996 World Solar Challenge*, chap. 9, Photovoltaics Special Research Center, University of New South Wales, Sydney, Australia, 1997.

8-3. Storey, J.W.V., A.E.T. Schinckel, and C.R. Kyle, *Solar Racing Cars*, chap. 9, Australian Government Publishing Service, Canberra, Australia, 1994.

8-4. Gillespie, T.D., *Fundamentals of Vehicle Dynamics*, chaps. 4 and 10, Society of Automotive Engineers, Warrendale, PA, 1992.

8-5. Milliken, W.F., and D.L. Milliken, *Race Car Vehicle Dynamics*, chaps. 2 and 14, Society of Automotive Engineers, Warrendale, PA, 1995.

8-6. Bastow, D., and G. Howard, *Car Suspension and Handling*, chap. 7, Society of Automotive Engineers, Warrendale, PA, 1993.

Chapter 9

Front Suspension Design

A. Wheel Selection

Once the tires are selected, a wheel must be selected that fits the tire. The wheel may be purchased or it may be manufactured to fit the tire. If the wheel is "dished" on the inside as illustrated in Fig. 9.1, the brake disk and calipers can fit in the dished area, and the fairing for the wheel can be thinner. This reduces aerodynamic resistance.

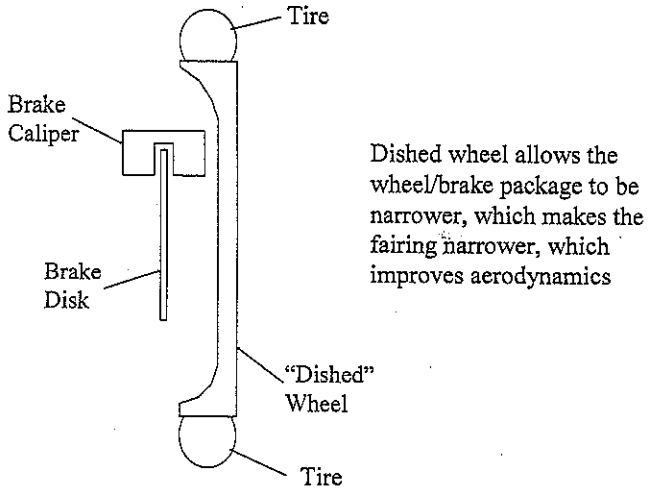

Fig. 9.1 Packaging the brakes within the dished wheel.

B. Brake Design

The brakes must be able to provide at least a 0.5g deceleration when braking to pass the braking test for races in the United States. There will be some reaction time for the driver, so the brakes will actually have to exceed the 0.5g requirement to accommodate the driver reaction time. To accomplish this, the brakes should be powerful enough to slide the front tires. When braking, the weight shifts toward the front of the car. If the car has 60–70% of the weight on the two front tires, a good assumption is that about 70–80% of the weight of the car will be on the front (35–40% on each front tire) during hard braking. If the tire is locked up and sliding, the braking deceleration is illustrated in Fig. 9.2.

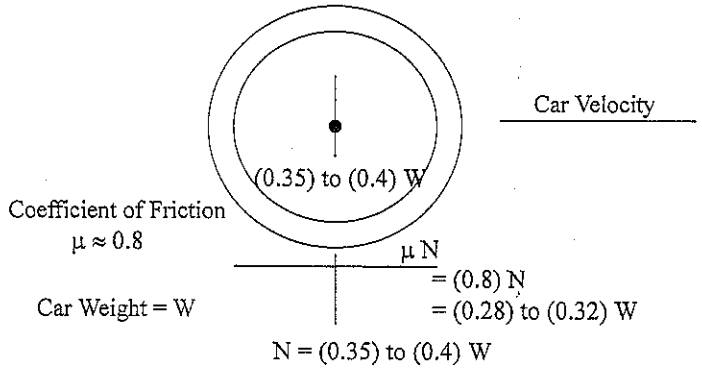

Fig. 9.2 Calculation of braking deceleration.

With these assumptions, the braking force is (0.28) W to (0.32) W for each front tire, or (0.56) W to (0.64) W when the front tires are locked up and sliding. This would yield a deceleration of 0.56–0.64g, which would meet the 0.5g requirement for brake performance and allow some reaction time for the driver.

If too much weight is on the rear tire, there will be less than 70% of the weight on the front when braking, and it will be difficult to achieve the 0.5g braking deceleration. On the other hand, if too much weight is on the front,

the nose will dive into the pavement and the rear will hop up into the air. Statistically, there should be 60–70% of the weight on the front to ensure good braking performance and control of the car.

If the center of gravity (CG) of the car is known, it is possible to calculate how much the weight shifts forward when braking, and the maximum braking force. The following example illustrates the process. Assume that the wheelbase for the car is 2.54 m (100 in.) and that the center of gravity is 1.016 m (40 in.) behind the front wheels and 0.508 m (20 in.) above the pavement. The geometry is illustrated in Fig 9.3.

For a braking force F and car weight W, the normal forces (weights) on the front and rear are:

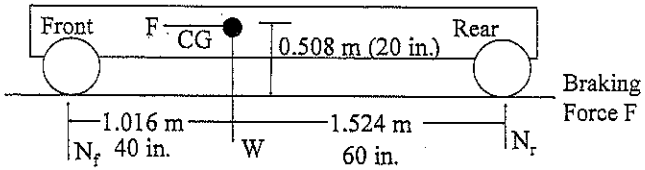

Balancing forces in the x-direction, the inertial braking force must be equal to the braking force F.

Fig. 9.3 Weight shift when braking.

F is the inertial force of braking, equal to the mass of the vehicle multiplied by the braking deceleration. The forces on the front and rear axles can be obtained by summing forces and moments, and are given in Eqs. 9.1 and 9.2.

$$N_f = \frac{(60)W + (20)F}{100} \tag{9.1}$$

$$N_r = \frac{(40)W - (20)F}{100} \tag{9.2}$$

1. *Front Wheel Only Braking.* If only the front wheels provide braking, the maximum braking force for the car is equal to the normal force on the front axles multiplied by the coefficient of friction between the tires and the road, that is, the maximum braking force is $F = (0.8)N_f$. The normal force on the front wheels is calculated using Eq. 9.3.

$$N_f = \frac{(60)W + (20)(0.8)N_f}{100}$$
$$N_f = (0.714)W \qquad (9.3)$$

So 71.4% of the weight is on the front axles in hard braking, compared with 60% on the front with no braking. The maximum braking deceleration is 0.8 times the normal force on the front axles, or 0.571g deceleration. Braking tests include the reaction time of the driver, so if a 0.5g brake performance is required, and a 0.571g brake is the maximum possible for the car, not much reaction time is left for the driver. A well-trained driver would be able to pass the test, but it would be extremely close.

2. *Front and Rear Braking.* If full braking is applied to the front and rear wheels, the car can theoretically achieve 0.8g deceleration. Front/rear braking is more difficult to design because the brakes must be proportioned. It is important that proportioning be done so that the rear brakes do not lock up and slide before the front brakes lock up. Sliding on the rear brakes will cause the car to go into a spin, and may cause the driver to lose control. If the front brakes lock up, the car will tend to slide in a straight line, and it is easier for the driver to regain control. For any vehicle, it is important for stability that the rear braking be controlled so that the rear tires do not lock up and throw the car into a spin.

To prevent sliding on the rear tires, the rear braking load should be limited to $0.5\,N_r$. The maximum braking force is 0.8 times the normal force on the front plus 0.5 times the normal force on the rear. Equation 9.4 is solved to get the normal and braking forces acting on the car.

$$F = (0.8)\left[(0.6)W + (0.2)F\right] + (0.5)\left[(0.4)W - (0.2)F\right] \qquad (9.4)$$

Solving the equation, $F = 0.723\,W$, $N_f = 0.745\,W$, and $N_r = 0.255\,W$. Here, 74.5% of the weight is on the front wheels in hard braking, compared with 60% static weight on the front wheels. The maximum braking deceleration is 0.723g. This illustrates that a relatively small braking force on the rear wheels will shift a little more weight to the front and significantly increase the braking deceleration.

In most cases the best approach in designing solar cars is to use the motor for regenerative braking on the rear, and have disk brakes on the front. A backup system should be available for safety reasons in case the disk brakes fail. Regenerative braking does not work if the batteries are fully charged, and it does not work well at slow speeds. A mechanical braking system such as redundant disk brakes or a cable brake should be employed for safety in case the disk brakes fail. Care must be taken when applying the regenerative brakes, especially on wet pavement. The regenerative brakes can cause the rear wheel to slide and make the car spin out of control. Several teams have had accidents and near misses when the regenerative brakes locked the rear wheel as the car was traveling downhill on wet pavement.

3. *Sizing the Brake System.* The pedal, master cylinder, brake caliper, and disk must be sized to achieve the required braking torque. This can be worked out in general with symbols, but as with most analysis, reasonable assumptions must be made to get to a solution. The assumptions are the manifestation of the design philosophy. In the analysis here, it was assumed that braking was applied only on the front wheels and that the coefficient of friction was 0.8 between the tires and road. N_f is the total weight on the front in hard braking, so $N_f/2$ is the weight on one front wheel, assuming that there are two front wheels. If the tire has a radius r_T, the required braking torque T_B to slide the tires is given by Eq. 9.5.

$$T_B = (0.8)\left(\frac{N_f}{2}\right)r_T = (0.4)(N_f)r_T \qquad (9.5)$$

If the normal force is equal to 0.745 W as in the example for front wheel only braking in item 1, then the braking torque is $0.298\,Wr_T$. The brake

disk will have a radius r_D to the center of where the brake pads in the calipers contact it, as illustrated in Fig. 9.4.

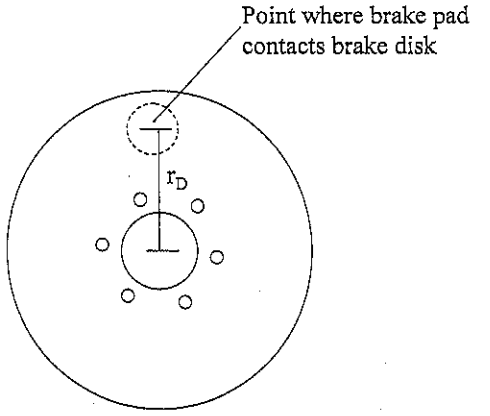

Fig. 9.4 Brake pads and brake disk.

The friction force between the pad and disk must generate the brake torque. With two pads, one on each side of the disk, the friction force required by the pad is given by Eq. 9.6.

$$F_P = \frac{T_B}{2r_D} \tag{9.6}$$

The coefficient of friction between the brake pad material and a steel disk is typically 0.2–0.4. The lower coefficient of friction occurs when the brake disk gets wet. It is good practice to design against the worst case of $\mu = 0.2$, so the normal force on the brake pads N_P is given by Eq. 9.7.

$$N_P = \frac{F_P}{0.2} \tag{9.7}$$

If the normal force on the front in hard braking is 0.745 W, the normal force on the brake pads is 0.745 $W(r_T/r_D)$. So under the assumptions of this design philosophy, the normal force required between the brake pads and the disk is equal to the total weight on the two front wheels in hard braking multiplied by the ratio of the tire radius to the radius to where the brake pads contact the brake disk. The radius of the wheel is generally between two and three times the radius to where the brake pad contacts the disk, so the compressive normal force between the brake pads and the disk must be two to three times the total weight on the front wheels in hard braking. This is a very substantial force. The normal force N_P on the pads is generated from the fluid pressure acting on the pistons in the brake calipers, as illustrated in Fig. 9.5.

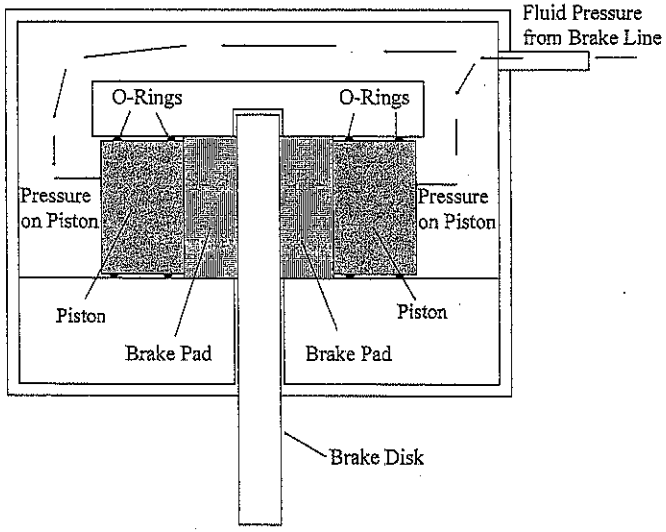

Fig. 9.5 Brake caliper schematic.

It is important to choose calipers that retract, pulling the brake pads back away from the disk when the brakes are not being applied. Nonretracting calipers tend to have brake scrub, which wastes energy. Fluid pressure

from the line pushes on the pistons, and the pistons push the brake pads against the brake disk. If the pistons in the brake calipers have a diameter d_P, the fluid pressure P required is given by Eq. 9.8.

$$P = \frac{N_P}{\frac{\pi}{4} d_P^2} \tag{9.8}$$

The brake line goes from the calipers to the master cylinder. The brake pedal must push on the master cylinder piston hard enough to generate the pressure P as illustrated in Fig. 9.6.

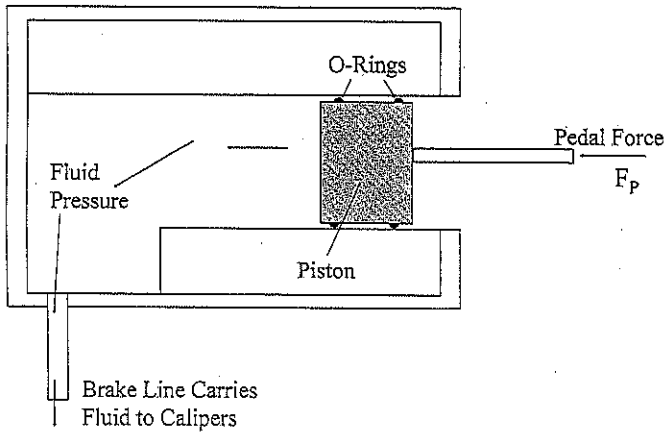

Fig. 9.6 Brake master cylinder schematic.

If d_M is the diameter of the piston in the master cylinder, the pedal force F_P required is given by Eq. 9.9.

$$F_P = P\left(\frac{\pi}{4} d_M^2\right) \tag{9.9}$$

The pedal force must be provided by the driver, so the system must be designed such that the driver is strong enough to provide the required pedal force. The brake pedal is designed as a lever to amplify the force of the driver's foot, and there are several possible approaches to designing the brake pedal. A common design is illustrated in Fig. 9.7.

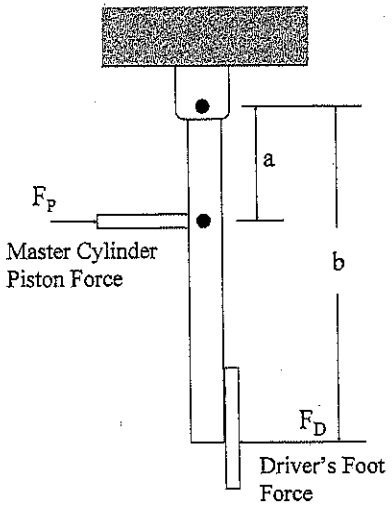

Fig. 9.7 Brake pedal schematic.

The leverage factor for this type of brake pedal design is b/a, that is, the force on the master cylinder piston will be b/a times the force of the driver's foot on the pedal. Plugging all this into the equations above, a relationship can be developed between the force the driver must push on the pedal F_D, the weight on the front wheels of the car in hard braking N_f, the radius of the tire r_T, the radius to where the brake disk pad contacts the brake disk r_D, the diameter of the master cylinder piston d_M, the diameter of the caliper pistons d_P, and the leverage factor on the brake pedal b/a. Eq. 9.10 illustrates this relationship.

$$F_D = N_f\left(\frac{r_T}{r_D}\right)\left(\frac{d_M^2}{d_P^2}\right)\left(\frac{a}{b}\right) \qquad (9.10)$$

It is reasonable to expect the driver to push with 446 N (100 lb) in hard braking. After setting F_D to a maximum of 446 N, Eq. 9.10 is helpful in selecting the right calipers, master cylinder, brake disk, and brake pedal to make the design work properly. It is a challenge to optimize the design. Increasing the diameter of the brake disk will increase r_D and reduce the amount of braking force required by the driver, but making the radius large pushes the disk down into the airstream and makes the front-wheel fairings wider.

Increasing the diameter of the pistons in the calipers reduces the amount of force required by the driver, but this increases the volume of fluid that must flow through the line to activate the brakes. Increasing the leverage factor on the brake pedal or decreasing the diameter of the master cylinder piston will reduce the force required by the driver, but both of these changes tend to reduce the amount of fluid flowing down the brake lines to activate the calipers. Once a geometry is selected, an analysis must be done to ensure that with the maximum brake pedal travel, the master cylinder displaces enough volume to activate the calipers. These details are illustrated in the following example.

Example. The team decides that to slide the tires the driver should push on the pedal with a force of 445 N (100 lb). The calipers selected have a piston diameter d_P = 24.5 mm (1 in.). The tire diameter is 482.6 mm (19 in.), and the radius to where the pad contacts the disk is 88.9 mm (3.5 in.). Master cylinders are available with piston diameters of 12.7, 19.0, 25.4, and 38.1 mm (0.5, 0.75, 1.0, and 1.5 in.). Select a master cylinder and design a brake pedal that is 305 mm (12 in.) long. The weight of the car and driver is 3559 N (800 lb) and in hard braking 74.5% of the weight is on the front wheels. The force analysis is shown in Eqs. 9.11 and 9.12.

$$445\text{ N} = (0.745)(3559\text{ N})\left(\frac{241.3}{88.9}\right)\left(\frac{d_M^2}{25.4^2}\right)\left(\frac{a}{305}\right) \qquad (9.11)$$

$$d_M^2 a = (12{,}167)\text{ mm}^3 \qquad (9.12)$$

From Eq. 9.12 it can be seen that there is a relationship between the leverage factor for the brake pedal (a/12) and the master cylinder diameter. The different possibilities are listed in Table 9.1.

TABLE 9.1
RELATIONSHIP OF MASTER CYLINDER DIAMETER AND BRAKE PEDAL LEVERAGE FACTOR

d_M	a
12.7 mm (0.5 in.)	75.4 mm (2.97 in.)
19.0 mm (0.75 in.)	33.5 mm (1.32 in.)
25.4 mm (1.0 in.)	18.8 mm (0.74 in.)
38.1 mm (1.5 in.)	11.9 mm (0.47 in.)

The most reasonable solution is probably the 0.5-in.-diameter master cylinder, although the 0.75-in. master cylinder would work. As the leverage factor (a) gets very short it becomes difficult to design the pedal. This example illustrates the basic analysis process, but there are certain details that must be taken care of. The components must be capable of handling the fluid pressure and all of the forces applied to them. Besides strength requirements, there are also the fluid volume and travel requirements for the brake system to work properly.

The master cylinder must be able to displace enough volume of fluid to push the brake pads into contact with the disk. There must be space between the brake pads and the disk when driving the car, or there will be brake scrub, which wastes a lot of energy. A well-designed system will have about 1.5 mm (0.06 in.) clearance between the brake pads and the disk when the pads are retracted. With two front calipers (one per front wheel) and two pistons in each caliper, four pistons must be activated when activating the front brakes. The required fluid volume to be displaced is calculated from Eq. 9.13.

$$\text{Volume} = 4\frac{\pi}{4}d_P^2 t_P \qquad (9.13)$$

where t_P is the clearance between the brake pads and the rotor when the brake system is not activated. If t_P is 1.5 mm (0.06 in.) and the caliper piston diameter is 25.4 mm (1.0 in.), the volume of fluid to be displaced is 3080 mm^3 (0.188 $in.^3$). *The actual volume required will be greater than this because of flexibility in the brake lines and other components in the brake system.* As a rule of thumb it is a good idea to double the calculated volume to account for flexibility in the system.

If a master cylinder with a diameter of 12.7 mm (0.5 in.) is selected and the rule of thumb is applied to the required volume, the piston must travel 48.8 mm (1.92 in.) to activate the brakes, so a master cylinder must be selected that has at least 48.8 mm (1.92 in.) of travel. From Table 9.1 the length a is to be 75.4 mm (2.97 in.), so the brake pedal must travel a distance of 48.8(305/75.4) = 197 mm (7.75 in.) where the driver pushes on it to activate the brakes. This is an acceptable design, but it may be difficult to find a master cylinder with a diameter of 2.7 mm (0.5 in.) with 48.8 mm (1.92 in.) of travel.

If a master cylinder with a diameter of 19 mm (0.75 in.) is selected, the piston must travel 21.6 mm (0.85 in.) to activate the brakes. From Table 9.1 the length a is to be 33.5 mm (1.32 in.) and the brake pedal will travel 197 mm (7.75 in.) to activate the brakes. (The distance that the driver's foot must move to activate the brakes is the same no matter which master cylinder is selected.)

C. Homework for Brakes

The following homework exercise leads the reader through the design of a braking system.

1. Calipers have been selected with a piston diameter d_P= 38.1 mm (1.5 in.), a pad diameter of 25.4 mm (1 in.), have a maximum pressure rating of 5.53 MPa (800 psi), and there is a coefficient of friction of 0.2 between the pads and the rotor. Find the maximum friction force for one brake pad. [1260 N (283 lb)]

2. The car weight is 2675 N (600 lb) and it is estimated that 74.5% of the weight will be on the front wheels when the car experiences hard braking. The tires are 482.6 mm (19 in.) in diameter and there is a coefficient of friction of 0.8 between the tires and road. Find the required radius to where the pads should contact the disk r_D so that it is possible to slide the tires, and estimate a minimum disk diameter. [r_D = 80.3 mm (3.16 in.), disk diameter = 93 mm (3.66 in.) because the whole pad has to fit on the disk]

3. Master cylinders are available with piston diameters of 12.7, 19.0, 25.4, and 38.1 mm (0.5, 0.75, 1.0, and 1.25 in, respectively). The brake pedal can be a maximum of 254 mm (10 in.) long. Select a combination of master cylinder and distance on the pedal as illustrated in Fig. 9.6 so that the driver need push with only 669 N (150 lb) to slide the tires. (The solution options are illustrated in Table 9.2.)

TABLE 9.2
HOMEWORK: RELATIONSHIP OF MASTER CYLINDER DIAMETER AND BRAKE PEDAL LEVERAGE FACTOR

d_M	a
12.7 mm (0.5 in.)	81.5 mm (3.21 in.)
19.0 mm (0.75 in.)	36.3 mm (1.43 in.)
25.4 mm (1.0 in.)	20.3 mm (0.80 in.)
38.1 mm (1.5 in.)	13.0 mm (0.51 in.)

[Probably the most reasonable solution is to use the master cylinder with a diameter of 19.0 mm (0.75 in.) and make a = 36.3 mm (1.43 in.).]

4. If the pads withdraw when the brakes are released so that there is 2 mm (0.08 in.) clearance between the pads and disk, find the volumetric displacement on the master cylinder and the required travel on the master cylinder and brake pedal. Use the rule of thumb of doubling the calculated volumetric displacement in calculating the required travel distances.

[18,517 mm^3 (1.13 in.^{3}) volumetric displacement. The master cylinder must have 65.0 mm (2.56 in.) displacement if the 19.0-mm (0.75-in.) master cylinder is used, or 36.6 mm (1.44 in.) travel if the 25.4-mm (1.0-in.) master cylinder is used. The pedal will travel 455 mm (17.9 in.) in either case.]

5. The solution to this point is not practical because it will not be possible to allow 455 mm (17.9 in.) travel on the brake pedal. If the clearance between the brake pads and the disk can be reduced to 1 mm (0.04 in.) the required travel is reduced by a factor of two to 228 mm (9 in.) which is a more practical amount. This small amount of clearance may cause brake scrub. Precise manufacturing and high stiffness in the calipers and caliper mounting brackets will be required to keep the brakes from scrubbing. Another approach is to use smaller-diameter pistons in the brake calipers and rework the problem, but this will increase the diameter of the brake disk. The designer must consider the components available and develop a system that will work.

D. Hub and Spindle

At this point in the design process for the front suspension the tire was chosen for minimum rolling resistance, a wheel was chosen to fit the tire, dished if possible to allow for good packaging of the brake calipers and disk, and the brake system was designed. Wheels, tires, and brakes are usually purchased components and a design must be developed around what is available to be purchased and the cost of the components. The hub and spindle are components that are usually designed and built by the team.

1. *Hub Design.* The purpose of the hub is to connect the wheel to the brake disk, and to house the bearings that the wheel assembly spins on. The hub must be structurally capable of carrying the braking torque and the bearing loads. This is not usually a problem because to connect the wheel to the brake disk requires that the hub be approximately 12.5 cm (5 in.) in diameter. The hub is usually made of aluminum to minimize the weight. The brake disk connects to one side of the hub and the wheel connects to the other side. The hub must be wide enough to provide clearance between the brake calipers and the wheel as illustrated in Fig. 9.8.

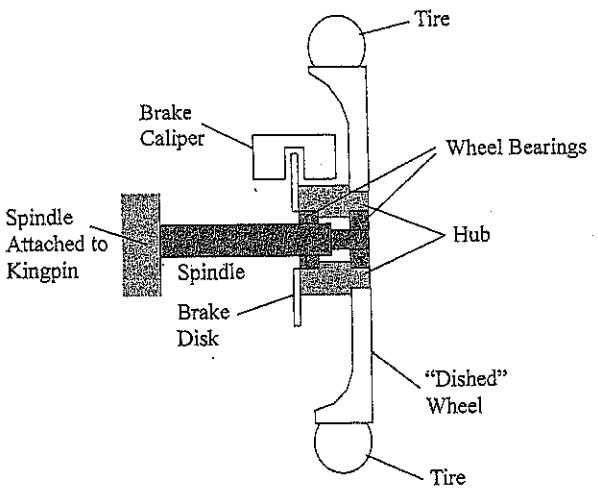

Fig. 9.8 Hub and spindle schematic.

Some secondary design issues exist for the hub. There is a small amount of play in the wheel bearings that will allow the wheel to rock back and forth. All bearings must have a small amount of play to be able to rotate. This creates a small amount of scrub that causes tire wear and increases the car's energy consumption. Locating the wheel bearings as far apart as is practical in the hub will minimize the scrub and make a slight improvement in the energy efficiency of the car. Spreading the bearings apart also reduces the bearing forces when cornering, which reduces the loads on the hub and spindle.

A solid aluminum piece machined to accommodate the wheel, disk, and wheel bearings works well for the hub, but a stress analysis will show that there is a lot of extra material and that the hub is heavier than it needs to be. Reducing the weight of the spindle should not be a priority because the amount of weight to be saved is small. It requires a lot of effort for a small savings in weight, and the effort may be better spent on other aspects of designing or manufacturing the car. The spindle is a component that will see some abuse when the team gets in a hurry

changing tires during the race. The maximum normal stress in the hub should be limited to 70 MPa (10,000 psi) when optimizing the design of the hub.

2. *Spindle Design.* The purpose of the spindle is to carry the wheel-bearing loads and to transmit those loads to the kingpin. The spindle is a cantilevered shaft and it is a highly stressed component. The spindle should be designed to carry a 3g bump, a 1g brake, and a 1g corner in either direction. The bending moment is much larger where the inner bearing is located than where the outer bearing is located, so the spindle is usually stepped as illustrated in Fig. 9.8. The maximum bending moment occurs where the spindle attaches to the kingpin.

   Steel is the recommended material for the spindle. If structural steel is used the maximum normal stress should be limited to 125 MPa (18,000 psi). If chrome-alloy steel (4130 steel) is used the maximum normal stress should be limited to 245 MPa (35,000 psi). *Aluminum should not be used for the spindle* because it does not have the fatigue strength, stiffness, or surface hardness required for such a highly stressed component. Titanium can be used if the maximum normal stress is limited to 350 MPa (50,000 psi), but the designer must recognize that titanium has a lower modulus than steel and that stiffness of the spindle is a factor in wheel alignment and scrub.

3. *Load Cases.* The load cases for the hub, spindle, and other suspension components are the 3g bump, the 1g brake, and the 1g cornering load in either direction. Experience has shown that if the components are designed to carry these loads, then they will hold up well in service. All of the load cases are based on the weight W_T on the wheel, so reducing the weight of the vehicle will reduce the loads the suspension components will have to carry. Static analysis is used to find the bearing loads, and then these loads are used to calculate stresses in the components. The stress analysis is beyond the scope of this book, but a limited amount of discussion of the load cases is provided. The 3g bump is illustrated in Fig. 9.9.

   In Fig. 9.9, P_{BI} and P_{BO} are the loads on the inner and outer wheel bearings, and l_I and l_O are the horizontal distances between the center of the

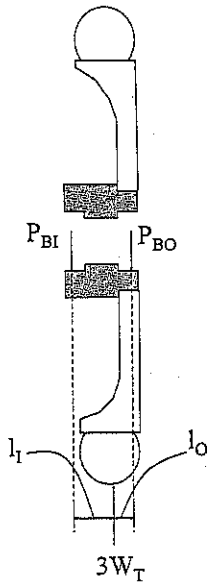

Fig. 9.9 Loads for 3g bump.

tires and the inner and outer wheel bearings, respectively. The loads on the wheel bearings are given by Eqs. 9.14 and 9.15.

$$P_{BI} = 3W_T\left(\frac{l_O}{l_I + l_O}\right) \tag{9.14}$$

$$P_{BI} = 3W_T\left(\frac{l_O}{l_I + l_O}\right) \tag{9.15}$$

The loads for a 1g cornering are illustrated in Fig. 9.10. Cornering in the direction shown yields the higher cornering stresses, and is usually the largest stress case for the suspension components.

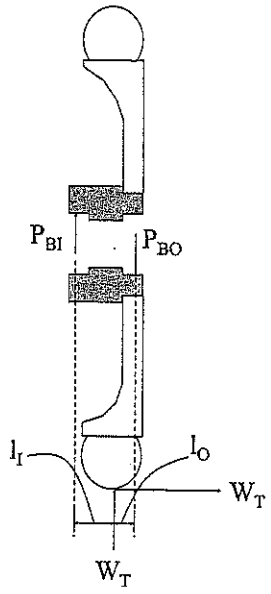

Fig. 9.10 1g cornering loads.

For the outer corner load illustrated in Fig. 9.10, the weight on the tire and the cornering load combine to produce a large bending moment on the spindle, which is then transmitted to the kingpin and other suspension components. Assuming r_T as the radius of the tire, the wheel-bearing loads are given in Eqs. 9.16 and 9.17.

$$P_{BO} = W_T\left(\frac{l_I + r_T}{l_I + l_O}\right) \tag{9.16}$$

$$P_{BI} = W_T\left(\frac{r_T - l_O}{l_I + l_O}\right) \tag{9.17}$$

For a 1g braking load the stress on the spindle is always less than the stress for the 3g bump. Braking often generates high stresses on the

kingpin and a-arms, but is not a problem for the spindle. For the case of the 1g braking load, a load equal to the weight on the tire is placed where the tire contacts the road. The torque that this load creates around the spindle axis is balanced by the friction force that the caliper exerts on the brake disk.

E. Suspension and Chassis Design Philosophy

The suspension and chassis components are highly important for the safety and performance of the car. Failure in the suspension or chassis will often make the car go out of control, so it is very important that these components do not fail. It is tempting for the mechanical engineer to design these components to the limit of the strength of the material to minimize their weight. Keeping the weight under control is extremely important for solar cars, but it is not good design philosophy to design chassis and suspension components near their limit for any vehicle, including solar cars.

The difference between having a safety factor of two and a safety factor of four in the chassis and suspension is only a few kilograms in the total weight of the vehicle, and it is worth it for the additional safety aspects of the car. Making the suspension components stronger also makes them stiffer, and there is a small improvement in wheel alignment if the suspension and chassis components are stiffer. The philosophy for designing suspension and chassis components should be to err on the side of safety, recognizing that there is some benefit to making the components stronger. Do not take on a lot of risk with these safety-critical components. On the other hand, do not tremendously overdesign the components. The stress limits proposed in this and other chapters are adequate.

F. Front-End Geometry and Steering

The geometry of the front end is set to minimize the energy the front suspension absorbs while the car is traveling down the road. Tires generate rolling resistance, which cannot be avoided, but the energy lost in the tires can be an order of magnitude higher if the front suspension geometry is not set up properly. The two fundamental mechanisms leading to energy loss in an

improperly designed suspension are tire misalignment and tire scrub [9-1, 9-2]. Misalignment is illustrated in Fig. 9.11.

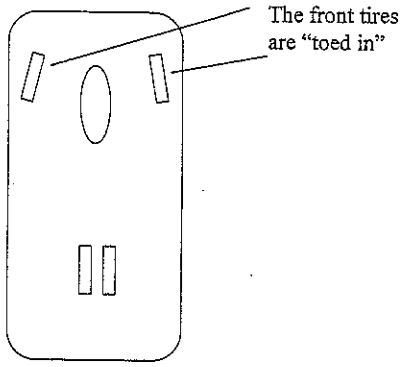

Fig. 9.11 Toe-in misalignment of the front tires.

The front tires should be parallel and aligned with the body of the car when it is traveling straight down the road. Figure 9.11 shows a greatly exaggerated misalignment, but even small angles of misalignment significantly increase the rolling resistance. The high-pressure tires used on solar cars are more sensitive to misalignment than passenger car tires. That is, for the same angle of misalignment, higher-pressure tires have a higher percentage increase in rolling resistance because they are stiffer and less able to accommodate the misalignment. Adjustments must be made in the steering linkage to allow the wheels to be properly aligned.

Even if the steering linkage is properly adjusted, there can still be alignment problems. If the suspension has low stiffness so that it flexes noticeably under load, it will flex back and forth as the car travels down the road, and the wheels will always be misaligned to some extent. Flexibility in the suspension always leads to misalignment and increased rolling resistance [9-1 to 9-5]. Similarly, if the connections in the ball joints, rod ends, or steering linkages are loose, the wheels will wobble because of the play in the linkage connections, and never be properly aligned. All connections must be tight.

If the tie rods are not of the proper length, the wheels will toe in and out as the car bumps up and down, a condition known as *bump steer* [9-2 to 9-5]. The suspension is constantly going through small up and down movements as the car travels down the road, so bump steer can waste a lot of energy. As the car turns corners the inner wheel should turn slightly more than the outer wheel, or the wheels will be misaligned when cornering. The tie rods and steering knuckles must be properly sized to achieve Ackerman steering to minimize the energy lost when cornering [9-3 to 9-5]. Poor adjustment of the suspension, flexibility, loose suspension connections, bump steer, and non-Ackerman steering are all examples of suspension problems that cause the tires to be improperly aligned. The suspension must be designed to minimize these energy losses, or the solar car will have high rolling resistance and will not be competitive.

The second energy loss mechanism is scrub. As the suspension bounces up and down, the "contact patch" between the tire and road can move in and out as illustrated in Fig. 9.12, a condition known as *scrub* [9-3 to 9-5]. This back-and-forth motion literally scrubs the tread off the tire, absorbing a lot of energy.

The goal in suspension geometry is to design a suspension and steering system that has minimal scrub and keeps the tires properly aligned while going

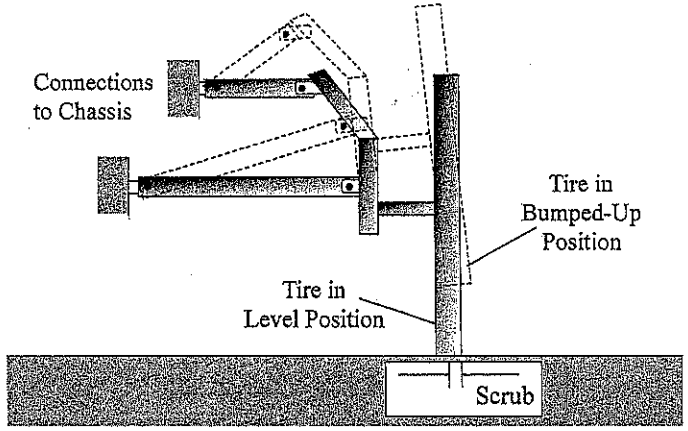

Fig. 9.12 Scrub of the front tires.

over bumps and around corners. As has been stated, an important aspect is to design a "stiff" suspension. The connectors, whether they are tie rods, spherical bearings, or ball joints, must fit tight so that there is little play in the system. Any play in the system will allow the tires to wobble around and introduce an apparent misalignment that cannot be corrected.

The first step is to choose the type of suspension to use. A double wishbone suspension will theoretically provide the best control of the front-end geometry, and has been used for many years for race cars and production cars [9-3 to 9-5]. A McPherson strut suspension is simpler than the double wishbone design and gives good control of the front-end geometry. However, to provide zero scrub, McPherson struts must be about 90 cm (36 in.) long, requiring a body that is 90 cm thick, which is unacceptable for solar car aerodynamics. Nearly all solar cars have used a double wishbone suspension (or a double a-arm suspension), so the discussion will focus on this type of design.

The double wishbone is a four-bar mechanism, and the equations governing its motion are complex. It is difficult to obtain an analytical solution. There are computer programs that can be used to solve the problem of defining front-end geometry, and it is recommended that the team obtain a program to assist in the front-end geometry design. A geometric construction technique is used in this chapter to illustrate front-end geometry design. It is an adequate method to design the front-end geometry, but is not as good or efficient as using a computer program. The geometric construction technique illustrates what occurs in the suspension, and helps the reader understand the suspension motion.

Before proceeding with the design of the suspension, the width of the chassis structure and the wheel track (distance between the front wheels) must be determined. The distance from the ground to where the lower wishbones will connect to the chassis must be decided too. There is no formula for selecting these three distances (chassis width, wheel track, and height above ground). The following general guidelines can be used in selecting these distances; the numbers in the brackets are good target values for the lengths or distances, but should not be regarded as rules. These are merely guidelines.

1. The chassis structure should be narrow where the front suspension is attached so that the lower wishbones in the suspension will be longer. Longer lower wishbones will reduce the scrub and bump steer and make the suspension more energy efficient. [23 cm (9 in.) is a good lower wishbone length for solar cars.]

2. A wider wheel track will also increase the length of the lower wishbones, so some consideration should be made to making the wheel track wide. However, a wider wheel track makes it harder to interface the front-wheel fairings with the body. The fairings will have to interface with the more rounded portion of the body near the edges with a wider wheel track. [For a car that is 1.8 m wide, a typical wheel track is 1.25 m (50 in.).]

3. The lower wishbones will transmit high loads to the chassis structure, so the point where the wishbones hook onto the chassis will need to be strong and stiff.

4. It is desirable to maximize the distance between the upper and lower wishbones. Making this distance larger reduces the wheel wobble due to play in the rod ends and improves the energy efficiency of the suspension. Making the distance large also reduces loads on the upper wishbone, and minimizes scrub and bump steer over a larger wheel bump travel distance. [23 cm (9 in.) is a good distance between the upper and lower wishbones.]

When these distances are selected, a portion of the front suspension geometry is defined as illustrated in Fig. 9.13.

Once the length of the lower wishbone has been determined, the next step is to select the angle for the kingpin axis as illustrated in Fig. 9.13. Selecting a vertical kingpin axis simplifies designing the steering system, and makes it easier to keep the wheels aligned when turning a corner. Angling the kingpin through the center of the tire patch causes the braking loads to have a zero moment around the kingpin axis. This allows braking loads to be separated from steering loads, and eliminates a phenomenon known as "brake steer." With a vertical kingpin, having one tire "grab" or "slip" against the pavement while braking will cause the car to try to turn, because the braking force on the tire will have a moment around the kingpin axis. The driver will fight the

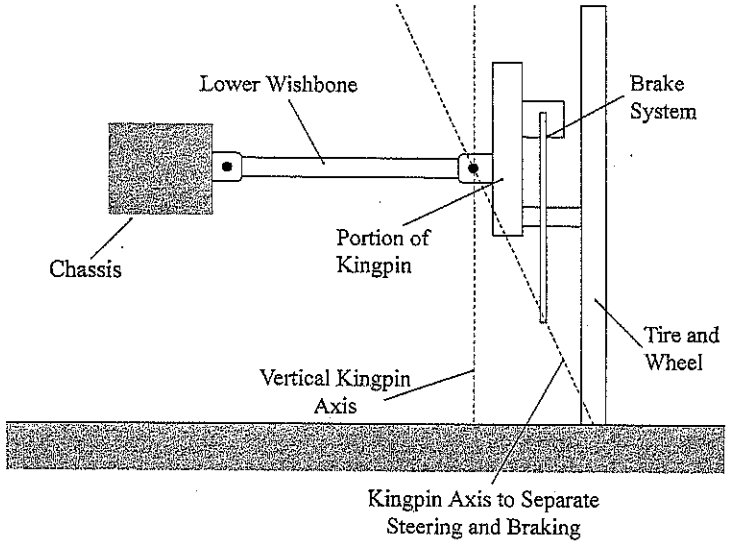

Fig. 9.13 A portion of the front-end geometry.

steering wheel in hard braking, and this can become a stability problem. Angling the kingpin axis makes the car more stable in hard braking, but complicates the steering design. For an angled kingpin the wheel will tilt slightly when turned, which slightly increases the rolling resistance when cornering. The vertical kingpin is the most energy-efficient design overall by a small margin.

There are advantages and disadvantages to the two angles shown. When passenger and race cars are being designed, usually some angle in between the two angles shown is chosen, compromising a small amount of cornering efficiency for an improvement in stability. Energy efficiency is very important for solar cars, and a strong argument can be made for using a vertical kingpin axis. A few solar cars have used a vertical kingpin axis, but most do not. Adequate stability can be achieved with a vertical kingpin axis, so angling the kingpin axis to improve stability of the solar car is not a good justification for having an angled kingpin axis.

Aerodynamics is extremely important for solar cars, and making the kingpin axis perpendicular to the belly pan will make it easier to interface the front fairings with the body. If the belly pan is flat and parallel to the ground around the front wheels, then a vertical kingpin will be perpendicular to the belly pan and is probably the best choice. In most solar cars the belly pan is curved upward to make the car thinner near the sides and to reduce the frontal area and surface area of the vehicle. If the kingpin is angled so that it is perpendicular to the belly pan, the front-wheel fairings will interface better with the body, and the aerodynamic energy savings is probably worth the small increase in rolling resistance when cornering. Angling the kingpin can also decrease the size of the hourglass-shaped holes that must be cut in the belly pan to allow clearance for the wheels to turn, which reduces ventilation drag. Angling the kingpin axis to reduce aerodynamic drag on the car is a good justification for an angled kingpin axis. An arbitrary kingpin axis will be used to illustrate how to choose the upper wishbone length to minimize the scrub.

As the car travels down the road, the tires will move up and down relative to the chassis. The movements are small on smooth pavement, but not insignificant. The upper wishbone must be located so that the contact patch between the tire and road moves straight up and down as the tire moves up and down. Any lateral movement of the tire patch is scrub, which scrubs the tread off the tires and wastes energy. The upper wishbone length must be selected to make the contact patch move as straight up and down as possible over the most probable range of motion. For the stiff suspensions used on solar cars, nearly all bumps in the road will cause the wheel to move up and down 25 mm (1 in.) or less, so the goal should be to develop a geometry that minimizes scrub over an upward and downward motion of 25 mm. Figure 9.14 illustrates the process of selecting the correct upper wishbone length to minimize the scrub.

1. Draw the wheel, spindle, kingpin, and lower wishbone in a CAD program as illustrated in the figure.

2. Rotate the lower wishbone around the left connection so that the right connection moves up 25 mm (1 in.).

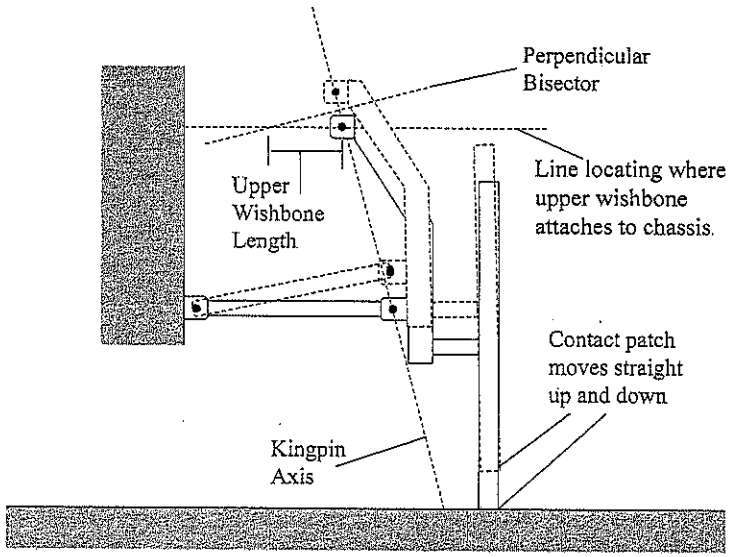

Fig. 9.14 Minimizing the scrub.

3. Rotate the wheel, spindle, and kingpin assembly so that the contact patch moves straight up. This will require a slight counterclockwise rotation of the assembly.

4. A line is drawn at the height where the upper wishbone will connect to the chassis. The goal is to decide how long the upper wishbone will be and where it will connect to the chassis.

5. Draw a perpendicular bisector between the original upper connection point on the kingpin and the "bumped-up" upper connection point. The point where this line intersects the line in item 4 is where the upper wishbone should connect to the chassis to minimize scrub over an upward bump of 25 mm.

6. The process should be repeated for a 25-mm (1-in.) downward bump. The downward bump will yield a slightly different upper wishbone length.

Average the two lengths for the upper wishbone to get the best overall solution using this method.

The method described here yields an acceptable solution for the upper wishbone length. As discussed previously, computer software is available that will do a slightly better job, and using the software is the recommended method. The final design is shown in Fig. 9.15.

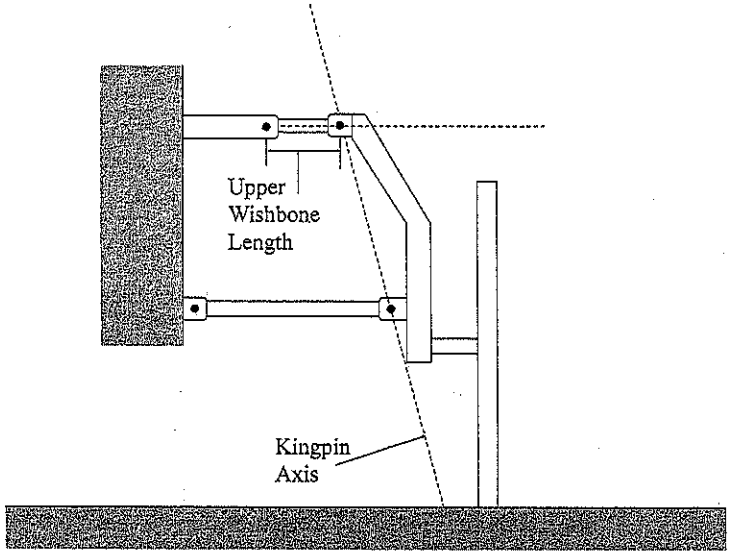

Fig. 9.15 Double wishbone suspension design.

The next step in designing the front suspension is to estimate the length of the tie rods used for the steering. Tie rod length affects both bump steer and Ackerman steering. The location of the steering knuckle also affects bump steer and Ackerman steering. An iterative solution must be used to get the optimal length of the tie rods and the location of the steering knuckle.

If the steering bar or rack is to be located in front of the front axle, then the steering knuckle must be located outside of the kingpin axis. If the steering

bar or rack is to be located behind the front axle, the steering knuckle must be located inside the kingpin axis. Figure 9.16 shows how to make a first estimate of the optimal location for the steering knuckle. This is only a rough estimate; the optimal location of the steering knuckle will not lie exactly on these lines. This will be used for a starting point, and will be refined using the analysis.

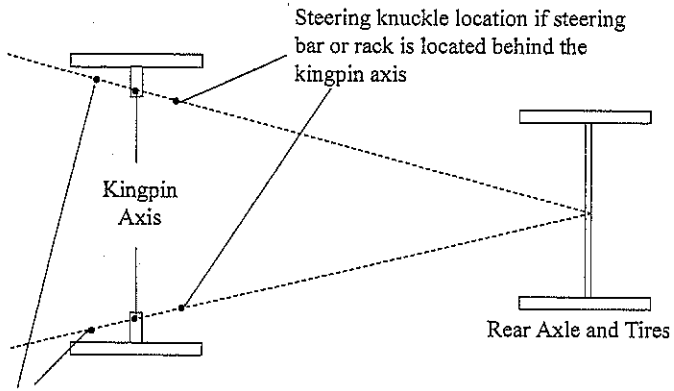

Fig. 9.16 Location of steering knuckle for Ackerman steering.

Because of the way the kingpin is designed, it is generally easier to design the steering knuckle and weld it to the kingpin if the steering bar or rack is located in front of the front axle. The kingpin axis will lie inside the kingpin structural member as illustrated in Fig. 9.17. Locating the steering knuckle outside the kingpin axis will make it approximately even with the kingpin structural member, which makes it easy to weld to the member. If the steering knuckle is located inside the kingpin axis, then it must be curved or come off the kingpin structure at an unusual angle, and it will be more difficult to manufacture. Either approach will work, and fitting the steering system to the driver position in the chassis is the most important consideration. If it is

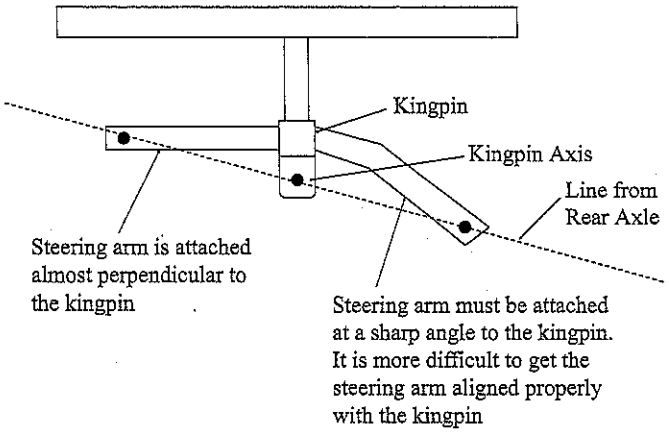

Fig. 9.17 Attaching steering knuckle to kingpin

an arbitrary choice, it is best to locate the steering knuckle in front of the front axle. Besides simplifying manufacturing of the kingpins, this also moves the points where the tie rods connect to the steering bar or rack outward, away from the chassis structure, and alleviates the potential of interface problems occurring involving the tie rods hitting the chassis structure when the car corners or hits a bump.

Once the steering knuckle is located, the tie rods are sized to minimize the bump steer. If the tie rods are too long or too short, the wheel will turn (toe in or toe out) as the wheel bumps up and down. Bump steer wears the tires and wastes energy, so it is important to get the tie rods sized to the proper length. The tie rods are sized using exactly the same procedure used to determine the length of the upper wishbone, as illustrated schematically in Figs. 9.18 and 9.19.

After the steering knuckle and tie rod have been located and the lengths specified to minimize the bump steer, the Ackerman steering is checked. When cornering, the inner front wheel in the corner should turn more than the outer wheel. As with scrub and bump steer, steering can be optimized over a range. Nearly all turns of interest involve the front wheels turning 10° or less. The

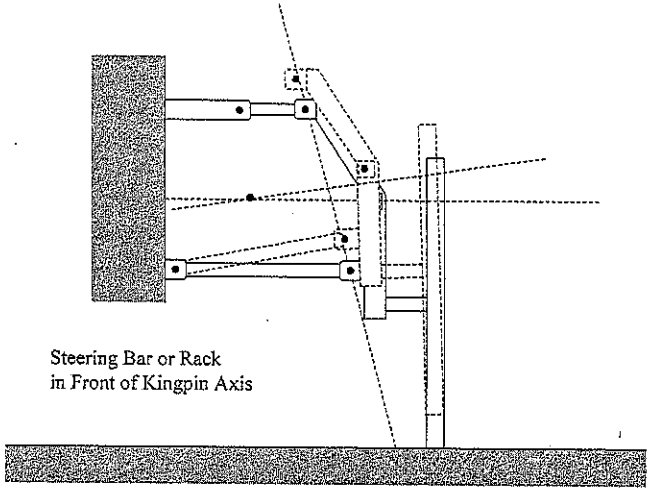

Fig. 9.18 Adjusting tie rod length to minimize bump steer steering knuckle in front of front axle.

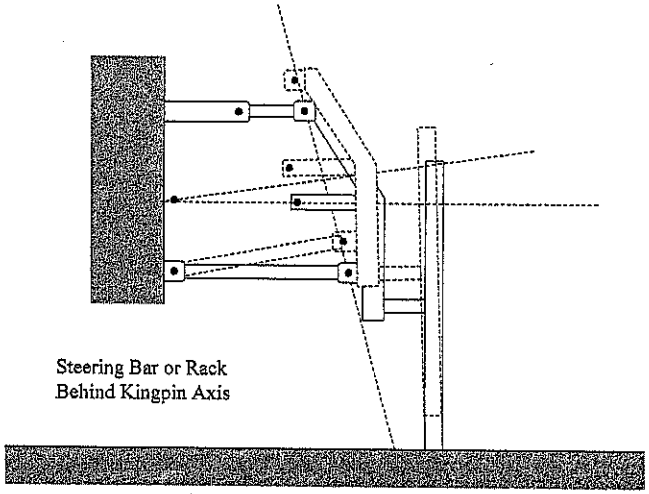

Fig. 9.19 Adjusting tie rod length to minimize bump steer steering knuckle behind front axle.

wheels will turn more sharply than this when maneuvering in a parking lot or turning at a stop sign, but in a road race or track race the wheels will seldom turn more than 10°. If the inner wheel is turned 10°, the angle that the outer wheel turns can be calculated using Fig. 9.20 and Eq. 9.18.

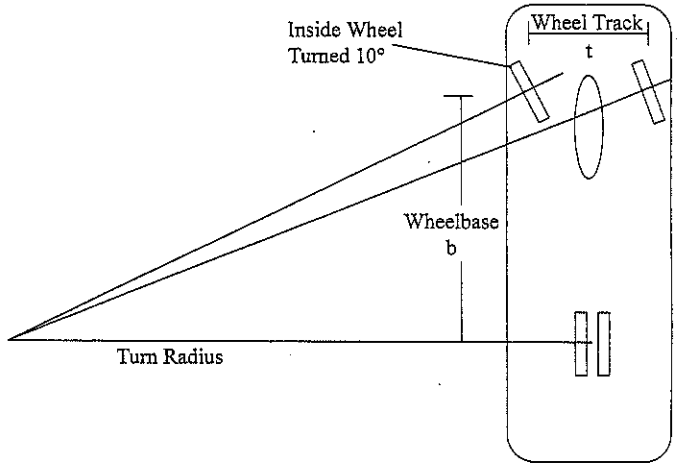

Fig. 9.20 Ackerman steering.

$$\text{Outside wheel angle} = \arctan\left(\frac{b}{b\,\csc(10^\circ) + t}\right) \qquad (9.18)$$

where b is the wheelbase and t is the wheel track as illustrated in Fig. 9.20. The goal is to adjust the steering knuckles and tie rods so that the car has Ackerman steering and minimal bump steer. Figures 9.21 and 9.22 illustrate how to check for Ackerman steering once it has been determined how much the outer wheel should rotate when the inner wheel rotates 10°.

The process is to rotate the inside tire 10° around the kingpin axis. Track where the tie rod on that side goes, where the rack goes, and where the tie rod

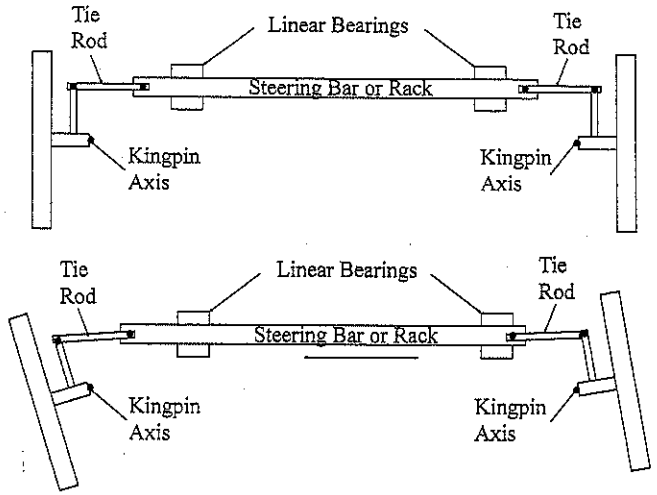

Fig. 9.21 Left turn with steering bar in front of front axle.

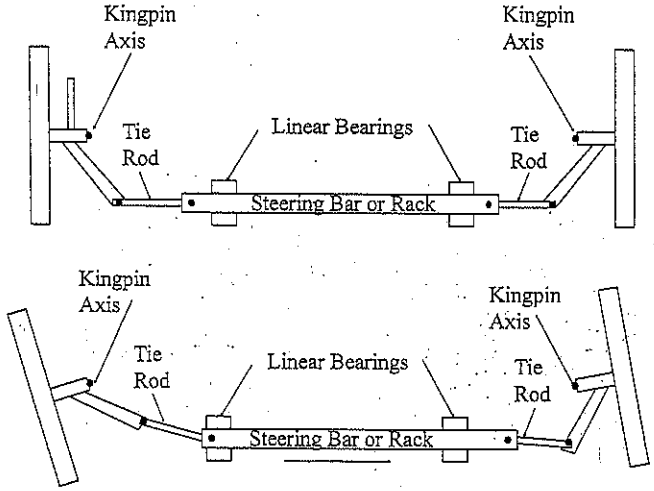

Fig. 9.22 Left turn with steering bar behind front axle.

and tire on the other side go. Ultimately find what angle the outside tire rotates through when the inside tire rotates 10°. Modify the tie rod length and steering knuckle location until Ackerman steering is approximated when turning the inside tire by 10°.

A difficulty arises if a vertical kingpin is not used. If the kingpin is not vertical, the steering arm does not rotate in the two-dimensional plane as illustrated, which is a disadvantage of using an angled (rather than a vertical) kingpin. The connection between the tie rod and steering arm actually rotates into or out of the page. This requires that the drawings be done in three-dimensional form to get an accurate representation of the geometry. A vertical kingpin will simplify the geometry and make it easier to achieve Ackerman steering.

After the steering knuckle and tie rod have been altered to achieve Ackerman steering, there will be some bump steer, and the process for zeroing the bump steer must be repeated, selecting a new tie rod length to zero the bump steer. Achieving Ackerman steering and zeroing bump steer therefore becomes an iterative process. The last step should be zeroing the bump steer because it affects the car all the time, while Ackerman steering affects the car only when it is turning. Both are important, but bump steer is a little more important.

Adjustments and Alignment. The wishbones and tie rods must be able to be adjusted to zero the camber and toe. Rod ends on the ends of these components are commonly used for the necessary adjustments. This brings up the issue of the location of the suspension attachment points on the chassis. These attachment points must be properly located, or the suspension will have scrub and misalignment problems, even if the suspension was very well designed. For example, if its attachment points are not properly located, the top wishbone will have to be made either longer or shorter than the desired length for the purpose of adjusting the camber of the tire. This introduces scrub, changes the roll center, and causes inefficiencies in the suspension.

G. Homework for Front Suspension Geometry

1. The lower wishbone, kingpin, tire, and axle are shown in Fig 9.23. Point K is the location of the steering knuckle, which is located 127 mm (5 in.)

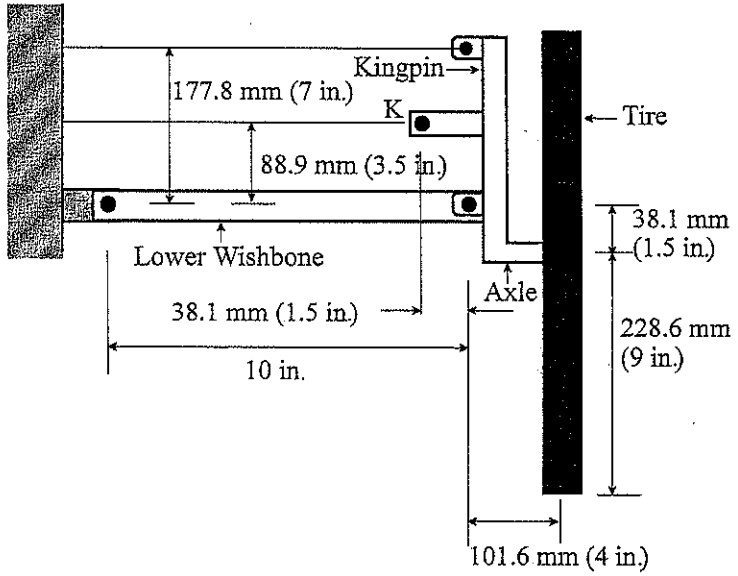

Fig. 9.23 Homework Problem 1.

in the z-direction (out of the page). Use a CAD package to solve for the length of the upper a-arm and the roll center connection for the tie rod for a 25 mm (1 in.) upward bump of the tire. Draw to scale showing where the upper a-arm should be connected to the chassis and where the tie rod should connect to the steering bar or rack. [Top wishbone is 153.1 mm (6.0219 in.) long, tie rod is 189.2 mm (7.4503 in.) long.]

2. Using the tie rod lengths from Problem 1 above and assuming that the left wheel turns counterclockwise 10° in Fig. 9.24, calculate how much the right wheel turns. For what (front to rear) wheelbase would this be perfect Ackerman steering? [9.388125°, 3.437 m (135.3 in.)]

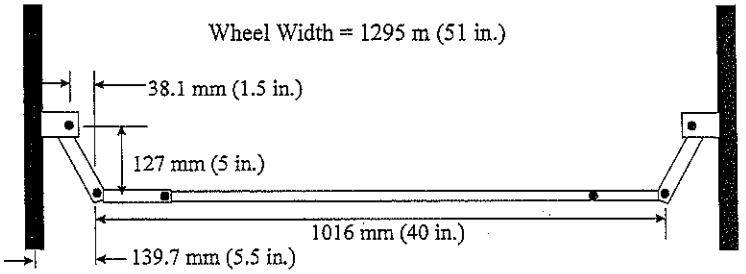

Fig. 9.24 Homework Problem 2.

H. References

9-1. Roche, D.M., A.E.T. Schinckel, J.W.V. Storey, C.P. Humphris, and M.R. Guelden, *Speed of Light: The 1996 World Solar Challenge*, chap. 9, Photovoltaics Special Research Center, University of New South Wales, Sydney, Australia, 1997.

9-2. Storey, J.W.V., A.E.T. Schinckel, and C.R. Kyle, *Solar Racing Cars*, chap. 9, Australian Government Publishing Service, Canberra, Australia, 1994.

9-3. Gillespie, T.D, *Fundamentals of Vehicle Dynamics*, chaps. 4 and 10, Society of Automotive Engineers, Warrendale, PA, 1992.

9-4. Milliken, W.F., and D.L. Milliken, *Race Car Vehicle Dynamics*, chaps. 2 and 14, Society of Automotive Engineers, Warrendale, PA, 1995.

9-5. Bastow, D., and G. Howard, *Car Suspension and Handling*, chap. 7, Society of Automotive Engineers, Warrendale, PA, 1993.

Chapter 10

Rear Suspension, Drive, and Chassis Structure

A. Rear Suspension and Drive Design

Choosing a tire, wheel, and spindle for the rear of the car is essentially the same process that was used for the front. Low rolling resistance is important on the rear, just as it was on the front. In most designs, the rear tires do not brake or steer, except for regenerative braking. The rear suspension should be stiff. It should not flex significantly under side loads. Low stiffness always generates tire scrub or misalignment and wastes energy.

Solar cars have used swing-arm designs for the rear suspension almost without exception [10-1 to 10-3]. A single rear wheel with a single trailing swing arm is the most common. However, tandem rear wheels with a single swing arm have been used on several cars. Two rear swing arms have been used on some four-wheel car designs. The trailing swing arm, similar to what is used on many motorcycles, is the most common design. A few teams have used the double wishbone swing-arm design, which is more complex, but offers higher stiffness and better adjustments to align the wheel. Some passenger cars have refined double wishbone rear suspensions with several other links to control the suspension when the car is cornering, braking, and traveling on rough roads.

Most solar cars have one rear wheel (three-wheeled cars), while some have two (four-wheeled cars). A car with a single rear wheel is lighter in weight, less complex to design and manufacture, has simpler rear alignment, and is generally more energy efficient. There are significant performance advantages to using only one rear wheel. The disadvantage to this design is that if traction is lost on the rear, the car will go into a spin [10-4 to 10-7]. Many

accidents have occurred when the rear-wheel tire blew out on a solar car and the car spun out of control. A car with two rear wheels is safer, but not as energy efficient. The car will be more stable if most of the weight is on the front. Cars with single rear wheels should have 60–70% of the weight on the front wheels for stability in case of a rear blowout, as well as for braking. The single trailing swing arm is illustrated in Fig. 10.1.

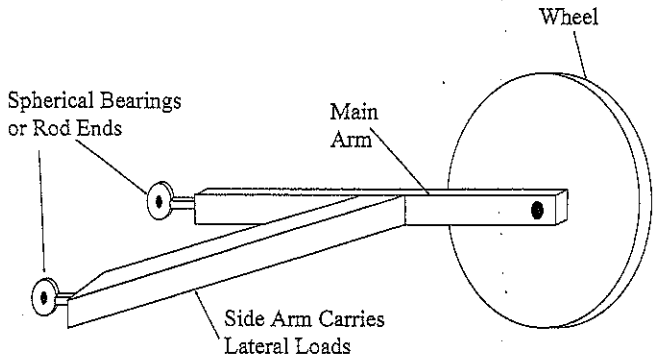

Fig. 10.1 Single trailing swing arm.

The rear swing arm must be rigid. Torsional rigidity of the main arm is required to keep the tire from tilting under a lateral (cornering) load. When the car corners, there will be significant side loads. The side arm and main arm must carry the lateral and torsional loads and keep the rear wheel(s) aligned with the chassis.

The weakest part of the design is often the rod ends. Rod ends must be capable of carrying the side loads when cornering. Cornering loads are what usually determines the minimum rod end size required. The cornering loads bend the rod ends, as illustrated in Fig. 10.2, and may cause failure at the root where the rod ends connect to the swing arm. A better and stiffer design involves using spherical bearings pressed into the main structural parts of the swing arm, but many teams use rod ends because it simplifies the manufacturing of the swing arm. Failure of a rod end or any part of the structure of

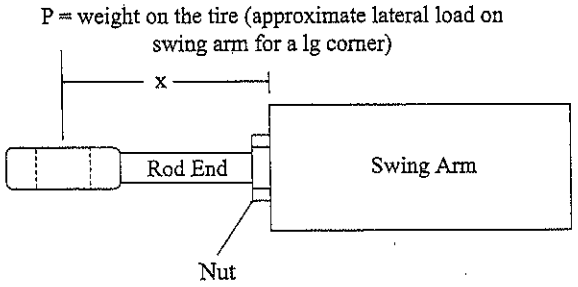

Allow 250 MPa (35 ksi) bending stress for top quality high-strength rod ends. Because the side load is actually shared by two rod ends, there is a safety factor of two built into the analysis. The actual bending strength of the rod ends is greater than 250 MPa (35 ksi), so the safety factor is probably between three and four.

Fig. 10.2 Rod end loading and analysis.

the rear swing arm will cause the car to go out of control. Figure 10.2 illustrates the recommended design analysis for rod ends.

In Fig. 10.2, x is the maximum distance the rod end can be extended from the swing arm for any adjustment. Some adjustment will be required to align the swing arm with the chassis. If the swing arm is not aligned with the chassis, the car will crab down the road, which hurts its aerodynamic properties, and because of Ackerman steering the front tires will not be properly aligned with each other. Whatever design is chosen for the rear swing arm, there must be a method to get the tire aligned with the chassis, and rod ends work well in providing this adjustment.

There must also be a method of adjusting the swing arm to make the rear wheel vertical, and the swing-arm design does not lend itself well to this adjustment. A common way of making this adjustment is to locate the rod end on the side arm after the chassis mounts and other parts are complete. The car should be driven around before the rod end is located, to be sure that the rear wheel is vertical. A suggested approach is pictured in Fig. 10.3.

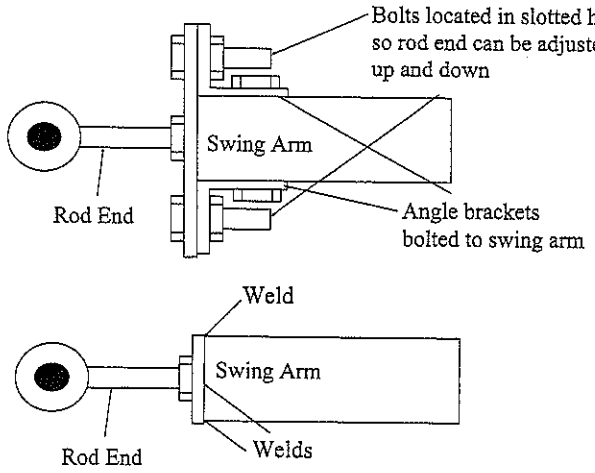

Fig. 10.3 Adjustment of rod end position to align rear tire.

Angle brackets are mounted to the swing arm, and the rod end is mounted in a plate that is bolted to the angle brackets. Slotted holes are cut in the plate or brackets so the plate can slide up and down, which adjusts the angle of the rear tire. Adjustments should be made until the rear tire is vertical when the car is loaded and driving. The bolted arrangement can be used for testing the car until the car is completed. When the team is sure that the rod end is located where it should be, the front and back of the plate are first welded to the swing arms. The bolts and angle brackets are then removed, the plate is cut off flush with the swing arm, and the top and bottom of the plate is welded to the swing arm.

The rod ends can be used to keep the rear wheel(s) aligned with the centerline of the car by screwing them in or out. The main arm must have adequate torsional stiffness to keep the wheel or tire from tilting under load, or in cornering. If a significant amount of lateral or tilting deflection is noticed in the rear tire when the solar car is being followed by the chase van, the rear swing arm is probably not stiff enough. Any noticeable deflection of the rear tire will increase the rolling resistance. It is better to have a heavier stiff

swing arm than a lighter-weight swing arm that flexes under load. The spring must also yield the correct spring rate for the rear. Connecting the spring near the rear axle will reduce bending stress on the main arm, as illustrated in Fig 10.4.

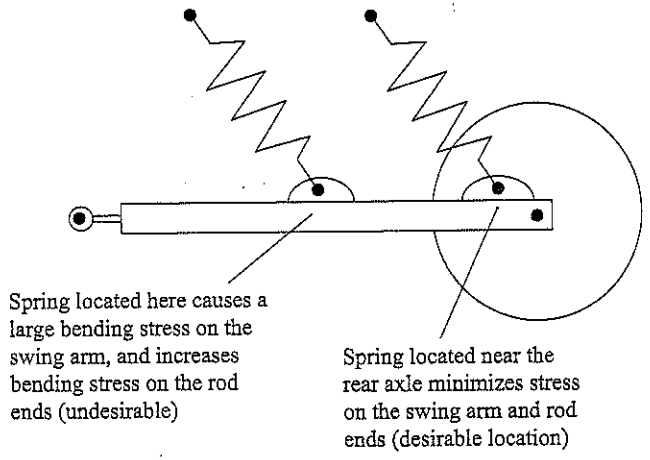

Fig. 10.4 Location of spring on rear swing arm.

Figure 10.5 illustrates the swing-arm design used for most solar cars, and illustrates how it is incorporated into the chassis.

In the rear swing-arm concept illustrated in Fig. 10.5, the load on the rear tire is carried primarily by the spring. There are loads in the swing arm and rod ends, but they are small compared with the weight on the rear tire for normal driving. The loads on the rod ends and swing arm increase significantly in hard cornering. This yields a simple, lightweight, efficient design. Ideally the spring would be vertical, but angling the spring up to 30° from vertical is acceptable. Larger angles are not recommended because it puts high loads on the rod ends and connections.

Some teams have used a horizontal spring concept, which is illustrated in Fig. 10.6. This design performs well, but the spring in this design is horizontal,

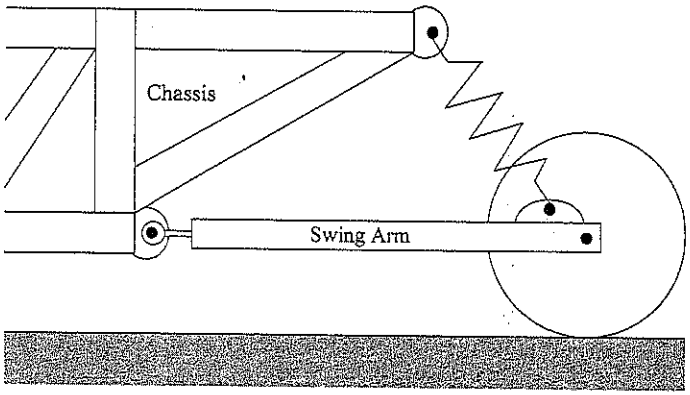

Fig. 10.5 Rear swing-arm concept.

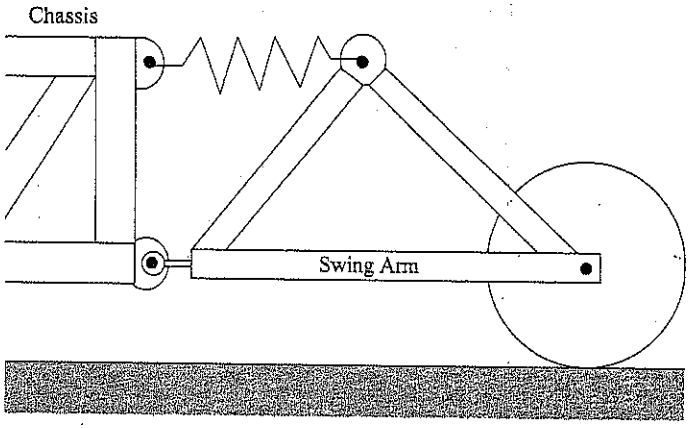

Fig. 10.6 Horizontal spring concept.

and cannot carry the vertical loads on the swing arm. The weight on the rear tire is transferred to the rod ends, which means that the weight on the rear tire will always be bending the rod ends. This design yields a heavier swing arm, but a lighter chassis, so the weight difference is probably insignificant. This

design requires larger rod ends. The rod ends should be designed for a 3g bump in this case, which means that three times the weight on the wheel should be used as the side load in selecting the rod end size.

A few teams have also used a double wishbone rear suspension, as illustrated in Fig. 10.7. This design has a lot of adjustments built in, and probably makes it easier to align the rear wheel, but it is more complex. It is similar to the front suspension design, except that the wishbones are attached to the back of the car rather than the side. The wishbones do not have to be sized to zero the scrub, because there is no tendency for the tire to move laterally as it bumps up and down.

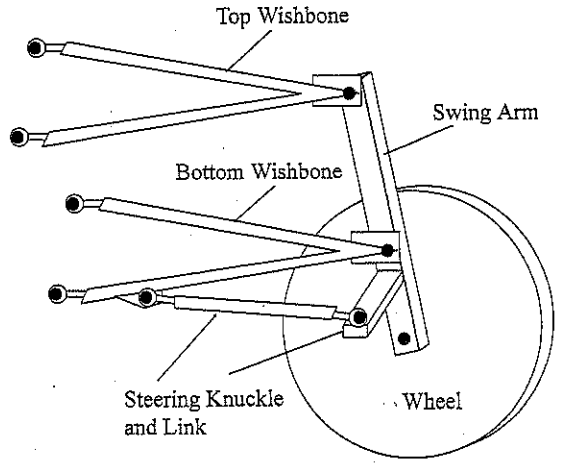

Fig. 10.7 Double wishbone rear suspension concept.

The springs/shocks are usually attached to the lower wishbone, just as in the front suspension. Rod ends on the wishbones are adjusted to keep the wheel vertical. A steering knuckle and link are used to align the wheel with the centerline of the chassis. Careful geometric control is required with the steering knuckle and link to make sure there is no bump steer. In most cases, the increased complexity of this design is not worth the increase in adjustment. A simple swing arm is the best choice in most cases.

B. Drivetrain

The drivetrain should be simple and should consume as little energy as possible. Energy efficiency is the most important consideration. The trend is for solar cars to use hub motors, where the motor is hooked directly to the wheel and there is no drivetrain. This is the simplest and most energy-efficient arrangement. The hub motor has made this section of the book obsolete for most teams, but it is included because there are still a few teams that use a single-reduction chain or belt drive.

Teams have used multiple chain or belt reductions. However, it is almost always more efficient to operate the motor at a lower efficiency with a single reduction, because of the energy lost in a second reduction. A single-reduction drive is simpler and will probably have better overall efficiency. Gear drives are less efficient than chain or belt drives and should not be used.

Single-Reduction Drive. In this type of drive system, the motor drives a small pulley or sprocket, which is connected to a larger pulley or sprocket on the rear tire or axle. This is the drive system used on bicycles or motorcycles. It is simple and energy efficient. A chain/sprocket drive is slightly more energy efficient than a pulley/belt drive, provided the chain and sprocket are clean and properly lubricated. Poor lubrication or lots of dust on the chain reduces the efficiency. Belt/pulley drives require no lubrication and are less susceptible to dirt.

Problems associated with this type of drive are obtaining proper tension of the belt or chain and properly aligning the pulleys or sprockets. Improper tensioning or alignment will reduce the energy efficiency of the drivetrain, and may cause premature failure. The precision required for proper alignment of the pulleys or sprockets is not easy to achieve. Teams using a single-reduction drive should not take the design of this system lightly because a considerable amount of energy can be wasted in a poorly aligned drive system. Considerable thought should be given during design to make sure that the tension can be adjusted, the shafts can be aligned, and the pulleys and sprockets can be aligned. There are several ways the alignment can be off, as illustrated in Figs. 10.8–10.10.

The first issue is improper alignment of the shafts. As the belt/chain is tensioned, there is a tendency to pull the shafts out of alignment as illustrated in Fig 10.8. A high degree of stiffness is required in the motor mounts, shafts, and wheel bearings to prevent this misalignment.

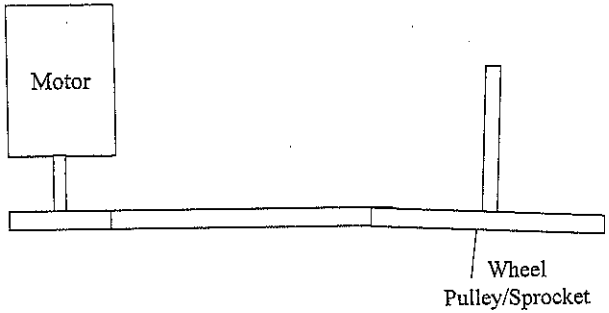

Fig. 10.8 Improper alignment of shafts.

Another possible misalignment is improper alignment of the pulleys and sprockets as illustrated in Fig. 10.9. In this case the shafts are aligned, but the pulleys are not. The system must be designed for adjustment so that the pulleys can be aligned. This is usually accomplished by incorporating a slide

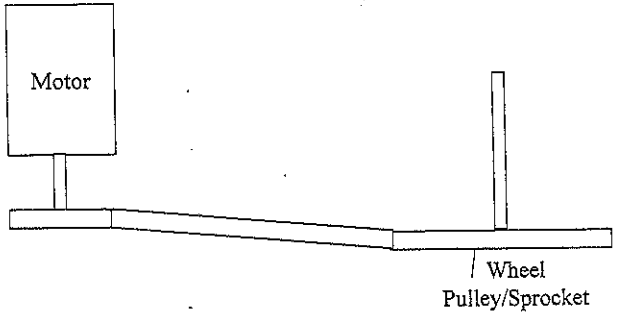

Fig. 10.9 Improper alignment of pulleys or sprockets.

adjustment for the pulley on the motor shaft, which can be slid to align the belt or chain.

A third possibility is that the shafts can be skewed as illustrated in Fig. 10.10. The shafts are skewed up and down relative to each other. This twists the belt and chain during operation and absorbs energy. It is the most difficult misalignment to detect, because most methods of measurement will show the system to be in alignment. Torsional twisting of the swing arm is a common source of this type of misalignment because the weight on the tire tends to twist the swing arm. *The suspension and drivetrain must have high stiffness to be energy efficient.*

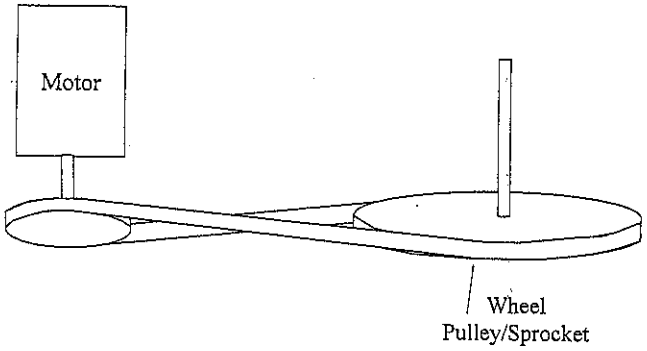

Fig. 10.10 Skewed shafts.

There are two methods of setting up the drivetrain: the live axle and the spindle and hub design as illustrated in Figs. 10.11 and 10.12. The live axle design is slightly more compact, but requires that a key-way connection be developed for at least one end of the live axle. The spindle and hub arrangement is similar to the spindle and hub design of the front suspension except that the brake disk on the front is replaced by a gear or sprocket on the rear. The live axle is the more commonly used design.

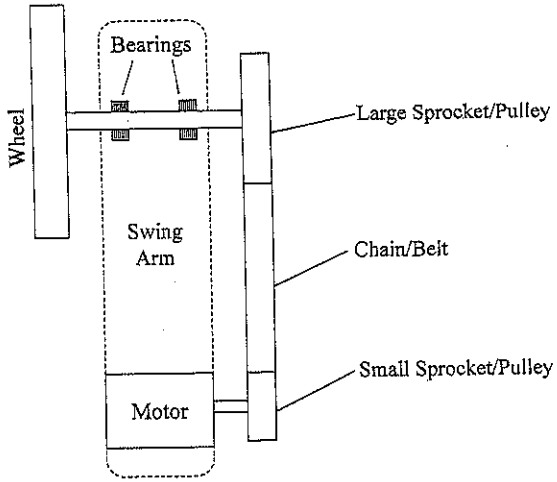

Fig. 10.11 Live axle design.

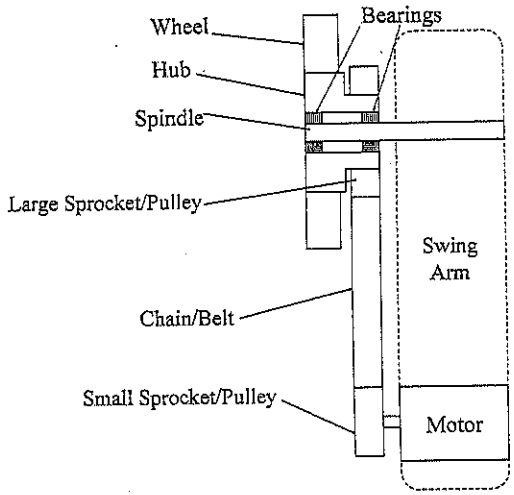

Fig. 10.12 Spindle and hub design.

C. Electric Motors

Electric motors work by passing a current through a wire that is in a magnetic field. If a current is passing through a wire in a magnetic field (the N-S poles of the magnet shown), a force F develops on the wire that is proportional to the product of the current I and the strength of the magnetic field B as illustrated in Fig. 10.13.

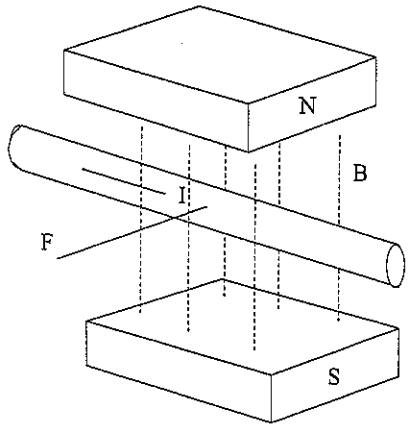

$$\vec{F} = \vec{I} \times \vec{B}$$

Fig. 10.13 Force of a magnetic field on a wire carrying current.

In the two-pole electric motor diagram shown in Fig. 10.14, the circles with a dot in the center indicate a wire carrying current "out of the page" and the circles with the x's indicate a wire carrying current "into the page." The wires on the left make a downward force, and the wires on the right make an upward force. This makes a torque on the inner circle (the rotor) causing it to rotate in the direction shown. If a permanent magnet is used (as shown) the amount of torque generated is controlled by controlling the current in the wires on the rotor [10-1 to 10-3].

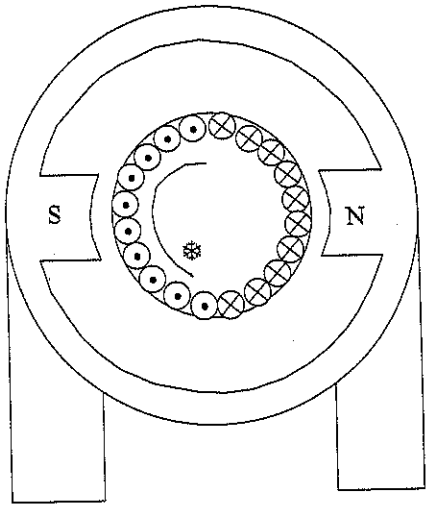

Fig. 10.14 Two-pole electric motor.

Once the rotor rotates 90°, a zero torque point is reached, with half the wires causing torque in one direction, and half in the other. Going past 90° generates a net torque in the opposite direction. At the 90° point, it is necessary to switch directions of the currents in the wire. Inexpensive motors use a brush and commutator arrangement to switch the direction of the current. High-efficiency motors use electronic switches (transistors).

A two-pole magnet was used to illustrate how the electric motor works. In practice, multiple poles are used, and the current direction in the windings must be switched every few degrees of rotation, rather than the 180° for the two-pole motor illustrated.

A permanent magnet can be used, or windings can be used to make an electromagnet. Permanent-magnet motors are inherently more energy efficient because of the power loss in the electromagnet. However, permanent-magnet motors tend to be heavy because of the weight of the magnets. Ceramic

magnets are the most common, but also the heaviest. More exotic materials are used in motors for solar cars.

Disk Motor versus Drum Motor. Most motors are of the drum type, with the windings on a drum-shaped rotor and the magnets on the stationary part of the motor (stator). The gap between the stator and rotor is important because the strength of a magnetic field decreases with distance. A motor with a small gap will have higher torque compared to one with a higher gap, but a motor with a narrow gap will not produce as high a revolutions-per-minute (RPM) rate when it is operating. With a drum-type design (one drum rotating inside the other) the gap between the stator and rotor cannot be adjusted.

With a disk-type motor, the magnets are placed on one disk, and the windings on the other. One disk is stationary and the other rotates. The advantage of this design is that the gap between the stator and rotor can be adjusted to make a low-speed, high-torque motor or a high-speed, low-torque motor. This adjustment allows the same motor to operate at high efficiency over a broad range of revolutions per minute. Hub motors have been designed (disk type) that are 90%+ efficient over a broad range of torques and revolutions per minute. The disadvantage to the disk-type design is that the enormous attractive force between the disks puts a tremendous thrust load on the bearing. This causes a bearing loss not present in the drum-type design. For the drum design the attractive force is radial and cancels out, yielding no net force on the bearings.

To maximize the efficiency of the motor, the currents in the coils must be precisely controlled. The motor will have a "sweet spot" where the coil is between two magnet poles, as illustrated in Fig. 10.15.

High currents are drawn to produce a high torque in the motor at the "sweet spot." Currents are shut off as the coil becomes close to being on top of a pole, because energy would be wasted in that position. The motor controller adjusts the magnitude and timing of the currents in the coils to make the motor operate at high efficiency. Pulse-width modulation (PWM) is used to control the amount of torque the motor produces. In PWM control, the controller will send the current to the motor in pulses, turning the current off and on at a high frequency. The percentage of time the current is on determines the amount of torque the motor will produce. The best motor controllers use

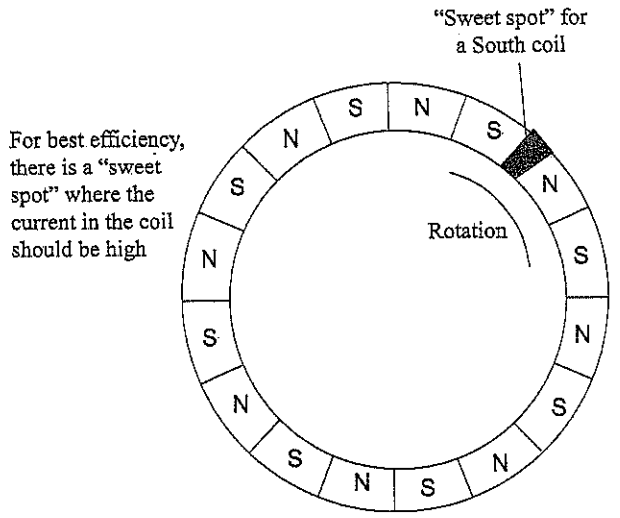

Fig. 10.15 Schematic of a twelve-pole motor.

PWM and vary the current magnitude in the coils in approximately a sinusoidal manner. Figure 10.16 shows how the efficiency of a typical electric motor varies with power output, torque, and revolutions per minute.

Figure 10.16 illustrates that it is important to size the motor to the amount of power it must provide. Efficiency improves as the revolutions per minute increases, and is best at the maximum revolutions per minute. The efficiency is good at speeds above 50% of the maximum revolutions per minute. The efficiency is poor when the motor is producing only 10% of its rated output at any revolutions per minute. It is typical for a solar car to use 2 kW of power on average when driving down the road, so it would be foolish to select a 20-kW motor for the car. The best efficiency occurs when the motor is producing 50–80% of the maximum rated power.

When Figure 10.16 is examined, it would appear that the most efficient design would be a motor that used about 75% of its rated output when the car is

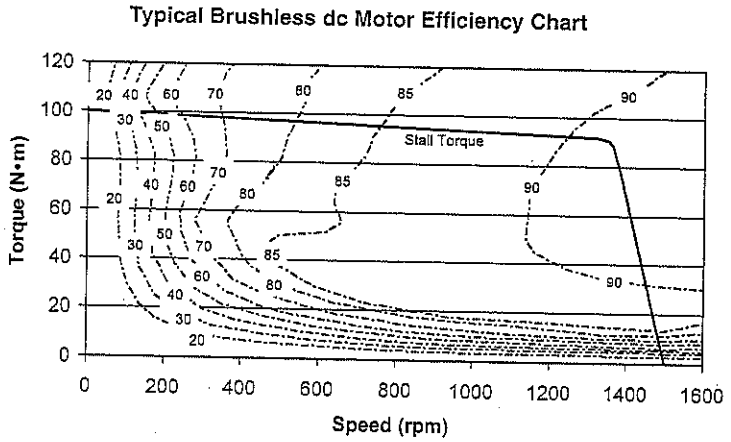

Fig. 10.16 Power and speed mapping of a typical brushless direct current (dc) motor.

cruising down the road. This choice would work well on a flat track, but would probably not generate enough power to push the car up hills on a road race. For road races it is recommended that the motor be capable of generating enough static (stall) torque to push the car up a 10% grade. For example, if the car weighs 3790 N (850 lb) as would be typical for a stock-class car, the motor should be capable of providing 379 N (85 lb) thrust to the car. If the tire has a radius of 25.4 cm (10 in.), 96.3 N•m (850 lb-in.) of torque must be applied to the rear wheel. A hub motor must be able to produce this much torque without being geared down. Other motors can be geared down with a single-reduction chain or belt drive to achieve the required torque. Climbing grades is the biggest power requirement the motor/drive system will face. Assuming a good brushless dc motor is used that is capable of providing static torque for a 10% grade, and capable of providing enough revolutions per minute to reach the desired speed, it is almost certain that the motor/drive system will be adequate. An 8-kW motor is suitable for most solar car designs.

D. Chassis Structure

The most difficult parts of chassis design, and the design aspects that must be specified first, involve providing a location for everything that connects to the chassis, and keeping the car's weight properly balanced on the tires. This is not straightforward; it is a trial-and-error process that is complicated because every major subsystem connects to the chassis. Structural design and analysis should be started after all of the major subsystems have been located on the chassis. It is important to carry out structural analysis to ensure that the chassis does not fail in driving and that it provides protection to the driver in the event of an accident. The chassis is complex enough that a finite element code must be used to do a realistic analysis, which is a straightforward process.

1. The heavier subsystems are the driver, batteries, and body. The CG of these items must be such that the proper amount of weight is on the tires (60–70% on the front tires).

2. The driver takes up a lot of space. Adequate space must be allocated for the driver and the steering, braking, and other controls the driver must operate.

3. Battery subsystems are most efficient if all the batteries are the same temperature, and it is good practice to locate all the batteries in the same box.

4. Location of the driver's head and roll cage on the chassis must correspond to the location of the canopy on the body. This seems obvious, but it is sometimes overlooked. The canopy and driver must be located so that there is space for the driver and the car is balanced.

5. The body and chassis groups of the team must come to an agreement as to how thick the car will be at various locations along the length. The body goes over and around the chassis, so it must always be thicker than the chassis.

6. The team must decide on a wheelbase (front and rear) and width (distance between the front tires). It is necessary to decide on these measurements

so the car's weight can be balanced and allowance can be made for wheel clearances in the body.

The first stage of chassis design is to locate the major subsystems. Extra space should be designed in so the motor controller, power converters, and other small electrical and mechanical components can be located later. The body and chassis groups must work together in the initial stage to be sure the two pieces will fit together. Center of gravity (CG) calculations, as described in Chapter 8, should be made to keep the car balanced. As the body and chassis groups are in the first stage of design, the suspension groups should be completing their geometry. The chassis must provide "hook-on" points for the suspensions. It is not necessary to design in all the bracing initially; bracing can be added later. At this stage a box-type shape should be made that will have the right geometry to connect the suspension.

The next stage is to add the roll cage and bracing, and do an analysis to ensure that the chassis will withstand the required load cases. Steel, aluminum, titanium, and composites have all been used for chassis structure. A brief description of the different types of materials that have been used for the chassis follows.

1. *Composites.* Composites can (theoretically) yield the lightest-weight chassis, but it is difficult to optimize the design when using them. The strength of composite materials is highly dependent on the process used for making them. A great deal of experience and expertise in designing with composites are required to take full advantage of their strength. In structural analysis the designer must know the *reliable* strength of the material. Finite element analysis is meaningless unless the strength of the material is known.

   Teams that have used composites in the past have generally used extremely conservative estimates of the strength of the material. The result is a composite structure that is heavier than a steel or aluminum tubular truss-frame design. A major advantage of the composite chassis is that it is easy to build. Composite panels are cut up and glued together to make a box-type chassis design. Hard mount points are made of aluminum, steel, or titanium for the suspension mounts. Bracing is required to get reasonable chassis stiffness. A disadvantage of the composite chassis is that it

is not as stiff as the other designs, and the lower stiffness probably increases rolling resistance. A composite chassis design is illustrated in Fig. 10.17.

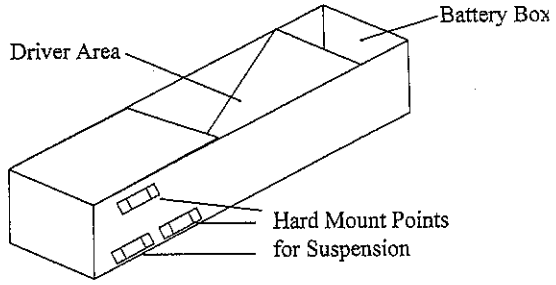

Fig. 10.17 Schematic of composite chassis.

2. *Titanium.* Welded titanium tube truss-frame structures have been used successfully by several teams. Titanium is expensive and difficult to weld, but if the team has the resources and technology it is probably the best choice. Titanium will provide the lightest-weight metal chassis. The disadvantage of using titanium is that it is difficult to repair or modify the chassis because of the difficulty involved in welding titanium. A tubular frame chassis, which could be titanium, aluminum, or steel, is illustrated in Fig. 10.18.

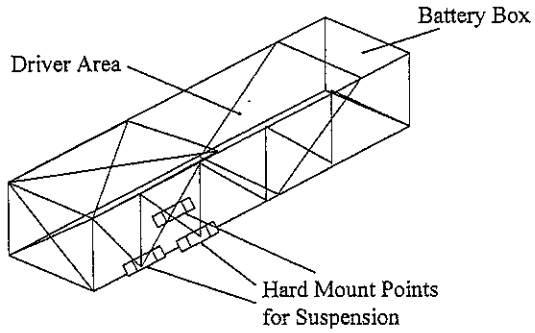

Fig. 10.18 Schematic of a titanium tube chassis.

3. *Aluminum.* An aluminum chassis is only slightly heavier than a titanium chassis. It is much less expensive and easier to weld than titanium. A good weldable aluminum alloy is 6061-T6. A tungsten–inert gas (TIG) welder is required to get good welds with aluminum. Students can learn to weld aluminum with some practice. An unfortunate attribute of aluminum is that it cracks in service. The chassis must be inspected regularly for cracks, and the cracks must be welded up. Much of the strength of the 6061-T6 aluminum alloy comes from the heat treatment, which will be partially removed by welding. Welding diminishes the heat treatment at the weld to about a T-4 level. Welding does not significantly change the ultimate strength of the material.

4. *Steel.* Steel chassis have been widely used in solar cars. Most teams choose 4130 steel, which is also used in race cars. A steel chassis is heavier than one made of aluminum, but has the advantages of being easier to weld and is more resistant to cracking. A disadvantage of steel, compared to aluminum, is that it rusts over time. This may not be an issue for the race, but will affect the looks of the car unless it is painted. This could be an issue if the car will be shown after the race.

   Solar cars tend to use high-performance materials and components, and it might appear that the trend would be toward using composites and titanium for the chassis. In fact, the opposite is true. The trend appears to be toward using 4130 steel. There will be many minor modifications to the chassis as the car is built. Carrying a little extra weight in the car body may be worth the flexibility steel has to offer during the manufacturing phase.

Structure Analysis. The car's chassis should be designed to protect the driver in the event of an accident. A sturdy roll cage should be used around the driver, not just a roll bar behind the driver. The driver should be completely enclosed inside the roll cage. Solar cars often travel at speeds of 100 km/h or faster and at these speeds a roll bar provides insufficient protection for the driver. Once the preliminary design is completed, the structure is put into a finite element code and modifications to the design are made until a lightweight design that will carry all the load cases is achieved. The recommended load cases follow. Satisfying these load cases ensures that the chassis will carry the suspension loads and protect the driver in a collision.

1. *3g Bump.* For each wheel (individually) assume an upward force of three times the weight on the tire, and calculate the loads transmitted to the chassis.

2. *1g Corner.* Assume a force equal to the weight on the tire acting laterally at the tire patch. Calculate the loads transmitted to the chassis, including the static weight on the wheel.

3. *1g Brake.* Assume a braking force equal to half the weight of the car on each front tire patch. Calculate the loads transmitted to the chassis, including the static weight on the wheel.

4. *5g Front Impact.* Assume five times the weight of the car applied over the front of the chassis, and restrain the back.

5. *5g Rear Impact.* Assume five times the weight of the car applied over the back of the chassis, and restrain the front.

6. *3g Rollover.* Assume three times the weight of the car pressing down on the roll cage.

7. *5g Side Impact.* Assume five times the weight of the car applied over one side of the car, and restrain the other side.

8. *3g Angular Impacts.* At 30 and 60° from the axes that line up with the chassis, assume three times the weight of the car is applied over whatever portion of the chassis makes sense for such an impact.

E. References

10-1. Roche, D.M., A.E.T. Schinckel, J.W.V. Storey, C.P. Humphris, and M.R. Guelden, *Speed of Light: The 1996 World Solar Challenge*, chaps. 4 and 7, Photovoltaics Special Research Center, University of New South Wales, Sydney, Australia, 1997.

10-2. Storey, J.W.V., A.E.T. Schinckel, and C.R. Kyle, *Solar Racing Cars*, chaps. 5 and 7, Australian Government Publishing Service, Canberra, Australia, 1994.

10-3. Kyle, C.R., *Racing with the Sun: The 1990 World Solar Challenge,* chaps. 6 and 7, Society of Automotive Engineers, Warrendale, PA, 1991.

10-4. Gillespie, T.D., *Fundamentals of Vehicle Dynamics*, chap. 5, Society of Automotive Engineers, Warrendale, PA, 1992.

10-5. Milliken, W.F., and D.L. Milliken, *Race Car Vehicle Dynamics*, chap. 6, Society of Automotive Engineers, Warrendale, PA, 1995.

10-6. Bastow, D., and G. Howard, *Car Suspension and Handling*, chap. 3, Society of Automotive Engineers, Warrendale, PA, 1993.

10-7. Starr. P., "Designing Stable Three Wheeled Vehicles, with Application to Solar Powered Racing Cars," unpublished work, May 1996.

Chapter 11

Battery Systems

A. Battery Fundamentals

An ideal battery pack would store electric energy at whatever rate it was put into the pack, and deliver the energy back at whatever rate it was needed. It would be 100% efficient in the sense that 100% of the energy put into it would be returned. It would also be lightweight [11-1 to 11-5]. No such battery exists. Batteries are heavy, and they are not 100% efficient in storing and releasing energy. Some terms that are important in developing the battery pack are as follows [11-4, 11-6]:

1. *Energy Density.* The amount of energy the battery will store, per weight of the battery (watt-hours per kilogram). A high energy density is desirable.

2. *Amp-Hour Capacity.* The total amount of charge the batteries can hold (1 amp hour = 3600 Coulombs). The amp-hour capacity is a function of the rate of charge and discharge for all battery systems. A well-designed battery will be at least 90% efficient as far as amp-hour capacity. That is, if 100 A-h of charge is put into the batteries, it should be possible to draw at least 90 A-h from the battery.

3. *Watt-Hour Capacity.* The total amount of energy the battery can hold (1 W-h = 3600 J). The usable energy in the batteries is sensitive to the charge and discharge rates for all battery systems. Charging and discharging at high currents reduces the watt-hour capacity of the battery system, because a higher percentage of the energy is converted to heat.

4. *Charge Efficiency.* The fraction of charge (amp hours) that will be returned after charging. Batteries that have a poor charge efficiency

are not acceptable for solar cars. For batteries with water-based electrolyte [lead-acid, nickel-metal-hydride (NMH), nickel-cadmium (NiCd), and silver-zinc], some of the charge is always lost in the electrolysis of water. Batteries with an organic or polymer-based electrolyte (lithium-ion and lithium-polymer) tend to have nearer 100% charge efficiency.

5. *Energy Efficiency.* Batteries are charged up along one voltage curve and discharged along a (lower) different curve, as illustrated in Fig. 11.1.

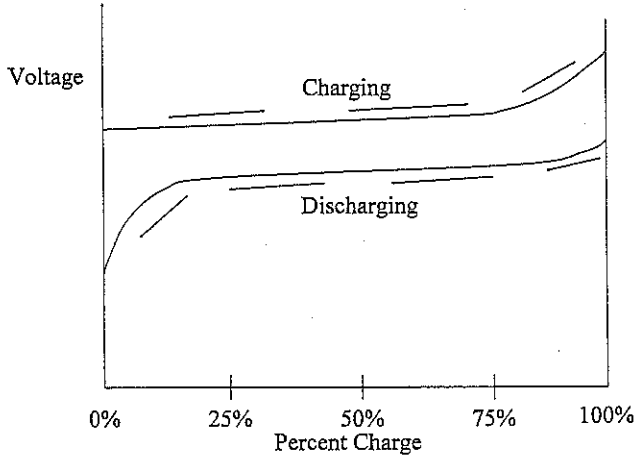

Fig. 11.1 Charge and discharge curves for a typical battery.

If the battery has a charge efficiency of 100%, the efficiency would be the ratio of the average discharging to charging voltages. Accounting for the charge efficiency, Eq. 11.1 shows the definition of the energy efficiency of the batteries.

$$\text{Energy efficiency} = \frac{V_{\text{Discharge}}}{V_{\text{Charge}}} \times \text{Charge efficiency} \qquad (11.1)$$

Batteries have poor efficiency at low states of charge because the discharge voltage is low. They are inefficient at high states of charge because the charge voltage is high. A common "rule of thumb" is that the batteries operate most efficiently between 25 and 75% state of charge. This can be illustrated graphically by taking the ratio of the discharge and charge voltages at various states of charge in Fig. 11.1.

The ideal choice would be a battery that has a high energy density (to reduce the weight of the car) and a high energy efficiency so that only a small fraction of the energy stored in the battery is lost. It is much easier to get information on the energy density of the battery system than the energy efficiency, but both quantities are important. Before the development of the lithium-ion and lithium-polymer batteries, the silver-zinc batteries had the highest energy density and were significantly better than any other battery chemistry. Before 2001, most of the top cars in the World Solar Challenge used silver-zinc batteries, a further indication that they were probably the best choice. In recent years, lithium-ion and lithium-polymer batteries have been developed that have an energy density comparable to silver-zinc batteries, and in 2001 all of the top teams in the World Solar Challenge and American Solar Challenge used either lithium-ion or lithium-polymer batteries. It appears that at the time of this writing the lithium-ion and lithium-polymer batteries are the best choice.

Nearly all battery manufacturers rate the energy density of their batteries, but very few provide information on the energy efficiency. Most designers have assumed that a lighter battery pack is better, but there is a point where an improvement in efficiency would justify carrying more weight. An example of this is in using NiCd or NMH batteries instead of lead-acid. NiCd or NMH batteries have a significantly higher energy density than lead-acid batteries, but they have a lower energy efficiency. Historically, solar cars powered by lead-acid batteries seem to perform as well as those powered by the NiCd or NMH batteries.

Efficiency is important because a lot of energy flows into and out of the batteries during a race. It is obvious that energy flows into the batteries when the body is on the array stand during the charging periods in the early mornings and late evenings. What is sometimes overlooked is that energy flows from the solar array into the batteries any time the car is going down a slight

grade or using regenerative braking. A higher-efficiency battery pack will provide more energy for the car to use. Lithium-ion and lithium-polymer batteries offer a lot of promise for solar cars. They have high energy density, high energy efficiency, and are less expensive than silver-zinc batteries.

B. Fundamentals of Battery Chemistry

The electrical energy in the batteries is stored as a chemical potential, the Gibbs free energy ΔG [11-4, 11-6]. The Gibbs free energy is the change in chemical potential energy between the two sides of the equation in the chemical reaction. The Gibbs free energy is the maximum amount of energy that the battery can deliver with the chemical reaction, that is, it is the energy delivered assuming 100% battery efficiency. Gibbs free energy is defined in Eq. 11.2.

$$G = -nFV_r \tag{11.2}$$

where n is the number of electrons involved in the chemical reaction, F is the Faraday constant = 96,485 C/mol, and V_r is the reversible (open-circuit) cell voltage. The Gibbs free energy is the change in energy between two states. To talk about energy values of different chemical states, it is necessary to define the energy level of one state to be zero. For this reason, the standard hydrogen potential was defined to be zero. If the potentials for the two electrode materials are known, then it is possible to determine the open-circuit potential voltage of the battery (which is not exactly the same as the open-circuit voltage). The standard hydrogen potentials for hydrogen, copper, and zinc are shown in Eq. 11.3 [11-4].

$$\begin{array}{lll} \text{Hydrogen} & \rightarrow V^0 = & 0.0 \\ \text{Copper} & \rightarrow V^0 = & 0.337 \\ \text{Zinc} & \rightarrow V^0 = & -0.763 \end{array} \tag{11.3}$$

Using this information, the open-circuit potential voltage of a copper-zinc battery is the difference between the hydrogen potentials of copper and zinc, $V^0 = 0.337 - (-0.763) = 1.1$ V. The standard hydrogen potentials are a relatively simple way to estimate the cell voltage of a battery, and yield a value that is approximately correct. The actual measured open-circuit voltage

depends on the state of charge in the battery. When at a higher state of charge, the battery will have a higher open-circuit voltage than when at a lower state of charge. The Nernst relationship in Eq. 11.4 relates open-circuit voltage V_r to open-circuit potential voltage V^0 [11-4, 11-6].

$$V_r = V^0 - \frac{RT}{nF} \ln\left[\frac{\text{(activities of products)}}{\text{(activities of reactants)}}\right] \tag{11.4}$$

where R is the universal gas constant and T is absolute temperature. The activities of the products and reactants change with the state of charge in the battery, and it is this change in activities that causes the open-circuit voltage to change with state of charge. A detailed discussion of the activities is beyond the scope of this book. The Nernst relationship also shows that open-circuit voltage is a function of temperature. In general, the voltage drops as the temperature increases, but temperature also affects the activities of the reactants and products, so it is not a simple linear change with temperature.

As current flows in or out of the battery the voltage shifts away from the equilibrium open-circuit voltage. The voltage increases when charging the battery and decreases when discharging the battery. The change from equilibrium is called *cell overpotential* and the overpotential has two components.

1. *Activation or Charge-Transfer Overpotential.* Charges (electrons) flowing off of or on to an electrode reduce or increase the potential of the electrode. The common definition is that the amount of overpotential is proportional to the current density (amps per cross-sectional area) of the electrode [11-4]. This is technically correct, but the common definition does not convey that the cross-sectional area of the plate changes as the chemical reaction proceeds. The battery may be charged or discharged at a constant amperage, but the effective cross-sectional area on the plates changes with the state of charge of the battery. If the battery is being charged from a low state of charge, the area is essentially the entire plate area. As the charging proceeds a large portion of the plates become reacted out and do not participate in the chemical reaction of charging the battery. The active area decreases as the battery is charged, hence the current density and cell overpotential increase as the battery is charged. As the battery approaches full charge, the area becomes small and the

voltage shifts significantly away from the open-circuit voltage. The charging rate (amperage) must be reduced as the battery approaches full charge because the high current density and cell overpotential will damage the battery.

If a fully charged battery is discharged at a constant amperage, the voltage will drop below the open-circuit voltage. This is still termed cell overpotential, but in this case it is a negative amount. The effective area on the plates decreases as the battery is discharged. As the battery approaches complete discharge, the current density and cell overpotential increase. Discharge rate (amperage) must be reduced as the battery approaches complete discharge to prevent damaging the battery.

2. *Concentration or Mass Transfer Overpotential.* This type of overpotential is caused by changes in the ion concentrations in the electrolyte near the electrodes [11-4]. The charges are delivered from the positive electrodes to the negative electrodes (or vice versa) by ions moving through the electrolyte. When current is flowing, the ions in solution near the plates are "used up" in the chemical reaction. The density of ions in the electrolyte near the plates will be less than the equilibrium concentration of ions in the electrolyte. The effect is sometimes termed *mass transfer* because the ions must flow through the electrolyte fast enough to maintain the chemical reactions at the electrodes. Increasing temperature, stirring the electrolyte, or other means of helping the ions move to the electrodes will reduce the cell overpotential caused by concentration or mass transfer.

   For most batteries, the cell overpotential caused by ion concentration near the electrodes is proportional to the amperage, and is not dramatically affected by the state of charge of the battery. If there were only enough ions in the electrolyte solution to exactly charge and discharge the battery, state of charge would be a major factor in the cell overpotential. Theoretically, the battery only needs enough ions to complete the chemical reaction, but this does not work out well in practice. As the chemical reaction nears completion, the ions in solution must find the areas on the electrodes that have not been reacted out, and the chemical reaction must slow down. Battery manufacturers put many more ions in the electrolyte solution than will be used in the chemical reaction during charging and

discharging the battery to reduce cell overpotential and make the batteries operate more efficiently. If the equilibrium concentration of ions in solution changes dramatically during the charge-discharge cycle, state of charge will significantly affect the cell overpotential caused by concentration of ions in the electrolyte. (As examples, lead-acid batteries use up the ions in the electrolyte so that the concentration changes significantly with state of charge. Nickel-cadmium batteries do not use up the ions in the electrolyte, so the concentration does not change with state of charge.)

3. *Internal Resistance.* Because cell overpotential is approximately proportional to current density, the battery can be modeled to have an internal resistance R [11-4]. The value of R is dependent on the state of charge of the battery because cell overpotential is proportional to the state of charge of the battery. The internal resistance is dependent on the state of charge of the battery and on temperature. The internal resistance is highest when the battery is being discharged at low states of charge, or charged at high states of charge. For the moderate charge and discharge rates for which the battery was designed to deliver, the internal resistance is fairly constant between 25 and 75% states of charge. If the manufacturer gives an internal resistance for the battery, it is probably for 50% state of charge, room temperature, and a moderate current draw, though there is no "standard" way of measuring internal resistance. Recognizing the limitations on defining an internal resistance, and using the Nernst relationship, the charge and discharge voltages can be written approximately as shown in Eq. 11.5 [11-4].

$$V_{discharge} = V^0 - IR$$
$$V_{charge} = V^0 + IR \qquad (11.5)$$

   where I is the discharge or charge current and R is the internal resistance of the battery. These equations are reasonably accurate and R is reasonably constant for the 25–75% state of charge of the battery and for reasonable currents, that is, currents the battery was designed to deliver. When using this model it is important to recognize that it is a rough

approximation, and that the internal resistance is actually dependent on the state of charge of the battery and temperature. The energy efficiency of the battery is the ratio of the discharge and charge voltages and can then be approximated as shown in Eq. 11.6.

$$\text{Energy efficiency} = (\text{Charge efficiency})\left(\frac{V^0 - IR}{V^0 + IR}\right)\times 100\% \qquad (11.6)$$

This efficiency model illustrates that the battery efficiency decreases as the current increases. As an example, consider a typical 60 A-h deep-cycle lead-acid battery with an internal resistance of 0.07 Ω, an open-circuit voltage of 12.6 V, and a charge efficiency of 97%. Figure 11.2 illustrates how the model predicts the battery efficiency to vary with the charge and discharge current. In this example, it is assumed that the battery is at approximately 50% state of charge and that the charge and discharge currents are equal.

Many solar cars have been designed using seven or eight lead-acid batteries wired in series with properties similar to those illustrated in Fig. 11.2. If the battery system were charged and discharged at 20 A, nominally

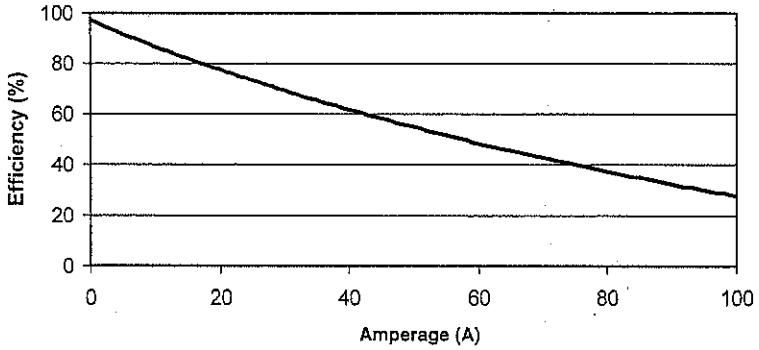

Fig. 11.2 Model prediction for battery efficiency as a function of amperage.

2000 W power, the efficiency of the battery system would be 78%. It would be common for the car to draw 20 A discharge from the batteries, but uncommon for the batteries to be charged with 20 A of current. If it were assumed that the batteries were discharged at 20 A and charged at 10 A, the efficiency would be 84%. A higher-efficiency battery system, such as lithium-ion, would have a lesser slope than the lead-acid battery system and the efficiency would be less sensitive to current. A less efficient battery system, such as NMH, would have a steeper slope and the efficiency would be more sensitive to current.

4. *Heat Generation.* The chemical reaction in the batteries will be endothermic in one direction and exothermic in the other direction [11-4, 11-6]. The endothermic reaction absorbs heat and tends to cool the battery, while the exothermic reaction tends to heat the battery. The I^2R term from the internal resistance always adds heat to the batteries. All batteries generate heat when they are cycled (repeatedly charged and discharged). They tend to generate more heat in one direction or the other because of the chemical reaction.

   The chemical reaction for lead-acid batteries is endothermic on discharge and exothermic on charge. For the same charge and discharge current, they will generate a lot more heat when being charged than when being discharged. Extra care must be taken when charging the batteries to prevent them from overheating.

   The chemical reaction for NMH batteries is exothermic on discharge and endothermic on charge. They generate a lot more heat when being discharged than when being charged. These batteries may require extra ventilation in the battery box to prevent them from overheating while driving the car.

C. Lead-Acid Batteries

The plates in lead-acid batteries are made of lead and lead oxide, and the electrolyte is sulfuric acid. Lead is the negative plate, and lead oxide is the positive plate. The sulfuric acid contributes sulfate ions and hydrogen ions to assist in the chemical reaction. Figure 11.3 is a schematic of a lead-acid

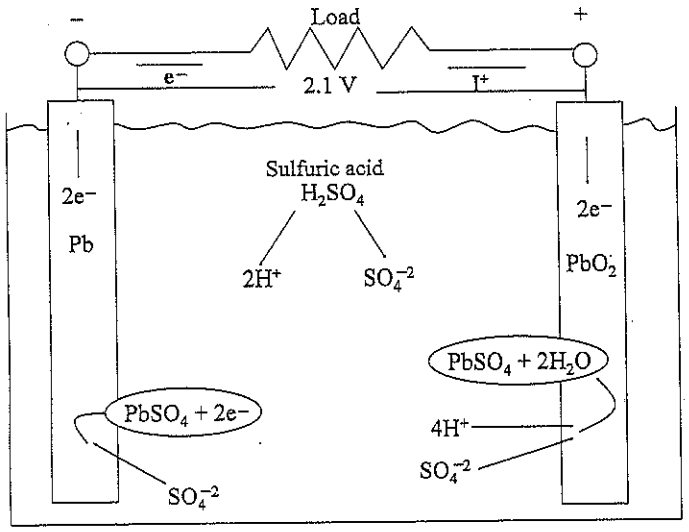

Fig. 11.3 Schematic of lead-acid battery chemistry.

battery. The chemical reactions in the figure are for discharge of the battery, and are reversed when the battery is charged [11-4, 11-6].

Negative Plate. Lead combines with the sulfate ion to make lead sulfate ($PbSO_4$) and generate two free electrons that go up through the load and down to the positive plate.

Positive Plate. Lead oxide separates into lead and oxygen ions, and then combines with four hydrogen ions and one sulfate ion and two free electrons to make $PbSO_4$ and two water molecules. The chemical reactions are illustrated in Eq. 11.7.

$$\begin{aligned}
&\text{Negative Plate:} && Pb + SO_4^{-2} \rightarrow PbSO_4 + 2e^- \\
&\text{Positive Plate:} && PbO_2 + 4H^+ + SO_4^{-2} + 2e^- \rightarrow PbSO_4 + 2H_2O \quad (11.7) \\
&\text{Total Reaction:} && Pb + PbO_2 + 2H_2SO_4 \rightarrow 2PbSO_4 + 2H_2O
\end{aligned}$$

The reactions in Eq. 11.7 are the description for discharging of the battery. As the reaction proceeds, the plates are both coated with $PbSO_4$. The sulfuric acid is "used up," so that the acidity becomes weaker as the reaction proceeds. As the sulfuric acid is used up in the chemical reaction, the specific gravity of the electrolyte decreases, so the state of charge in the battery can be determined by measuring specific gravity of the electrolyte.

As the battery nears complete discharge, the plates are nearly completely coated with $PbSO_4$. The reaction can proceed only when four free hydrogen ions and one free sulfate ion all come together at an uncovered spot on the PbO_2 plate. From a probability standpoint, this becomes less likely to happen, and the chemical reaction must slow down. There is still a significant amount of energy that can be drawn out of the battery, but the energy must be drawn out slowly. Trying to drive the reaction too fast leads to $PbO \cdot PbSO_4$ and other interesting chemical compounds on the positive plate. Some of the chemical reactions are almost irreversible, and degrade the energy storage capacity of the battery by partially coating the plates.

When several battery cells are in series, as is the case for solar cars and nearly all battery power systems, there is always a "weakest" cell. The "weakest" cell is the one that has the lowest charge capacity. When the battery system (made up of several cells) is run to a low state of charge, the "stronger" cells will drive current through the "weakest" cell, and cause the positive plates in the "weakest" cell to be coated with $PbO \cdot PbSO_4$ compounds. This reduces the charge capacity of the "weakest" cell, making it weaker. Because the battery cells are in series, the charge capacity of the "weakest" cell is the charge capacity of the battery system. Batteries and battery systems often fail because one cell becomes sulfated out, as described here.

Deep-cycle lead-acid batteries have more positive plate area than negative plate area, because the chemical reaction on the positive plate is more complex. This makes the batteries more tolerant of being run to a low state of charge, but it is never a good idea to run the battery completely dead. There is always a "weakest" cell that will be damaged and reduce the charge capacity of the battery. The negative plates in the battery cells are not as much of a problem because the chemical reaction is less complex. Energy efficiency of the battery is best when the power is drawn out at a rate so that the chemistry can proceed according to the design.

If a battery becomes damaged by $PbO \cdot PbSO_4$ compounds forming on the positive plates, it can be rejuvenated to some extent. Charging the battery with a slow pulsating current will break up some of the compounds and get them back into solution. It will not be possible to break them all up, but this charging method can significantly increase the charge capacity of the batteries.

In the charging cycle, as the battery nears complete charge, hydrogen and oxygen ions must find the remaining $PbSO_4$ on the positive plate. This becomes unlikely, and charging must slow down toward the end to allow the chemistry to take place. Too much current going into the battery will cause the water to be broken into free hydrogen and oxygen, which is a dangerous situation. Some free hydrogen is always generated when charging the battery, so ventilation is required.

Lead-acid batteries have been studied more than any other battery chemistry, and there are some important empirical relationships that have been developed. Because the sulfate ions in the electrolyte are used up during the discharge chemical reaction, the specific gravity of the electrolyte decreases as the battery is discharged. The open-circuit voltage and state of charge vary with the specific gravity of the electrolyte. For open-celled batteries it is common to measure state of charge of the battery by measuring specific gravity of the electrolyte. Solar cars use sealed batteries, and it is not possible to access the electrolyte.

When the battery is discharged at a high rate, the surface of the plates get covered quickly with $PbSO_4$, which limits the depth of the plates participating in the reaction. This reduces the apparent charge capacity of the battery at the high rate. Most of the charge capacity can usually be recovered if the rate is reduced. The Peukert relationship of Eq. 11.8 was developed for the discharging of lead-acid batteries [11-4].

$$\text{Capacity} = \frac{C}{I^{(n-1)}} \tag{11.8}$$

where the capacity measured is the battery charge capacity (amp-hour capacity), I is the current, and C and n are constants. Also, n is the Peukert number,

and it is between 1.2 and 1.3 for deep-cycle lead-acid batteries that might be used for solar cars. A lower Peukert number indicates that the battery will have higher efficiency, so a lower Peukert number is desirable. The capacity at a given current draw also depends on temperature. Equation 11.9 is an empirical relationship that was developed for temperature variation of lead-acid batteries.

$$\text{Capacity} = C_{30}[1 + 0.008(T - 30)] \tag{11.9}$$

where C_{30} is the amp-hour capacity at 30°C and T is temperature of the battery (Celsius).

Electrolysis of Water. Electrons on the negative plate combine with H^+ in the electrolyte to make H_2. Oxygen ions give up electrons to the positive plate at the same time and form $O_2(2O^{-2} \rightarrow O_2 + 4e^-)$. This electrolysis of water is one way that the current appears to flow through the battery when too much current is used in charging the battery. An external meter will measure current going into the batteries and it will appear that the battery is being charged, but in reality what is happening is that water is being converted to hydrogen and oxygen and vented out of the box. Too much of this can deplete the electrolyte, "boiling it away."

Self-Discharge. Lead-acid batteries will self-discharge over time, and should always be trickle-charged when not in use. The self-discharge reactions on the plates are illustrated below.

1. *Positive Plates*

   a. *Oxygen Evolution.* The lead oxide on the plates gives up its oxygen atoms and combines with sulfate ions in the electrolyte to form $PbSO_4$ on the plates as illustrated in Eq. 11.10. Water and oxygen are released into the electrolyte solution.

$$PbO_2 + H_2SO_4 \rightarrow PbSO_4 + H_2O + \frac{1}{2}O_2 \tag{11.10}$$

b. *Oxidation of Organics X^R.* The material used in separating the plates usually contains polymers (organics) that can oxidize and gradually discharge the battery as illustrated in Eq. 11.11.

$$2PbO_2 + X^R + 2H_2SO_4 \rightarrow 2PbSO_4 + 2H_2O + CO_2 + X^0 \quad (11.11)$$

c. Corrosion of lead in the current collectors is illustrated in Eq. 11.12.

$$Pb + PbO_2 + 2H_2SO_4 + 2H_2O \rightarrow 2PbSO_4 + 2H_2O \quad (11.12)$$

d. Corrosion of alloying constituents in the current collector is illustrated in Eq. 11.13.

$$5PbO_2 + 2Sb + 6H_2SO_4 \rightarrow (SbO_2)SO_4 + 5PbSO_4 + 6H_2O \quad (11.13)$$

2. *Negative Plates*

a. *Hydrogen Evolution.* The hydrogen ions in the electrolyte collect electrons from the negative plates and bubble off as hydrogen gas, as illustrated in Eq. 11.14.

$$Pb + H_2SO_4 \rightarrow PbSO_4 + H_2 \quad (11.14)$$

b. Oxygen recombination is illustrated in Eq. 11.15.

$$Pb + H_2SO_4 + \frac{1}{2}O_2 \rightarrow PbSO_4 + H_2O \quad (11.15)$$

c. Antimony can dissolve into solution from the positive plates and diffuse to the negative plates where it enhances oxygen recombination.

D. Silver-Zinc Batteries

Silver-zinc batteries are a high-performance option for solar car racing. They have a high energy density. The disadvantages are that they are expensive

and have a short life. Some silver-zinc batteries can be charged and discharged only a few times before they are worn out. Silver-zinc batteries are extremely sensitive to overcharge and high charging rates. In general, they require more care and caution and are less forgiving of misuse than lead-acid batteries. When fully charged, the plates in the batteries are Zn and AgO, and the electrolyte is potassium hydroxide (KOH) dissolved in water. The reaction during discharge is shown in Eq. 11.16 [11-4, 11-6].

$$Zn + AgO + H_2O \rightarrow Zn(OH)_2 + Ag \quad (11.16)$$

The Zn plate is coated with $Zn(OH)_2$ and the AgO plate is coated with Ag. When the batteries are being charged, the reaction goes in the opposite direction. Open-circuit voltage of a fully charged battery cell is 1.86 V, but drawing significant current will drop the voltage to about 1.5 V. The KOH in the electrolyte does not appear in the chemical reaction, but is necessary for the reaction to proceed at a reasonable rate. Most of the $Zn(OH)_2$ comes from Zn combining with the OH^- available from the KOH electrolyte; only a small amount is available from decomposition of the H_2O. The K^+ ion is helpful in separating the AgO into Ag and K_2O, which then separates back into $2K^+ + O^{-2}$, and the oxygen ion finds two hydrogen ions (H^+) and makes water. The silver-zinc cell is illustrated in Fig. 11.4.

E. Nickel-Cadmium (NiCd) Batteries

Nickel-cadmium (NiCd) batteries have been used by a few solar car teams. They have slightly higher energy density than lead-acid batteries and are less expensive than silver-zinc batteries. Rechargeable batteries for many tools and toys are NiCd, so the batteries are available in many sizes. They are good, reliable batteries, but their energy efficiency is lower than that of lead-acid batteries, and overall performance is probably not as good as lead-acid batteries. NiCd batteries generate significant heat when discharging, and may require additional cooling or ventilation in the battery box to prevent them from overheating. The chemistry of NiCd batteries is illustrated in Fig. 11.5 [11-4, 11-6].

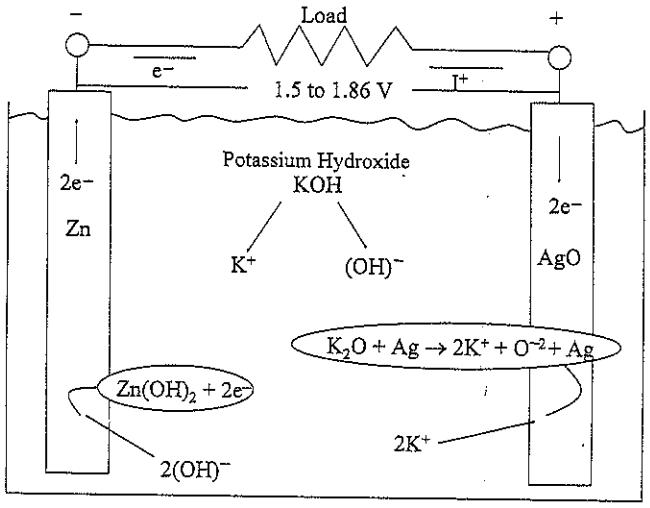

Fig. 11.4 Schematic of silver-zinc battery chemistry.

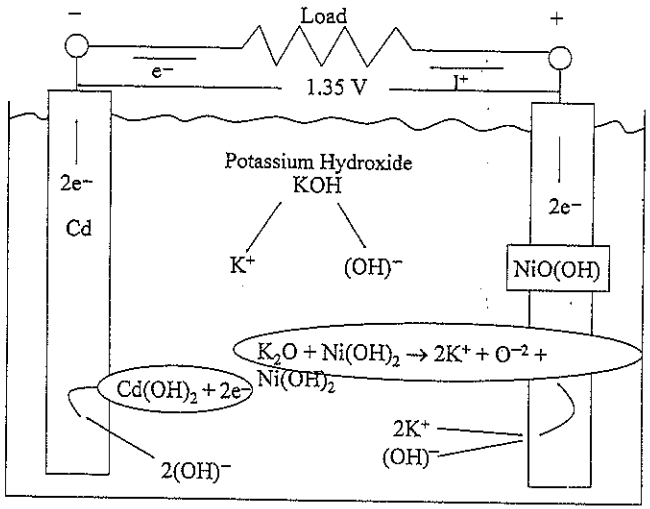

Fig. 11.5 Schematic of nickel-cadmium (NiCd) battery chemistry.

When fully charged, the plates in the batteries are Cd and NiO(OH), and the electrolyte is KOH dissolved in water. The reaction during discharge is shown in Eq. 11.17.

$$Cd + 2NiO(OH) + 2H_2O \rightarrow Cd(OH)_2 + 2Ni(OH)_2 \qquad (11.17)$$

The Cd plate is coated with $Cd(OH)_2$ and the NiO(OH) plate is coated with $Ni(OH)_2$. When the battery is being charged the reaction goes in the opposite direction. Operating voltage is approximately 1.35 V.

The KOH does not appear in the chemical reaction, but is necessary for the reaction to proceed at a reasonable rate. Most of the $Cd(OH)_2$ comes from Zn combining with the OH^- available from the KOH electrolyte. The K^+ ion is helpful in separating the oxygen O from the NiO(OH) so it can form $Ni(OH)_2$. The K_2O then separates back into $2K^+ + O^{-2}$, and the oxygen ion finds two hydrogen ions (H^+) and makes water.

F. Nickel-Hydrogen and Nickel-Metal-Hydride (NMH) Batteries

The plates in these batteries are NiO(OH) and hydrogen gas. Because it is not possible to make a plate out of a gas, the NMH battery is the most common one of this type where the hydrogen is stored as a metal hydride on the negative plates. The battery chemistry is illustrated in Fig. 11.6 [11-4, 11-6].

Negative Plates. The catalyst on the electrode assists with the chemical reaction. The hydrogen combines with hydroxides in the electrolyte and forms water and two free electrons as shown in Eq. 11.18.

$$H_2 + 2(OH^-) \rightarrow 2H_2O + 2e^- \qquad (11.18)$$

Positive Plates. The potassium ions help strip the oxygen out of the nickel-oxy-hydroxide, forming potassium oxide as an intermediate step. The potassium oxide then dissolves back into the electrolyte solution. The nickel then combines with two hydroxides to form nickel hydroxide. The chemical reaction is illustrated in Eq. 11.19.

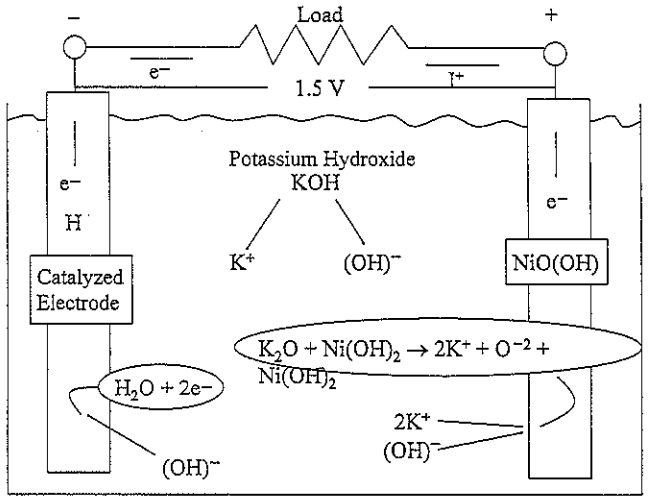

Fig. 11.6 Schematic of nickel-hydrogen battery chemistry.

$$2NiO(OH) + 2OH^- + 4K^+ + 2e^- + 4H^+ \rightarrow 2Ni(OH)_2 + 2K_2O + 4H^+ \rightarrow 2Ni(OH)_2 + 4K^+ + 2O^{-2} + 4H^+ \rightarrow 2Ni(OH)_2 + 4K^+ + 2H_2O \quad (11.19)$$

The chemical reaction on the positive plates is complex. Care must be taken when charging and discharging the batteries or the positive plates will be coated with compounds that are difficult, if not impossible, to remove. The net chemical reaction for NMH batteries is shown in Eq. 11.20.

$$2NiO(OH) + H_2 \rightarrow 2Ni(OH)_2 \quad (11.20)$$

G. Lithium-Ion and Lithium-Polymer Batteries

Lithium-ion and lithium-polymer batteries have the highest energy efficiency and the highest specific energy of all the batteries currently being used in solar car racing. They are different from the other batteries discussed because

they use an organic electrolyte, and current passes by transporting lithium ions between the positive and negative plates. The chemistry of these batteries is illustrated in Fig. 11.7 [11-4].

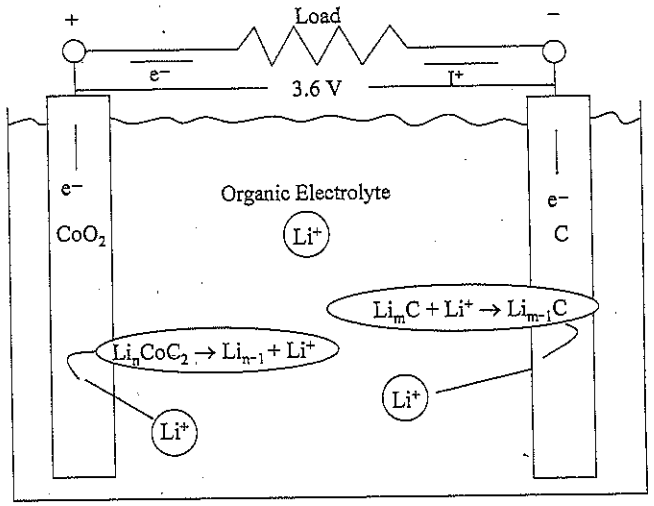

Fig. 11.7 Schematic of lithium-ion battery chemistry.

Lithium is a lightweight element, number 3 on the periodic table. Experimental lithium batteries have existed for many years because of the potential of developing a battery with a high energy density. The main problem has been that metallic lithium is extremely explosive and unsafe. The first breakthroughs were in 1976 and 1978 with the intercalation of lithium into titanium sulfide [11-7]. The battery chemistry that was developed is shown in Eq. 11.21.

$$xLi^+ + TiS_2 + xe^- \leftrightarrow Li_xTiS_2 \quad (11.21)$$

The intercalation of lithium did not significantly change the crystal structure of the titanium sulfide; it just changed the lattice parameter. Intercalation was rapid and reversible. Other materials were developed for intercalation

of lithium, but the problem of a pure lithium metal, negative electrode remained and the battery was never used commercially.

The breakthrough that made the commercial lithium battery possible was the discovery of intercalation of lithium ions into carbon, up to an amount LiC_6 [11-4]. The negative electrode could then be made of carbon, and the positive electrode made of a mix of cobalt oxide, nickel oxide, and manganese oxide, commonly referred to as a metal oxide electrode. Using the symbol MO_2 to represent a metal oxide on the positive terminal, the chemical reaction for the battery is shown in Eq. 11.22.

$$Li_xMO_2 + 6C \leftrightarrow Li_{(1-x)}MO_2 + LiC_6 \qquad (11.22)$$

Manganese oxide is the least expensive metal oxide to use for the positive electrode, but it is also the heaviest and yields the lowest energy density. Nickel oxide is the second least expensive and yields the highest energy density. Cobalt oxide is the most expensive of the three metals that can be used for the positive electrode and yields the second highest energy density. Cobalt oxide is used for the example in Fig. 11.7 because it was used in the earliest lithium-ion batteries.

The metal oxides all become chemically unstable at temperatures above 100°C, liberating oxygen and forming undesirable compounds. Careful voltage control is necessary when charging the battery to prevent damaging the positive electrode.

H. Charge-Discharge Curves

Figure 11.8 shows a typical charge-discharge curve for a battery being charged and discharged at a C/3 rate. (The C rating indicates the rate at which the battery is charged and discharged so that C/3 indicates that the charge is drawn out in 3 h.) C ratings are somewhat misleading because the battery has a maximum voltage for charging and a minimum voltage for discharging.

In Fig. 11.8, the battery is charged at a C/3 rate until the maximum allowable charge voltage is reached, and then the charging rate is cut in half. Charging continues until the maximum charge voltage is reached and then the charging

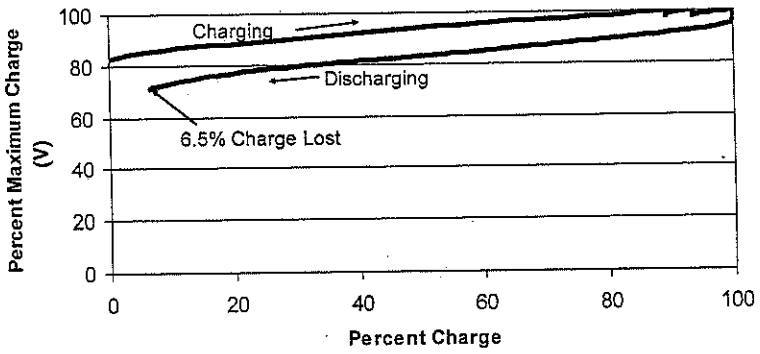

Fig. 11.8 Typical battery charge-discharge curve.

rate is cut in half again (to one-quarter of the original C/3 rate). Charging continues until the maximum charge voltage is reached for the third time, and then the charge portion of the cycle is complete. The battery is discharged at the C/3 rate until the minimum discharge voltage is reached for the discharge portion of the cycle.

When testing, the charge-discharge cycle shown here is repeated several times. Data for the first couple of tests are usually a bit erratic as they depend on the initial state of charge in the batteries. As a result, the data for the first couple of cycles are not very useful in analyzing the battery. Starting at about the third cycle, the data will become repeatable and more useful. Figure 11.8 is representative of what a typical battery would do after several cycles.

One point on Fig. 11.8 is labeled "6.5% Charge Lost." As this battery was cycled, it took 6.5% more to charge the battery than was returned when the battery was discharged. The "lost" charge can be caused by internal leakage (shorting within the battery) or electrolysis of the electrolyte. The charge efficiency for this battery is 93.5%, which is typical for well-designed lead-acid, silver-zinc, and NMH batteries with water-based electrolyte. Batteries with polymer-based electrolyte, such as lithium-ion or lithium-polymer batteries, can have charge efficiencies above 99%. Poorly designed batteries

may have a lower charge efficiency, but such batteries would not be used in solar car racing.

In Fig. 11.8, the area under the "charging" curve represents the energy required to charge the batteries. The area under the "discharging" curve represents the energy that the battery will deliver when discharged. Because batteries are charged at a higher voltage and discharged at a lower voltage, the energy efficiency of the battery is considerably lower than the charge efficiency. The energy efficiency of this battery is 83.9%, which is typical for well-designed lead-acid batteries. NMH batteries are typically 10% less energy efficient than lead-acid batteries. Lithium-ion and lithium-polymer batteries can have energy efficiencies above 90% when discharged at a C/3 rate.

The energy efficiency of the battery increases when it is charged and discharged at a slower rate, and decreases when the charge and discharge rates are increased. Charge efficiency increases slightly when the battery is charged and discharged at a slower rate. It is difficult to draw charts to illustrate the effect of charge rate on the batteries. If the battery is discharged from a fully charged state at a C/1 rate, it will reach its minimum allowable voltage with fewer amp-hours drawn out of the battery than if the discharge rate is C/3. The capacity is reduced and the energy efficiency is reduced. If the battery is discharged at a C/8 rate, it will deliver more amp-hours before reaching its minimum allowable voltage than at the C/3 rate. The usable capacity, charge efficiency, and energy efficiency of the battery all vary with charge-discharge rate. Charging and discharging at a slower rate is best for the batteries, but may not always be the best strategy for racing.

I. Battery Modeling

The capacity and efficiency of batteries are dependent on the rate at which they are charged and discharged, along with many other variables specific to the battery chemistry. Batteries are extremely important in solar car racing, and it is important to include a reasonably accurate model for the batteries in the power management model. The Peukert equation is the most respected approach to modeling battery capacity. This equation was developed for lead-acid batteries, and has been applied with reasonable success to other battery chemistries. It must be stressed that the Peukert equation is empirical, is for discharge only, and is only accurate over a range of currents. In

particular it is not accurate for small currents, recognizing that the definition of what constitutes small currents depends on the size and design of the battery system.

The goal is to develop a relationship between the energy capacity of the battery system (watt-hours) and the rate (in watts) at which power is being drawn out of the batteries. Because the battery voltage is approximately constant, the Peukert equation can be modified to yield a relationship between the capacity and the power P as shown in Eq. 11.23.

$$\text{Capacity} = \frac{C}{P^{(n-1)}} \tag{11.23}$$

To solve for the constants n and C, it is necessary to measure the capacity for different discharge rates and then perform a least-squares fit on the data. Unfortunately, it is difficult to perform constant power rate testing. Testing is generally done at a constant current rate. The voltage decreases during the test, so the power rate is not exactly constant, but it is approximately constant. This is an approximate model, and it is acceptable to use the data from a constant current test as if it were a constant power test. There is probably very little to be gained in developing equipment to perform constant power rate testing. The following example illustrates the process used in developing the Peukert model.

Example. Assume that a lead-acid battery being tested has a nominal charge capacity of 60 A-h. It is cycled a few times and then trickle-charged to full capacity. The battery is then discharged at a rate of 20 A (C/3 discharge) until it reaches the minimum allowable voltage of 10.5 V. (The battery would deliver about 56 A-h at this rate.) Integrating the data, it is found that the battery provided 630 W-h of energy during the discharge cycle. It is assumed that the battery has a capacity of 630 W-h at a power draw of 210 W.

Assume that the same battery is tested at a current draw of 10 A (C/6) and that it delivers 708 W-h of energy at this rate. It would be assumed that the battery capacity is 708 W-h at a power draw of 118 W. Also assume that the battery is tested at a power draw of 60 A (C/1) and that it delivers 515 W-h of energy at this rate. It is assumed that the battery delivers 515 W-h at a power

draw of 515 W. A least-squares approach can be used to determine values for the constants in the battery model equation for this battery, yielding Eq. 11.24.

$$\text{Capacity} = \frac{1930}{P^{(1.21-1)}}\ \text{W-h} \tag{11.24}$$

The Peukert number for this battery is 1.21 and the other constant in the Peukert equation is 1930. Equation 11.24 is useful for estimating the battery capacity for different power draws on the battery. The equation is not accurate for extremely low power draws. As an example, assume that the power is drawn out at 1 W (a very low power draw for this battery). The equation predicts 1930 W-h of energy in the battery, but the battery will not really provide that much energy. It is impossible to make the Peukert equation accurate for extremely low power draws and for the more typical power draws in solar car racing. The equation is accurate only over a range of values, and should be fitted to a range of data typical for the energy a solar car would draw when racing.

J. Battery Pack Modeling

A battery pack is usually made of more than one battery. If two batteries are used instead of one, each battery will deliver only half as much power for the same total power draw. Reducing the power draw increases the capacity of the individual batteries, so there is more than a twofold increase in battery capacity by doubling the size of the battery pack.

This phenomenon is consistent with the model developed. Assume that individual batteries follow the Peukert equation. If a battery pack contains m batteries, and the power is drawn out at mP, then the capacity of the pack would be increased by a factor of m, because each battery would be providing a power of P. Eqs. 11.25 and 11.26 apply in developing a model for using m batteries in a battery pack.

$$\text{Capacity} = \frac{C}{P^{(n-1)}} \tag{11.25}$$

$$\text{m(Capacity)} = \frac{C'}{(mP)^{(n'-1)}} \tag{11.26}$$

where n and C are the constants that go with the individual batteries and n′ and C′ are the constants that go with the battery pack. These equations can be satisfied only when Eqs. 11.27 and 11.28 are satisfied.

$$C' = mC \tag{11.27}$$

$$n' = n - (n-1)\frac{\text{Ln}(m)}{\text{Ln}(mP)} \tag{11.28}$$

The significance of writing the equations this way is that the Peukert number of the battery pack is less than that of the individual batteries. The other constant is simply m times the constant for one battery, which is to be expected, but by increasing the size of the battery pack the effective Peukert number is reduced. This means that for any power draw P, the battery pack will have more than m times as much capacity than if the power P is drawn out of a single battery. It also means that the battery pack will operate at a higher efficiency than a single battery for the same power draw. The following example illustrates the effect.

Example. Suppose that seven lead-acid batteries of the type used in the example above (n = 1.21 and C = 1930) are put together to make a battery pack. The battery pack will need to deliver between 300 and 2000 W power during the race. Plot the battery capacity as a function of power.

One way to estimate the capacity of the battery pack (the wrong way) would be to find the capacity on one battery over the range of 300–2000 W power draw, and multiply by 7 because there are seven batteries in the pack. This method underestimates the energy capacity of the battery pack. Equations 11.27 and 11.28 should be used to get the correct constants for the battery pack. The comparison between simply multiplying the capacity of one battery by 7 and calculating the correct capacity for the battery pack is shown in Fig. 11.9.

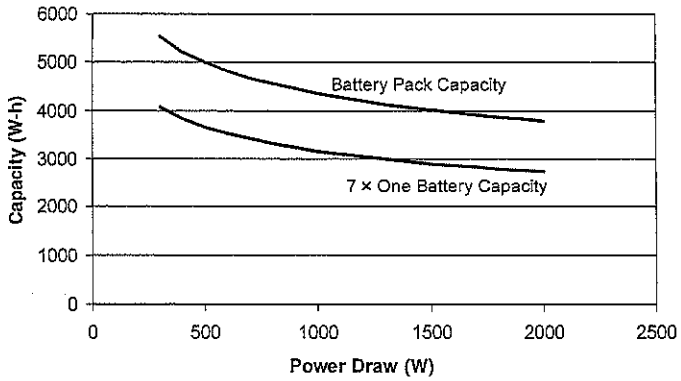

Fig. 11.9 Battery pack capacity vs. individual battery capacity.

Homework. Assume that a battery pack consisting of nine lithium-ion cells in parallel was tested. The pack provides 62 W-h energy at a power of 20 W, 67 W-h at a power of 8 W, and 58 W-h at a power of 58 W.

1. Find the Peukert equation describing the battery performance.

2. If the nine-cell pack weighs 400 g and each cell operates at a nominal voltage of 3.7, design a battery pack that operates at nominally 100 V and weighs 30 kg or less.

3. What equation would be used for the capacity of the battery pack?

4. Plot capacity versus power from 300 to 2000 W.

The slope of the curve for the lithium-ion pack in the homework problem is much lower than that for the lead-acid pack. This means that the lithium-ion pack will deliver more energy at high power draws, which is a desirable characteristic. On sunny days the car can be driven at high speeds up and down hills with little regard for the batteries. The lithium-ion pack is usually the better choice on a sunny day. It is often overlooked that the lead-acid pack will deliver more energy at low power draws, as might be the case for a

cloudy, rainy day. If the two battery packs have the same capacity when the power is drawn out at a C/3 rate, the lead-acid pack will deliver more energy at lower power draws and the lithium-ion will deliver more energy at higher power draws. Lead-acid batteries are much heavier, and it is difficult to imagine a case when it would be better to use lead-acid batteries than lithium-ion batteries, but there are cases where lead-acid batteries will deliver more energy. The power management models should be used to determine which battery pack is best for the car.

K. Wiring of the Battery Box

As the car travels down the road the batteries will consume some energy because of resistance in the wires and the connections on the battery terminals. These are commonly referred to as i^2R losses. A typical car draws about 20 A from the battery on average, with spikes of 80 A for climbing hills on a sunny day. A total resistance of 1 Ω would cause a power loss of 400 W for a 20-A current and 6400 W for an 80-A current. Clearly, the resistance in the main power bus must be extremely low. An example of a typical main power bus is shown in Fig. 11.10.

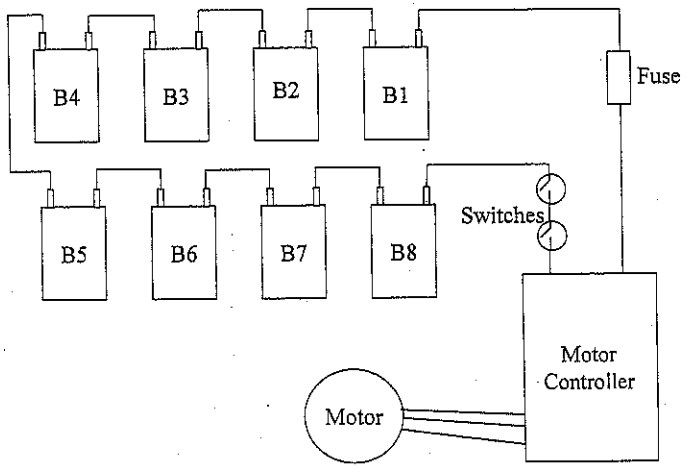

Fig. 11.10 Main power bus.

The main power bus includes the batteries, the two switches required by race rules, and the motor and motor controller. High currents exist in all of these wires and connections. There is a minimum of two connections per battery, a fuse, four switch connections, two switches, five motor controller connections, three motor connections, internal resistance in the motor and controller, and the wire connecting everything together.

If the goal is to limit total loss to less than 10 W at 80 A, the total resistance of all the wires and connections must be less than 0.0015625 Ω = 1.56 mΩ. *One corroded connection could have this much resistance.* Although 1 mΩ of resistance is a lot for any wire, connection, or switch, there are many connections. Cleaning the battery terminals, sizing the wires, and ensuring that all the connections are good are important.

L. Battery Safety

The batteries must be tied down securely to the frame, or encased in the battery box so they will be contained in the event of an accident. The main concerns are holding the batteries down so they do not become projectiles, and containing battery electrolyte should the batteries break open or leak.

For most batteries there will be some electrolysis of water during charging of the batteries, which releases hydrogen and oxygen gases into the battery box. There must be a vent fan and ventilation system to constantly push the hydrogen out into the atmosphere. Buildup of hydrogen in the battery box could cause an explosion.

A fuse is required to prevent the battery from generating excessive current. The fuse must burn out at a safe current and yet have essentially zero resistance for the current that the car will use.

M. References

11-1. Roche, D.M., A.E.T. Schinckel, J.W.V. Storey, C.P. Humphris, and M.R. Guelden, *Speed of Light: The 1996 World Solar Challenge*, chap. 8, Photovoltaics Special Research Center, University of New South Wales, Sydney, Australia, 1997.

11-2. Storey, J.W.V., A.E.T. Schinckel, and C.R. Kyle, *Solar Racing Cars*, chap. 8, Australian Government Publishing Service, Canberra, Australia, 1994.

11-3. Kyle, C.R., *Racing with the Sun: The 1990 World Solar Challenge*, chap. 8, Society of Automotive Engineers, Warrendale, PA, 1991.

11-4. Rand, D.A.J., R. Woods, and R.M. Dell, *Batteries for Electric Vehicles*, Research Studies Press Ltd., Taunton, U.K., 1998.

11-5. Bogner, S., N. Chorneau, and D. Pickett, *GM Sunraycer Case History Lecture 3-4: Design and Performance of the GM Sunraycer Battery*, Society of Automotive Engineers, Warrendale, PA, 1992.

11-6. Besenhard, J.O. [ed.], *Handbook of Battery Materials*, Wiley-VCH, Weinheim, Germany, 1999.

11-7. Whittingham, M.S., "Intercalation of Lithium into TiS_2," *Prog. Solid State Chem.*, vol. 12, pp. 41–99, 1978.

Chapter 12

Electrical Systems

A. Introduction

The electronics field changes rapidly, and the best electronic components at the time of this writing will not be the best components in the future. Some aspects of the electrical systems do not change as rapidly, and these are the focus of this chapter. Wires, connectors, and fuses must be sized to minimize the electrical losses, and there are safety concerns in any electrical system design.

The driver must be isolated from high voltage to avoid any chance of electrocution. To be conservative, anything above 24 V should be treated as high voltage. Driver controls should all be low-voltage controls that activate a metal oxide semiconductor field effect transistor (MOSFET) or other relay-type device outside the driver compartment to control the higher-power system voltage. Connectors should be covered to prevent shock hazards when working on the car. If possible, the batteries and array should be disconnected when working on the car. One hundred volts from a typical power system is lethal, and some common sense is required to avoid injury.

B. Wiring Diagram

A typical schematic of the wiring of the car is shown in Fig. 12.1. This is not a detailed wiring diagram. There are separate wiring diagrams showing the designs of the motor controller, driver-user interface (DUI), power point trackers, dc–dc converters, turn signals, and motor blower controller. The diagram in Fig. 12.1 shows the overall layout of a typical car.

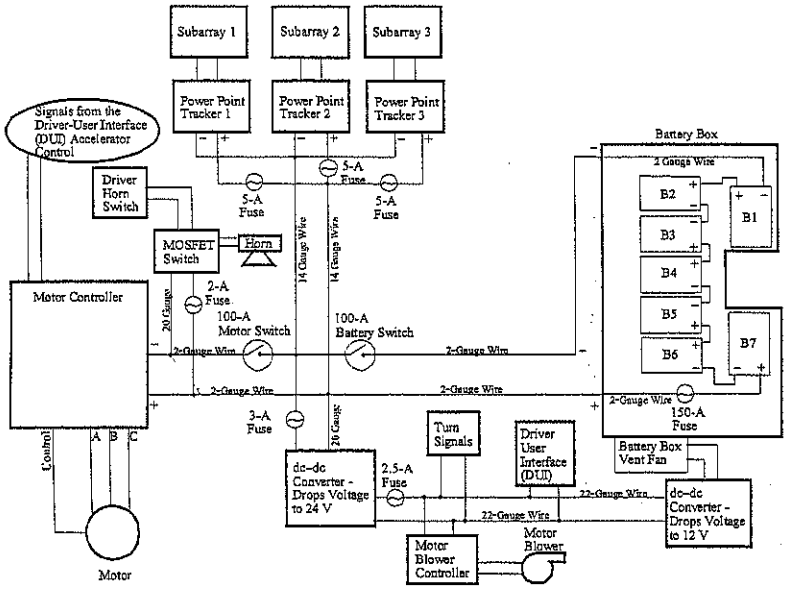

Fig. 12.1 Typical wiring diagram.

The "main power bus" wires are the 2-gauge wires that run from the battery box to the motor controller. Power flows from the batteries to the motor down these wires. There are two 100-A switches in the wires: the motor switch and the battery switch. Power from the array comes in between the two switches. Two switches must be included for safety reasons. If both switches are opened, there is no way for power to flow, and the car is "off." For safety reasons the car must be off and no electric power should flow when the main power switches are off. Most race rules require that the car be off when the main power switches are thrown, so this is in most cases a race rule in addition to a safety rule.

Toggle switches are typically used for the main power switches, and there is a small power loss associated with the switches. Probably every electrical engineer designing such a system has spent some time trying to figure out how to get by with one switch and reduce the power loss. But with power

coming from two sources, the battery pack and the array, there appears to be no way to do this.

At night both switches are opened to turn the car off. If the switches were left closed, the battery pack would drive some small current through the array and/or through the motor controller or accessories and deplete the power in the batteries. There are diodes to prevent this from happening, but diodes allow a small reverse current, so there is some power loss. An open switch allows no current and is the best solution.

When the car is stopped during the day, the motor switch is open (off) and the battery switch is closed (on). This is the configuration for charging the batteries off the array. In this configuration, no power can flow to the motor controller or the horn system. This provides a level of safety because while the car is sitting and the batteries are being charged, it is not possible to inadvertently start the car moving. The battery vent fan must be running anytime the batteries are being charged to vent the hydrogen gas created when charging, so the battery box will not explode. This is important. The batteries probably create more hydrogen gas when being charged off the array than when the car is being driven down the road. The power converters that provide power to the battery box vent fan must be connected between the two main power switches so that it is powered when the car is being charged.

When both main power switches are closed (on), power is available to all components and the car can be driven. The only subsystem that must be active when the car is stopped is the battery box vent fan. Everything else can be hooked in to the left of the motor switch, and be taken completely out of the circuit when the car is stopped and the batteries are being charged. Note that technically, with the array providing power and both main power switches open (off), power is being provided to the dc–dc converter, and the motor blower, turn signals, DUI, and battery box vent fan can still operate. This appears to technically violate the race rule that the main power switches must turn everything off. However, inspectors have been willing to allow this type of configuration provided there is a separate switch in the dc–dc converter, and that the team has a policy of always disconnecting the array umbilical cord when turning the switches off. Most teams use a similar configuration.

The problem is that a race rule requires that the battery fan must be running anytime power is going into or out of the batteries. This is necessary for safety and is a good and important rule. The fan could be wired directly to the batteries so that it runs all the time, day and night, which would satisfy the rule. But from a strategy and energy management point of view, it is desirable to turn the fan off at night so it does not continue to drain the batteries. There is no reason to run the fan at night, so there must be a switch somewhere to turn the fan off. If the switch were to be placed on the fan, the team members would forget to turn it on in the mornings and this would lead to a safety problem. Inspectors are not willing to accept a switch on the fan; the switch that turns off the fan must also turn off any power going into or out of the batteries at the same time.

A third main power switch can be installed to isolate the array power, and this would satisfy the rule that the car must be completely off under all circumstances. Shock hazards would still be presented by the wires coming out of the battery box and the array umbilical wires. It is not possible to completely eliminate shock hazards. It is unacceptable to have power going to the motor when the car body is on the array stand charging the batteries in the morning and evening. The car could be started inadvertently and cause damage or injury. Providing power to the other systems increases the shock hazard to some extent, but is probably an acceptable risk.

C. Fuses

Fuses should be used to prevent too much current from flowing and burning up the wiring or components. They represent an added level of safety. Fuses should be properly sized for the current flowing through the wires. The fuses shown in the schematic (Fig. 12.1) are the minimum required. Many of the subsystems will have additional fuses built in to protect them. Fuses serve two purposes:

1. They prevent a short circuit from overheating the wiring and causing a fire (safety feature).

2. They protect expensive electronic components, keeping them from being damaged by too much current.

Putting a fuse in the wire absorbs a small amount of power, so fuses should not be used without a reason. In general, a fuse with a higher amperage rating absorbs less power than one with a lower amperage rating because the higher-amperage fuse has a lower electrical resistance. The fuses must be properly sized. Putting a 10-A fuse in a wire that can only safely carry 5 A does not make sense. The fuse must trip before damage occurs or a fire starts, but a large power loss at the fuse is not desirable. If possible, the fuses should be soldered in place to reduce the resistance at the connections, but this makes them harder to replace.

D. Wire Sizing

Thicker, lower-gauge wire is designed to carry more current than thinner, higher-gauge wire. The thicker the wire, the lower the electrical resistance, and thus the lower the power loss in the wire. Electrical losses can be minimized by using heavy copper wire for all wiring, but this makes the car very heavy. Copper has a higher specific gravity than steel, and it does not take a lot of thick copper wire to add a significant amount of weight to the car. Power lost is commonly referred to as i^2R loss.

The resistance in a wire is linearly proportional to its length, so the wires should be made as short as practical to minimize i^2R losses. Resistance is also proportional to the cross-sectional area of the wire. A larger-diameter wire will have lower resistance, but the weight increases with cross-sectional area too. There is an optimal wire diameter designed to carry a given current. The power lost in the wiring should be small. It cannot be eliminated; it can only be made small. As a target value or goal, it would be reasonable to decide that the main wires in the diagram could absorb 1 W of power for the maximum rated current. For the 100-A main power bus the resistance of the wire selected should be 0.0001 Ω or less. For the 2-A dc–dc converter the wire should have a resistance of 0.25 Ω or less.

This is the kind of logic that must be used throughout the electrical system design. Most of the parasitic power lost is lost due to i^2R losses. A car will lose about 30 W in a well-designed system, which comprises about 100 wires, switches, connectors, and fuses. So as a general "rule of thumb" it is necessary to keep the power losses below 1 W for each electrical component. The

designer should never deliberately increase the power loss, so some common sense must be applied with the "rule of thumb" mentioned above. Power losses less than 0.01 W are probably insignificant. Table 12.1 shows suggested wire sizes for given currents. It is important to recognize that these are general guidelines, and there can be good reasons for an exception.

TABLE 12.1
SUGGESTED CURRENT LIMITS FOR WIRE SIZES

Wire Gauge Size	Copper Single	Copper Bundled	Wire Gauge Size	Copper Single	Copper Bundled
0000	380 A	225 A	16	22 A	5 A
000	328 A	200 A	18	16 A	10 A
00	283 A	175 A	20	11 A	7.5 A
0	245 A	150 A	22	9 A	5 A
1	211 A	125 A	24	NR	NR
2	181 A	100 A	26	NR	NR
4	135 A	80 A	28	NR	NR
6	101 A	60 A	30	NR	NR
8	73 A	46 A			
10	55 A	33 A			
12	41 A	23 A			
14	32 A	17 A			

NR = Not Rated. Suitable only for very small currents such as sensor wires.

E. Connectors and Switches

If the wires are sized properly, the connectors and switches will probably be the largest i^2R loss in the system. There are many ways to make connections from wire to wire or wire to component, and no single method works for all of them. The goal is to use a connector with as low a resistance as practical.

1. *Solder Connections.* Soldered connections have the lowest resistance. The resistance of a good soldered connection is almost zero. The

disadvantage of a soldered connection is that it cannot be easily taken apart and reassembled. Soldered connections are the lowest power loss choice, and should be used except where there is a compelling reason to be able to easily connect and disconnect.

2. *Bolted Connections.* The larger-amperage connections are usually bolted together. The bolt provides leverage so that the surfaces can be clamped together very tightly. Clamping the surfaces together tightly and having lots of area of contact tends to reduce the resistance of the connection, as illustrated in Fig. 12.2. Bolted connections have more resistance than soldered connections, but less resistance than crimp connections.

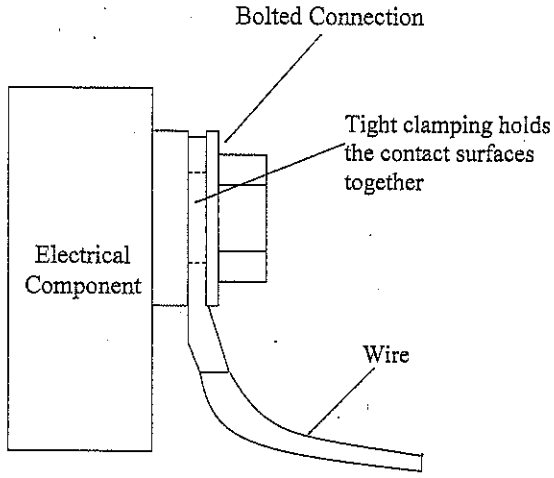

Fig. 12.2 Bolted connection.

3. *Crimp Connections.* Crimp connections come in many styles. A wall outlet is an example of a crimp connection. The advantage of a crimp connection is that it is easy to take apart and reassembled. As the connector slides together, the crimping action between the pieces causes a fairly tight contact between the contact surfaces. The wires should be soldered to the two pieces to minimize resistance in the connection. A common spade connector is illustrated in Fig. 12.3.

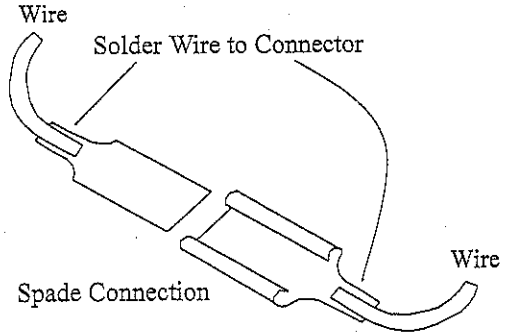

Fig. 12.3 Crimped connection.

4. *Mechanical Switches.* A mechanical switch has about the same resistance as a crimp connection. It could be a little more or a little less depending on the design. If the wires are soldered to the switch connections, there is little difference between the resistance in a switch and a crimp connector.

5. *General Connection Design.* Electrons flowing through the wires and connectors are analogous to fluid flow. The connectors should not restrict the flow of electrons. Make sure that the cross-sectional areas the current must flow through when going through the connectors are at least as large as the cross-sectional area of the wire, as illustrated in Fig. 12.4.

F. Electrical Subsystems

1. *Motor Controller.* The motor controller provides the interface between the main power system and the motor. To achieve a high-efficiency design, the motor controller must be matched with the motor. The team will probably not design their own motor controller, but will need to learn how to optimize the performance of the one purchased. Use the technical information from the manufacturer and also experiment with the motor and controller to see what works best.

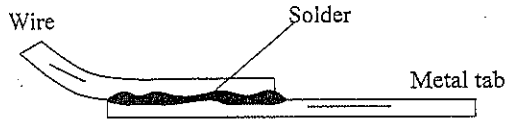

Make sure the path through the solder is larger than the wire. It should be larger because the solder will have more resistance per sectional area.

Fig. 12.4 General connector design.

2. *Array and Power Point Trackers.* These take the solar energy and convert it to electrical power at the system voltage. Operation of these subsystems was covered in Chapter 4 on solar arrays.

3. *Horn System.* Design of this system depends on the operating voltage of the horn. For the system shown schematically in Fig. 12.5, the horn was

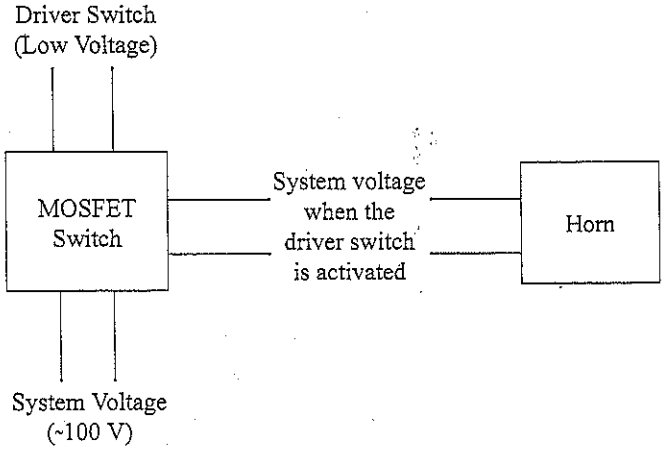

Fig. 12.5 Schematic of horn system.

designed to operate at the main power system voltage. For safety (shock hazard), any wires carrying system voltage should not be in the cockpit near the driver. A MOSFET electronic switch was used in this design to power the horns. The driver pushes a low-voltage switch that activates the MOSFET, which in turn activates the horn.

4. *dc to dc Converter.* Most of the electronic subsystems on the car operate at a voltage lower than system voltage, so a dc–dc power converter is needed to provide the lower voltage. System voltage may vary between 70 and 105 V, depending on the state of charge of the batteries and the power draw. The dc–dc converter illustrated schematically in Fig. 12.6 is a step-down transformer that converts system voltage to a fairly constant 24 V to power the other subsystems.

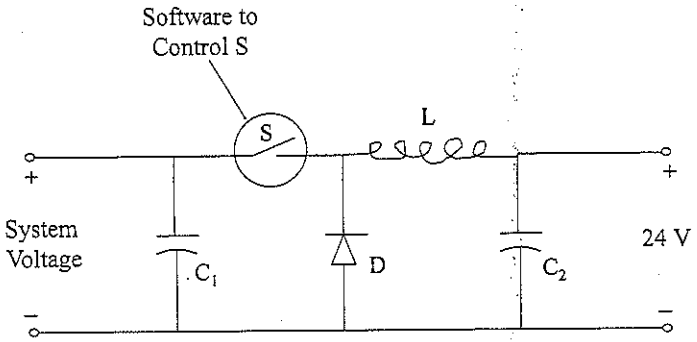

Fig. 12.6 dc–dc converter.

The switch is controlled by software to regulate the voltage to 24 V. It is important that this power converter be a high-efficiency design.

a. When the switch S is closed, the full battery voltage is applied, pushing current through the inductor L and into the 24-V power system. The voltage across the 24-V power system increases.

b. When the voltage across the 24-V system is getting too high, the switch S opens, disconnecting from the batteries. Current will continue to flow up through the diode D as the inductor L and capacitor C_2 both push current into the 24-V system. The voltage decreases as the capacitor and inductor discharge. Capacitor C_1 is charged up during this part of the cycle.

c. As the voltage to the 24-V system goes down slightly below 24 V, the switch S is closed again, and the batteries and capacitor C_1 push current through the inductor and into the 24-V system. Current through the diode D ceases and capacitor C_2 is charged up during this part of the cycle.

The cycle described above repeats. The software takes readings from sensors measuring the voltage of the 24-V system. The opening and closing of switch S (MOSFET switch) causes a ripple in the voltage, so the voltage is not a constant 24 V, but oscillates from slightly above that figure to slightly below it. This ripple must be controlled so that it is acceptable for the car's electronic components.

The primary power loss mechanisms in the dc–dc converters are resistive losses primarily in the inductor, switching losses in the MOSFET switch S (a MOSFET is a very energy-efficient switch), capacitive losses as the capacitors are charged and discharged, and the energy to forward-bias the diode. The diode is the largest energy loss, but all of these are significant.

All power flows through the inductor, so all that can be done is to choose as low a resistance inductor (and other wiring) as practical to minimize the i^2R losses. The switching, capacitive, and diode losses occur each time the switch is opened and closed, so operating at a slower frequency is desirable. The switching frequency goes up as system voltage becomes larger than 24 V; that is, if the system voltage is slightly higher than 24 V, the switching frequency is low. If the system voltage is much higher than 24 V, the switching frequency must be higher. The switching frequency can be reduced by allowing a larger "ripple" in the voltage too. The more precisely we try to control the voltage, the faster the converter must switch, which reduces its efficiency.

5. *Turn Signals and Brake Lights.* The lights for the turn signals and brake lights can use a lot of power. An important part of this system is using low-power lights [light-emitting diode (LED) type] for turn signals and brake lights. As the lights blink for turn signals, front and rear lights should alternate so that power is drawn at a more constant rate. Blinking the front and rear lights at the same time causes a larger power draw. The driver's switch must be integrated into the design so that the driver can turn the turn signals and brake lights on and off.

   The brake lights must come on when the driver hits the brakes, when the driver releases his or her foot from the dead man switch, and when the motor kicks into regenerative braking mode. Ultimately, a microprocessor, digital signal processor (DSP), or computer will probably be used to take signals from the driver and motor controller and decide how to light the lights on the front and rear of the car. This seems simpler than it is because most people use turn signals and brake lights every day, but the system of logic involved is actually rather complex. It takes a carefully designed program to take all the inputs and logically reason out what the lights should do.

6. *Motor Blower Control.* It is possible that the motor selected for the car will need a cooling fan to keep it from overheating. Some of the motors used in solar car racing require a cooling fan and some do not. If a cooling fan is required, a logic circuit system must be developed to take input from the motor thermocouple and provide the required air flow to cool it. Too little airflow will allow the motor to overheat. The motor operates less efficiently when hot, and will shut down completely if it gets too hot. Providing too much airflow wastes energy in the blower, but it is best to err on the side of too much airflow. It is frustrating to have the motor shut down or fail during the race because of overheating. A separate microprocessor could be used to control the motor blower, or it could be controlled by a central DSP or computer.

7. *Driver-User Interface.* The DUI is the interface the driver uses to control speed and acceleration of the car. A trained driver can operate the car in a more efficient manner than a computer because the driver can see what is going on around the car and anticipate when to accelerate and decelerate. It is important to allow the driver to control the throttle. A

simple potentiometer can be used on most motor controllers, and this is probably the best solution. Computer systems have been designed to limit the acceleration of the driver, or provide a buffer between the driver and the motor controller, but these systems do not seem to improve the efficiency of the car.

8. *Battery Box Vent Fan.* This fan must be on anytime the battery switch is on, which means it is only off at night. A very low-power fan is desirable. At the time this chapter was written the most efficient fan that could be found operated at 12 V. A separate dc–dc converter was used to step the power down from 24 to 12 V to take advantage of the increased efficiency of the fan, as shown on the general schematic of the car. Even small power savings are worth considering for the vent fan because it runs continually.

Index

Page numbers followed by *f* or *t* refer to figures or tables, respectively.

About the Author

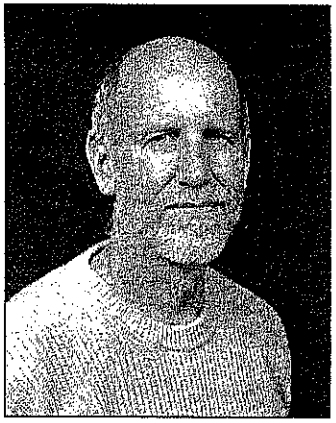

Dr. Douglas R. Carroll received his B.S. degree from Southwest Missouri State University in 1980 and his M.S. degree from Texas A&M University in 1982. He worked for the U.S. Air Force for six years at Tinker AFB and then returned to college and earned his Ph.D. degree from the University of Missouri–Rolla in 1991.

After graduation, Dr. Carroll accepted a faculty position in the Basic Engineering Department at the University of Missouri–Rolla and almost immediately began working with the solar car team in designing its first solar car. Designing the first few cars was difficult, and the cars were not very competitive in the races.

The designs improved with time and experience, and the Missouri–Rolla team finished first in the 1999 Sunrayce, second in the 2000 Formula Sun Grand Prix, second in the 2001 American Solar Challenge, fourth in the 2001 World Solar Challenge, and first in the 2002 Formula Sun Grand Prix, and first in the 2003 American Solar Challenge.

Dr. Carroll is currently a professor in the Basic Engineering Department and continues to work with the solar car team in designing a new car for the 2003 race season.